NASA Contractor Report CR- 189225

LUNAR PMAD TECHNOLOGY ASSESSMENT

Kenneth J. Metcalf
Rockwell International
Rocketdyne Division
Canoga Park, California

February 1992

PREPARED FOR
LEWIS RESEARCH CENTER
UNDER CONTRACT NAS3-25808

NASA

NATIONAL AERONAUTICS AND
SPACE ADMINISTRATION

CONTENTS

FIGURES

FIGURES

TABLES

TABLES

NASA CR–189225

1.0 SUMMARY

The purpose of this report is to document the initial set of power conditioning models created to estimate power management and distribution (PMAD) component masses and sizes. This first set contains converter, rectifier, inverter, transformer, remote bus isolator (RBI), and remote power controller (RPC) models. The objective is to form a library of PMAD models that will allow system designers to assess various power system architectures and distribution techniques quickly and consistently. It is recommended that the models developed during this study only be used for conceptual design studies which require "ballpark" PMAD mass estimates. To determine specific PMAD design choices such as component topologies, and transmission and distribution voltages and frequencies requires specific power system requirements and more detailed analyses.

These models are designed primarily for space exploration initiative (SEI) missions that require continuous power and support manned operations. The model development is based on the fact that power conditioning components have common stages and that their interconnection and control determines the function and operation of the component. The stages contained in a component are defined, their masses calculated, and the control and monitoring, enclosure, and thermal management masses are added to determine the mass of the complete component. The models are based on components that use passive or active thermal management and they estimate component heat sink, coldplate, and radiator masses (the masses of pumps, plumbing, etc. are not included). The model documentation explains the component equations, including their constants and exponents; identifies model limitations; specifies valid input ranges; and discusses methods for applying the component models. A separate section explains how to link individual models to form a complete power transmission and distribution system model.

Before creating the power conditioning models, a power element technology assessment was conducted to gauge the amount of advancement one could reasonably expect by the year 2000. From this assessment, component characteristics consistent with future PMAD designs were generated. The model development was initiated by identifying common component stages and obtaining mass breakdowns for these stages from electronic hardware elements proposed for near term missions such as the Space Station. Technology advances were then incorporated to generate hardware masses consistent with the 2000 to 2010 time period. These projected mass breakdowns served as benchmarks, and they were the basis for mass breakdowns generated at other operating points. Equations representing the various component stages were developed from these data points using curve fitting techniques. The final step was to assimilate selected equations into a spreadsheet to form a complete component model.

The previously identified power conditioning component models allow certain studies to be performed; however, other models are required to conduct a thorough evaluation of lunar base PMAD alternatives and perform other PMAD system studies. A list of these component and transmission line models is contained in the conclusions and recommendations section of this report. It is suggested that models be created for these PMAD components during follow up task orders.

2.0 INTRODUCTION

This task was initiated to develop and document easy to use, standardized PMAD models for power system studies. Earlier centralized versus decentralized lunar base power system analyses used simple power conditioning and transmission line models to conduct architecture, voltage, and frequency trade studies (Ref. II-1). These models were obtained by NASA LeRC and questions were raised about their development, applications, and capabilities. It became apparent that additional models were required to allow a wider variety of power systems to be evaluated and that the earlier created models needed to be revised to include the latest information, enhanced in capability and flexibility, and most importantly documented to allow critical review by experts in the field. This report represents a beginning in this process. Subsequent reports containing additional power conditioning and transmission line models will allow a library of PMAD models to be formed. First though, the models presented in this report must be evaluated since it is important to reach a consensus on the approach employed and the model accuracy before proceeding with future work.

The models contained in this report are intended to be simple to use and yield useful results. While these objectives are desirable, individuals not familiar with PMAD systems may assume the components are easy to design and the technology is mature. This is clearly wrong. New design approaches and emerging technologies are continually being studied to achieve better performance and reduce mass. Consequently, to develop representative PMAD models it was necessary to review different technologies and evaluate these against proposed space exploration initiative (SEI) applications. The objective was to conceive a set of component characteristics and operating conditions that would be consistent with future PMAD designs.

Anticipated improvements in PMAD components are reflected in the models and discussed in the sections dedicated to those devices. Although a concentrated development effort is necessary to achieve many of these performance levels, this report does not propose methods for realizing them or identify critical technology areas. This is not its intent. Technology projections will be addressed on a case by case basis, but in general they are based on information obtained from related power system studies and discussions with experts in the PMAD field. The purpose of this report is not to contribute component design information, but to present models representative of future PMAD components and explain the rationale employed during their development. Subsequent tasks will need to identify the critical technology areas that must be developed to fabricate and deploy proposed SEI power systems.

Every SEI application will have different operating requirements, many of which are not even envisioned at the present time. Although the models in this report are designed to accept a wide range of operating parameters, they are not capable of addressing all aspects of a particular application. It was necessary to assume typical values for some parameters. This naturally introduces a certain amount of error and it is one reason model outputs should be compared with other sources of information. These models also address a specific type of power system operation. To understand their scope, it is necessary to briefly discuss other power system operating methods and models developed to represent them.

Depending on their application, PMAD systems tend to fall into two broad categories, burst or continuous power. Burst power systems are suited for short term operation, generally less than fifteen minutes. Continuous power systems are designed for reasonably steady state operation and they typically operate for years. These operating differences lead to different design approaches, especially in the area of thermal management.

The short operating life of a burst power system allows adiabatic or cryogenic cooling techniques to be employed. Adiabatic cooling relies on the heat capacity of the component and adjacent structure to absorb generated heat. Mass constraints essentially limit adiabatic cooling times to under 120 seconds. Cryogenic cooling normally uses liquid hydrogen or nitrogen to cool the power conditioning components to near cryogenic temperatures. The cryogenic liquid and its tankage can be quite heavy; hence, cryogenic cooling is often employed only when that liquid can cool several items or is needed for other reasons on the platform. It generally is not practical to condense the gas byproduct back into its liquid form because cryogenic refrigeration processes are not very efficient. For these reasons, cryogenic cooling is also limited to relatively short periods.

A PMAD system designed for long term operation requires radiators and passive and/or active thermal management techniques. Components in a passive system contain internal heat sinks and thermal paths that conduct generated heat to a coldplate. Heat pipes routed through the coldplate then transport this heat out to a radiator for dissipation. An active cooling system employing a coldplate would use a pumped loop containing a liquid to carry heat from the coldplate to a radiator surface. An alternate active cooling technique eliminates the need for a dedicated coldplate and greatly reduces the amount of passive heat transfer within a component by pumping a liquid directly over the surfaces of the power carrying devices and out to a radiator.

A. S. Gilmour developed power conditioning models for burst power systems that relied on adiabatic cooling (Ref. II-2). Estimates generated by J. J. Moriarty were for space based power conditioning components that operated in either burst or continuous power modes (Ref. II-3). In Moriarty's concept, waste heat was passively conducted to spacecraft walls held at a constant temperature of 20° C. Power conditioning algorithms developed by E. T. Gerry and W. J. Shaefer were based on hydrogen cooled components operating from 200 to 1000 seconds (Ref. II-4). An unlimited supply of hydrogen ranging from 150 to 250 K was considered to be available. These reports provided valuable insight and some of the mass trends contained in them were helpful in formulating the models contained in this report. However, these models were developed for specific applications, applications very different than those portrayed in SEI reports. Since Gilmour's models are based on adiabatic cooling, they do not include any factors for passive or active thermal management subsystems. The hardware necessary to passively cool a device may account for 80 to 90% of its total mass. Moriarty's estimates include the hardware mass needed for passive heat transfer within a component, but they do not include the mass of the external passive or active cooling system required to cool the spacecraft walls. The algorithms developed by Gerry and Shaefer assumed an unlimited supply of hydrogen was available for cooling, an assumption that is not practical for long duration missions. An individual using these models will nearly always obtain power conditioning mass estimates that are much lower than those forecast for a continuous, steady state power system. In some cases, the values may be less than one-tenth of the expected mass. Using values that originate from work done by Gilmour, Moriarty, or Gerry and Shaefer for SEI mass estimates is therefore strongly discouraged.

Another factor affecting PMAD mass is whether the platform is manned or unmanned. Man critical systems have higher reliability, availability, and maintainability requirements. Consequently, a more conservative design approach is usually employed. Components are operated at lower power densities and temperatures. This increases PMAD mass because added thermal management hardware is required and larger power devices are used throughout the system. The components in a manned system may also need to be designed for easy removal and maintenance. This also drives up PMAD mass because components will need to be equipped with electrical connectors, mechanical disconnects, and heat exchangers or fluid couplings to provide detachable heat transfer paths.

Since many proposed SEI missions are manned or support manned expeditions, reliability considerations influenced the model development. A detailed reliability analysis was not conducted during this study, therefore it was necessary to make some basic assumptions. It is anticipated that the lunar base requirements will specify at least a ten year operating life for power conditioning components. Because many of the present Space Station Freedom (SSF) components are designed to meet a ten year mean time between failure (MTBF), this data was relied on heavily during the model development. Reliability is normally improved in two ways: (1) key elements within a component can be made redundant, and (2) multiple smaller units, each sized to handle a percentage of the power, can replace a single large unit. Unfortunately, reliability considerations typically increase power system mass and place added demands on the instrumentation and control subsystem. Incorporating internal redundancy into a component increases its mass since additional elements are required. Replacing a single power conditioning unit with multiple smaller units increases mass because some economies of scale are sacrificed and ancillary hardware such as the enclosure, and control and monitoring now occupy a larger percentage of the total component mass. The size and complexity of the instrumentation and control (I&C) subsystem that oversees the entire power system is also expanded since it must monitor a larger number of units and coordinate their operation. The mass impacts associated with an enlarged I&C subsystem are not addressed by these models since they only pertain to individual power conditioning components.

The models contained in this report are primarily targeted for SEI missions that demand continuous power for long time periods and support manned operations. They are based on the use of passive or active thermal management techniques and include equations to estimate the masses of component heat sinks, coldplates, and radiators. Just as Gilmour's, Moriarty's, and Gerry and Shaefer's models and estimates are only suitable for certain applications, the models in this report are also oriented toward certain applications. They should only be used to estimate masses, volumes, and efficiencies of components in highly reliable PMAD systems designed for long duration, steady power delivery.

3.0 POWER CONDITIONING MODEL DEVELOPMENT

Before beginning to develop power conditioning models, a power element technology assessment was conducted to determine the amount of advancement one could reasonably expect by the year 2000. After considering anticipated technology advances in the context of proposed SEI missions, general conclusions were reached. Numerous improvements are projected for converter elements, thermal management subsystems and packaging techniques. It is anticipated that carbon-carbon will be used extensively for enclosures and heat pipes, replacing aluminum in many applications. Component radiators will also utilize carbon-carbon extensively. Improvements in the magnetic materials area are expected to be fairly minor and occur mainly in the high frequency region. High frequency transformer and inductor core masses and losses should decline as a result. Incremental improvements in capacitors should yield modest gains in energy density and efficiency. Presently, most individual semiconductor switches are limited to operating voltages below 500 V (Ref. III-1). Recent advances in metal-oxide-semiconductor field-effect-transistors (MOSFETs) and MOS controlled thyristors (MCTs) indicate substantially higher voltage devices can be developed by the year 2000, possibly as high as 5000 V (Ref. III-2, III-3, III-4). Although silicon controlled rectifiers (SCRs) are already available at voltages up to 5000 V, their turn off requirements limit their applications[1] (Ref. III-5). The development of high voltage, high power semiconductor switches should decrease the mass of converters and improve their efficiency. It should be noted that the technology advances predicted here and throughout this report are highly speculative since a key driver is development funding and it varies considerably.

Based on this technology assessment a set of component characteristics were developed that were deemed to be consistent with future PMAD designs. This data served as a foundation for the actual component model development. Models were generated using a six step process: (1) the specific stages in a component were identified; (2) mass breakdowns for these stages were obtained by studying component designs or hardware; (3) projected technology advances were considered and used to adjust these mass breakdowns to yield mass values consistent with the 2000 to 2010 time period; (4) these adjusted mass breakdowns were used as benchmarks and they were extrapolated from to generate mass tabulations at other operating points; (5) equations were generated to fit these points using curve fitting techniques; and (6) selected equations were assimilated to form a complete model. This entire process is based on the theory that the mass of a power conditioning component can be estimated by summing the masses of its power processing stages and associated hardware (this approach is treated in detail in the next section).

The tables contained in Appendix A illustrate many of the model development steps. Referring to the "Chopper Mass Breakdown Tables" for example, note that some of the mass breakdowns are shaded. These shaded areas depict power processing stage mass breakdowns derived from present element masses. They were gener-

---

[1] An SCR cannot be turned off by simply removing the gate signal, the current flow must either be interrupted or forced to flow in the opposite direction. For ac switching or rectification, these turn-off requirements are acceptable because the current naturally crosses through zero each half cycle. However in a DC application, such as an inverter switch, they aren't usually acceptable.

ated by listing the masses of the present elements in a stage and incorporating gains expected from technology advances. Because it was easier to estimate the improvements for a single item, each element in a stage was evaluated individually. These derived mass breakdowns served as benchmarks for subsequent extrapolations. To generate mass breakdowns at other operating points each of the operating parameters such as power, voltage, efficiency, and frequency were considered separately. The mass impact that a change in an operating parameter had on a stage was again evaluated element by element. This matrix like approach, where one axis represented the elements in a stage and the other axis the change in operating parameters, was used because it simplified the extrapolation process and resulted in greater confidence in the values.

3.1 Power Conditioning Stages Approach

Power conditioning components tend to have common stages. For example, the dc/dc converter, the dc/ac inverter and the ac/ac frequency converter, each have a chopper stage. The interconnection and control of these stages determine the function and operation of the total converter. Hence, one can define the stages contained in a specified converter, calculate their individual masses, and then add these values to the control and monitoring hardware mass, the enclosure mass and the thermal management and radiator subsystem mass to determine the total mass of a complete converter.

The masses of power conditioning components were estimated by defining the stages in a component and generating a mass equation for each one using the previously described six step process. Much of the information used to develop these equations was obtained from SSF documentation. These designs were considered to best typify proposed lunar base hardware and represent the latest space based components, operating at the highest steady state power levels. Since the lunar base will be erected about ten years in the future, mass figures were modified to incorporate projected technology advances. Equations were then developed to determine the mass of ancillary hardware such as controllers, data interface modules and monitoring sensors. The masses of the individual stages and ancillary hardware are summed to determine the total mass of the electronics related elements contained in the component. Based on this mass and a factor computed for the density of electronics, the surrounding enclosure and selected thermal management hardware mass was estimated. These values are then summed to obtain the component mass. Finally, a mass is computed for the radiator and added to this component mass to obtain the total mass of the power conditioning component.

Since the power conditioning component models consist of interconnected stages, the easiest way to explain the model formulation is to address the models for the component stages individually. The equations used to estimate the masses of these stages will be further broken down and these parts will be discussed separately. This should allow the supporting rationale to be presented in a clearer manner. Since most effects can not be easily explained or justified using mathematical procedures, graphs will be used liberally to display the effects that have been noted as operating conditions are varied over the ranges being considered. The equations were developed by studying technical reports, program documentation, textbooks, design manuals, and vendor catalogues. These sources will be identified during the model discussions.

3.1.1 Chopper Stage Model

The chopper stage is utilized to convert dc into ac, and it is included in the inverter, dc/dc converter and frequency converter models. A chopper can follow several different topologies, depending on the design requirements. These chopper stage equations, however, are general in nature and only intended to provide rough mass estimates for component comparison purposes. For more accurate mass estimates and topology comparisons, specific designs should be generated by a circuit designer.

The chopper section is composed of switch modules, each containing a semiconductor switch and a snubber circuit; and ancillary hardware, consisting of inductors, capacitors, diodes, and resistors. The snubber circuitry facilitates switching and mitigates the voltage and current spikes that occur during switching. The switch modules operate together to switch the incoming dc voltage and generate an alternating voltage. Precise, synchronized switching is required to provide a constant frequency and fine voltage regulation. Mass breakdowns for a present and projected switch module capable of handling 1 kWe are shown in Table 1. A 1 kWe power level was selected to develop a per unit basis for later mass extrapolations. The present mass values were estimated from briefing packages prepared by TRW, Ford Aerospace, and Rocketdyne in support of SSF, and a power MOSFET catalogue (Ref. III-1, III-6, III-7, III-8). The projected mass breakdown originates from articles discussing future power conditioning component developments and discussions with experts in the field of power conditioning (Ref. III-4, III-9, III-10). It was used as a basis for subsequent equation development.

Table 1
1 kWe Switch Module Mass Breakdown

Hardware Element	Present Mass (grams)	Projected Mass (grams)
Active Switch Element	7	5
Snubber Circuitry	20	15
Heat Sink, Thermal Management	48	35
Gate Drive Circuitry	25	15
Switch Control Logic	20	5
Packaging and Mounting	40	25
Total Switch Module	160	100

Advances in switch fabrication techniques, better switch geometries, and continuing size reductions in integrated logic circuitry should reduce the mass of switch elements. Much of the development expended on semiconductors is expected to be aimed at improving their efficiency because the main limiting factor in electronics mass reduction is the inability to remove waste heat (Ref. III-11). The increasing use of graphite based fibers in heat sinks should facilitate heat removal and cut mass because graphite has superior heat transfer characteristics and its specific weight is about two-thirds that of aluminum.

In addition to the switch module mass, ancillary hardware is required in the chopper circuit itself to manage internal energy flows. A parallel resonant topology has a tank circuit consisting of an inductor and capacitor that stores energy to facilitate current circulation and switching; a current fed push-pull topology requires an input inductor to maintain a constant current supply. Mass gains in this area are expected to be relatively small. Alternate magnetic materials are being developed, but they often times are brittle or exhibit poor thermal conductivity. This limits their usefulness in high power applications and proven materials such as supermalloy are expected to remain the standard. Capacitor development continues to yield improvements in energy storage density and reliability, but progress is fairly slow. Overall the mass of the tank hardware in a chopper circuit was expected to decline about 10%.

The chopper mass breakdowns contained in this report are based on a parallel resonant Mapham converter topology. This topology was originally selected for use in the main inverter units when the SSF power system utilized a 20 kHz PMAD system. It is well suited for high frequency applications and exhibits a low mass and high efficiency. The resonant operation of this converter also allows zero current switching. This greatly reduces switching losses, switch stress, and switching induced noise. The lower switching noise and sinusoidal nature of the waveform improves the output power quality and reduces filtering demands (Ref. III-12). Because the Mapham resonant topology uses two sets of switches to switch the input voltage, the full input voltage is not impressed across a single switch. This feature and the reduced switching stress should facilitate a high voltage chopper design. However, because there are two switches in the conduction path, the switch voltage drop is doubled. This is a serious drawback in a low voltage converter. One reason the present SSF dc/dc converter units utilize a current fed push-pull topology is because of concerns raised about the technological maturity of the resonant converter. The resonant converter has a higher parts count and tends to be more complex (Ref. III-13). Resonant converter development has been rapid, however, and these equations are intended for components anticipated to be available after the year 2000. This is adequate time to fully develop and verify the operation and reliability of a resonant converter.

For a present 1 kWe, 20 kHz chopper stage, the mass of the chopper tank hardware was judged to be 330 grams. Anticipated circuit and component improvements should drop this value to 300 grams by the year 2000. A full wave chopper stage based on a Mapham resonant topology uses four 500 watt switch modules, each weighing 50 grams, and tank hardware estimated to weigh 300 grams, the total mass of a future 1 kWe chopper is projected to be about 500 grams.

The subsequent paragraphs will explain the development of the single-phase and 3-phase chopper stage equations in detail. The variables that will be used during this discussion are shown in Table 2. When a factor is being discussed it will be underlined. Graphs will accompany each section to illustrate the parameters that have been incorporated into the equations. Chopper mass breakdown tables are located in Appendix A on pages A-1 and A-2. The values in these mass breakdowns were mainly generated from information obtained from NASA LeRC, General Dynamics, and TRW (Ref. III-11, III-14, III-15).

Table 2
Chopper Model Variable Definitions

1CSM	Single-Phase Chopper Stage Mass
3CSM	3-Phase Chopper Stage Mass
CSE	Chopper Stage Efficiency (96%)
CSAM	Chopper Stage Available Modules
CSRM	Chopper Stage Required Modules
CSP_O	Chopper Stage Power Output (kWe)
CSV_I	Chopper Stage Voltage Input (Vdc)
CSF	Chopper Stage Frequency (kHz)

Mass Coefficient

$$1CSM=\underline{0.39}*((EXP(0.025/(1-CSE)))/1.86)*(CSAM/CSRM)*CSP_O*((CSP_O/CSRM)^{-0.05}$$
$$*(CSV_I/(CSV_I-2))^7*EXP(CSV_I/40000)*(20/CSF)^{0.45}*EXP(CSP_O{}^{0.1}*CSF/160))$$

$$3CSM=\underline{0.4}*((EXP(0.025/(1-CSE)))/1.86)*(CSAM/CSRM)*CSP_O*((CSP_O/CSRM)^{-0.05}$$
$$*(CSV_I/(CSV_I-2))^7*EXP(CSV_I/40000)*(20/CSF)^{0.45}*EXP(CSP_O{}^{0.1}*CSF/160))$$

To calculate an appropriate value for the chopper stage mass coefficients, the equations were calibrated to yield values consistent with the above 1 kWe mass breakdown and actual component designs (Ref. III-6, III-7, III-16).

Efficiency Factor

$$1CSM=0.39*\underline{((EXP(0.025/(1-CSE)))/1.86)}*(CSAM/CSRM)*CSP_O*((CSP_O/CSRM)^{-0.05}$$
$$*(CSV_I/(CSV_I-2))^7*EXP(CSV_I/40000)*(20/CSF)^{0.45}*EXP(CSP_O{}^{0.1}*CSF/160))$$

$$3CSM=0.4*\underline{((EXP(0.025/(1-CSE)))/1.86)}*(CSAM/CSRM)*CSP_O*((CSP_O/CSRM)^{-0.05}$$
$$*(CSV_I/(CSV_I-2))^7*EXP(CSV_I/40000)*(20/CSF)^{0.45}*EXP(CSP_O{}^{0.1}*CSF/160))$$

The factors underlined above estimate the changes in specific weight that occur over a range of chopper efficiencies. Within reason, the interconnecting wiring and ancillary hardware resistive losses, and the switch conduction losses can be reduced by increasing the size of the wiring and ancillary hardware, and the active switch element area and snubber component ratings. If the switch losses are always less over the full operating range, it should be possible to reduce the heat sink mass. By gauging the effect of power losses on individual elements within a switching module, chopper mass estimates were developed for efficiencies ranging from 95 to 97%. An efficiency factor was then calculated and incorporated into the chopper mass equation. Figure 1 shows a graph of the resulting specific weight versus efficiency values that were developed with this approach. Note that the depicted chopper efficiency range is relatively narrow.

Figure 1

CHOPPER SPWT VS EFFICIENCY

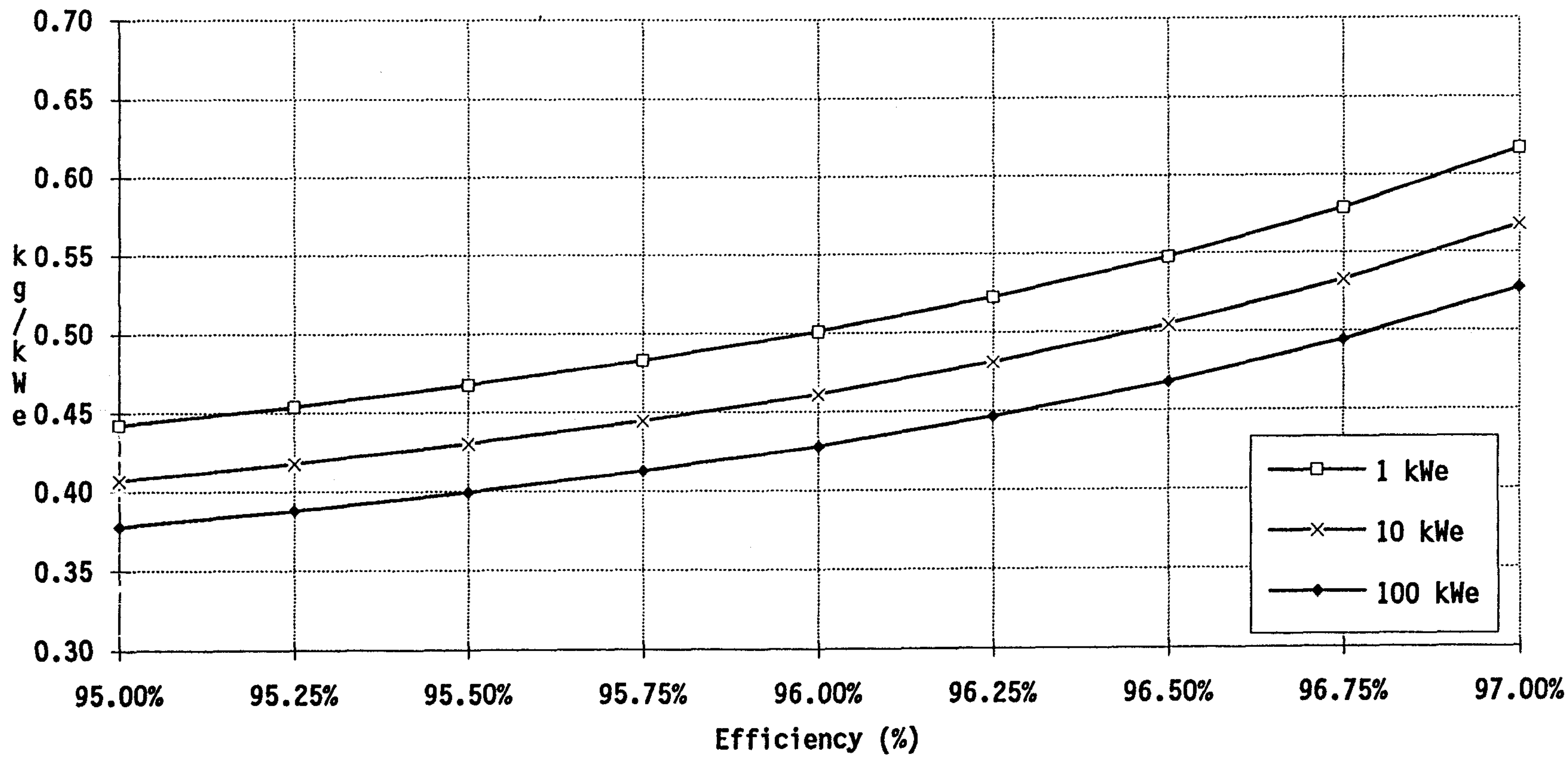

Chopper efficiencies higher than about 97% are not considered practical due to limitations in circuit topology designs and switch fabrication techniques. Lower efficiencies are undesirable because of the increased thermal management and radiator mass. However, low operating voltages cause addition losses and result in efficiencies poorer than those shown. This will be explained further in the discussion pertaining to the voltage factors.

Redundancy Factor

$$1CSM=0.39*((EXP(0.025/(1-CSE)))/1.86)*\underline{(CSAM/CSRM)}*CSP_O*((CSP_O/CSRM)^{-0.05} *(CSV_I/(CSV_I-2))^{7}*EXP(CSV_I/40000)*(20/CSF)^{0.45}*EXP(CSP_O{}^{0.1}*CSF/160))$$

$$3CSM=0.4*((EXP(0.025/(1-CSE)))/1.86)*\underline{(CSAM/CSRM)}*CSP_O*((CSP_O/CSRM)^{-0.05} *(CSV_I/(CSV_I-2))^{7}*EXP(CSV_I/40000)*(20/CSF)^{0.45}*EXP(CSP_O{}^{0.1}*CSF/160))$$

The redundancy mass impacts that will occur for this stage when modules are added to enhance reliability are reflected in the above factor. This redundancy factor does not include the increased system control and monitoring requirements and their associated mass. The "available modules" value is the actual number of modules present in the component; the "required modules" number is the actual number of modules required to achieve full output power. If a design requires 4/3 redundancy to meet the reliability requirements, each channel will be rated to carry 33% of the power. 4 channels are available, but only 3 channels are needed to supply full power. The fourth channel represents the mass penalty incurred in this particular stage to achieve a higher reliability.

Power Level Multiplier

$$1CSM=0.39*((EXP(0.025/(1-CSE)))/1.86)*(CSAM/CSRM)*\underline{CSP_O}*((CSP_O/CSRM)^{-0.05} *(CSV_I/(CSV_I-2))^{7}*EXP(CSV_I/40000)*(20/CSF)^{0.45}*EXP(CSP_O{}^{0.1}*CSF/160))$$

$$3CSM=0.4*((EXP(0.025/(1-CSE)))/1.86)*(CSAM/CSRM)*\underline{CSP_O}*((CSP_O/CSRM)^{-0.05} *(CSV_I/(CSV_I-2))^{7}*EXP(CSV_I/40000)*(20/CSF)^{0.45}*EXP(CSP_O{}^{0.1}*CSF/160))$$

The equations can be used to calculate the mass or specific weight of the chopper. When the above multiplier is included, the value that results is a chopper mass estimate. To obtain the specific weight of the chopper, remove this multiplier.

Power Level Factor

$$1CSM=0.39*((EXP(0.025/(1-CSE)))/1.86)*(CSAM/CSRM)*CSP_O*(\underline{(CSP_O/CSRM)^{-0.05}} *(CSV_I/(CSV_I-2))^{7}*EXP(CSV_I/40000)*(20/CSF)^{0.45}*EXP(CSP_O{}^{0.1}*CSF/160))$$

$$3CSM=0.4*((EXP(0.025/(1-CSE)))/1.86)*(CSAM/CSRM)*CSP_O*(\underline{(CSP_O/CSRM)^{-0.05}} *(CSV_I/(CSV_I-2))^{7}*EXP(CSV_I/40000)*(20/CSF)^{0.45}*EXP(CSP_O{}^{0.1}*CSF/160))$$

As the power level of the chopper increases, certain economies of scale present themselves and allow a reduction in specific weight. Although, the active switch element, snubber circuitry, and thermal management hardware sizes will increase nearly linearly with power level, the mass of the gate drive circuitry and switch control logic will rise at a slower rate. This causes switch module specific weights to decline as power levels rise. The specific weight of the tank hardware also declines slowly as the power level rises because the inductors, capacitors, diodes, resistors and interconnecting wiring forming this subsystem can be fabricated and configured more efficiently. Components can also be packaged more effectively at higher power levels, further reducing the packaging volume and mounting mass.

The masses of individual elements of a single-phase chopper were extrapolated to generate mass estimates for a complete unit at power levels ranging from 0.5 to 100 kWe. Based on these mass estimates, it was concluded that the specific weight of a single-phase chopper would decline at the 0.05 power as power level rose. The results of this evaluation are illustrated in Figure 2.

A 3-phase chopper consists of three single-phase choppers operating in unison. Assuming a dc link resonant converter is employed, each phase will require its own resonant tank hardware. This is necessary to generate three separate waveforms, each offset 120 degrees from the other. Power handling devices can not be shared between phases, only the control hardware is common. 3-phase chopper mass estimates were calculated by summing the masses of three single-phase choppers, each assumed to be processing exactly one-third of the power. Separate gate drive circuitry was assumed for each switch, but the switch control logic was integrated into a single unit to ensure synchronized operation and facilitate voltage regulation and frequency control. 3-phase chopper mass estimates were generated for power levels ranging from 10 to 250 kWe. These estimates indicated the specific weights of 3-phase choppers also decline at the 0.05 power as power levels increase. The specific weights of 10 to 250 kWe single- and 3-phase choppers are compared in Figure 3 at two resonant frequencies.

The required number of modules is also included in this segment. A modular design approach consists of multiple modules, each designed to process a percentage of the total assembly output power. For this reason, the specific weight of each chopper is calculated at the power level that that particular module is operating at and not the power level of the complete assembly.

Voltage Level Factors

$$1CSM=0.39*((EXP(0.025/(1-CSE)))/1.86)*(CSAM/CSRM)*CSP_O*((CSP_O/CSRM)^{-0.05} *\underline{(CSV_I/(CSV_I-2))^7}*\underline{EXP(CSV_I/40000)}*(20/CSF)^{0.45}*EXP(CSP_O{}^{0.1}*CSF/160))$$

$$3CSM=0.4*((EXP(0.025/(1-CSE)))/1.86)*(CSAM/CSRM)*CSP_O*((CSP_O/CSRM)^{-0.05} *\underline{(CSV_I/(CSV_I-2))^7}*\underline{EXP(CSV_I/40000)}*(20/CSF)^{0.45}*EXP(CSP_O{}^{0.1}*CSF/160))$$

It was necessary to include two factors to cover the full voltage range that will be encountered by a chopper. The first, "$(CSV_I/(CSV_I-2))^7$", addresses the influences on power conductor and switch mass as the voltage level declines. The second, "$EXP(CSV_I/40000)$", addresses the mass increases occurring as voltages increase.

Since conduction losses are calculated with the equation I^2R, and current levels rise as voltage declines, the chopper efficiency will be poorer at lower

CHPR1PWR.XLC

Figure 2

Chopper SPWT vs Power Level

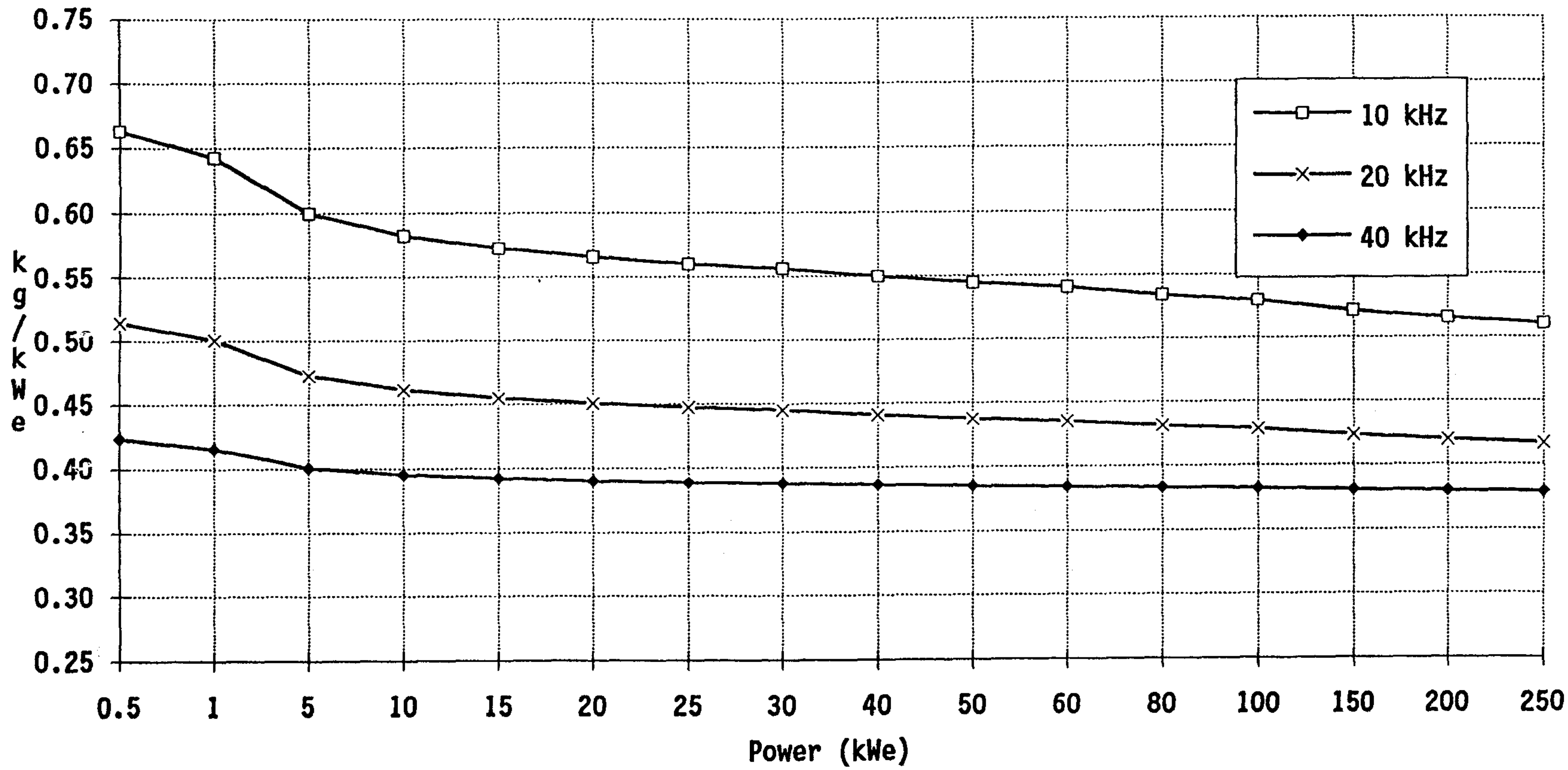

CHPRGRPH.XLS

6/10/91

Figure 3

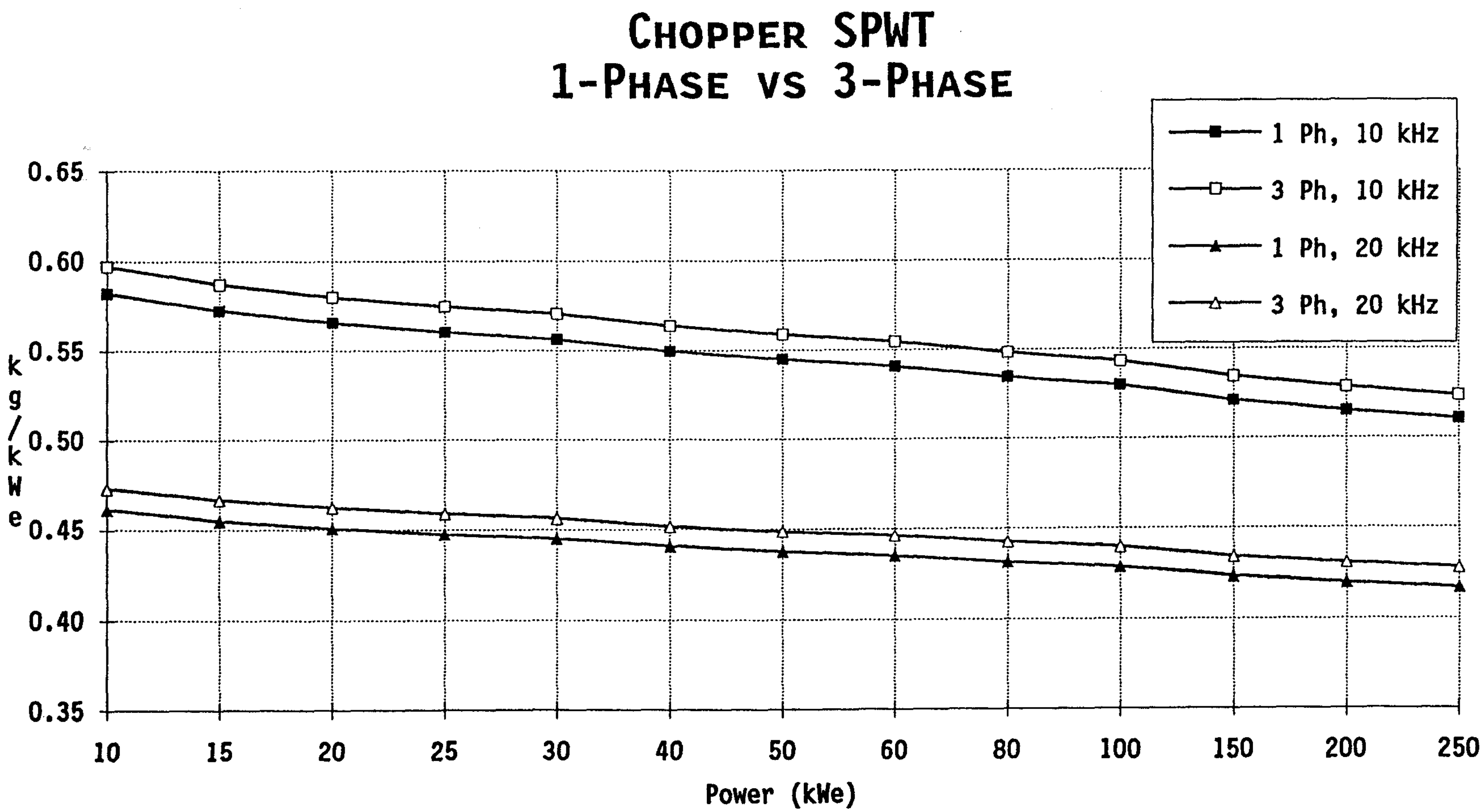
CHOPPER SPWT
1-PHASE VS 3-PHASE
1 Ph, 10 kHz
3 Ph, 10 kHz
1 Ph, 20 kHz
3 Ph, 20 kHz
kg/kWe
0.65
0.60
0.55
0.50
0.45
0.40
0.35
10
15
20
25
30
40
50
60
80
100
150
200
250
Power (kWe)

voltage levels[2]. In most designs, these higher losses are partially offset by lowering the resistances of circuit elements. To accomplish this the cross sectional areas of the conductors and switches must be increased, which causes their mass to increase. To obtain proper mass estimates for low voltage choppers, the efficiency parameter that is input into the chopper module should be decreased in accordance with Table 3. Using the values shown here, smooth specific weight versus input voltage curves are generated for resonant converter chopper designs. These values reflect the increase in mass and reduction in efficiency that occurs at lower voltages. The specific weight curves generated with these values are shown in Figure 4 for 0.5 and 1 kWe power levels.

Table 3
Efficiency Corrections for Low Voltage Chopper Mass Estimates

Input Voltage (Vdc)	Resonant Chopper Input Efficiency (percent)
120	96.00
110	96.00
100	95.97
90	95.93
80	95.87
70	95.76
60	95.63
50	95.40
40	95.07
30	94.40
20	92.00

High voltage chopper designs will require alternate design approaches. Currently metal-oxide-semiconductor field-effect-transistors (MOSFETs) are utilized most often for chopper switches, although MOS controlled thyristors (MCTs) are expected to become prominent in the future due to their lower losses, and higher voltage and power capabilities (Ref. III-9, III-10, III-17). To switch very high voltages, the switch modules will need to be connected in series. Theoretically, since the voltage across a single module is not increased, the insulating requirements and mass of the individual modules are unchanged. In practice, this probably will not be true. Added hardware will be needed to force the switch modules to voltage share and limit parasitic capaci-

---

2 The equation I^2R also applies in high frequency applications, but the skin effect drives the effective resistance of the conductors up. This increased resistance can be partially offset by employing alternate conductor constructions such as Litz wire, but mass and thermal conduction penalties are incurred. For 20 kHz designs a typical guideline is that the ac resistance of a conductor is 1.3 times the dc resistance.

Figure 4

CHOPPER SPWT VS VOLTAGE

(LOW VOLTAGE REGION)

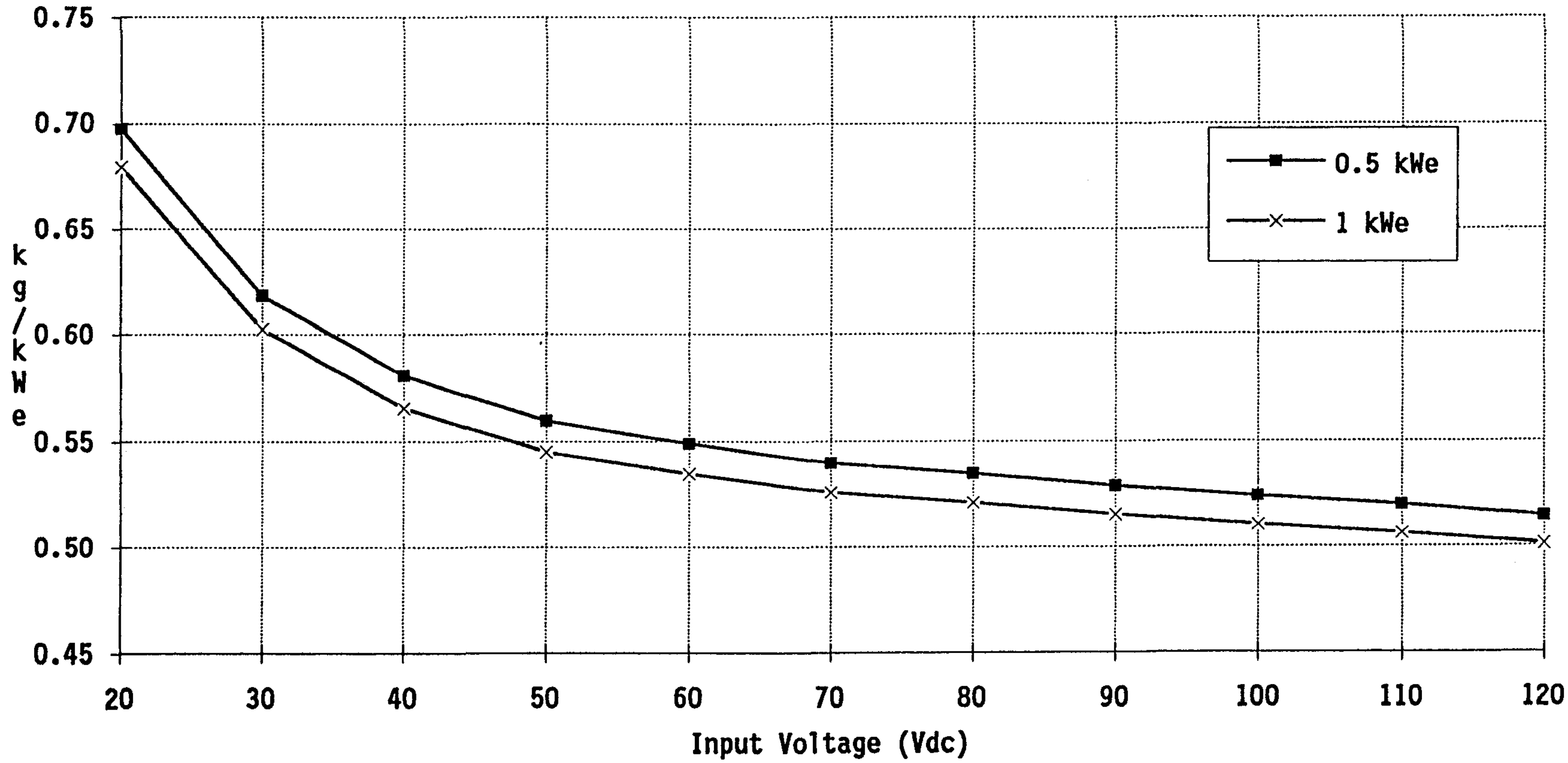

tance. Even with this added hardware, the insulation and switch ratings may need to be increased to tolerate uneven or improperly applied voltages. It is expected that the switch synchronization problems that are a concern in any chopper design will be exacerbated in a high voltage design. Unfortunately, little information is available on actual design techniques since there is not much demand for a high voltage chopper at the present time and very little space suitable hardware is rated for high voltage applications.

In fact, only one very high power design is known to be currently in progress. General Electric is evaluating a 1 MWe inverter design for NASA (Ref. III-18). It uses a module containing four parallel strings, each containing 100 amp MCTs. This module is rated for 200 amps total. Each string is composed of ten 1000 volt MCTs stacked in series to provide a 5000 volt switching potential. Based on the design results noted to date, the operating limits of the composite assembly will be lower than the sum of the individual parts. Topology and component design modifications are necessary to insure proper voltage and current sharing between MCTs. These constraints result in size, mass, and loss penalties. It will also be challenging to achieve synchronized switching with these 40 MCTs at high frequencies. Poor synchronization will lead to excessive losses in the snubber circuits and result in a low switching efficiency. No mass information was available at the present time, but its status will be tracked.

A survey of high power, high voltage MOSFET manufacturers indicates a MOSFET device with a 5000 volt drain to source breakdown voltage, a 250 amp current rating, and a 20 kHz switching speed is achievable by 1995-2000 (Ref. III-2). Present literature states that MOSFETs with drain to source breakdown voltages in excess of 1000 volts can be purchased (Ref. III-3). For this study, it was assumed that switches with a 5000 volt breakdown voltage and a 20 kHz switching speed will be available by 2000. The acceptable operating voltage for a semiconductor device is approximately half the breakdown voltage; therefore, two series connected solid state switches would be required in each switch module to switch a 5000 Vdc voltage.

Based on the items previously discussed, the following observations were made about high voltage chopper designs and masses. The data obtained to date from the high power inverter study indicates high voltage designs will incur mass penalties to insure voltage sharing and limit parasitic capacitance. The switch ratings and insulation levels will probably need to be increased to guard against potential voltage imbalances. Even power conditioning devices as rugged as transformers rise in mass as voltage levels increase. It is expected that the mass of a chopper will rise at a faster rate with voltage than a transformer since its components tend to be much more sensitive to over voltage conditions and voltage spikes. Based on this reasoning, the factor underlined in the above equation was developed. Specific weight curves for high voltage chopper designs obtained from this equation are shown in Figure 5 at 10, 100, and 250 kWe power levels.

Frequency Factors

$$1CSM=0.39*((EXP(0.025/(1-CSE)))/1.86)*(CSAM/CSRM)*CSP_0*((CSP_0/CSRM)^{-0.05} *(CSV_I/(CSV_I-2))^{7}*EXP(CSV_I/40000)*\underline{(20/CSF)^{0.45}}*\underline{EXP(CSP_0^{0.1}*CSF/160)})$$

Figure 5

Chopper SPWT vs Voltage

(High Voltage Region)

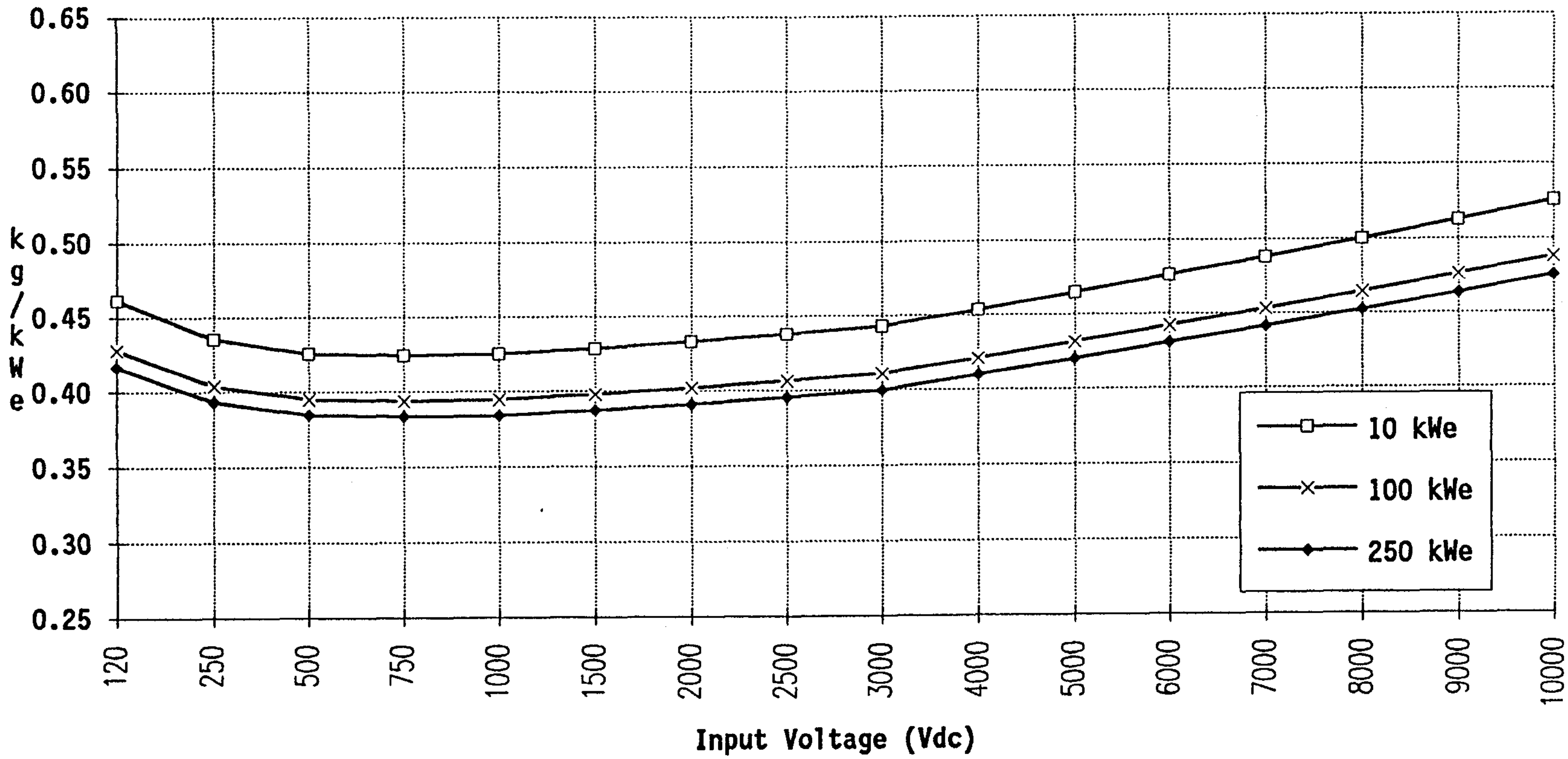

$$3CSM=0.4*((EXP(0.025/(1-CSE)))/1.86)*(CSAM/CSRM)*CSP_O*((CSP_O/CSRM)^{-0.05}$$
$$*(CSV_I/(CSV_I-2))^7*EXP(CSV_I/40000)*\underline{(20/CSF)^{0.45}}*\underline{EXP(CSP_O^{0.1}*CSF/160)})$$

The masses of the chopper switches are relatively unaffected by changes in frequency. However, the component values contained in the resonant converter tank and the circuit parasitic reactances are a function of the resonant frequency. The resonant frequency of a resonant circuit is calculated by the equation:

$$2\pi f=1/(L*C)^{0.5}$$

Where: f = the resonant frequency in hertz
L = the circuit inductance in henries
C = the circuit capacitance in farads

From this equation one can see that the inductor and capacitor values, and their associated masses, are a function of frequency. While this equation is correct, it does not convey all the factors that must be considered in a converter design. It indicates the mass of the tank hardware will change linearly in a direction opposite to the frequency change. This is not entirely true. Other factors such as parasitic reactances in the circuit and hysteresis and eddy current losses must be considered. Depending on the resonant frequency, they may have a strong influence on the converter design.

At low frequencies, parasitic reactances are small and hysteresis and eddy current effects are minor. This allows more common, often lighter weight component types and materials to be employed. Other converter topologies may also be used because the mass increases occurring in the tank hardware of a resonant converter may be unacceptable for low frequency applications. Pulse-width-modulation (PWM) and push-pull topologies may be better. Assuming a designer selects the topology that minimizes mass and considering the effects of frequency and circuit parasitics, chopper mass estimates were generated at several frequencies. These estimates were extrapolated from known designs and they are documented in Appendix A. They were utilized to develop the frequency factors contained in the chopper mass equations. Figure 6 compares the specific weights obtained with these equations for single- and 3-phase designs at 10 and 100 kWe power levels for frequencies ranging from 1 to 50 kHz. Note that the 3-phase design is slightly heavier over the full frequency range due to its higher parts count.

As the resonant frequency rises, the effects of parasitic reactances and hysteresis and eddy current losses become more pronounced and strongly influence the converter design. They will largely offset supposed improvements and cause the design to reach a point where further mass reductions can not be realized by increasing the frequency. The product of power and frequency approaches a constant value. This is the reason the mass of the chopper circuit levels out above 20 kHz and may actually begin to rise at frequencies beyond this point. Since most of the available design information was based on 20 kHz and 40 kHz inversion frequencies, the equations were calibrated to yield good results at these frequencies. The single-phase resonant topology specific weight curves shown in Figure 7 depict the strong influence frequency has on chopper mass and show the specific weight of a chopper approaches a constant value of 0.38 kg/kWe as the frequency and power level rises.

Figure 6

Chopper SPWT vs Frequency
Single- and 3-Phase Designs

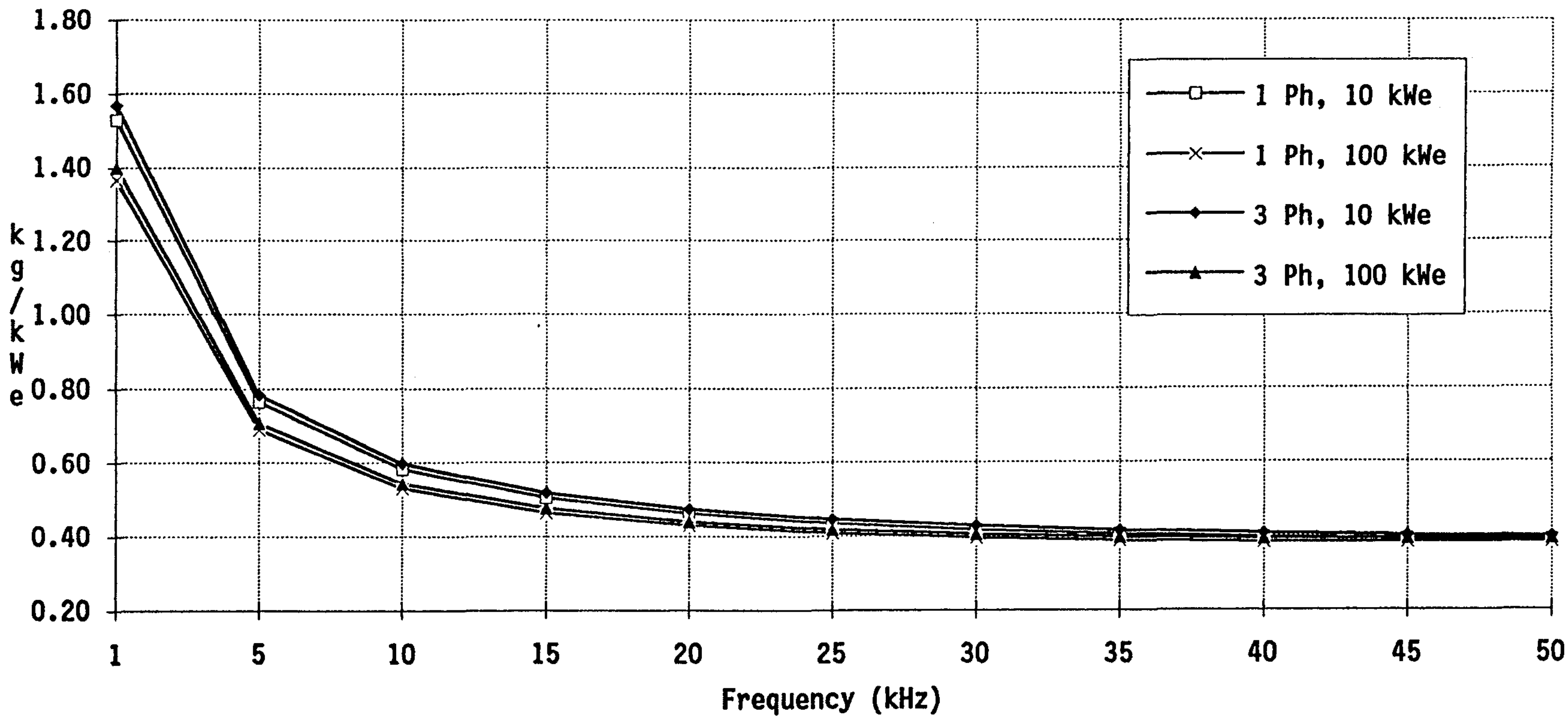

Figure 7

CHOPPER SPWT VS FREQUENCY SINGLE-PHASE DESIGNS

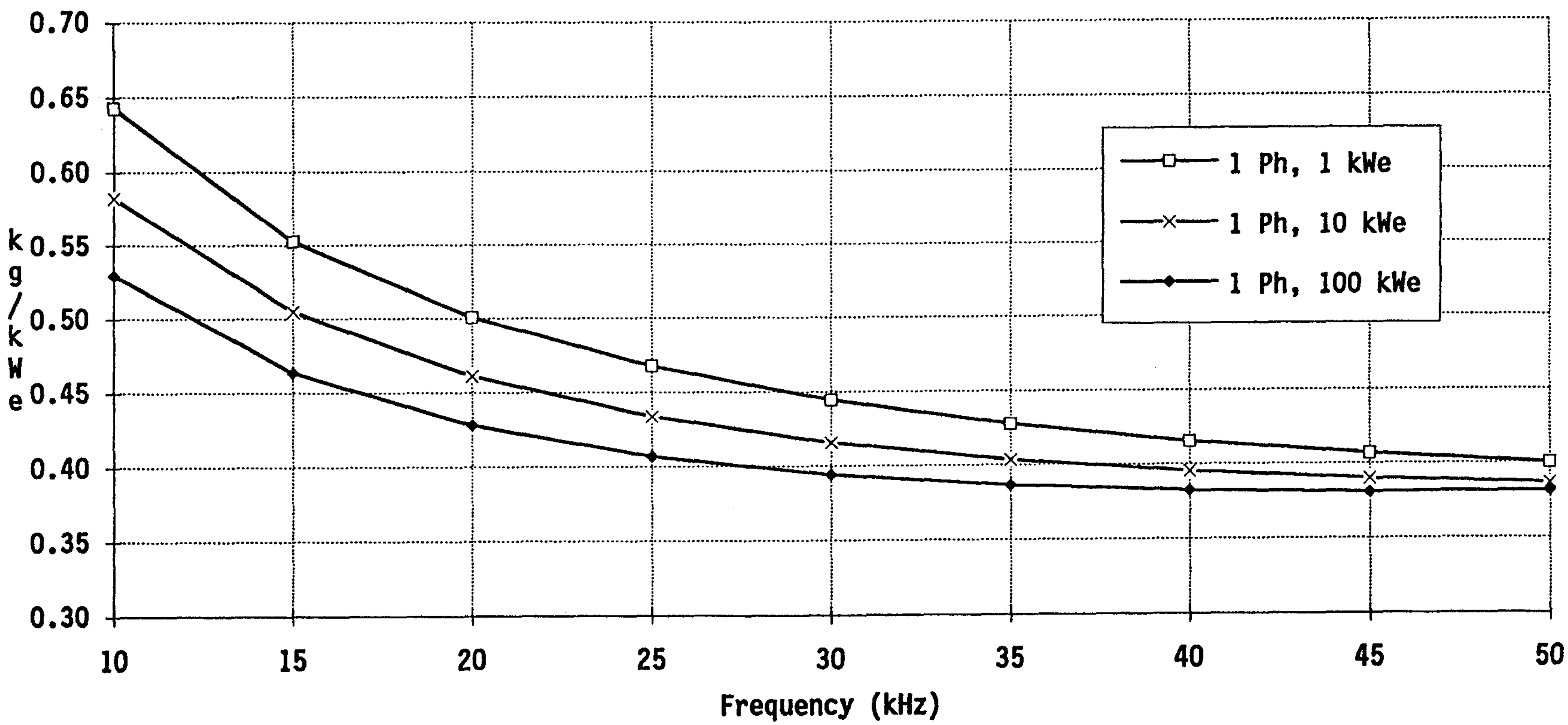

Before leaving this subject, it should be noted that at high power and frequency levels fewer switching devices are available and the sizes of resonant tank elements may become impractical. Therefore, even if there is not any circuit limitation that precludes the use of a high resonant frequency, the availability of suitable parts may force the designer to settle for a lower frequency design. To make higher operating frequencies practical, high power switching devices that exhibit faster switching speeds are currently under development. For example, the 1-2 μsec switching times being projected for MCTs represent a significant improvement in high power switching. Parasitic inductive and capacitive reactances, though, will still drive the resonant frequency downward as power levels rise. The point is: Even though the model will generate a mass estimate for a high power chopper based on a high frequency, one must consider whether the design is really practical. Table 4 is offered as a guide to assist the model user in selecting inversion frequencies appropriate for future component power levels.

Table 4
Resonant Converter Frequency Input Guide

Converter Power Level	Suggested Inversion Frequency Limit
Under 500 Watts	60 kHz
500 to 5000 Watts	50 kHz
5 to 50 kWe	40 kHz
50 to 100 kWe	30 kHz
Greater than 100 kWe	20 kHz

3.1.2 Inverter and Standard Transformer Models

Two types of transformers may be utilized in the lunar base PMAD system depending on the architecture and user needs: inverter transformers that are an integral part of a converter circuit, and standard transformers. These transformers will be significantly different because the operating frequencies, and waveform harmonic content are different for the two applications. For this reason, it was necessary to create two model types to address the characteristics of the two designs. The inverter transformer design will be presented first because it tends to be more involved and cover a wider range of design considerations. The standard transformer discussion will rely heavily on the information and rationale previously presented in the inverter transformer section.

3.1.2.1 Inverter Transformer Stage Model

The inverter transformer stage is contained in the inverter, dc/dc converter and frequency converter models. In an actual power conditioning component, an inverter transformer follows a chopper section. It is used to step up or down the input voltage, and/or to provide isolation between the input and output.

Although transformer design guidelines have been established to deal with most operating requirements; there are many practical design and materials limitations that continue to hinder transformer fabrication. These design difficulties are more pronounced at higher frequencies; consequently, high frequency transformer design techniques require more development. High frequency designs proposed for high power and/or voltage levels are especially complicated. However, established transformer design principles can provide insight into how these problems might be solved and in turn the evolution of transformer design. For this reason, design manuals were frequently referred to to guide the equation development (Ref. III-19, III-20, III-21). The variables that will be used in the inverter transformer stage model discussion are shown in Table 5.

Table 5
Inverter Transformer Model Variable Definitions

1ITSM	Single-Phase Inverter Transformer Stage Mass
3ITSM	3-Phase Inverter Transformer Stage Mass
ITSE	Inverter Transformer Stage Efficiency (99%)
ITSAM	Inverter Transformer Stage Available Modules
ITSRM	Inverter Transformer Stage Required Modules
$\mathbf{ITSP_O}$	Inverter Transformer Stage Power Output (kWe)
$\mathbf{ITSV_I}$	Inverter Transformer Stage Voltage Input (Vrms)
$\mathbf{ITSV_O}$	Inverter Transformer Stage Voltage Output (Vrms)
ITSF	Inverter Transformer Stage Frequency (kHz)

The equations used to estimate the mass of single-phase and 3-phase transformers are shown below. They will be discussed piece by piece to identify the parts that correspond to specific parameters. The subsequent paragraphs will explain the development of the factors and constants contained in these equations. The factor being discussed will be underlined and accompanying graphs will be used to illustrate results and trends determined during this study.

Mass Coefficient

$$1ITSM=\underline{1.27}*((EXP(0.003/(1-ITSE)))/1.35)*(ITSAM/ITSRM)*ITSP_O*((ITSP_O/ITSRM)^{-0.08} *EXP(ITSV_I/200000)*EXP(ITSV_O/200000)*ITSF^{-0.47}+(ITSF/300)^{1.4})$$

$$3ITSM=\underline{2.75}*((EXP(0.003/(1-ITSE)))/1.35)*(ITSAM/ITSRM)*ITSP_O*((ITSP_O/ITSRM)^{-0.25} *EXP(ITSV_I/200000)*EXP(ITSV_O/200000)*ITSF^{-0.47}+(ITSF/300)^{1.4})$$

The constants, "1.27" and "2.75", were determined by calibrating these mass equations against the masses of known inverter transformer designs. They are designed to yield acceptable mass estimates over the ranges specified for each of the input parameters. These constants are largely determined by the wave form factor[3] and are 10% larger than the corresponding constants contained in the standard transformer discussion. Since the chopper rapidly switches a dc input to fabricate an ac output, the inverter transformer input is not a smooth sinusoid and it exhibits many square wave characteristics. Square waves have a high harmonic content; consequently, they generate higher losses in the transformer core. Calculations and design procedures contained in design manuals indicate an inverter transformer core must be sized 10% larger to lower the core flux density and manage the added losses resulting from the square wave harmonics (Ref. III-19, III-20, III-21).

Efficiency Factor

$$1ITSM=1.27*\underline{((EXP(0.003/(1-ITSE)))/1.35)}*(ITSAM/ITSRM)*ITSP_0*((ITSP_0/ITSRM)^{-0.08} *EXP(ITSV_I/200000)*EXP(ITSV_0/200000)*ITSF^{-0.47}+(ITSF/300)^{1.4})$$

$$3ITSM=2.75*\underline{((EXP(0.003/(1-ITSE)))/1.35)}*(ITSAM/ITSRM)*ITSP_0*((ITSP_0/ITSRM)^{-0.25} *EXP(ITSV_I/200000)*EXP(ITSV_0/200000)*ITSF^{-0.47}+(ITSF/300)^{1.4})$$

The factor underlined above is used to estimate the mass effects that will occur when the transformer efficiency is changed. To reduce losses and increase transformer efficiency, the flux density in the core is lowered and the resistance of the windings is reduced. A lower core flux density will reduce core losses; however, Faraday's law shows the core effective cross sectional area must be increased to compensate.

$$E=4B_mA_cNfx10^{-5} \quad \text{(square wave)}$$

Where: E = applied voltage (rms)
4 = square wave form factor
B_m = flux density in gauss
A_c = core effective cross sectional area in cm^2
N = number of primary turns
f = frequency in kHz

This naturally increases core mass. To reduce the winding resistance and losses, the winding conductor area must be increased. This can be seen by referring to the equation used to calculate conductor electrical resistivity.

$$R=\rho l/A$$

Where: R = conductor resistance
ρ = volume resistivity ($\mu\Omega\cdot$cm)
l = length in cm
A = cross sectional area in cm^2

To raise the transformer efficiency from 99% to 99.5%, transformer losses would need to be cut in half. Core loss versus flux density tables contained in transformer design manuals indicated a 25% reduction in flux density would reduce losses 50%. To achieve this the core cross sectional area and associated mass

---

[3] The form factor is the ratio of the root-mean-square value to the average absolute value, averaged over a full period of the waveform.

would increase 33%. To cut the winding losses in half, the conductor area would need to double. This doubles the conductor mass. Summing only these two effects and using a ratio of about 2:1 for winding mass to core mass with a 20 kHz transformer results in a transformer mass increase of about 75%. However, increasing the core size further increases in the conductor mass due to the added length of the turns; and the larger winding size will enlarge the core window. Clearly the core and winding dimensions are interrelated; there are no closed form transformer design equations. After including estimates for these interdependent influences, a mass increase of 85% was obtained. The trends reflected by the resulting efficiency factor are shown in Figure 8 for 10 and 20 kHz frequencies and 10 and 100 kWe transformer power levels.

Redundancy Factor

$$1ITSM=1.27*((EXP(0.003/(1-ITSE)))/1.35)*\underline{(ITSAM/ITSRM)}*ITSP_O*((ITSP_O/ITSRM)^{-0.08}$$
$$*EXP(ITSV_I/200000)*EXP(ITSV_O/200000)*ITSF^{-0.47}+(ITSF/300)^{1.4})$$

$$3ITSM=2.75*((EXP(0.003/(1-ITSE)))/1.35)*\underline{(ITSAM/ITSRM)}*ITSP_O*((ITSP_O/ITSRM)^{-0.25}$$
$$*EXP(ITSV_I/200000)*EXP(ITSV_O/200000)*ITSF^{-0.47}+(ITSF/300)^{1.4})$$

The above factor addresses redundancy mass impacts that occur to enhance reliability. The available modules is the actual number of modules present in the component; the required modules is the actual number of modules required to achieve full output power. An example will illustrate. Assume a design requires 4/3 redundancy to meet the reliability requirements. This means each channel is rated to handle 33% of the power and 4 channels are available. This factor shows a 4/3 redundancy design will be 33% heavier. Only 3 channels are needed to supply full power; the fourth channel represents the mass penalty incurred to enhance reliability.

Power Level Multiplier

$$1ITSM=1.27*((EXP(0.003/(1-ITSE)))/1.35)*(ITSAM/ITSRM)*\underline{ITSP_O}*((ITSP_O/ITSRM)^{-0.08}$$
$$*EXP(ITSV_I/200000)*EXP(ITSV_O/200000)*ITSF^{-0.47}+(ITSF/300)^{1.4})$$

$$3ITSM=2.75*((EXP(0.003/(1-ITSE)))/1.35)*(ITSAM/ITSRM)*\underline{ITSP_O}*((ITSP_O/ITSRM)^{-0.25}$$
$$*EXP(ITSV_I/200000)*EXP(ITSV_O/200000)*ITSF^{-0.47}+(ITSF/300)^{1.4})$$

The equations can be used to calculate either transformer mass or transformer specific weight. When the above multiplier is included, the calculations will yield the transformer mass. To obtain the transformer specific weight, simply remove this multiplier.

Power Level Factor

$$1ITSM=1.27*((EXP(0.003/(1-ITSE)))/1.35)*(ITSAM/ITSRM)*ITSP_O*\underline{((ITSP_O/ITSRM)^{-0.08}}$$
$$*EXP(ITSV_I/200000)*EXP(ITSV_O/200000)*ITSF^{-0.47}+(ITSF/300)^{1.4})$$

$$3ITSM=2.75*((EXP(0.003/(1-ITSE)))/1.35)*(ITSAM/ITSRM)*ITSP_O*\underline{((ITSP_O/ITSRM)^{-0.25}}$$
$$*EXP(ITSV_I/200000)*EXP(ITSV_O/200000)*ITSF^{-0.47}+(ITSF/300)^{1.4})$$

Figure 8

INVERTER TRANSFORMER SPWT VS EFFICIENCY

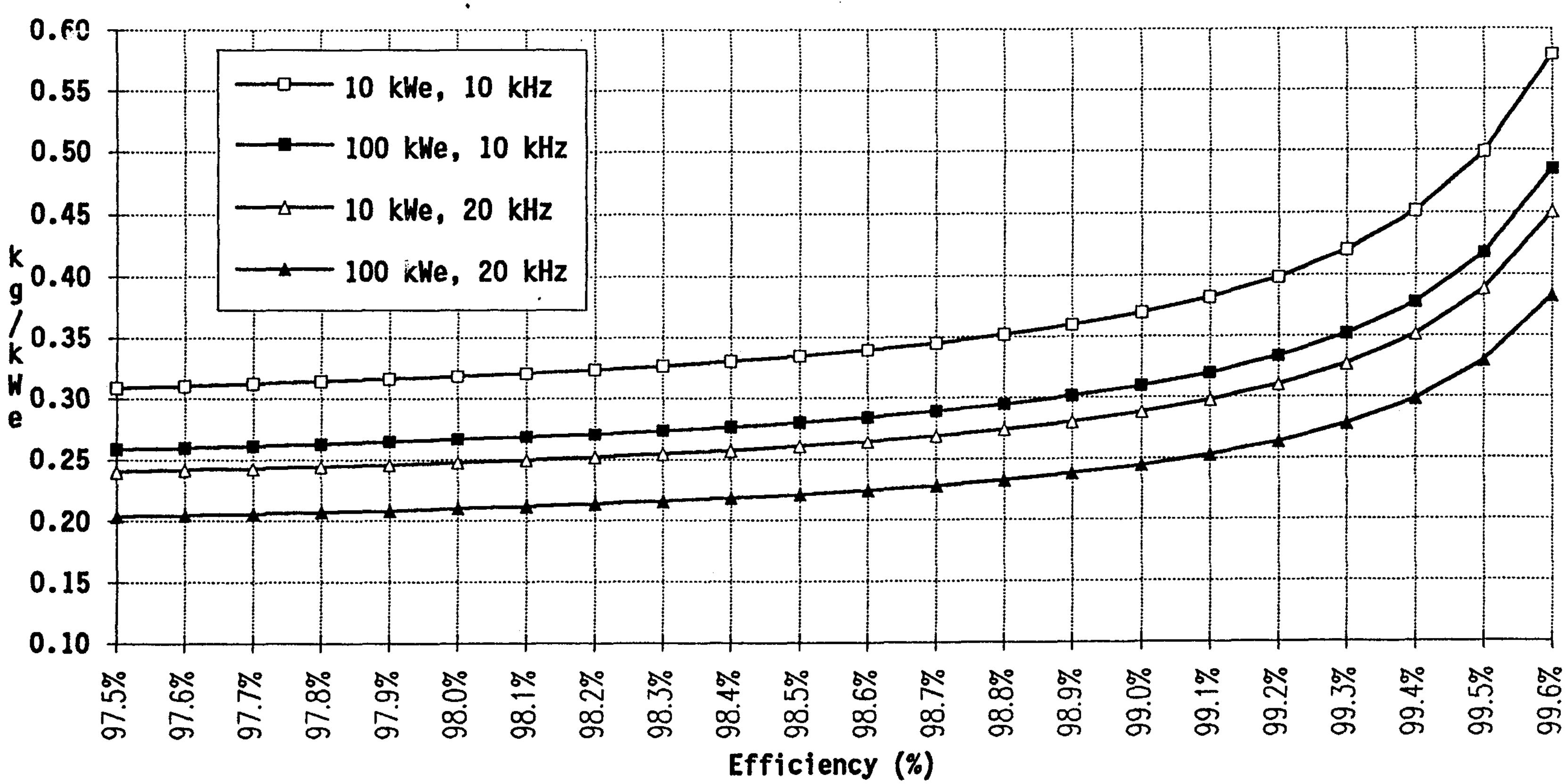

XFMRGRPH.XLS 6/26/91

As transformer size increases, the core can be better utilized, and the current density increased in the windings to reduce their cross sectional area. These economies of scale result in a transformer specific weight reduction at higher power levels. The "Standard Handbook for Electrical Engineers" indicated the specific weight of a 3-phase transformer would decline by the 0.25 power with power level (Ref. III-22). This was verified for 60 Hz transformers by referring to the transformer masses contained in a vendor catalogue (Ref. III-23). This factor was also assumed to hold for high frequency 3-phase transformer designs, although there was not any mass information available to confirm it. The same vendor catalogue showed the specific weight of a low frequency single-phase transformer would decline by the 0.08 power with power level. Mass figures obtained from another source indicated this factor also held true for high frequency single-phase transformer designs (Ref. III-19). The specific weights of single- and 3-phase transformer designs are compared in Figure 9. This figure shows that a 1 kHz single-phase transformer will weigh less than a 3-phase one until a power level of about 100 kWe is reached. This value was projected from information contained in a vendor catalogue and a transformer design handbook (Ref. III-23, III-24). It was estimated that the mass cross over point for higher frequency single- and 3-phase transformers occurs at a higher power level. The mass gains achievable with a change from a single- to 3-phase design occur mainly in the core. These gains are expected to be less at higher frequencies because the core mass occupies a smaller percentage of the transformer mass. With this assumption incorporated into the equations, Figure 9 shows that a single-phase 20 kHz transformer design is more weight efficient below 250 kWe. Figure 10 shows only single-phase transformer designs and allows specific weight comparisons at several frequencies over a wide power range. Figure 11 also depicts single-phase designs, but it concentrates on the power levels and frequencies expected to be used most often in inverter transformer designs.

The total power level is divided by the required number of modules. A modular design consists of several modules, each designed to only process a percentage of the total assembly output power. The specific weight of each transformer must be calculated at the power level of the individual module and not the complete assembly power level.

Voltage Level Factors

$$1ITSM=1.27*((EXP(0.003/(1-ITSE)))/1.35)*(ITSAM/ITSRM)*ITSP_O*((ITSP_O/ITSRM)^{-0.08} *\underline{EXP(ITSV_I/200000)}*\underline{EXP(ITSV_O/200000)}*ITSF^{-0.47}+(ITSF/300)^{1.4})$$

$$3ITSM=2.75*((EXP(0.003/(1-ITSE)))/1.35)*(ITSAM/ITSRM)*ITSP_O*((ITSP_O/ITSRM)^{-0.25} *\underline{EXP(ITSV_I/200000)}*\underline{EXP(ITSV_O/200000)}*ITSF^{-0.47}+(ITSF/300)^{1.4})$$

The voltage factor development had to consider two viewpoints, the influence of insulation stress on transformer mass as voltage rises, and high voltage transformer design limitations occurring as frequency rises. Only the insulation stress effects will be addressed initially. It is mainly the volts per turn not the terminal voltage that determines the stress placed on the insulation and consequently its thickness. The thickness of the insulation can be calculated from its dielectric strength, usually expressed in volts per mil. For typical operating ranges, the dielectric strength of most insulating materials is reasonably constant regardless of the transformer frequency. This information indicates the voltage mass effects occurring at low frequency also apply at higher frequencies.

Figure 9

INVERTER TRANSFORMER SPWT
1-PHASE VS 3-PHASE

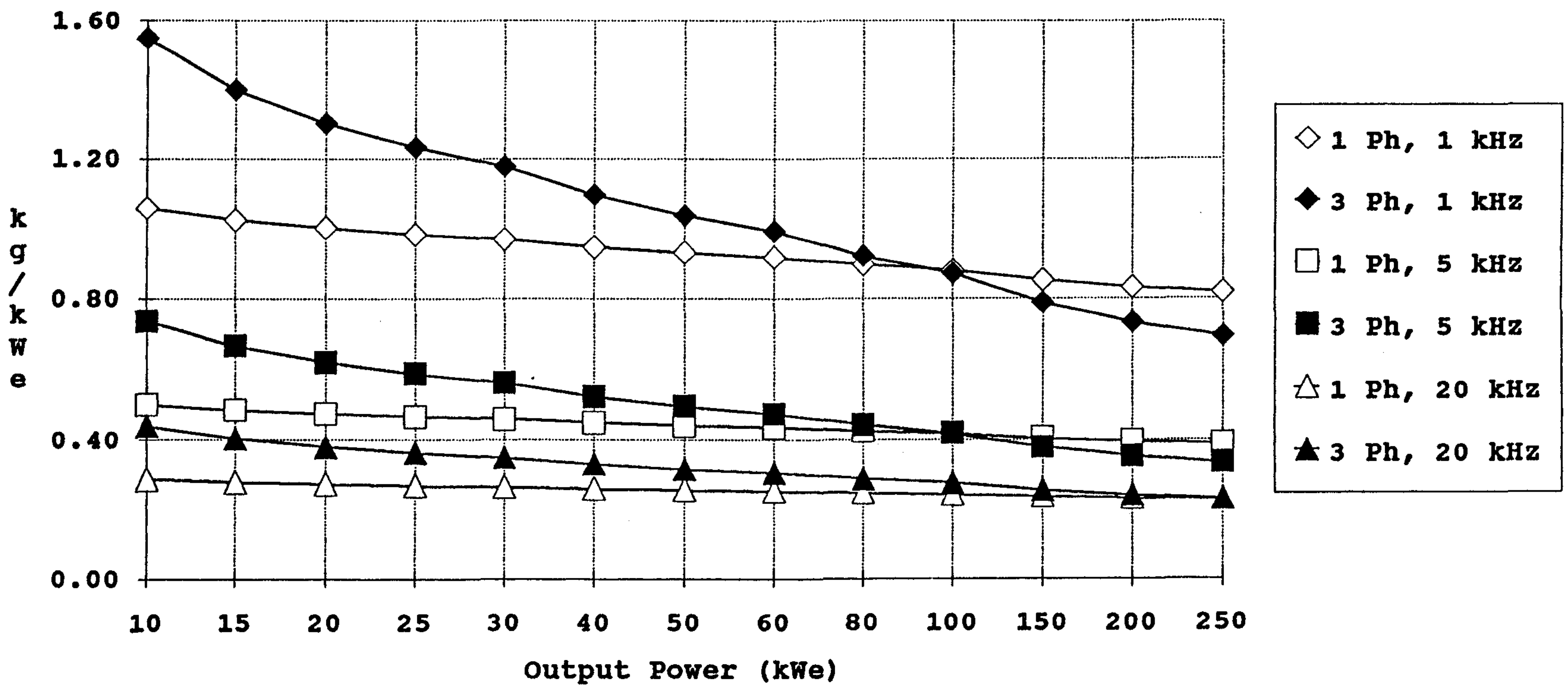

Figure 10

INVERTER TRANSFORMER SPWT VS POWER

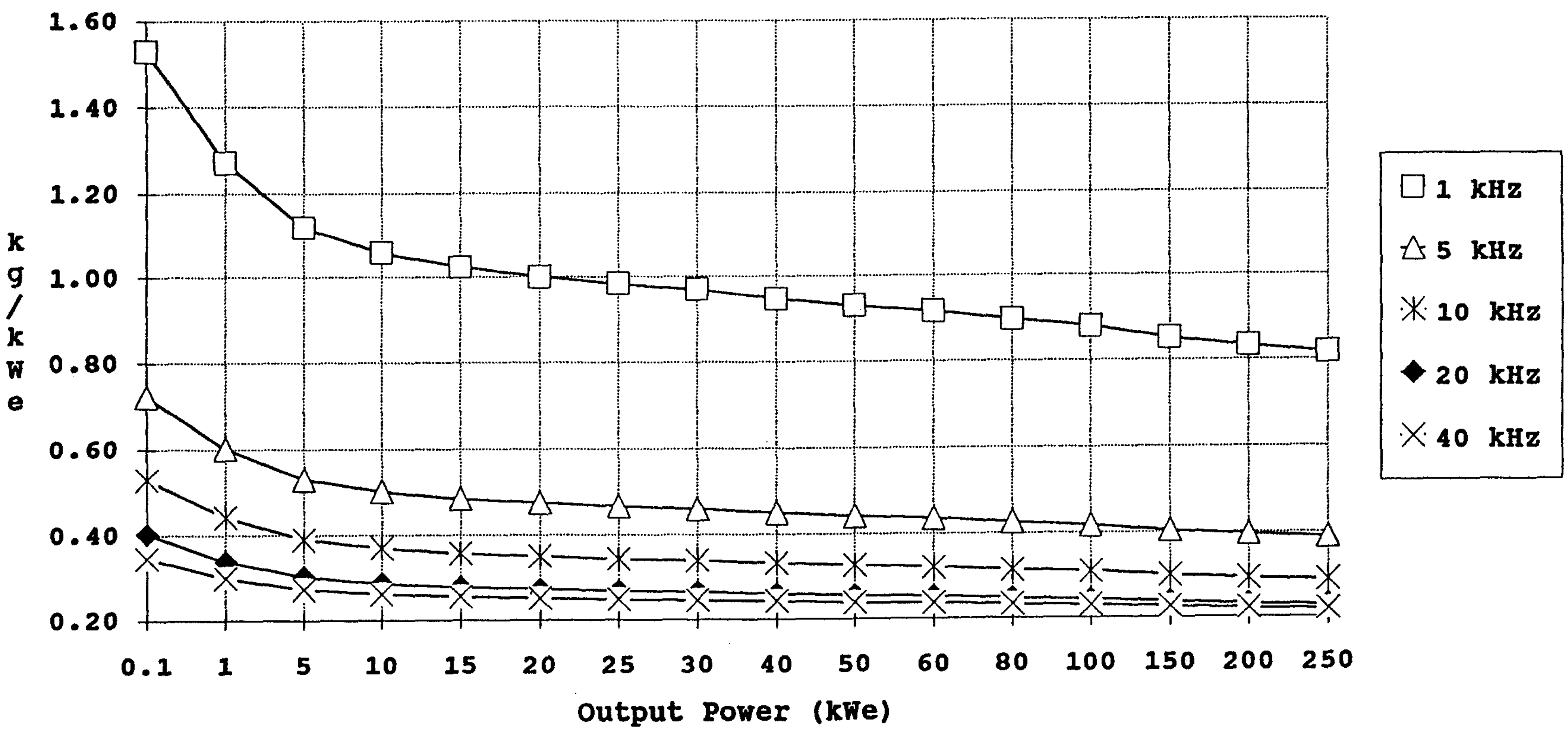

XFMRPF2.XLC

Figure 11
Inverter Transformer SPWT vs Power

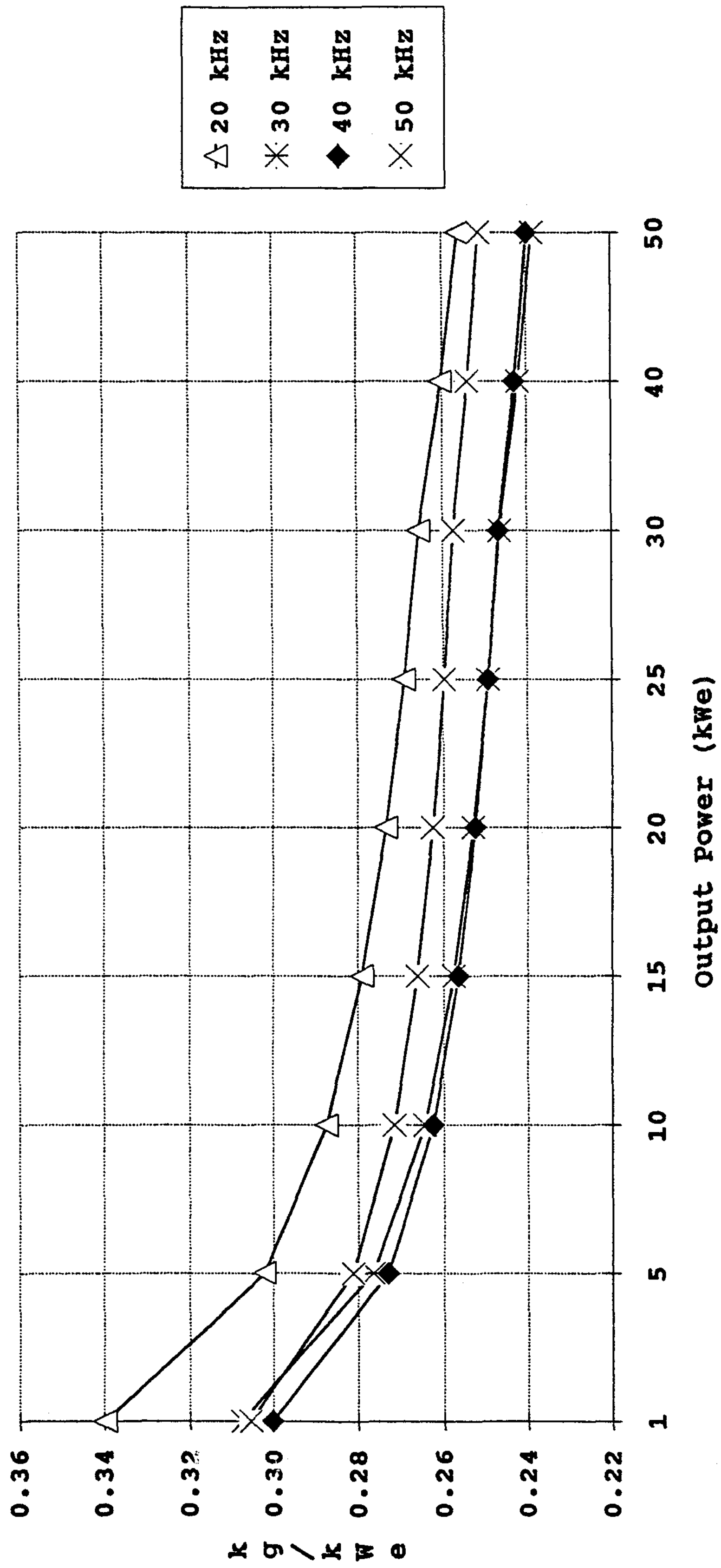

XFMRGRPH.XLS

4/25/91

This observation is important since the information on high voltage transformers is limited to low frequency designs. Low frequency, commercial transformer data showed transformer specific weight rose slowly until voltage levels approached 20 kV. This is well above the 10 kV voltage level expected to be used for the lunar base. The minor increase in specific weight was attributed to the additional insulation needed to prevent insulation breakdown between windings, and the need for high voltage terminations. This added winding insulation will increase the winding cross sectional area and necessitate a slightly larger core window area. However, the impact is minor. In addition, the insulation mass is a very small percentage of the total transformer mass, so it can increase substantially and the transformer mass will only change slightly. The information obtained from this analysis was sufficient to develop a transformer voltage factor, but it was not enough to know how to properly apply it. The voltage factor determined at this point is shown for different transformer power levels in Figure 12. It shows transformer mass will only rise about 5% when the primary or secondary voltage is increased from 20 to 10,000 Vrms.

It was previously stated that the volts per turn determined the insulation thickness and that the dielectric strength of an insulating material is basically independent of frequency. However, frequency does influence the calculated volts per turn and this ultimately impacts the voltage characteristics of the complete transformer. Referring back to Faraday's law and rearranging the terms, one can see that the volts per turn is a function of frequency.

$$E/N = f(K, B_m, A_c, f)$$

Where: E = applied voltage (rms)
K = form factor constant
B_m = flux density
A_c = core effective cross sectional area
N = number of primary turns
f = frequency

Because of nonlinearities in transformer design, particularly in core material characteristics, the product of core cross sectional area and flux density can not be linearly changed to accomodate an increasing frequency. This situation indicates a designer will encounter voltage restraints as frequency rises. To verify this conclusion, a transformer design analysis was conducted and transformer point designs were evaluated. They showed that the volts per turn will increase significantly when moving from 60 Hz to 20 kHz, possibly enough to increase the insulation level on the turns. Thicker insulation will lead to greater separation distances between the primary and secondary windings, and reduce transformer coupling. This results in higher leakage flux. Because leakage flux increases if additional winding insulation is needed and the effects attributable to turn-to-turn capacitance rise with frequency, a high frequency transformer tends to have more reactance. High voltage transformers have more turns, which increases the total turn-to-turn or winding capacitance. Although these effects are compounding, they probably are not enough to preclude the design of a high voltage, high frequency transformer; however, they do complicate its design and emphasize the need to minimize turn-to-turn capacitance.

It was already mentioned that a high voltage transformer has a higher winding capacitance; and transformer coupling is poorer if thicker winding insulation is required. Leakage inductance also rises as the distance between the windings

Figure 12

INVERTER TRANSFORMER SPWT VS VOLTAGE

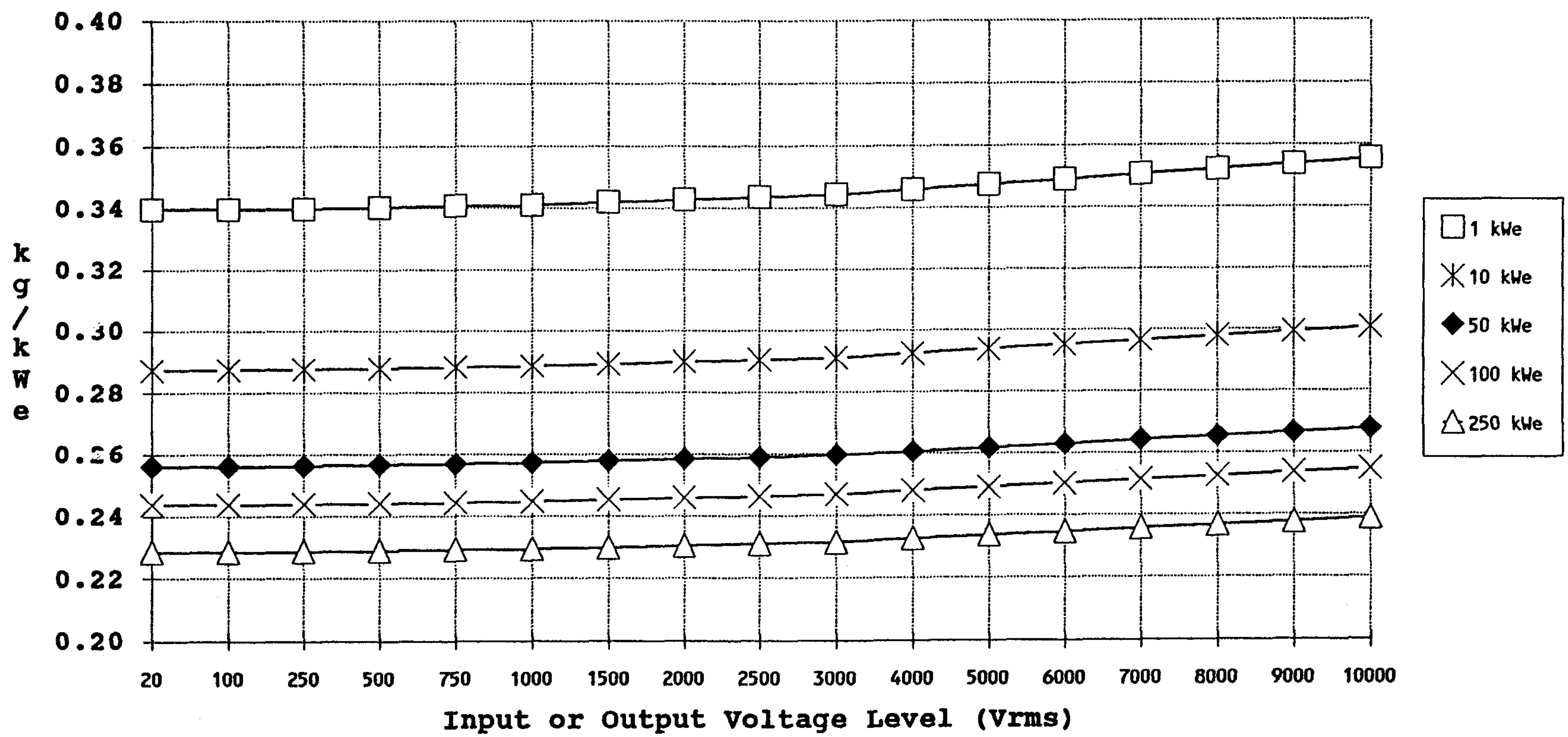

increases. To maximize transformer coupling and minimize leakage inductance, the primary and secondary windings must be in close proximity. However, this is difficult to accomplish in a transformer that has a high voltage ratio because thick insulation levels are required to prevent primary to secondary voltage breakdown. Most loads require a relatively low voltage; therefore, the voltage will need to be stepped down further in a system that uses high voltage transmission. This forces the distribution transformers to utilize higher voltage ratios and leads to higher leakage inductance.

Oscillations in the power system, a phenomenon known as ringing, may result from the leakage capacitance and inductance present in high voltage transformers. Ringing occurs because the parasitic capacitive and inductive reactances transfer energy back and forth during operation and after turn off until it is damped out by element resistances. This increases transformer losses and may lead to damage if high voltage spikes result. Ringing is frequency related because the effects attributable to parasitic capacitive and inductive reactances grow as frequency rises. Power may also be a factor because it may be more difficult to limit stray capacitance and inductance due to fabrication constraints resulting from the transformer's larger physical size.

Ringing limits the acceptable voltage ratio of the transformer. In a discussion with John Beiss, he indicated the step ratio of a present 20 kHz transformer is probably limited to about 6 or 7 due to ringing. However, a transformer design generated by Space Power Incorporated exhibited a voltage ratio of 10, 180 divided by 18 Vrms. Its demonstrated efficiency of 98.2% indicates this step ratio is feasible, although it will be harder to achieve good operating characteristics at higher voltages. Commercial transformer data indicates a step ratio of 145 is obtainable with a 60 Hz transformer. Using these two values, an empirical relationship was developed to estimate reasonable step ratios for transformers at several different frequencies. This relationship is shown below and it was used to generate the values shown in Table 6. This table is only offered as a guide; its main intent is to point out the need to include step ratio effects when evaluating a high voltage power transmission design. It shows that it may be necessary to connect transformers in series to utilize a high voltage transmission system with input or output components that require fairly low voltages, especially if high frequency distribution is employed.

$$SR=39.7*f^{-0.46}$$

Where: SR = acceptable step ratio
f = frequency in kHz

Table 6
Transformer Step Ratio Guidelines

Transformer Frequency (kHz)	Suggested Step Ratio Limit
0.060	145
0.070	135
0.400	60
1	40
5	19
10	14
15	11
20	10
25	9
30	8
35	8
40	7
45	7
50	7

Frequency Factors

$$1ITSM=1.27*((EXP(0.003/(1-ITSE)))/1.35)*(ITSAM/ITSRM)*ITSP_O*((ITSP_O/ITSRM)^{-0.08} *EXP(ITSV_I/200000)*EXP(ITSV_O/200000)*\underline{ITSF^{-0.47}+(ITSF/300)^{1.4}})$$

$$3ITSM=2.75*((EXP(0.003/(1-ITSE)))/1.35)*(ITSAM/ITSRM)*ITSP_O*((ITSP_O/ITSRM)^{-0.25} *EXP(ITSV_I/200000)*EXP(ITSV_O/200000)*\underline{ITSF^{-0.47}+(ITSF/300)^{1.4}})$$

Transformer core mass declines with increasing frequency. Faraday's law shows the flux density required to generate a voltage is lower at a higher frequency. Because the flux density is lower, the transformer core volume and mass are reduced. Winding mass also declines because the mean length of the turns is less. However, core mass does not decrease linearly with frequency as Faraday's law appears to indicate. Alternate core materials must be employed at higher frequencies to hold down losses. While these materials are more efficient, they must be operated at lower flux densities. For transformer operating frequencies ranging from 10 to 60 kHz, the selected core materials might progress from 50-50 Ni-Fe, to Permalloy, to Supermalloy, to Metglas. For this materials progression, the operating flux density will roughly decline from about 10,000 to 2,000 Gauss.

In addition to material limitations, other factors must be addressed during a transformer design. Thermal management considerations may limit how much the core size can be reduced. The surface area of a transformer must be sufficient to conduct away generated heat. At very high frequencies, roughly above 50 kHz, another set of effects begins to dictate the size of a power transformer core. The eddy current and hysteresis losses become high enough to actually drive the core volume and mass upward. Hence the optimum inverter transformer frequency typically lies between 20 and 40 kHz. At high power levels, 50 kWe and above for example, the preferred frequency is probably near 20 kHz. For power levels below about 5 kWe, the optimum frequency is most likely near 40 kHz.

To determine how transformer mass declines as frequency is increased, inverter transformer mass estimates were examined at 1, 2, 5, 10, 20, 40, and 60 kHz (Ref. III-6, III-19, III-25). Based on these designs, the mass gains occurring as frequency is increased are shown in Figure 13 for several power levels. Figure 14 concentrates on the frequencies envisioned to be used for most lunar base inverter transformer designs. It shows the optimum design frequency shifts downward as the transformer power level rises. This reflects a feature that has been incorporated into the transformer mass equations.

3.1.2.2 Standard Transformer Stage Model

The standard transformer stage will be contained in the transformer, and transformer/rectifier models. Standard ac transformers will be used in ac power transmission systems primarily at the user end to step down a high transmission voltage to a level suitable for secondary distribution. Standard ac transformers may also follow an alternator or inverter output in certain cases. However, this will not be as common because alternators can provide nearly any voltage desired and inverters and frequency converters will probably contain their own integral inverter transformer stage. Transformers following an alternator will experience frequencies less than 5 kHz. If the system utilizes inverters or frequency converters to change the characteristics of the power source, the transformers will probably be designed for frequencies between 10 and 20 kHz. The type of ac waveform encountered should be a smooth sinusoid with a low harmonic content. A pure sinusoid minimizes transformer core losses because the added eddy current and hysteresis losses resulting from high frequency harmonics are not present.

Because a fine transformer design manual existed, especially for low frequency transformer designs, it was frequently referred to to assist in the equation development (Ref. III-24). The variables used in the standard transformer stage model discussion are shown in Table 7.

Figure 13
INVERTER TRANSFORMER SPWT VS FREQUENCY

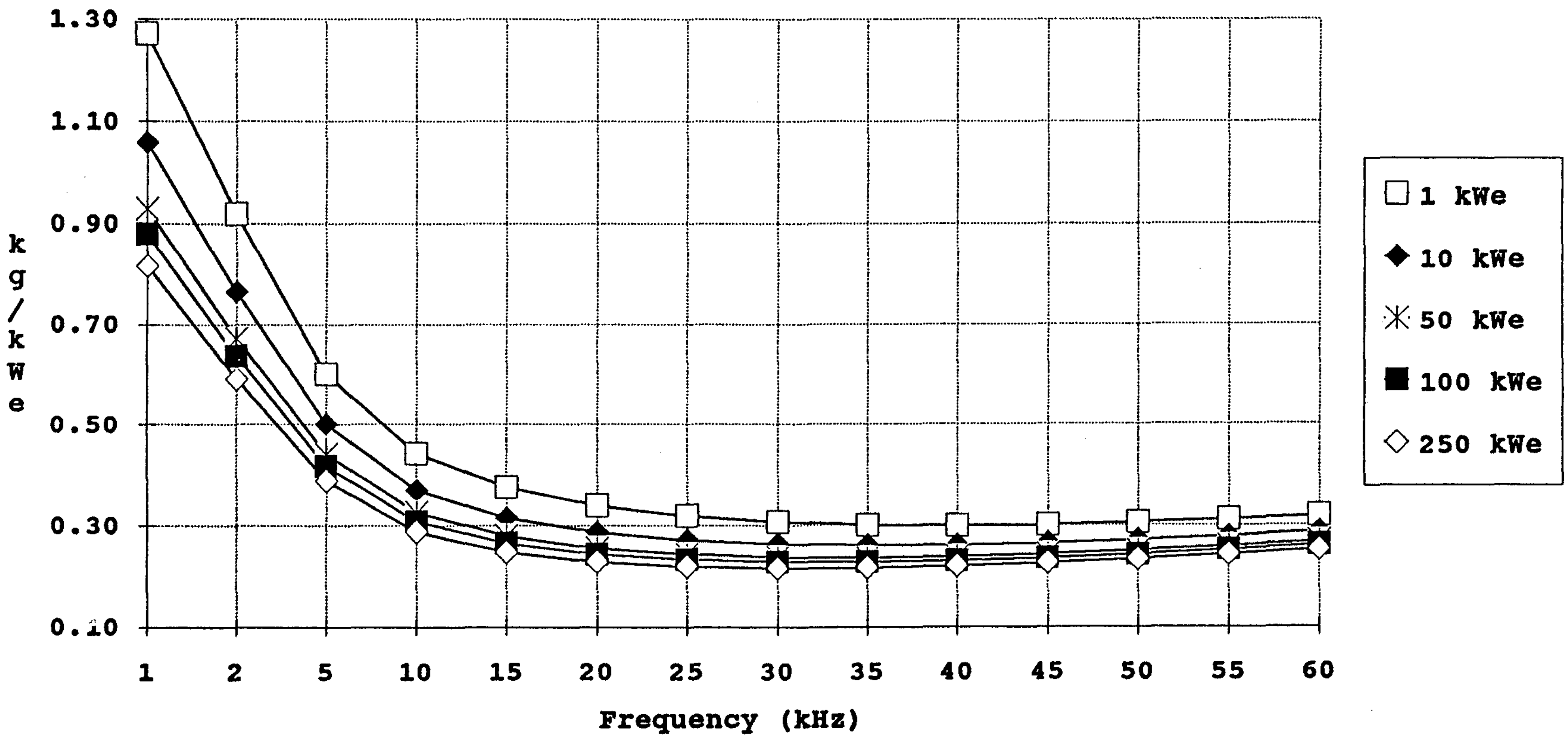

Figure 14
Inverter Transformer SPWT vs Frequency

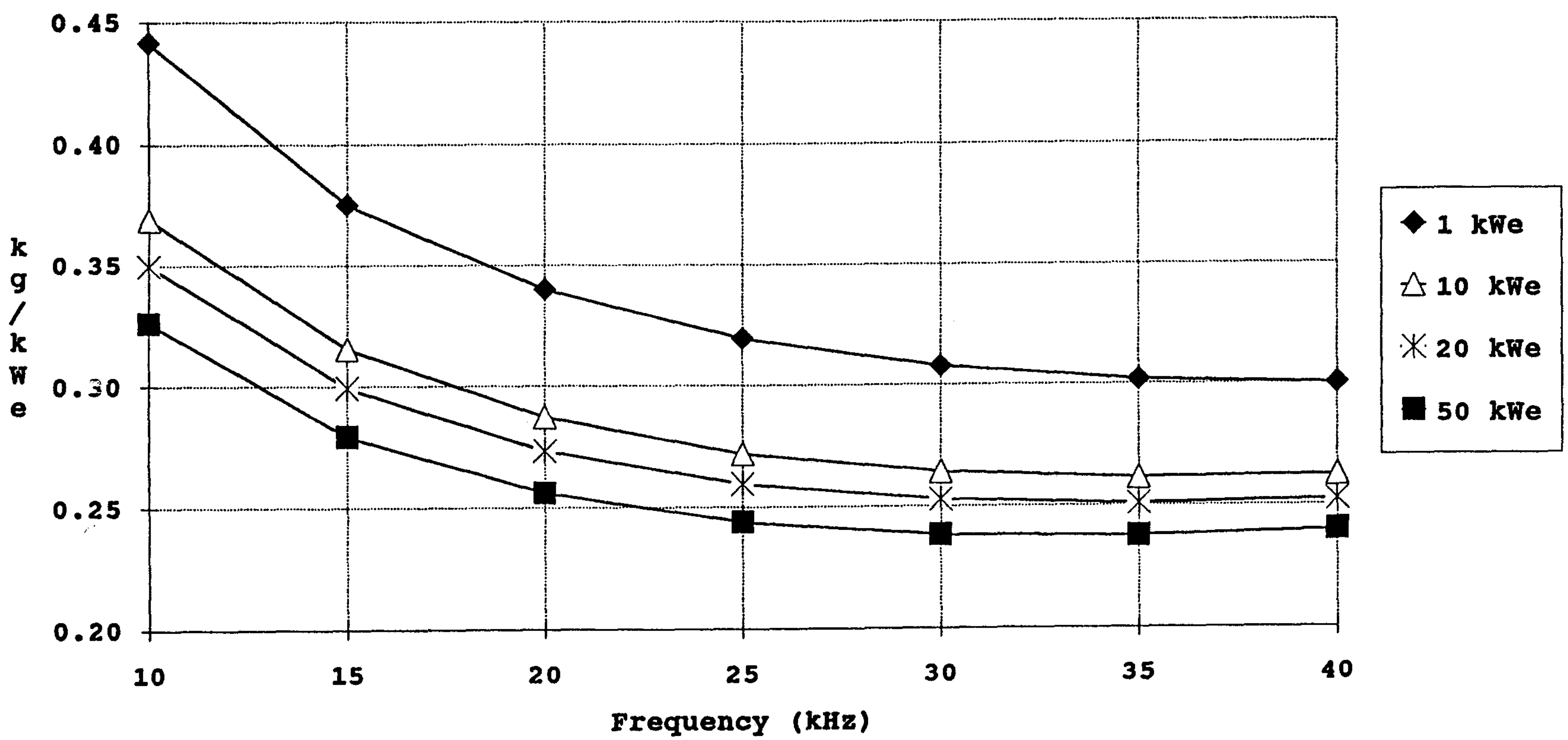

Table 7
Standard Transformer Model Variable Definitions

1STSM	Single-Phase Standard Transformer Stage Mass
3STSM	3-Phase Standard Transformer Stage Mass
STSE	Standard Transformer Stage Efficiency (98%)
STSAM	Standard Transformer Stage Available Modules
STSRM	Standard Transformer Stage Required Modules
$STSP_O$	Standard Transformer Stage Power Output (kWe)
$STSV_I$	Standard Transformer Stage Voltage Input (Vrms)
$STSV_O$	Standard Transformer Stage Voltage Output (Vrms)
STSF	Standard Transformer Stage Frequency (kHz)

The equations used to estimate the mass of single-phase and 3-phase standard transformers are shown below. Only the mass coefficient will be discussed here since the rest of the factors are identical to those contained in the section on inverter transformers. To see how the specific weight or mass of a standard transformer changes with efficiency, power level, voltage, and frequency refer to the graphs contained in the inverter transformer section and subtract 10% from each value. The shape of the curves will be identical for both designs, the standard transformer curves are simply shifted downward a slight amount.

Mass Coefficient

$$1STSM=\underline{1.15}*((EXP(0.003/(1-STSE)))/1.35)*(STSAM/STSRM)*STSP_O*((STSP_O/STSRM)^{-0.08} *EXP(STSV_I/200000)*EXP(STSV_O/200000)*STSF^{-0.47}+(STSF/300)^{1.4})$$

$$3STSM=\underline{2.5}*((EXP(0.003/(1-STSE)))/1.35)*(STSAM/STSRM)*STSP_O*((STSP_O/STSRM)^{-0.25} *EXP(STSV_I/200000)*EXP(STSV_O/200000)*STSF^{-0.47}+(STSF/300)^{1.4})$$

The constants, "1.15" and "2.5", were determined by calibrating these mass equations against the masses of standard transformer designs--minus their enclosures--contained in vendor catalogues (Ref. III-23). Initially, an individual might feel the mass of a terrestrial transformer would be heavier than a space-based transformer. However, the masses of low frequency commercial and space-based transformers were felt to be comparable. Most of the transformer mass is concentrated in the transformer core and windings, and this will be nearly equivalent in both designs. Because the space-based transformer mounting hardware needs to be stronger than similar earth-based mounting hardware to withstand the launch environment, the mass reductions possible by using alternate materials and space type packaging approaches will be largely offset. Terrestrial transformers mainly rely on convection for cooling, a space-based unit must include thermal management hardware and use conduction. Finally, the enclosure mass is calculated by a separate algorithm and not included in this equation.

These constants are designed to produce reasonably accurate mass estimates for the specified input parameters contained in the component models. They are 10% less than those shown in the inverter transformer section because the wave form factors of the power inputs differ. The waveform encountered by a standard transformer is a smooth sinusoid with a low harmonic content. A pure sinusoid minimizes transformer core losses because the added eddy current and hysteresis losses resulting from high frequency harmonics are not present. The square wave input of an inverter transformer has a high harmonic content; consequently, it generates higher losses in the transformer core. The design equations contained in design manuals indicate a standard transformer core can be 10% smaller due to these improved waveform characteristics. (Ref. III-19, III-20, III-21).

3.1.3 Rectifier Stage Model

The rectifier stage converts ac into dc. It is contained in the rectifier, transformer/rectifier, dc/dc converter, and frequency converter models. Two basic operating types of rectifiers are available, diode and switching. The diode rectifier is a static device that simply converts ac into dc. The switching rectifier is essentially a simplified chopper operating in reverse. Since it uses active switching devices such as SCRs or MOSFETs it can regulate the output voltage. SCRs accomplish this by adjusting the commutation angle, the point at which the switch is turned on to allow conduction. MOSFETs typically use PWM techniques. The equations presented in this section are only valid for diode rectifiers, equations should be developed for switching rectifiers in subsequent tasks. The rectifier stage equations presented here are only intended to provide rough mass estimates to facilitate component comparisons. For more accurate mass estimates, specific designs should be generated by a circuit designer.

The rectification stage consists of a diode network. Mass breakdowns for a present and projected diode capable of handling 1 kWe are shown in Table 8. Note that this breakdown is similar to the previous switch module breakdown contained in the chopper section. The main differences are: the snubber circuitry, gate drive circuitry, and switch control logic have been removed since diodes are not active switching devices; and the mass of the packaging and mounting hardware has been adjusted downward because there are fewer parts. Present mass values were estimated from briefing packages prepared by Rocketdyne, Ford Aerospace, and TRW in support of SSF (Ref. III-6, III-7, III-8). Projected mass improvements were obtained from articles on future power conditioning component developments (Ref. III-4, III-10).

Table 8
1 kWe Diode Module Mass Breakdown

Hardware Element	Present Mass (grams)	Projected Mass (grams)
Active Switch Element	7	5
Heat Sink, Thermal Management	48	35
Packaging and Mounting	20	15
Total Switch Module	75	55

Two full wave rectifier configurations are available, a center-tapped full-wave rectifier, or a bridge rectifier circuit. The center-tapped rectifier construction is simpler, but bridge rectifiers appear to be more attractive for high voltage applications because the peak inverse voltage imposed across each diode is half the center-tapped case. Bridge rectifiers also make better use of transformers. A center-tapped rectifier requires two 1 kWe diodes, each weighing 55 grams; a bridge rectifier uses four 500 watt diodes, each weighing 28 grams. The total mass in each case is 110 grams. Based on this analysis, the total mass of a future 1 kWe rectifier is projected to be about 110 grams.

The subsequent paragraphs will explain the development of the single-phase and 3-phase rectifier stage equations in detail. These sections will use the format presented earlier in the chopper stage discussion since the items are comparable in many respects. The variables that will be used during this discussion are shown in Table 9. Rectifier mass breakdown tables are located in Appendix A on page A-3.

Table 9
Rectifier Stage Model Variable Definitions

1RSM	Single-Phase Rectifier Stage Mass
3RSM	Three-Phase Rectifier Stage Mass
RSE	Rectifier Stage Efficiency (98.5%)
RSAM	Rectifier Stage Available Modules
RSRM	Rectifier Stage Required Modules
RSP_O	Rectifier Stage Power Output (kWe)
RSV_I	Rectifier Stage Voltage Input (Vrms)

Mass Coefficient

$$1RSM=\underline{0.1}*((EXP(0.005/(1-RSE)))/1.4)*(RSAM/RSRM)*RSP_O*(RSV_I/(RSV_I-2))^6 *EXP(RSV_I/80000)$$

$$3RSM=\underline{0.11}*((EXP(0.005/(1-RSE)))/1.4)*(RSAM/RSRM)*RSP_O*(RSV_I/(RSV_I-2))^6 *EXP(RSV_I/80000)$$

To calculate an appropriate value for the rectifier stage mass coefficients, the equations were calibrated to yield values consistent with the above 1 kWe mass breakdown and actual component designs (Ref. III-6, III-7).

The diodes comprising three single-phase full wave rectifiers are interconnected to form a 3-phase full wave rectifier. Six diodes are required and each processes a third of the power. The 3-phase rectifier design was judged to be slightly heavier because of the added number of diodes. This would probably enlarge the mounting area and increase the interconnecting wiring weight. Figure 15 compares the specific weights of single- and 3-phase rectifiers.

Efficiency Factor

$$1RSM=0.1*\underline{((EXP(0.005/(1-RSE)))/1.4)}*(RSAM/RSRM)*RSP_O*(RSV_I/(RSV_I-2))^6$$
$$*EXP(RSV_I/80000)$$

$$3RSM=0.11*\underline{((EXP(0.005/(1-RSE)))/1.4)}*(RSAM/RSRM)*RSP_O*(RSV_I/(RSV_I-2))^6$$
$$*EXP(RSV_I/80000)$$

The factor underlined above estimates the specific weight values associated with a range of rectifier efficiencies. Within reason, the interconnecting wiring and the diode conduction losses can be reduced by increasing the size of the wiring and the diode die area. An improved efficiency allows a reduction in the heat sink mass. The effect of power losses on individual elements within a diode module were assessed to develop rectifier mass estimates for efficiencies ranging from 97.5 to 99.5%. From this analysis, an efficiency factor was calculated and incorporated into the rectifier mass equation. Figure 16 shows a graph of the resulting specific weight versus efficiency values that were developed with this approach. Note that the depicted rectifier efficiency range is relatively narrow. Rectifier efficiencies higher than about 99.5% are not considered practical due to diode fabrication limitations. Lower efficiencies are undesirable because of the additional radiator mass. Because silicon diodes require a forward bias voltage of about 0.7 V before they will conduct, their efficiency is considerably less at lower operating voltages. This will be addressed later in the section on voltage factors.

Redundancy Factor

$$1RSM=0.1*((EXP(0.005/(1-RSE)))/1.4)*\underline{(RSAM/RSRM)}*RSP_O*(RSV_I/(RSV_I-2))^6$$
$$*EXP(RSV_I/80000)$$

$$3RSM=0.11*((EXP(0.005/(1-RSE)))/1.4)*\underline{(RSAM/RSRM)}*RSP_O*(RSV_I/(RSV_I-2))^6$$
$$*EXP(RSV_I/80000)$$

The above factor computes the redundancy mass impacts occurring when a modular design approach is used to improve reliability. The "available modules" number is the actual number of modules present in the component; the "required modules" value is the actual number of modules required to achieve full output power. If a design requires 4/3 redundancy to meet the reliability requirements, each channel will be rated to carry 33% of the power. 4 channels are available, but only 3 channels are needed to supply full power. The mass of the fourth channel is the penalty paid to obtain a higher reliability.

Power Level Multiplier

$$1RSM=0.1*((EXP(0.005/(1-RSE)))/1.4)*(RSAM/RSRM)*\underline{RSP_O}*(RSV_I/(RSV_I-2))^6$$
$$*EXP(RSV_I/80000)$$

Figure 15

Rectifier SPWT
1-Phase vs 3-Phase

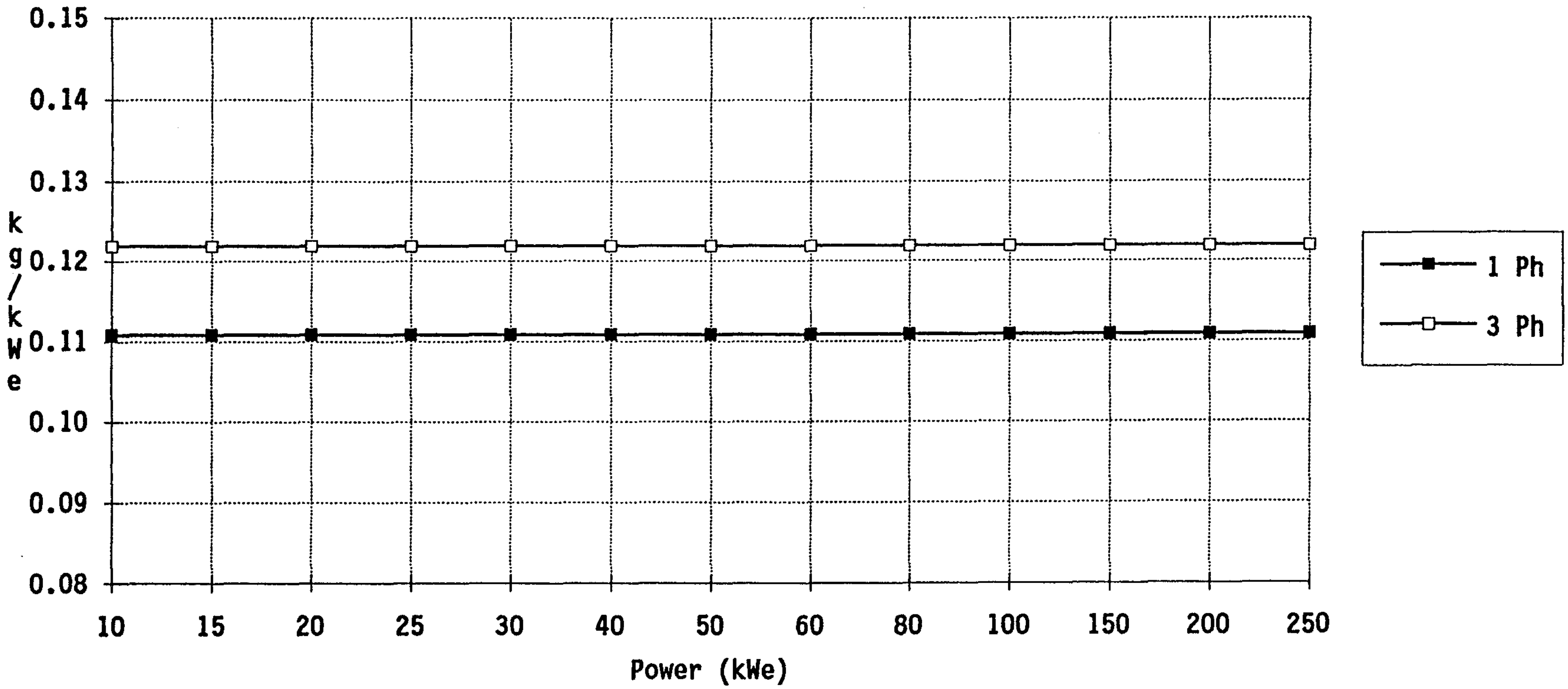

Figure 16

Rectifier SPWT vs Efficiency

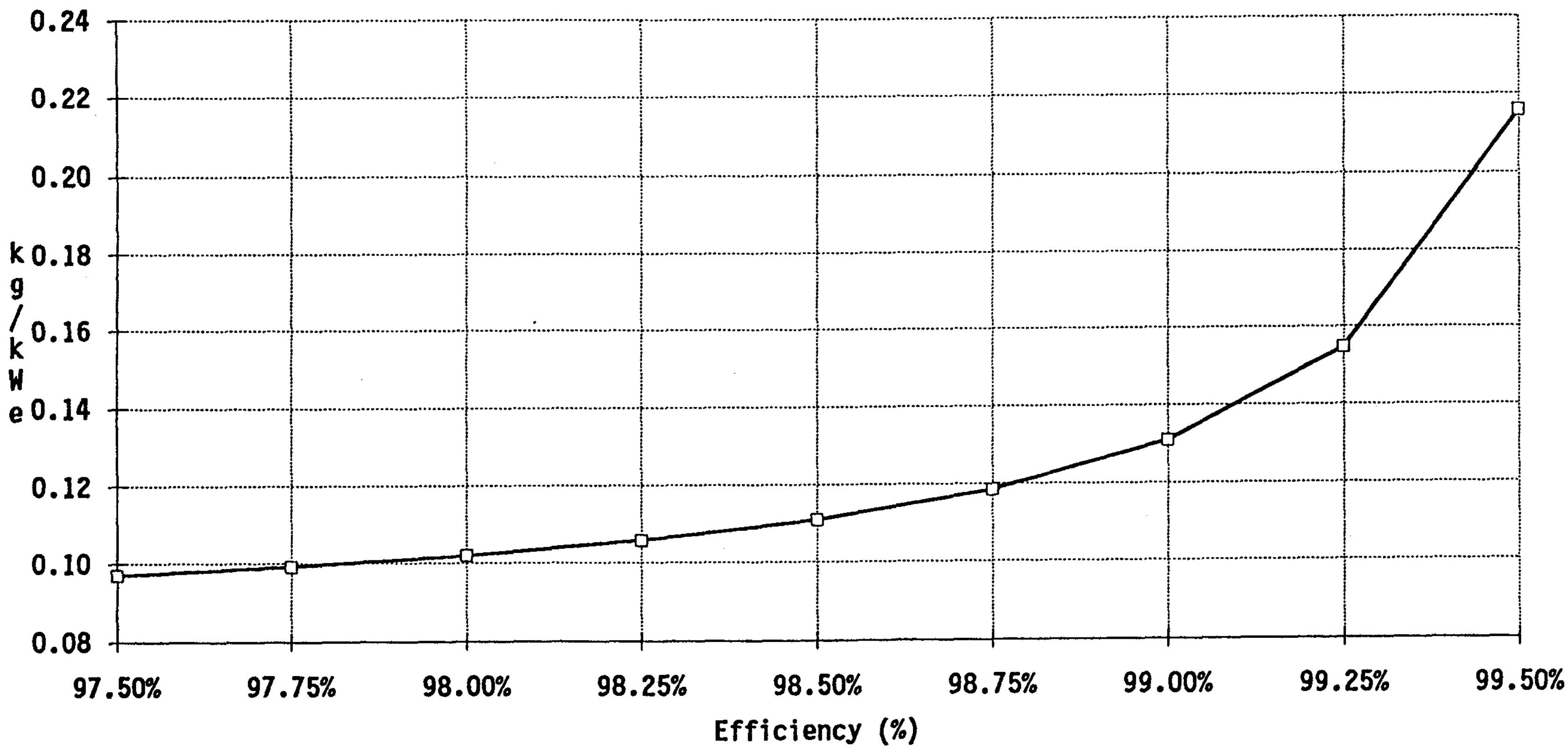

$$3RSM=0.11*((EXP(0.005/(1-RSE)))/1.4)*(RSAM/RSRM)*\underline{RSP_0}*(RSV_I/(RSV_I-2))^6$$
$$*EXP(RSV_I/80000)$$

The equations can be used to calculate the mass or specific weight of the rectifier. When the above multiplier is included, the value that results is a rectifier mass estimate. To obtain the specific weight of the rectifier, remove this multiplier.

A power factor was not included in the rectifier equation to improve the specific weight at higher power levels. As the rectifier power level increases, a slight reduction in specific weight may occur because it is possible to package larger sized units more compactly; however, this minor effect was considered to be to small to warrant the inclusion of an additional factor.

Voltage Level Factors

$$1RSM=0.1*((EXP(0.005/(1-RSE)))/1.4)*(RSAM/RSRM)*RSP_0*\underline{(RSV_I/(RSV_I-2))^6}$$
$$*\underline{EXP(RSV_I/80000)}$$

$$3RSM=0.11*((EXP(0.005/(1-RSE)))/1.4)*(RSAM/RSRM)*RSP_0*\underline{(RSV_I/(RSV_I-2))^6}$$
$$*\underline{EXP(RSV_I/80000)}$$

The voltage impacts on rectifier and chopper mass were judged to be similar; therefore, the approaches used to define the voltage factors are comparable. Two factors are required to cover the full voltage range expected to be experienced by a rectifier. The first, "$(CSV_I/(CSV_I-2))^6$", addresses the influences on power conductor and diode mass as the voltage level declines. The second, "$EXP(CSV_I/80000)$", addresses the mass increases occurring as voltages increase.

Two primary effects cause the rectifier efficiency to decline as the voltage level is reduced: the bias voltage imparted across the diode, and the conduction losses. Silicon diodes require a forward bias voltage of about 0.7 V before they will conduct. At lower voltage levels this bias voltage is a larger percentage of the device voltage; therefore, the efficiency is reduced. Conduction losses are calculated with the equation I^2R. Since current levels rise as voltage declines, the rectifier efficiency is poorer at lower voltage levels. Methods are available to partially offset these losses, but they have associated mass penalties. The resistances of circuit elements can be lowered by increasing the cross sectional areas of the conductors and leads, but it causes their mass to increase. Increasing the diode die area and reducing its current density will lower the conduction losses, but a heavy mass penalty can be incurred. An alternate approach is to replace these standard diodes with Schottky diodes, germanium rectifiers, or bipolar synchronous rectifiers (Ref. III-26). Schottky rectifiers have a lower forward voltage drop, but they generally are not as rugged. The bias voltage of a germanium rectifier is about 0.3 V, but it is more limited in temperature and has a lower breakdown voltage. The I-V characteristic of a bipolar synchronous rectifier is linear down to zero volts and it does not exhibit a bias voltage; however, it requires a more complicated circuit for operation.

Due to these factors, the efficiency parameter input for rectifier stage calculations should be decreased in accordance with Table 10. These values reflect the increase in mass and reduction in efficiency that occurs at lower voltages. These values will yield a smoothly increasing mass curve. The rectifier specific weight curve generated with these values is shown in Figure 17.

Table 10
Efficiency Corrections for Lower Voltage Rectifier Mass Estimates

Input Voltage (Vrms)	Input Rectifier Efficiency (percent)
120	98.50
110	98.50
100	98.48
90	98.46
80	98.42
70	98.36
60	98.30
50	98.18
40	98.00
30	97.75
20	96.50

Present diodes can withstand voltages up to 1600 V and diode assemblies are available up to 4400 V. These may be adequate for most power conditioning needs (Ref. III-27). Extremely high voltage rectifiers often utilize a pancake configuration consisting of diodes stacked in series. Ideally, if the voltage across a single diode is not increased, the insulating requirements and masses of the individual diodes are not increased. This probably is not totally true in actual applications. Because it is virtually impossible to guarantee a string of diodes will always conduct simultaneously, some diodes will briefly experience higher voltages. The insulation levels and diode ratings will need to be higher to withstand these high voltage transients. Hence, a high voltage rectifier will incur some mass penalties as voltage levels rise. Because a silicon rectifier is more robust than a chopper, but less than a transformer; the mass gain occurring with a rise in voltage is expected to fall in between these devices. Based on this reasoning, the factor underlined in the above equation was developed. A specific weight curve for a high voltage rectifier design obtained from this equation is shown in Figure 18.

Frequency Factor

Although it may be necessary to incorporate fast recovery diodes in a high frequency design, the effect of frequency on rectifier mass was considered to be minor. In fact it may even be desirable to incorporate fast recovery diodes in lower frequency designs to gain an improvement in efficiency. For these reasons, it was not considered necessary to include a frequency factor in the equations.

Figure 17

Rectifier SPWT vs Voltage

(Low Voltage Region)

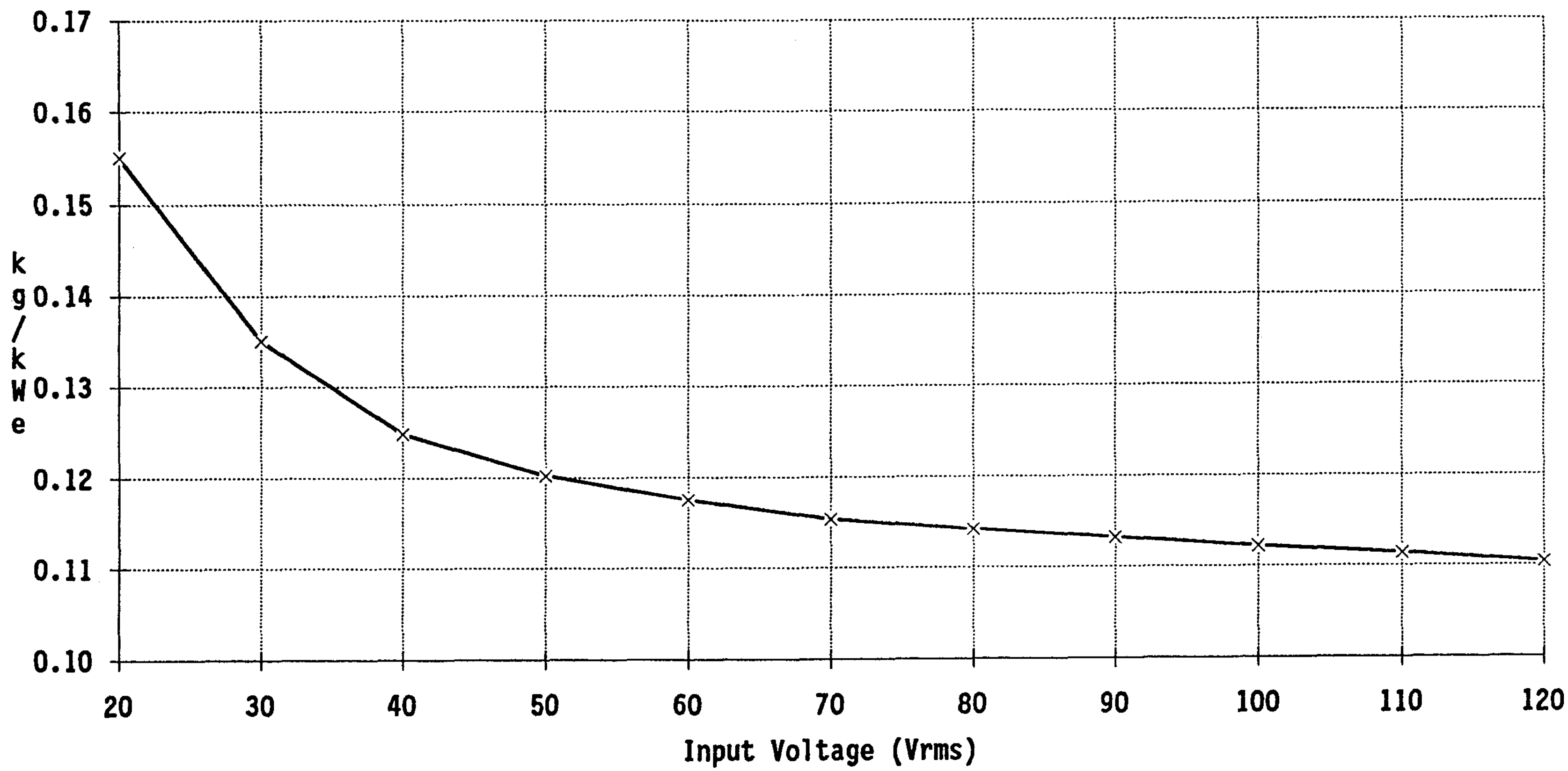

Figure 18

RECTIFIER SPWT VS VOLTAGE
(HIGH VOLTAGE REGION)

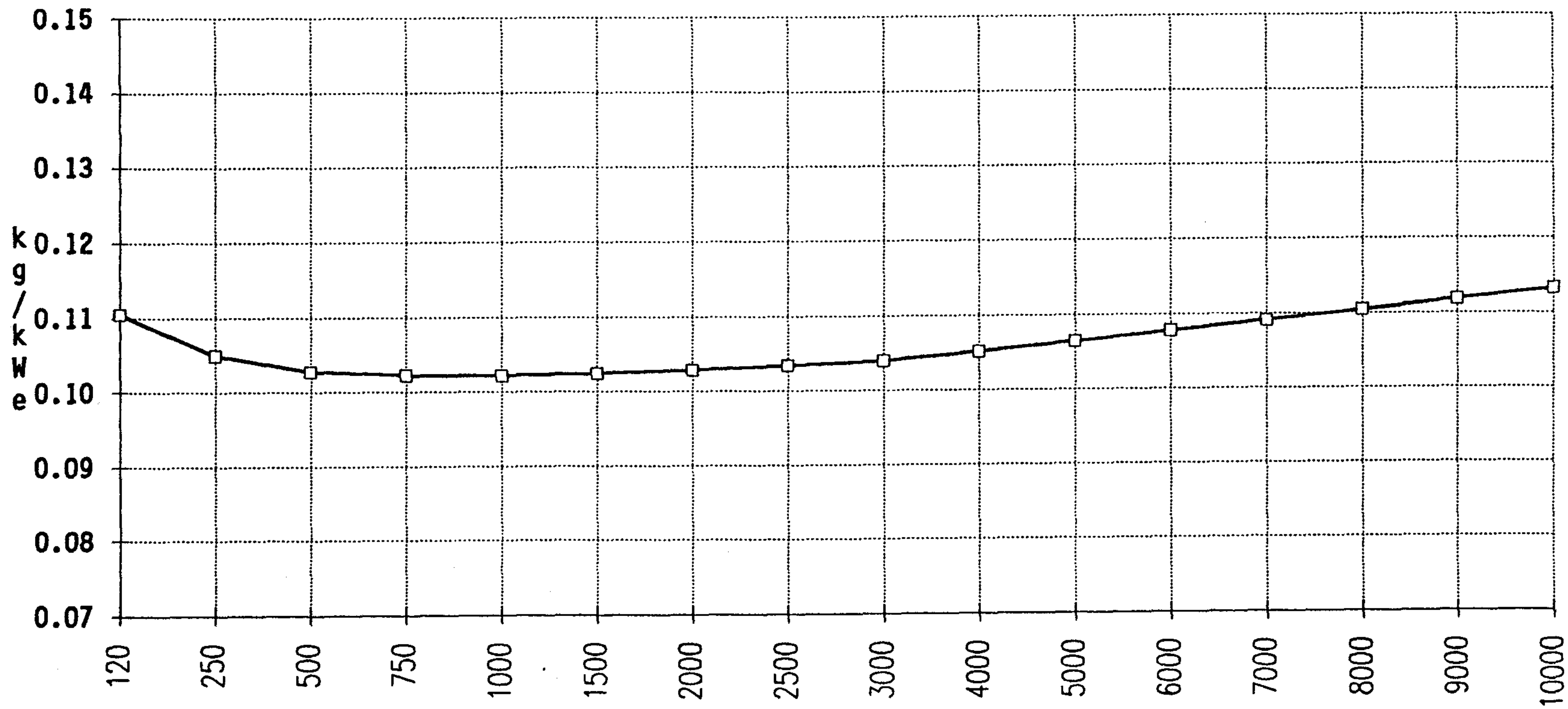

3.1.4 DC Filter Stage Model

The dc filter stage conditions the dc waveforms to achieve the power quality required by the system. Two dc filters may be required for a component, one on the input and another on the output. Most components containing a chopper or rectifier will require dc filtering; therefore, dc filter stages are contained in the rectifier, dc/dc converter, and inverter models. Filtering mass is difficult to estimate. The power quality requirements for lunar or Mars base applications are vague or nonexistent, and the design of a filter is a complex process that is heavily influenced by the circuit topology. The filter stage equations presented here are generalized and only intended to provide rough mass estimates to facilitate component comparisons. For more accurate mass estimates, power quality requirements must be defined and specific filter designs generated.

A single-stage filter design was assumed to precede the chopper and follow the rectifier. This configuration is relatively simple, consisting of a series inductor and a parallel capacitor. Since the input to a chopper and the output from a rectifier are periodically discontinuous and they have a high ripple content, filtering is needed to smooth the dc waveform and suppress voltage and current spikes. The masses of the filter hardware preceding the chopper and following the rectifier were assumed to be comparable because they are both performing similar functions, providing energy to smooth the dc lines during discontinuous conduction periods. Due to the approximations and inaccuracies already inherent in these models, it was not considered practical to identify differences in the two filter designs and develop alternate equations for both applications.

Presently, the mass of a filter following a 1 kWe, 120 Vdc single-phase rectifier, designed to reduce the output ripple to 1%, is 370 grams. This rectifier was assumed to be after a chopper stage operating at 20 kHz. The ripple frequency of a 3-phase rectifier is three times higher than a single-phase design. This decreases the amount of energy that must be stored in the filter hardware and reduces the filter mass. Consequently, the mass of a dc filter following a 3-phase rectifier also designed to reduce the output ripple to 1% is 125 grams. Fabrication advancements should reduce the single- and 3-phase dc filter masses to 330 and 110 grams respectively by the year 2000.

To develop the dc filter stage mass equations, the previous power conditioning model analyses by Gilmour, Moriarty, and TRW were referred to for guidance (Ref. II-1, II-2, III-28). The equations developed by TRW under contract NAS3-19690 were especially valuable since they allowed dc filter masses to be calculated for numerous conditions. The variables that will be used through out the dc filter stage model discussion are shown in Table 11.

Table 11
DC Filter Model Variable Definitions

1FSM	Single-Phase Dc Filter Stage Mass
3FSM	3-Phase Dc Filter Stage Mass
FSRF	Dc Filter Stage Ripple Factor (1 to 5%)
FSE	Dc Filter Stage Efficiency (99.5%)
FSAM	Dc Filter Stage Available Modules
FSRM	Dc Filter Stage Required Modules
FSP_o	Dc Filter Stage Power Output (kWe)
FSV_o	Dc Filter Stage Voltage Output (Vrms)
FSF	Dc Filter Stage Frequency (kHz)

The equations developed for the single-phase and 3-phase dc filter mass estimates are shown below. Each factor in the equations will be discussed separately. The factor being discussed will be underlined and accompanying graphs will be used to display the values generated by the equations. Dc filter mass breakdown tables are located in Appendix A on page A-4.

Mass Coefficient

$$1FSM=\underline{4700}*(1/(FSRF/0.01)^{0.5})*((1-0.995)/(1-FSE))*(FSAM/FSRM)*FSP_o*(FSV_o^{-2}+0.000001)*(20/FSF)$$

$$3FSM=\underline{4700}*(1/(FSRF/0.01)^{0.5})*((1-0.995)/(1-FSE))*(FSAM/FSRM)*FSP_o*(FSV_o^{-2}+0.000001)*(6.7/FSF)$$

A four step process was used to determine the mass coefficient used in the above dc filter equations. First, masses of actual LC filter designs were located in technical reports (Ref. III-6, III-7, III-29). Because the filter masses identified in these reports were under widely varying conditions, it allowed the later developed filter equations to be verified in different applications. The next step was to calculate filter masses using equations developed by TRW during a component mass optimization study (Ref. III-28). The parameters input into these filter mass equations were obtained from values contained in the reference reports. The third step compared the calculated filter masses with masses listed in reports. Finally, discrepancies were noted and investigated.

The TRW equations generally appeared to be quite accurate and seemed to correctly reflect the dc filter mass trends associated with voltage, frequency, and efficiency. Using a mass coefficient value of "4700", fairly good dc filter mass estimates were obtained for filters preceding resonant converters and filters following rectified alternator outputs. It was previously stated in the section discussing the chopper equation development that a resonant converter design would be employed through out the model development.

Ripple Factor

$$1FSM=4700*\underline{(1/(FSRF/0.01)^{0.5})}*((1-0.995)/(1-FSE))*(FSAM/FSRM)*FSP_0*(FSV_0^{-2}+0.000001)*(20/FSF)$$

$$3FSM=4700*\underline{(1/(FSRF/0.01)^{0.5})}*((1-0.995)/(1-FSE))*(FSAM/FSRM)*FSP_0*(FSV_0^{-2}+0.000001)*(6.7/FSF)$$

The ripple factor measures the amount of ripple existing on the dc waveform. It is calculated with the following equation:

$$RF=(V_R)/Vdc$$

where: RF is the ripple factor expressed as a percentage
V_R is the ripple voltage level expressed as a rms value
Vdc is the dc voltage level.

Naturally, the dc filter mass will increase as the ripple requirements get more stringent. Equations derived by Gilmore and later verified by the TRW calculations showed that the mass would change by the reciprocal of the square root of the increase in the ripple factor. This led to the factor underlined above. Figure 19 shows the rise in dc filter mass occurring as the ripple factor is reduced. To obtain filter masses consistent with SSF requirements or expected lunar base habitat needs, it is recommended that the ripple factor be set at 1%. For utility power applications, such as following a large alternator based power source or feeding drive motors, a value of 5% is suggested. Larger ripple factor values appear to be undesirable for the power transmission system and also cause the filter mass estimates to become less accurate. The subsequent graphs on filter characteristics will use a ripple factor of 1% unless otherwise noted.

Efficiency Factor

$$1FSM=4700*(1/(FSRF/0.01)^{0.5})*\underline{((1-0.995)/(1-FSE))}*(FSAM/FSRM)*FSP_0*(FSV_0^{-2}+0.000001)*(20/FSF)$$

$$3FSM=4700*(1/(FSRF/0.01)^{0.5})*\underline{((1-0.995)/(1-FSE))}*(FSAM/FSRM)*FSP_0*(FSV_0^{-2}+0.000001)*(6.7/FSF)$$

The efficiency of an LC filter network is determined by the equivalent series resistance (ESR) of the inductor and capacitor. To reduce the ESRs of these devices the inductor winding and core size, and the capacitor dielectric cross sectional area must be increased. This increases filter mass. The TRW equations were used to calculate filter masses for efficiency values ranging from 99.3 to 99.7%. They indicated there was a linear relationship between dc filter mass and efficiency. The factor underlined above was computed during this exercise and used to generate Figure 20. It depicts the change in dc filter specific weight occurring with a change in efficiency.

Figure 19

DC Filter SPWT vs Ripple Factor

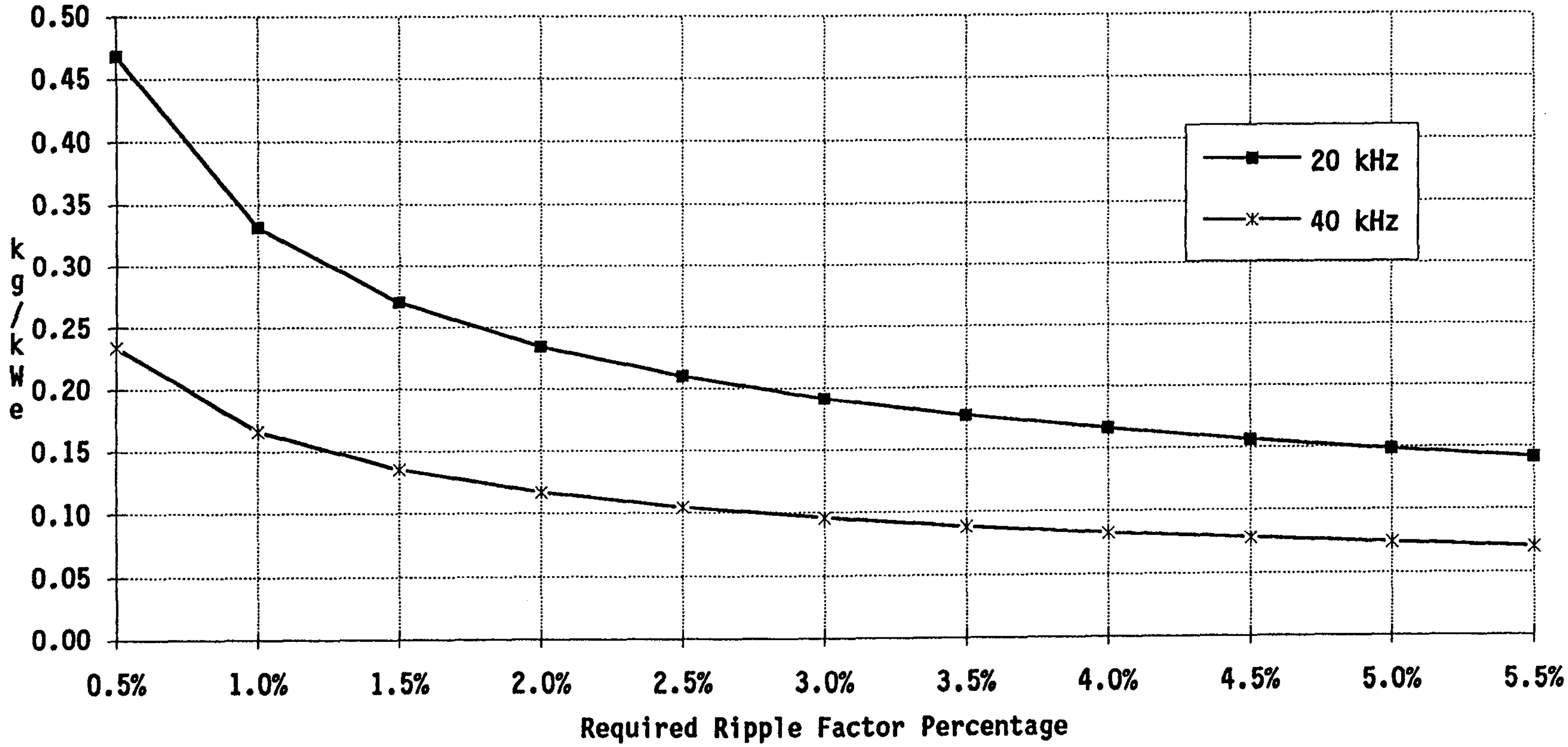

Figure 20
DC Filter SPWT vs Efficiency

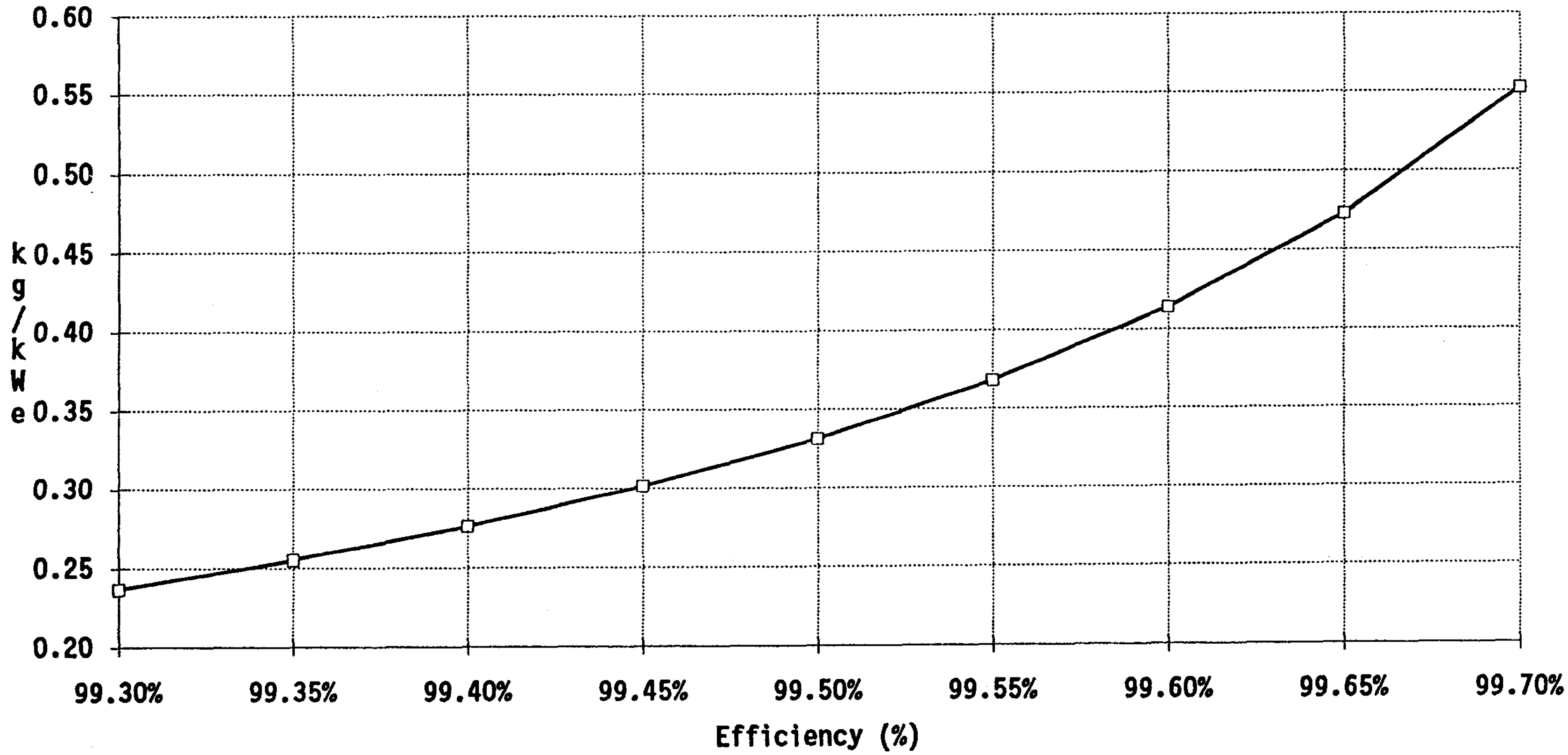

Redundancy Factor

$$1FSM=4700*(1/(FSRF/0.01)^{0.5})*((1-0.995)/(1-FSE))*\underline{(FSAM/FSRM)}*FSP_0*(FSV_0^{-2}+0.000001)*(20/FSF)$$

$$3FSM=4700*(1/(FSRF/0.01)^{0.5})*((1-0.995)/(1-FSE))*\underline{(FSAM/FSRM)}*FSP_0*(FSV_0^{-2}+0.000001)*(6.7/FSF)$$

The redundancy factor underlined above addresses the mass penalty associated with a more reliable system. The actual number of modules in the assembly is defined by the "available modules" value. The number of modules needed to provide full power is defined by the "required modules" value. If a design requires 4/3 redundancy to meet the reliability requirements, four 33% rated channels will be used. This increases the mass of the assembly at least 33%. The mass of the fourth channel is the penalty incurred to achieve a higher reliability.

Power Level Multiplier

$$1FSM=4700*(1/(FSRF/0.01)^{0.5})*((1-0.995)/(1-FSE))*(FSAM/FSRM)*\underline{FSP_0}*(FSV_0^{-2}+0.000001)*(20/FSF)$$

$$3FSM=4700*(1/(FSRF/0.01)^{0.5})*((1-0.995)/(1-FSE))*(FSAM/FSRM)*\underline{FSP_0}*(FSV_0^{-2}+0.000001)*(6.7/FSF)$$

The equations can calculate filter mass or specific weight. When the power level multiplier is included, the equations determine the mass of the dc filter. Remove this multiplier to obtain the dc filter specific weight.

Note that a power level factor is not included in the dc filter mass equations. The TRW equations indicated the filter specific weight remained constant with power level. This is shown in Figure 21 for single- and 3-phase filter designs. Because the energy density of the capacitors and inductors in the filter network remains constant regardless of the power level, the filter specific weight does not change. The gains that might be realized in packaging density as the component sizes increased, were considered to be insignificant.

Voltage Level Factors

$$1FSM=4700*(1/(FSRF/0.01)^{0.5})*((1-0.995)/(1-FSE))*(FSAM/FSRM)*FSP_0*\underline{(FSV_0^{-2}+0.000001)}*(20/FSF)$$

$$3FSM=4700*(1/(FSRF/0.01)^{0.5})*((1-0.995)/(1-FSE))*(FSAM/FSRM)*FSP_0*\underline{(FSV_0^{-2}+0.000001)}*(6.7/FSF)$$

In most LC filter designs, the mass of the capacitor is the largest portion of the filter mass. To determine the changes that will occur in filter mass as the voltage level rises, the changes occurring in capacitor mass must be identified. For a given power level and frequency, the energy that must be stored in the filter is constant regardless of the voltage level, but the filter capacitance is not. The energy stored in a capacitor is defined by the equation:

FILT1VS3.XLC

Figure 21

DC Filter SPWT vs Power
(1-Phase & 3-Phase Comparison)

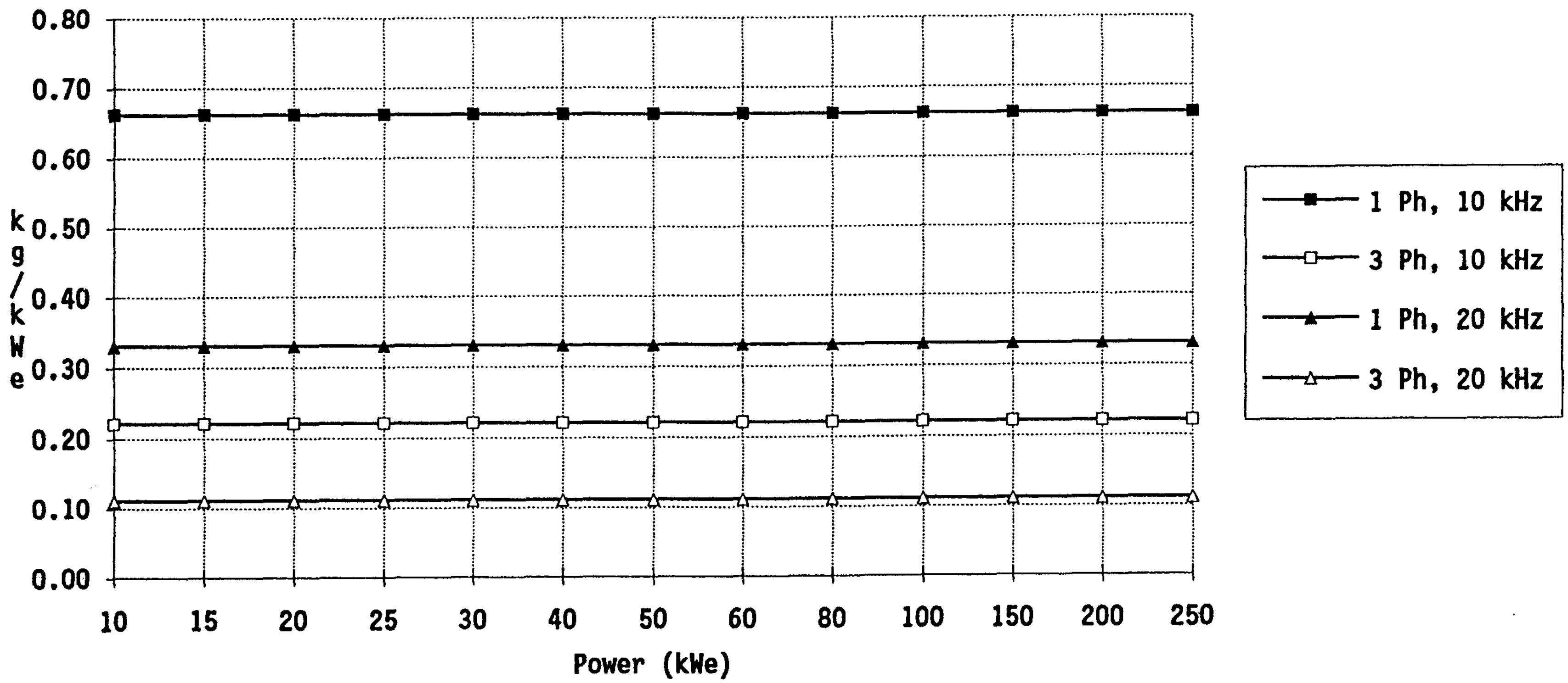

FILTGRPH.XLS

8/11/91

$$E=\frac{1}{2}CV^2$$

where: C is the capacitance in farads
V is the voltage level in volts.

By inspection, one can see that the energy stored in a capacitor rises with the voltage squared. If the voltage level is doubled, the capacitance can be reduced to one-fourth of its previous value and the amount of energy that is stored will remain the same. If a constant mass per farad is assumed, the capacitor mass will drop to one-fourth of its previous value. Because the mass of the capacitor dominates the filter mass at voltages below 1000 Vdc, most of the change in filter mass results from a change in capacitor mass. Below 120 Vdc this correlation is quite accurate. Figure 22 shows the relationship between filter mass and voltage for voltage levels below 120 Vdc.

Although there were not any restrictions associated with the constant mass per farad assumption contained in the TRW report, it is doubtful that the authors intended this assumption to be extended to high voltage applications. A survey of capacitors indicates there are a number of dielectric materials that can readily withstand voltages up to 1000 Vdc without greatly increasing the dielectric thickness. This seemed to indicate that this assumption had merit up to this voltage level. However, at voltages approaching 1000 Vdc, the need to increase the dielectric thickness to prevent voltage breakdown, will cause the mass per farad to rise.

Because capacitor mass initially declines quickly with voltage, the inductor mass becomes significant at voltages above 250 Vdc. For voltages above a 1000 Vdc, the reductions in capacitor mass that theoretically occur with a rising voltage are largely offset by the capacitor's rising mass per farad and increases in inductor mass. This causes the filter specific weight to become relatively constant. This is shown in Figure 23. The voltage factor underlined above is designed to cover a voltage range from 20 to 10000 Vdc and it was developed by assimilating the data from this analysis.

Frequency Factor

$$1FSM=4700*(1/(FSRF/0.01)^{0.5})*((1-0.995)/(1-FSE))*(FSAM/FSRM)*FSP_0*(FSV_0^{-2}+0.000001)*\underline{(20/FSF)}$$

$$3FSM=4700*(1/(FSRF/0.01)^{0.5})*((1-0.995)/(1-FSE))*(FSAM/FSRM)*FSP_0*(FSV_0^{-2}+0.000001)*\underline{(6.7/FSF)}$$

The mass of a dc filter is primarily determined by how much energy it must store. The energy storage requirements are in turn proportional to the ripple frequency. The further apart the wavecrests of the ripple voltage are, the more energy a filter must provide to the system to maintain a smooth dc output. The ripple frequency of a full wave rectified single-phase waveform is twice the input frequency. Because the three phases of a 3-phase system are superimposed after rectification, the ripple frequency of the output is six times the operating frequency. To best illustrate these points, the dc filters needed after linear and rotary alternator rectifiers are compared. The effects of different ripple frequencies and the features of single- and 3-phase systems can be evaluated in an application that is real and of considerable interest.

Figure 22

DC FILTER SPWT VS VOLTAGE (LOW VOLTAGE REGION)

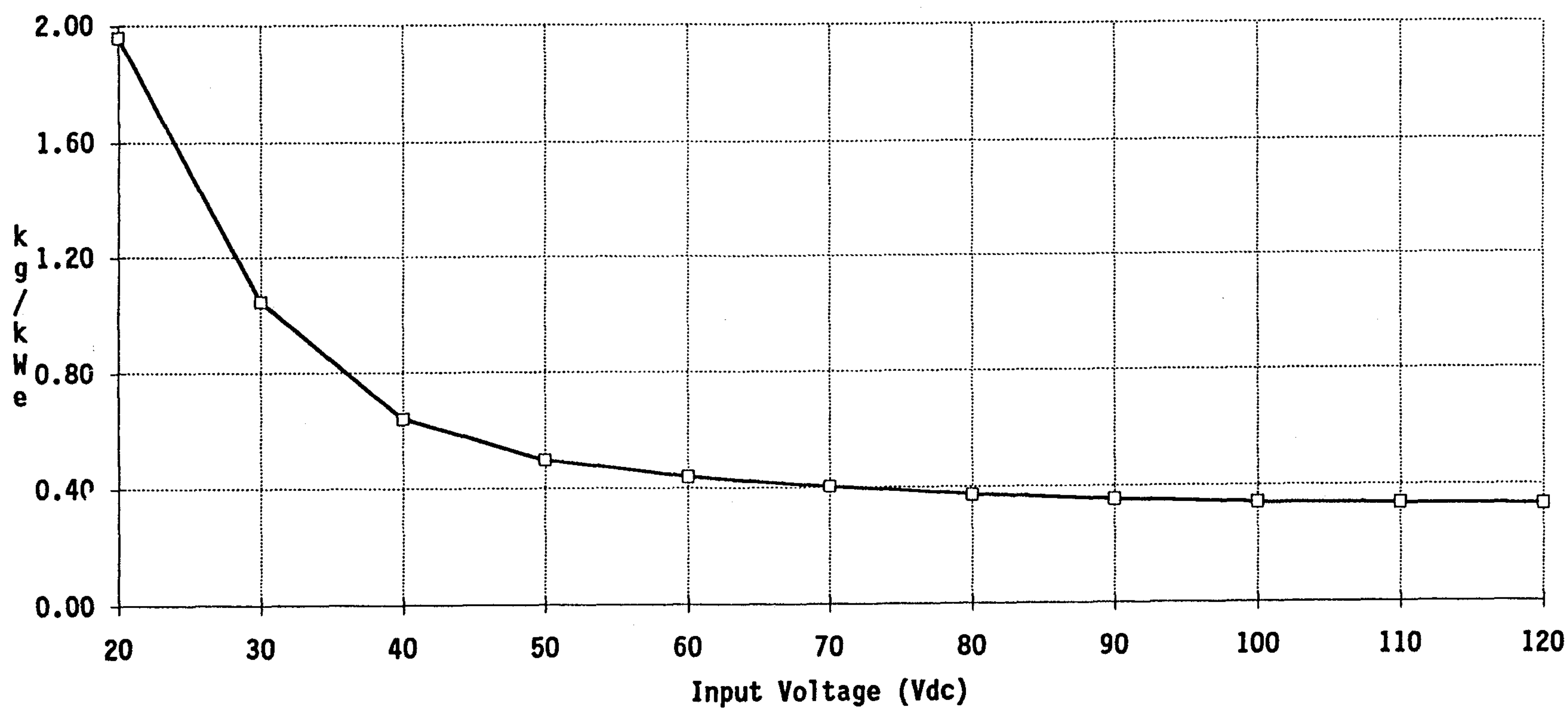

FILTGRPH.XLS

8/11/91

Figure 23

DC FILTER SPWT VS VOLTAGE (HIGH VOLTAGE REGION)

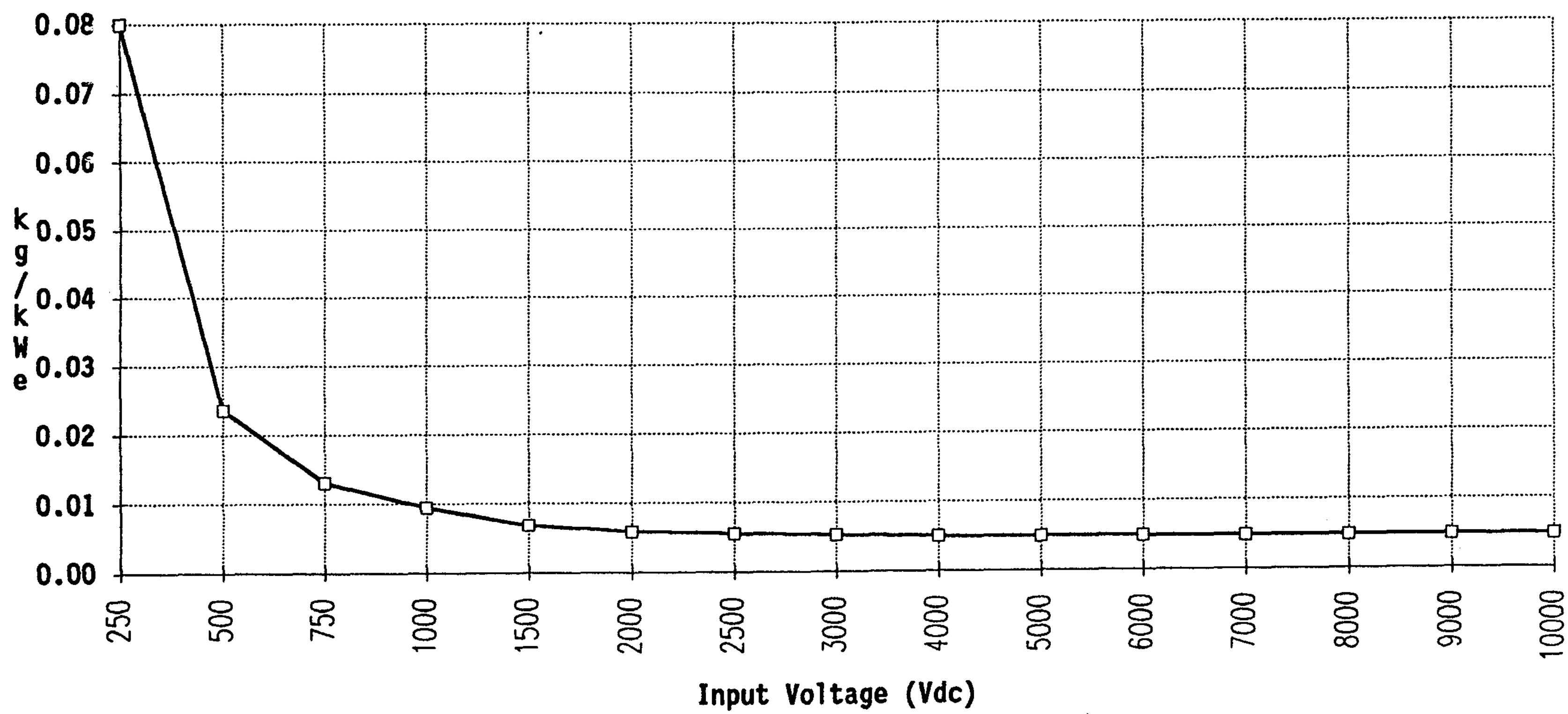

For some applications, the single-phase ac generated by a linear alternator will need to be converted into dc. To obtain dc, the output of the linear alternator is first rectified. An ideal linear alternator waveform is shown in Figure 24. Figure 25 shows the waveform obtained after perfect rectification. The waveform distortion that occurs when the power piston reverses direction, and the rectifier conduction and commutation losses have been disregarded for clarity[4]. Because the waveform depicted in Figure 25 has a very high ripple content, it would be unsatisfactory for most dc power transmission applications. It must be smoothed with a dc filter to make it better approximate a dc voltage.

One of the most common techniques for filtering a rectified waveform is to place an LC filter after the output. The capacitor in this filter provides energy to the system when the voltage level declines, reducing the dip between waveform crests. The effect of adding a simple LC filter is shown in Figure 26. Each shaded area depicts the relative amount of energy that must be stored in the capacitor. This energy level is proportional to the frequency and power quality requirements. The more energy the dc filter must store, the heavier it becomes. The waveform obtained from the rectification of the 70 Hz single-phase linear alternator output is relatively difficult to filter. To illustrate this point, the filtered linear alternator dc output will be contrasted with a rectified and filtered rotary alternator output.

The individual phases of a rotary alternator three-phase, 1 kHz waveform are shown in Figure 27. Notice that each phase is offset 120 degrees from the other two. (When comparing the rotary and linear alternator waveforms, note that the rotary alternator time scale has been expanded for clarity. For a true comparison the rotary alternator waveform would have slightly over 14 cycles for 1 cycle of the linear alternator waveform.)

The ac output of the rotary alternator can be converted into dc with a rectifier and dc filter. Figure 28 shows the perfect rectification of a rotary alternator output. Because the three-phases are evenly offset, a fairly smooth dc output results when they are rectified and superimposed. The ripple content of this waveform is much lower than in the linear alternator case. This occurs because the rotary alternator frequency is much higher, 1 kHz versus 70 Hz, and its output is three-phase instead of single-phase. These two factors result in a ripple frequency of 6 kHz, approximately 40 times the 140 Hz ripple frequency of the linear alternator.

In some cases, the rectified rotary alternator output may be adequate for dc transmission; however, some filtering will be required for most applications. Typically, an LC filter is placed across the output to make it better approximate a dc voltage. The addition of an LC filter is shown in Figure 29. Energy is supplied by the capacitor in this filter when the voltage dips, smoothing the waveform. The shaded areas between crests depict the amount of energy stored in the capacitor. Since the energy storage requirement of a filter is proportional

---

[4] Conduction losses occur due to the voltage drop across the diodes or silicon controlled rectifiers (SCRs) normally used to rectify an ac waveform. Commutation losses result when the current sequentially transfers or *commutates* from one SCR or diode to the next. These losses will cause discontinuities in a rectified waveform, especially near zero.

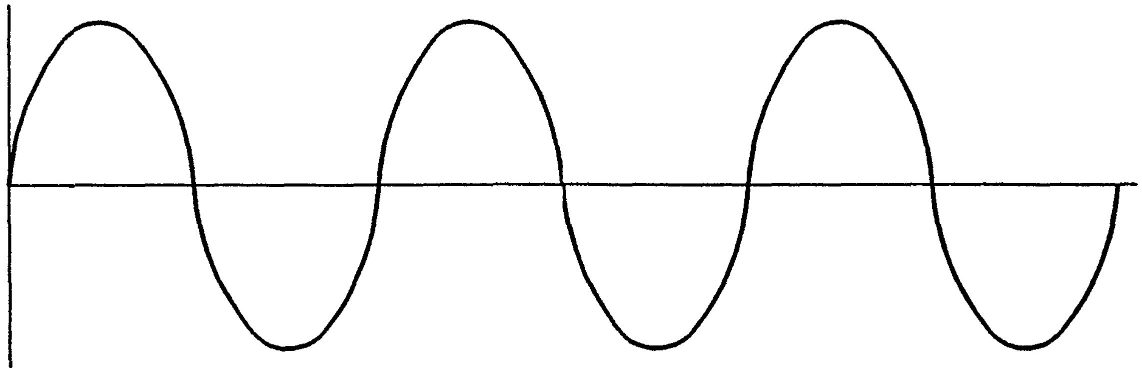

Figure 24 Linear Alternator Output Waveform

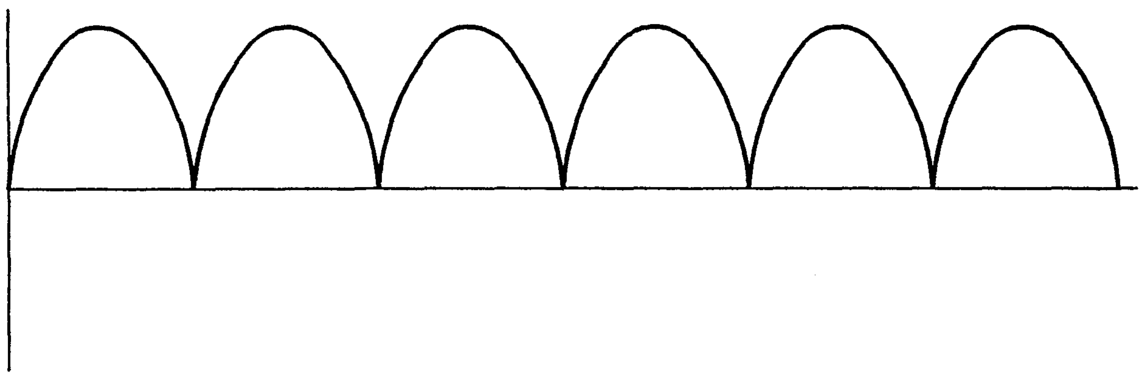

Figure 25 Rectified Linear Alternator Output

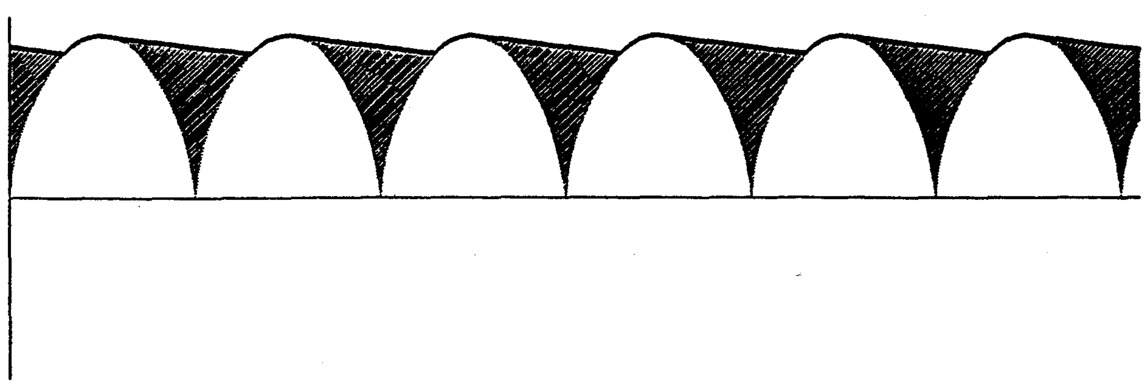

Figure 26 Rectified Output after Filtering

STLGWAVE
9-20-91

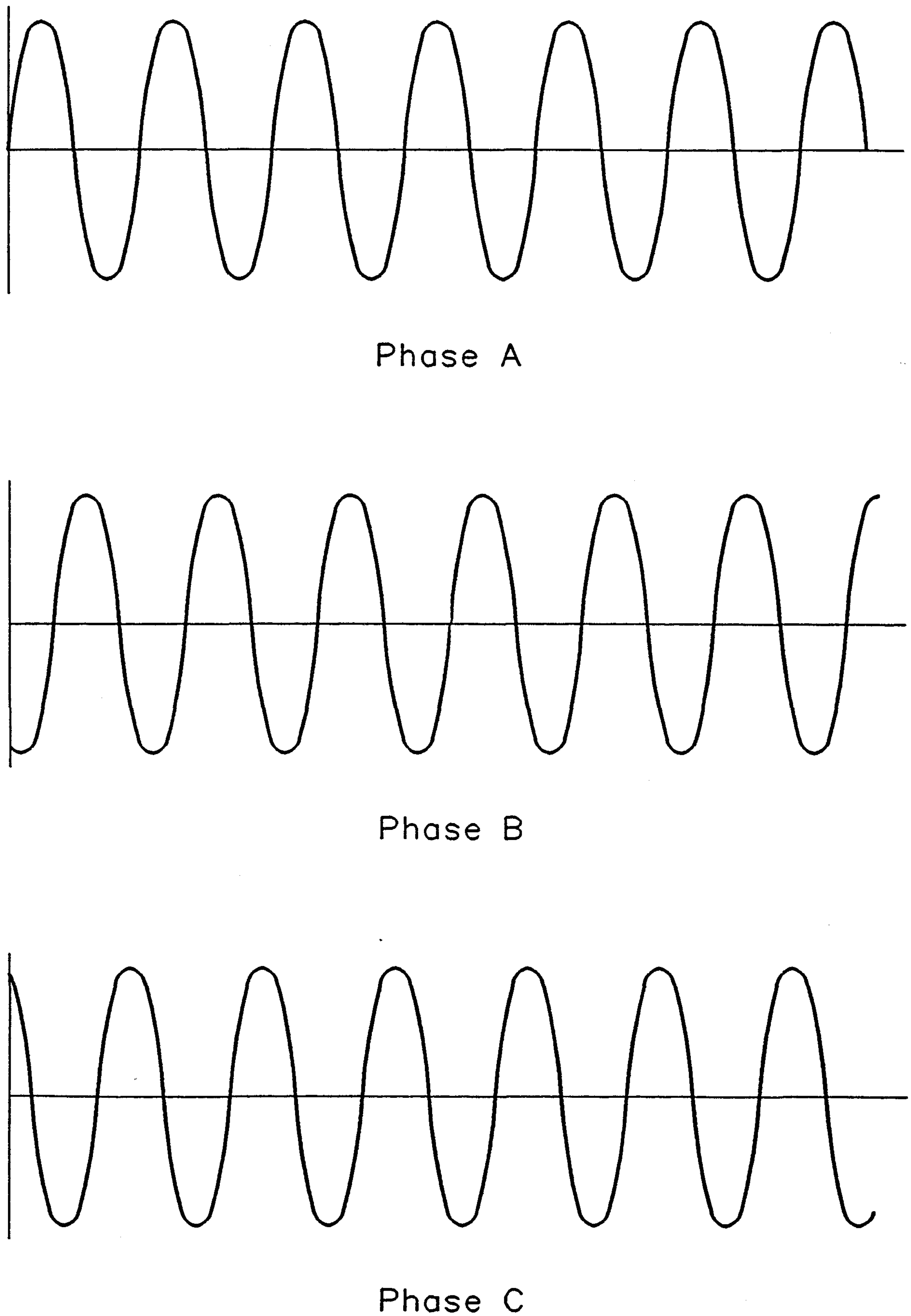

Figure 27 3–Phase Rotary Alternator Output Waveform

CBCWAVE1
9-20-91

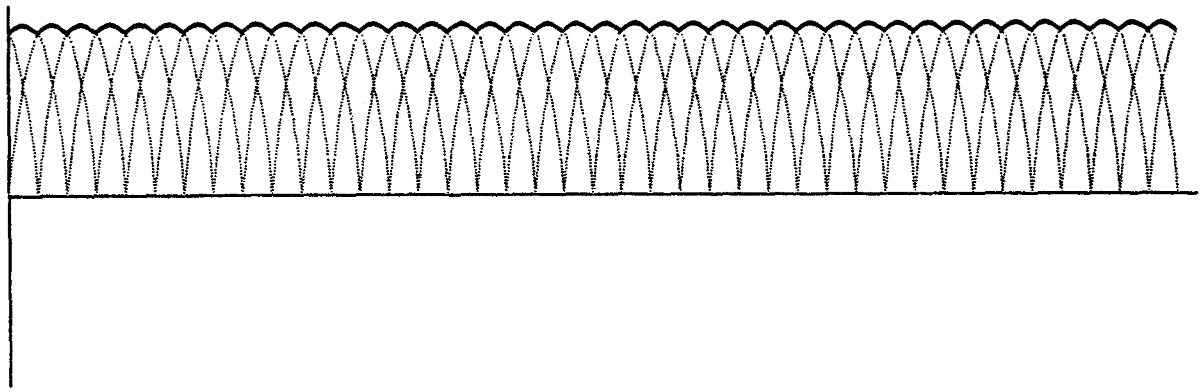

Figure 28 Rectified Rotary Alternator Output Waveform

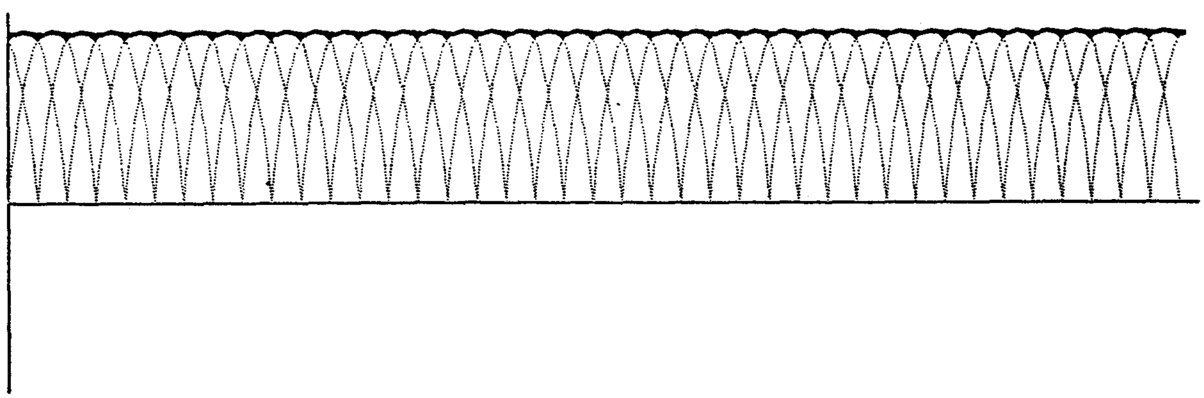

Figure 29 Rectified Output after Filtering

to the ripple frequency and the ripple frequency of the rectified rotary alternator output is about 40 times higher than the rectified linear alternator output, the energy that must be stored in the rotary alternator dc filter is much lower. Consequently, the mass of the rotary alternator dc filter is much less.

Using a ripple factor of 5%, Figure 30 graphically compares the masses of single- and 3-phase dc filters at the frequencies associated with linear and rotary alternators. One should not infer from this chart and the above discussion that the filter mass of the linear alternator must be 40 times that of the rotary alternator, this would be an extreme. A systems analysis must be conducted to determine appropriate filtering requirements. It may not be prudent to impose the same requirements on both alternator designs. If the power system pays a large mass penalty to heavily filter a rectified alternator output, it may be better to place filters on the inputs of sensitive equipment and only provide coarse filtering after the alternator rectifier.

Because the filtering associated with high frequency converters is also of interest, Figure 31 was generated. It compares the dc filter masses on the outputs of two dc/dc converters. These filters follow single- and 3-phase rectifier stages and are designed to meet 1% ripple requirements.

3.1.5 AC Filter Stage Model

Resonant converters can typically achieve less than 5% total harmonic distortion without filtering. This is adequate for most PMAD applications; however, a series harmonic trap is required to prevent external harmonics from being amplified within the converter. The mass of a harmonic filter is difficult to estimate. In discussions held with converter designers familiar with the design of harmonic filters, they indicated present harmonic filter designs are not optimized and quite a bit of improvement is expected. Many articles discuss harmonic distortion, but none were found that described a method for calculating the mass of a harmonic filter. Consequently, the following equations are approximate since there is very little concrete data. It is recommended that further work be done in this area when additional information becomes available. If more accurate mass estimates are required, it will be necessary to define power quality requirements and have a knowledgeable designer generate a specific filter design.

A harmonic filter is placed before the converter input or after its output, and it is connected in series with the source or load. The equations in this report are based on a series resonant circuit tuned to the inversion frequency of the converter. The filter configuration itself consists of a current transformer that is connected in parallel with a resistor, and a series connected inductor and capacitor combination (Ref. III-30). The current transformer is required to obtain reasonable values for the inductor and capacitor and to reflect adequate resistance into the line to inhibit harmonics (Ref. III-11). Much of the filter mass is concentrated in this current transformer and it can not be eliminated.

A technical presentation compiled by TRW indicated the mass of a harmonic filter placed on the output of a 5 kWe, 20 kHz inverter would weigh 1071 grams (Ref. III-7). The specific weight of this filter is about 0.21 kg/kWe. In a discussion held at the "High Frequency Power Distribution and Controls Technology Conference" in June 1991, John Biess indicated it might be possible to reduce

Figure 30

DC FILTER SPWT VS FREQUENCY SINGLE- AND 3-PHASE DESIGNS (LOW FILTERING LEVEL)

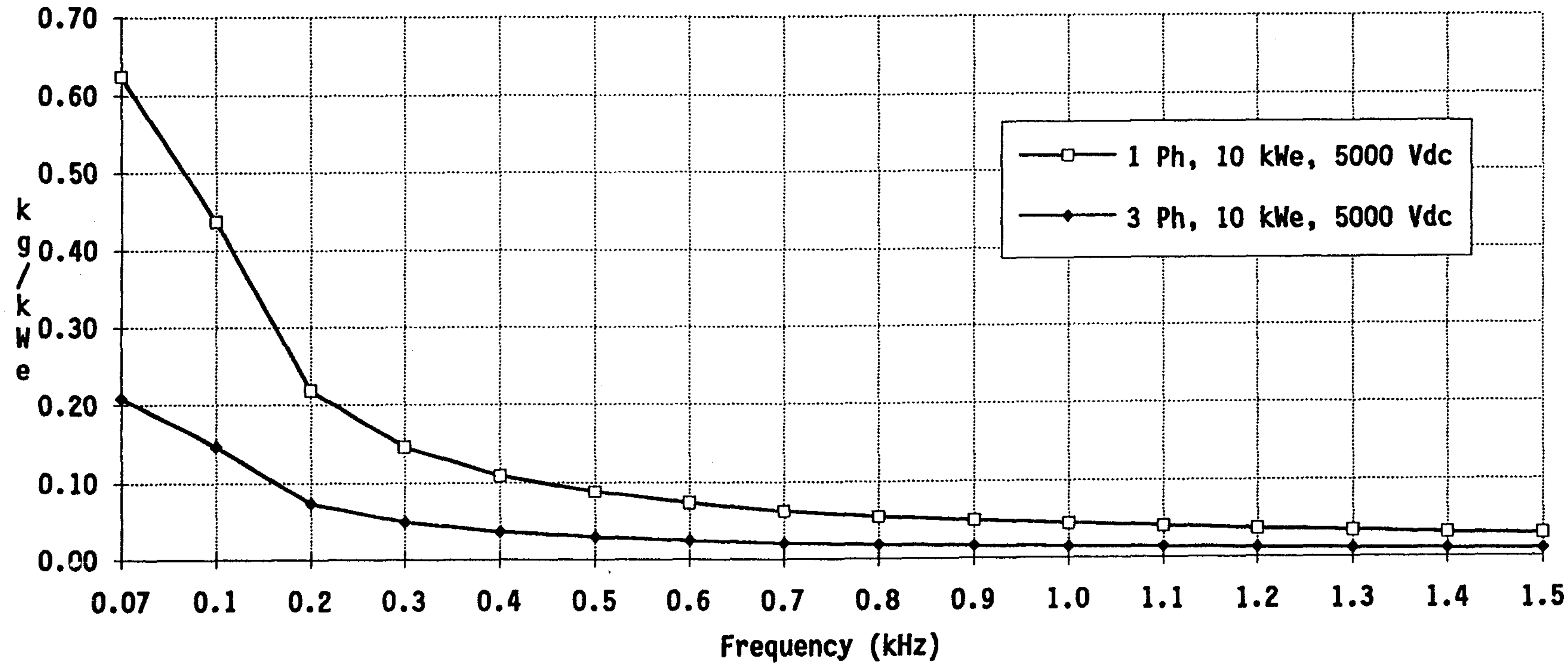

FILTGRPH.XLS

8/11/91

Figure 31

DC Filter SPWT vs Frequency Single- and 3-Phase Designs (High Filtering Level)

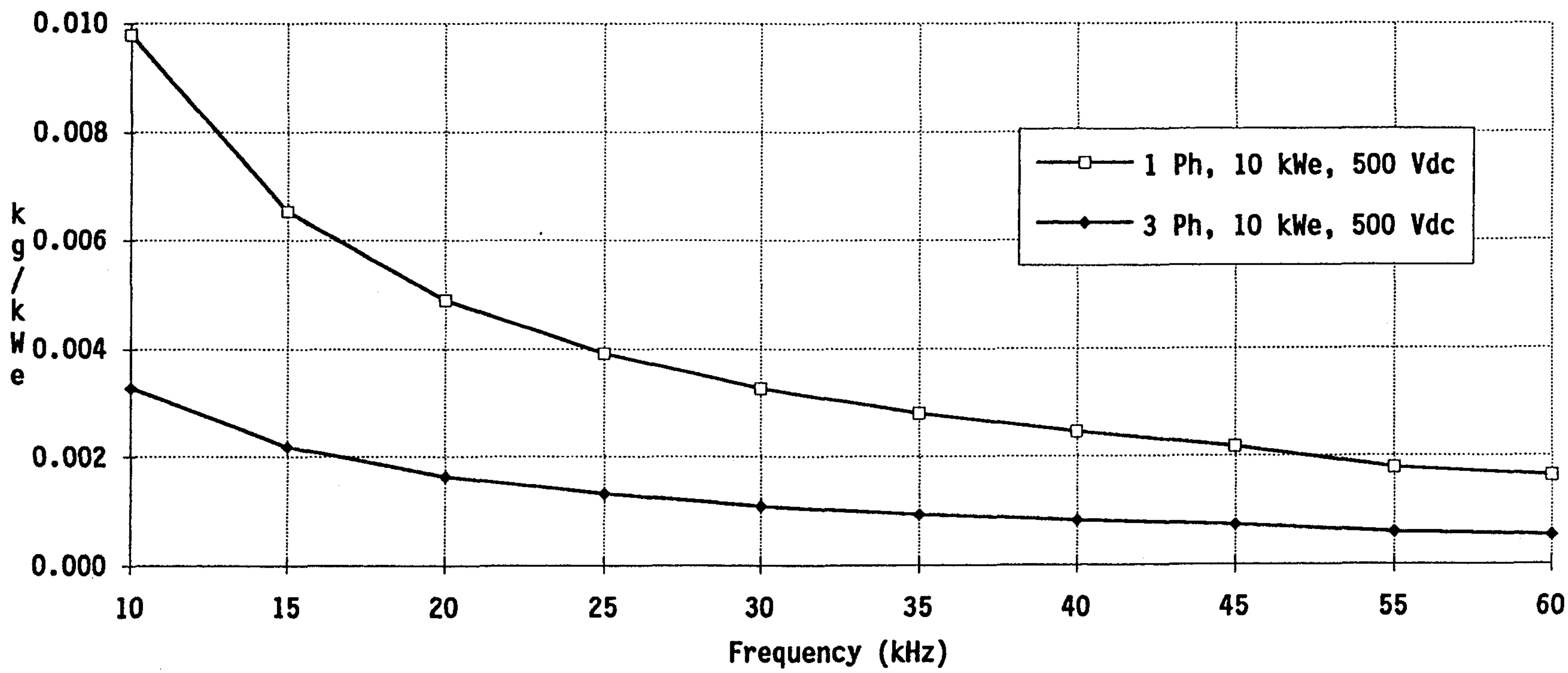

this filter design to one-third of its present weight with extensive analysis and optimization. This would result in a specific weight of about 0.07 kg/kWe (Ref. III-11). However, he also indicated this value might be optimistic. Based on this discussion, it was decided to use a value of 0.1 kg/kWe for a harmonic filter following a single-phase 1 kWe, 20 kHz inverter. The harmonic filter used for a 3-phase inverter was assumed to consist of three single-phase inverter filters each rated to carry one-third of the power. Its mass would be just slightly heavier due to economies of scale. The resulting filter masses for 1 kWe single-phase and 3-phase inverters was estimated to be 100 and 105 grams respectively.

The variables contained in the ac filter stage equations are shown in Table 12.

Table 12
AC Filter Model Variable Definitions

1FSM	Single-Phase Ac Filter Stage Mass
3FSM	3-Phase Ac Filter Stage Mass
FSE	Ac Filter Stage Efficiency (99.5%)
FSAM	Ac Filter Stage Available Modules
FSRM	Ac Filter Stage Required Modules
FSP_0	Ac Filter Stage Power Output (kWe)
FSF	Ac Filter Stage Frequency (kHz)

The equations generated to estimate the masses of single-phase and 3-phase ac filters follow. The factors in the equations will be discussed separately and underlined. Graphs will be used to depict the effects calculated by the equations. Mass breakdowns of ac filters designed for different operating conditions are located in Appendix A on page A-5. Note that none of these mass breakdowns is highlighted. This is because none of the individuals consulted felt the present masses of harmonic filters were optimized sufficiently to be used as reference designs.

Mass Coefficient

$$1FSM=\underline{0.1}*((1-0.995)/(1-FSE))*(FSAM/FSRM)*FSP_0*(FSP_0/FSRM)^{-0.03}*(FSF/20)^{-0.6}$$

$$3FSM=\underline{0.105}*((1-0.995)/(1-FSE))*(FSAM/FSRM)*FSP_0*(FSP_0/FSRM)^{-0.03}*(FSF/20)^{-0.6}$$

The single- and 3-phase ac filter stage mass coefficients were calibrated to yield specific weights of 0.1 and 0.105 kg/kWe respectively, when placed after a 1 kWe, 20 kHz inverter. This was based on the previously discussed conversation with John Biess (Ref. III-11). The mass coefficient for the 3-phase design is larger because it consists of three single-phase filters, each carrying one-third of the power. Economies of scale are lost in the current transformer as the filter power level declines. This causes the mass of the 3-phase filter to be slightly greater. The difference in masses of single- and 3-phase ac filters is illustrated in Figure 32. This figure compares the specific weights of these two designs at 10 and 20 kHz resonant frequencies.

Efficiency Factor

$$1FSM=0.1*\underline{((1-0.995)/(1-FSE))}*(FSAM/FSRM)*FSP_0*(FSP_0/FSRM)^{-0.03}*(FSF/20)^{-0.6}$$

$$3FSM=0.105*\underline{((1-0.995)/(1-FSE))}*(FSAM/FSRM)*FSP_0*(FSP_0/FSRM)^{-0.03}*(FSF/20)^{-0.6}$$

The ac filter design presented in this study contains a series resonant circuit. This circuit has the largest influence on filter efficiency and its efficiency is determined by the ESRs of the inductor and capacitor composing it. These ESRs can only be decreased by enlarging the inductor winding and core, the capacitor dielectric area, and the interconnecting lead wires. A larger filter mass will result. Since this same process occurred in the dc filter case, the efficiency factors were assumed to be the same. This factor generated the linear relationship for ac filter efficiency shown in Figure 33.

Redundancy Factor

$$1FSM=0.1*((1-0.995)/(1-FSE))*\underline{(FSAM/FSRM)}*FSP_0*(FSP_0/FSRM)^{-0.03}*(FSF/20)^{-0.6}$$

$$3FSM=0.105*((1-0.995)/(1-FSE))*\underline{(FSAM/FSRM)}*FSP_0*(FSP_0/FSRM)^{-0.03}*(FSF/20)^{-0.6}$$

A redundancy factor accounts for the additional mass needed to realize a more reliable system. The actual number of modules in the assembly is defined by the "available modules" value. The number of modules needed to provide full power is defined by the "required modules" value. A design requiring 4/3 redundancy has four 33% rated channels. The mass of this assembly will be at least 33% heavier and the mass of the fourth channel is part of the penalty associated with this higher reliability requirement.

Power Level Multiplier

$$1FSM=0.1*((1-0.995)/(1-FSE))*(FSAM/FSRM)*\underline{FSP_0}*(FSP_0/FSRM)^{-0.03}*(FSF/20)^{-0.6}$$

$$3FSM=0.105*((1-0.995)/(1-FSE))*(FSAM/FSRM)*\underline{FSP_0}*(FSP_0/FSRM)^{-0.03}*(FSF/20)^{-0.6}$$

These equations can calculate the mass or specific weight of the ac filter. If the power level multiplier is included, the mass of the ac filter will be calculated; removing it produces the filter's specific weight.

Power Level Factor

$$1FSM=0.1*((1-0.995)/(1-FSE))*(FSAM/FSRM)*FSP_0*\underline{(FSP_0/FSRM)^{-0.03}}*(FSF/20)^{-0.6}$$

$$3FSM=0.105*((1-0.995)/(1-FSE))*(FSAM/FSRM)*FSP_0*\underline{(FSP_0/FSRM)^{-0.03}}*(FSF/20)^{-0.6}$$

The heaviest element in the ac filter is the current transformer. As the filter power level increases and the size of this transformer grows, its core is better utilized, and the winding current density increases slightly. These economies of scale reduce the current transformer specific weight by the 0.08 power as the filter power level rises. Similar evaluations of the inductor, capacitor,

Figure 32

AC FILTER SPWT VS POWER (1-PHASE & 3-PHASE COMPARISON)

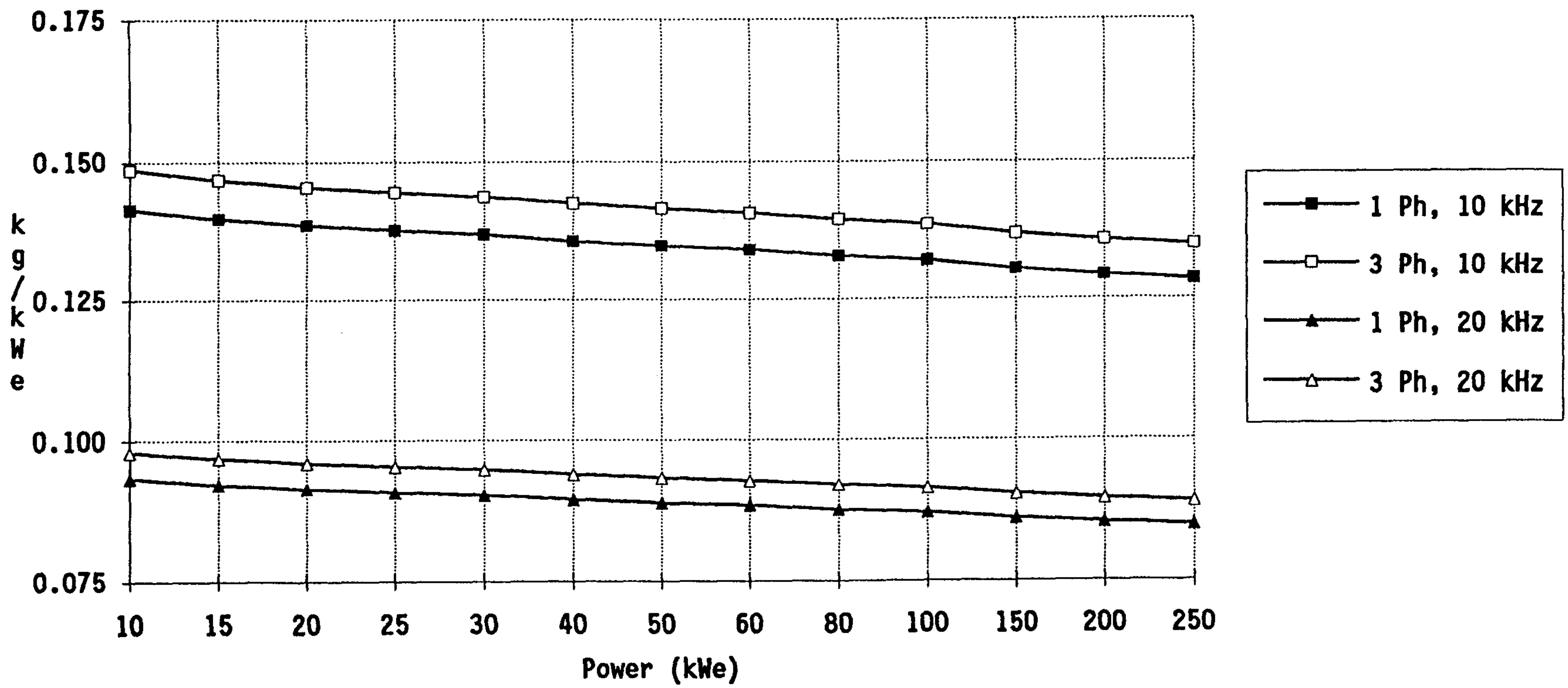

Figure 33

AC FILTER SPWT VS EFFICIENCY

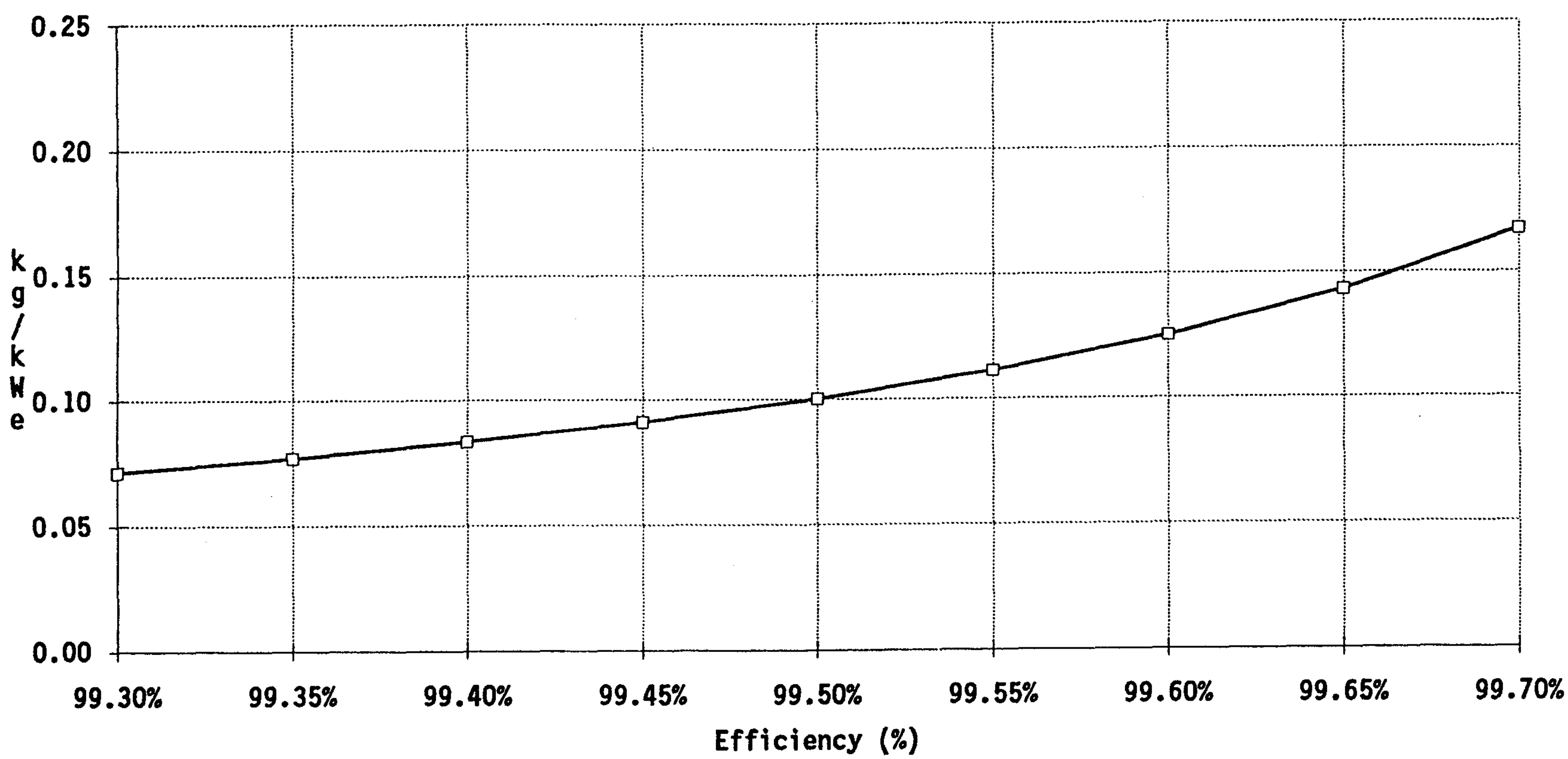

and resistor specific weights indicate they do not change with power level. Combining the specific weight properties of all the elements in the ac filter indicates the specific weight of the complete filter will decline at the 0.03 power as the ac filter power level grows. This influence is shown in Figure 34 for 10, 20, and 40 kHz single-phase ac filter designs.

The "required modules" figure is included in this factor to address the use of a modular design approach. The total output power of the assembly must be divided by the required number of modules since each module processes just a portion of this power. Because the specific weight of an ac filter changes with power, its mass must be calculated at the power level of the individual modules and not the power level of the complete assembly.

Frequency Factor

$$1FSM=0.1*((1-0.995)/(1-FSE))*(FSAM/FSRM)*FSP_0*(FSP_0/FSRM)^{-0.03}*\underline{(FSF/20)^{-0.6}}$$

$$3FSM=0.105*((1-0.995)/(1-FSE))*(FSAM/FSRM)*FSP_0*(FSP_0/FSRM)^{-0.03}*\underline{(FSF/20)^{-0.6}}$$

The combined impact of frequency on ac filter mass was determined by evaluating the influence frequency had on the current transformer, the series resonant circuit, and the resistor masses. The mass of the current transformer core will decline with increasing frequency because the flux density needed to generate a given voltage declines as frequency rises. This lower flux density reduces the transformer core volume and mass. A smaller core means less winding mass because the mean length of the turns is less. Totaling the overall effect shows the current transformer specific weight declines at the 0.47 power as frequency rises. The resonant frequency of the series resonant circuit is calculated with the following equation.

$$F_R=1/(LC)^{0.5}$$

Where: F_R is the resonant frequency,
L is the circuit inductance in Henries,
C is the circuit capacitance in Farads.

By inspection one can see the circuit inductance and capacitance must double if the resonant frequency is cut in half. This causes the inductor and capacitor mass to double and shows that the mass of a series resonant circuit is inversely proportional to frequency. The final element in the filter, the resistor, is unaffected by frequency. By adding these individual frequency effects together, a frequency factor was generated for the complete ac filter. This calculation indicated the specific weight of an ac filter would decline by the 0.6 power as its resonant frequency rose. The combined influence of frequency on filter mass is shown in Figure 35 for 1 and 40 kWe single-phase ac filter designs.

Voltage Factor

The current transformer contained in the ac filter is necessary to obtain reasonable values for the inductor and capacitor and to reflect adequate resistance into the line to inhibit harmonics. Consequently, the effects of different operating voltages on the resonant circuit elements and the resistor can be offset by selecting the proper turns ratio for this transformer. This means the only item that will be impacted by varying the voltage level is the current trans-

Figure 34
AC Filter SPWT vs Power Level

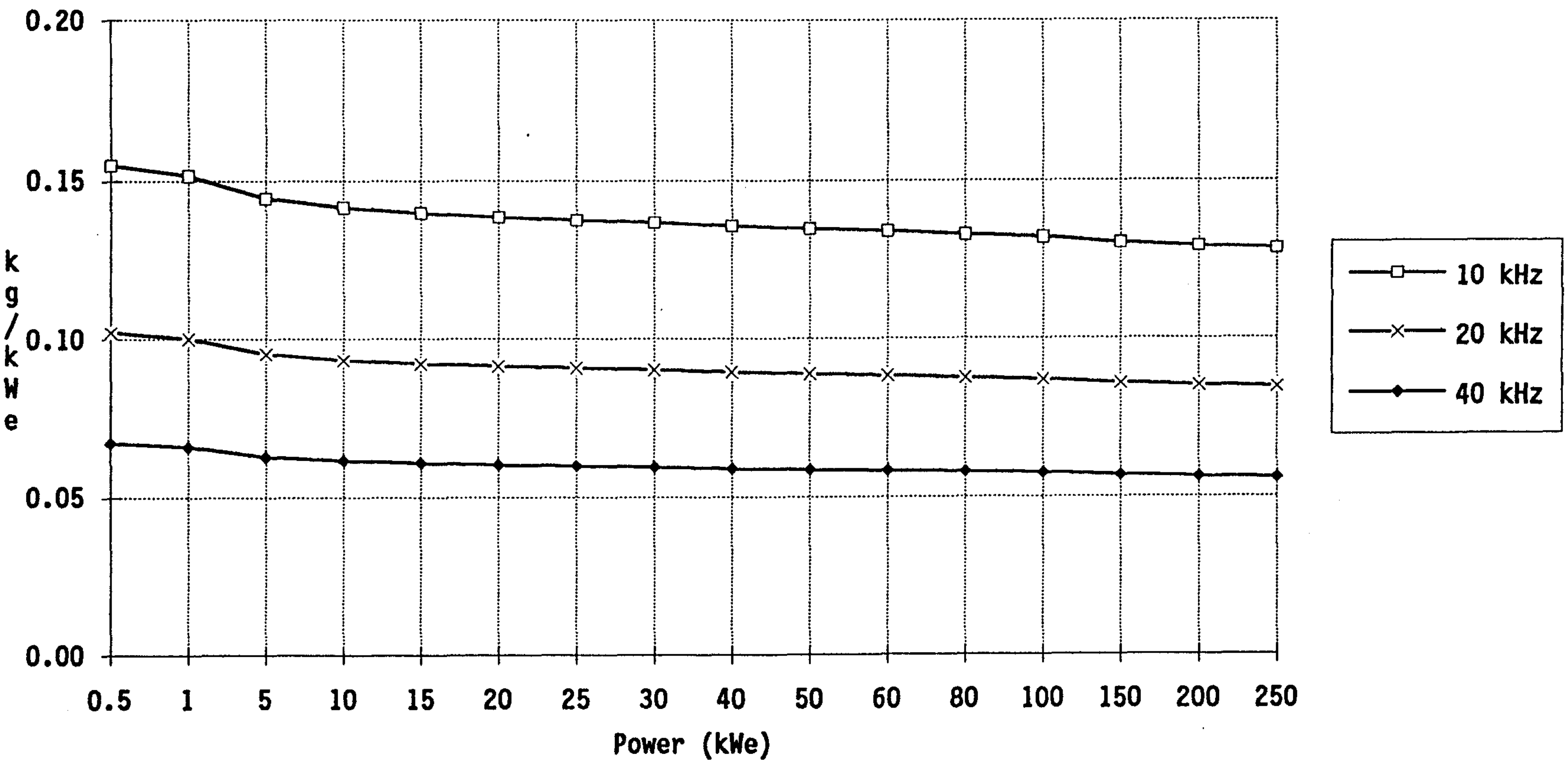

Figure 35

AC Filter SPWT vs Frequency
Single-Phase Design

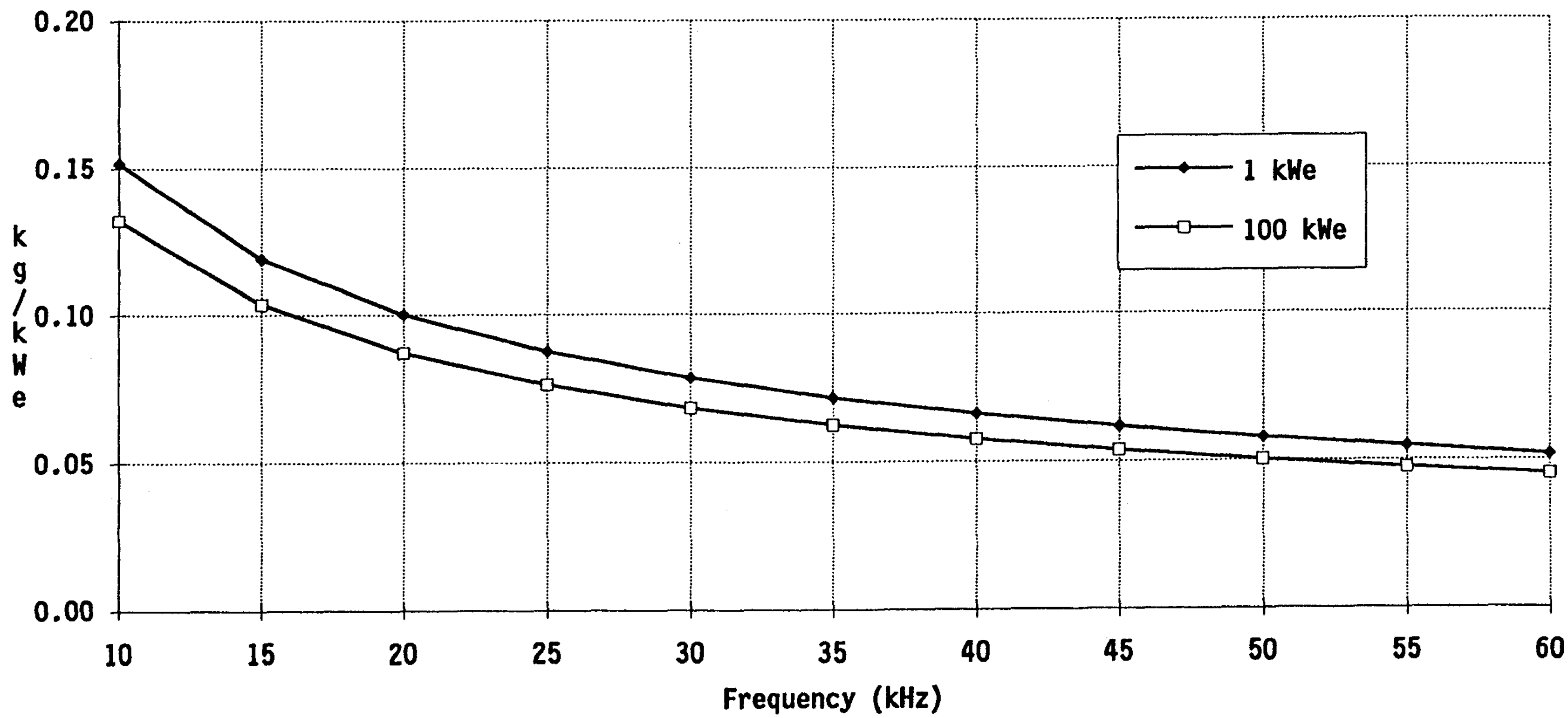

former itself. The effect of voltage on a transformer was previously investigated in section 3.1.2.1 and it was shown to be fairly minor. Since the transformer is only one element in the filter, the cumulative effect will be even less. After a short analysis, it was considered negligible and a factor was not included in the equations.

3.1.6 Ancillary Hardware Equations

Every power conditioning component requires ancillary hardware to perform its functions. In this report, the component ancillary hardware is considered to consist of the following items: power conductors and connectors, a control and monitoring subsystem, an enclosure, and a radiator. These items will be addressed individually in the subsequent sections.

3.1.6.1 Power Conductor and Connector Equations

Within a power conditioning component, conductors are required for internal power distribution. This section establishes a mass for the input and output power conductors and the conductors that transfer power from one stage to the next. It should be noted that the conductor mass value referred to here is only for power conductors, and not control and monitoring wiring. The wiring within a particular stage, for example the wiring in the chopper stage that interconnects its switches and tank hardware, is also not included. The control and monitoring wiring will be covered in section 3.1.6.2, and the wiring within the chopper stage was already included as part of the ancillary hardware mass referred to in section 3.1.1.

Power conductors and connectors are primarily sized on the basis of current; therefore, the conductor and connector mass is a function of the maximum steady state current levels within a component. If a voltage transformation occurs in the component, it is necessary to include separate factors for the input and output current levels. The information used to develop the following equations was obtained from SSF documentation (Ref. III-6, III-8, III-31). Table 13 defines the variables used in the equations. These equations are based on copper conductors because copper is more ductile and occupies a smaller volume than aluminum. Separate equations are provided for single- and 3-phase systems because the conductor sizes are calculated differently.

Table 13
Conductor and Connector Equation Variable Definitions

1CCM	Single-Phase Conductor and Connector Mass
3CCM	3-Phase Conductor and Connector Mass
CE	Component Efficiency
AM	Available Modules
RM	Required Modules
P_O	Power Output (kWe)
V_I	Voltage Input ($Vrms_{L-L}$ or Vdc)
V_O	Voltage Output ($Vrms_{L-L}$ or Vdc)

Single-Phase, 1 Voltage: $1CCM=0.056*(AM/RM)*((P_O*1000)/V_O)$

Single-Phase, 2 Voltages: $1CCM=(AM/RM)*(0.028*((P_O*1000)/V_O)$
$+0.028*(((P_O*1000)/CE)/V_I))$

3-Phase, 1 Voltage: $3CCM=(3^{0.5}/2)*0.056*(AM/RM)*((P_O*1000)/V_O)$

3-Phase, 2 Voltages: $3CCM=(AM/RM)*((3^{0.5}/2)*0.028*((P_O*1000)/V_O)$
$+(3^{0.5}/2)*0.028*(((P_O*1000)/CE)/V_I))$

3.1.6.2 Control and Monitoring Subsystem Mass and Parasitic Power Equations

Each of the power conditioning components will have some type of control and monitoring subsystem. This subsystem was assumed to consist of a controller card, a data interface module, a control and monitoring wiring harness, and various voltage, current, and temperature sensors. A component controller card responds to higher level commands and performs the minute steps necessary to implement these commands. Typical commands might inform a unit to change its output voltage setpoint or make the latest device temperatures available to the data bus. The monitoring system provides data on the component operating status to the internal controller or higher level computers. A data interface module, normally composed of numerous analog to digital conversion circuits, is required to convert the sensor signals into the proper form for data bus transmission.

SSF component documentation was utilized to formulate the control and monitoring mass equations (Ref. III-6, III-8, III-31). Table 14 defines the variables used in these equations. Because a 3-phase system has nearly three times as much monitoring data to collect and process, separate equations are provided for single- and 3-phase systems. The equations are broken into three parts, the controller card and data interface module, the control and monitoring wiring, and the sensors.

Table 14
Control and Monitoring Equation Variable Definitions

1CMM	Single-Phase Control and Monitoring Mass
3CMM	3-Phase Control and Monitoring Mass
1CMP	Single-Phase Control and Monitoring Power
3CMP	3-Phase Control and Monitoring Power
AM	Available Modules
RM	Required Modules
P_o	Power Output (kWe)

Single-Phase Mass: $1CMM=AM*(1.4+0.9*(P_o/RM)^{0.3}+0.25*(P_o/RM)^{0.3})$

3-Phase Mass: $3CMM=AM*(2+2.5*(P_o/RM)^{0.3}+0.75*(P_o/RM)^{0.3})$

Single-Phase Power: $1CMP=AM*55.6*(P_o/RM)^{0.1}$

3-Phase Power: $3CMM=AM*79.4*(P_o/RM)^{0.1}$

The present mass of a SSF component controller card and data interface module is 2.8 kg. Based on the rapid progress occurring in control and data processing, it was felt this value would decline 50% by the year 2000. A value of 2 kg was assumed for a 3-phase component due to the additional data handling requirements.

From SSF component mass breakdowns, it was determined that the average mass of a control and monitoring wiring harness for a component rated at around 10 kWe was about 3.6 kg. This value was expected to decline about 50% with the introduction of fiber optics (Ref. III-11). By replacing much of the present copper wiring with fiber optic cables, it was anticipated that the mass of the control and monitoring wiring could be reduced to 1.8 kg. Because a 3-phase system has nearly three times as many control devices and sensors, its wiring was estimated to weigh 5 kg. As a component's power level grows, its volume increases proportionally. Consequently, its linear dimensions increase by the cube root of the power, and the length of the control and monitoring wiring harness grows likewise. This accounts for the 0.3 exponent in this factor. Based on this previously described analysis, the single- and 3-phase control and monitoring wiring factors were designed to yield values of 1.8 kg and 5 kg respectively for 10 kWe rated components.

Again using SSF component mass breakdowns, a value of 0.6 kg was estimated for the mass of the monitoring sensors in a typical 10 kWe component. Anticipating technology improvements by the year 2000, this value was reduced to 0.5 kg. A 3-phase system should have almost three times as many sensors; hence, a value of 1.5 kg was used for it. The mass of the sensors will increase as the component power levels rise. A potential transformer used to measure high voltages will weigh considerably more than one measuring low voltages. It was estimated that the mass of the sensors would roughly double when the component power level went up by a factor of ten. To obtain this mass gain as power grew, an exponent of 0.3 was included in the sensor mass factor. The sensor mass factors were calibrated to yield 0.5 and 1.5 kg respectively for single- and 3-phase 10 kWe components.

Power must be obtained from the component input to operate the control and monitoring subsystem, the semiconductor switch gate drive circuitry and control logic, the control power converters, relay coils, heaters, etc. In this report, these power requirements are referred to as the parasitic power demand. An engineering information document written to describe the operation of the SSF electrical power system indicated the parasitic power demands of components rated for around 10 kWe would be approximately 100 watts (Ref. III-32). Since the largest portion of this power is demanded by the control and monitoring subsystem and improvements are expected in this area by the year 2000, this value has been reduced to 70 watts. 3-phase components contain more sensors and control devices. The additional power needed for these devices was expected to be about 30 watts; consequently, the parasitic power demand of a 10 kWe 3-phase component was judged to be 100 watts. It is expected that parasitic power demands will rise slowly as component power levels increase, because certain control and monitoring devices will need more power to perform their functions. The exponent 0.1 was included in the factor to account for these gradual power increases.

3.1.6.3 Component Volume, Dimension, and Enclosure Equations

Regardless of the power level, the density of the electronics in power conditioning components operating under similar conditions will normally be comparable. To determine an appropriate component electronics density, the electronics densities of several SSF components were computed. This information is presented in Table 15.

Table 15
SSF Power Conditioning Component Densities

Component	Electronics Density (grams/cubic cm)
DC/DC Converter Unit	0.293
DC Switching Unit	0.332
Battery Charge/Discharge Unit	0.282
Main Bus Switching Unit	0.338
Average	0.311

Assuming a 10% improvement in packaging densities will be realized by the year 2000, a value of 0.342 grams/cubic centimeter was used. Using this density, the component volume can be calculated using the following formula:

$$CV=CEM/(0.342*1000)$$

where: CV = Component Volume in cubic meters
CEM = Component Electronics Mass in kilograms

Knowing the component volume, it is possible to generate dimensions for the component. Referring to dimensions reported for SSF enclosures, the following per unit aspect ratios were determined for a typical component: height, 0.7; width, 1.1; and length, 1.3. Using these aspect ratios and computing the cube root of the volume, the component height, width, and length can be calculated.

$$Height=0.7*CV^{0.3333}$$

$$Width=1.1*CV^{0.3333}$$

$$Length=1.3*CV^{0.3333}$$

A component requires an enclosure to provide protection from the environment, but enclosure types vary depending on the application. Two types are mentioned here and offered as options in the models. The first type uses a finned heat exchanger to transfer heat from an internal component baseplate to an external coldplate assembly. The finned heat exchanger concept is relatively heavy and has a higher temperature drop than other approaches, but it was selected for the SSF to allow replacement of the power conditioning units. An advanced concept would replace the finned heat exchanger with high density fiber pads constructed from graphite or copper. These pads would rely on both fiber to fiber contact and radiation to pass heat between the surfaces and resemble two carpets laid face to face. Recent advances in this area indicate this technique is feasible and it definitely deserves further study. However, because there was not any concrete information available, it was not included in the models. The second approach mounts the electronics directly on a coldplate and relies on a fluid that is pumped through the coldplate for heat removal. For this approach, some type of quick disconnect is required. Only the coldplate mass is addressed, not the quick disconnect mass.

The enclosure consists of different parts, the housing, connector structure, mounting hardware, and depending on the concept a radiant fin baseplate or coldplate. The following breakdown was obtained for the orbital replacement unit (ORU) Type I box from SSF documentation (Ref. III-6). The Type I box is 68.6 cm in length, 58.4 cm in width, and 30.5 cm high.

Table 16
SSF ORU Box Mass Breakdown

Enclosure Subassembly	Mass (kg)
Box Housing	8.2
Connector Structure	0.6
Mounting Hardware	5.3
Radiant Fin Baseplate	13.4
Total	27.5

Of the radiant fin baseplate mass, about 50% is dedicated to the radiant fins, and the remainder is the aluminum baseplate and heat exchanger piping.

It is anticipated that carbon-carbon will replace much of the aluminum in future enclosures. The density of aluminum is 2.7 g/cm^3, carbon-carbon is 1.65 g/cm^3. This represents a reduction of about 39%. It will probably be impractical to replace the connector structure and mounting hardware materials with carbon-carbon, but it should be fine for the box housing. This would reduce the box housing, connector structure, and mounting hardware mass from 14.1 kg to 10.9 kg. Regarding the radiant fin baseplate, it was assumed that only the aluminum baseplate and heat exchanger piping could utilize carbon-carbon. This replacement reduced their mass from 6.7 kg to 4.1 kg. Anticipated difficulties in fabricating the radiant fins, precluded the use of carbon-carbon for this piece of hardware. Table 17 lists the projected mass breakdowns for the finned heat exchanger and coldplate enclosure concepts that were utilized as the basis for the subsequent enclosure equations.

Table 17
Projected Enclosure Mass Breakdowns

Enclosure Subassembly	Finned Heat Exchanger Enclosure Mass (kg)	Coldplate Enclosure Mass (kg)
Box Housing	5.0	5.0
Connector Structure	0.6	0.6
Mounting Hardware	5.3	5.3
Baseplate or Coldplate	4.1	4.1
Radiant Fins	6.7	N/A
Total	21.7	15.0

The enclosure mass is closely related to the component volume. Using a perfect cube as an example, the volume is the length of a side cubed, while the surface area is 6 times the length of a side squared. Therefore, the surface area is related to the volume by the 2/3 power or 0.6666. The enclosure mass is directly derived from the surface area. Depending on the enclosure type being considered, the mass of the baseplate and radiant fins, or the mass of the coldplate, is a function of the bottom side of the box. This is simply the length times the width. This logic was used to develop the following equations.

$$FHEM=44.26*CV^{0.6666}+27*(L*W)$$

$$CPEM=44.26*CV^{0.6666}+10.25*(L*W)$$

where: FHEM = Finned Heat Exchanger Enclosure Mass in kilograms
CPEM = Coldplate Based Enclosure Mass in kilograms
CV = Component Volume in cubic meters
L = Length in meters
W = Width in meters

The factor "$44.26*CV^{0.6666}$" calculates the mass of the box, connector structure and mounting hardware; the factors "27*(L*W)" or "10.25*(L*W)" estimate the mass of the finned heat exchanger baseplate and fins, or the coldplate. The coefficients "44.26", "27", and "10.25" were calibrated to yield enclosure mass estimates that are in agreement with the above mass breakdowns.

3.1.6.4 Radiator Area and Mass Equations

A radiator is used to dissipate waste heat generated in a power conditioning component. For the equation development, a two sided radiator was selected. It was assumed to be a vertical flat plate that stood under 4.5 meters in height. The mass of the radiator was calculated from the component power losses and the effective radiator and lunar surface sink temperatures. The radiator surface temperature was computed by assuming a 16.7° C temperature delta existed between the electronics coldplate and the radiator surface. Using a reflective blanket that was placed on the lunar surface, the effective sink temperature was reduced to 250 K.

$$RA=(1.1212E+10*Q)/(T^4-T_s^4)$$

$$RM=4.159*RA$$

where: RA = Radiator Area in square meters
RM = Radiator Mass in kilograms
Q = Heat to be Dissipated in kWt
T = Radiator Surface Temperature in Kelvin
T_s = Radiator Sink Temperature in Kelvin
(250 K is recommended)

The equations utilized a radiator efficiency of 0.873 and mass per square meter coefficient of 4.159. These values were calculated using Rocketdyne radiator codes. The radiator surface emissivity was assumed to be 0.9.

3.1.7 DC RBI Model

Dc remote bus isolators (RBIs) are smart circuit protection devices that incorporate current sensors and are used to switch dc power and interrupt fault currents. They will be located in dc switchgear units. This section discusses the equation developed to estimate their masses as a function of power, efficiency, and voltage. This equation is only capable of providing rough mass estimates for component comparison purposes. For more accurate mass estimates specific component designs will need to be developed.

The latest dc RBI switchgear design uses a channelized approach because the card cage assembly that controls and monitors the dc RBI operation can be shared among several units. A single RBI channel can assume three different configurations, a mechanical relay, a hybrid arrangement consisting of a mechanical relay paralleled with a semiconductor switch, or a semiconductor switch. The SSF RBIs use a mechanical relay and add a snubber circuit to suppress voltage transients occurring during opening and closing periods. A hybrid arrangement has certain advantages because the relay and semiconductor switch can function together to improve the operating characteristics of the RBI switch. The relay carries the bulk of the current during normal operation; this results in a high efficiency switch. The main need for the semiconductor switch is during opening and closing times. It closes immediately before relay closing to quell relay chatter transients, and it opens after the relay to suppress opening transients. The opening rate of the semiconductor can be varied to obtain the best opening characteristics. The design that only uses a semiconductor switch exhibits very good opening and closing characteristics, but the conduction resistance of a semiconductor is higher than a relay contact so the switch losses are significantly higher during normal operating periods.

The dc RBI model described in this report is based on a hybrid switch configuration. This design was considered to provide the best combination of mass, efficiency, and switching characteristics. However, as the RBI voltage rises the switch design will probably change from a relay in parallel with a single semiconductor to a vacuum switch in parallel with a number of series connected semiconductors. At the present time, the semiconductor devices in a dc RBI would probably be MOSFETs or insulated gate bipolar transistors (IGBTs). Future RBI designs will probably use MCTs. Mass breakdowns for dc RBIs are shown in Appendix A on page A-6 and A-7. These mass estimates were derived from a SSF RBI mass breakdown and information obtained from a Ford Aerospace briefing package (Ref. III-6, III-31). The RBI efficiency was calculated from RBI loss information contained in a SSF document written by Rocketdyne (Ref. III-33). They were utilized as a basis for the subsequent equation development.

The following paragraphs explain the dc RBI equation development. Graphs are used in conjunction with technical descriptions to explain the equation rationale. The variables used in this discussion are shown in Table 18.

Table 18
Dc RBI Model Variable Definitions

DRBM	Dc RBI Mass
DRBE	Dc RBI Efficiency (99.85%)
DRBAM	Dc RBI Available Modules
DRBRM	Dc RBI Required Modules
$DRBP_o$	Dc RBI Power Output (kWe)
$DRBV_o$	Dc RBI Voltage Output (Vdc)

Mass Coefficient

$$DRBM=\underline{0.12}*((EXP(0.0008/(1-DRBE)))/1.7)*(DRBAM/DRBRM)*DRBP_o*(DRBP_o/DRBRM)^{-0.15}*(DRBV_o/200)^{0.13}$$

The dc RBI mass coefficient was developed from SSF dc RBI mass breakdowns. To be consistent with the previously discussed future design, the design of the SSF dc RBI was revised to include a semiconductor switch in parallel with the mechanical relay, the snubber circuitry was removed since it was no longer required, and mass benefits obtained from minor hardware advancements were incorporated. Mass breakdowns of future dc RBIs are contained in Appendix A on pages A-6 and A-7. The mass coefficient was calibrated to yield values consistent with these mass breakdowns.

Efficiency Factor

$$DRBM=0.12*\underline{((EXP(0.0008/(1-DRBE)))/1.7)}*(DRBAM/DRBRM)*DRBP_0*(DRBP_0/DRBRM)^{-0.15}*(DRBV_0/200)^{0.13}$$

The above underlined factor estimates the change in specific weight occurring with a change in dc RBI efficiency. The efficiency of an RBI is quite high and it does not appear practical to change it much. However, it can be increased by reducing the resistances of the relay contacts and semiconductor. To accomplish this, the conduction areas of these elements must be enlarged. Basically, doubling the masses of the relay contacts and semiconductor switch will cut their losses in half. Since the losses are cut in half, the thermal management hardware changes likewise. The rest of the RBI elements will also change slightly to conform to the new relay, semiconductor, and thermal management hardware designs. The variation in RBI mass was estimated for efficiencies ranging from 99.8 to 99.9% and it was used to generate the above efficiency factor. A graph of RBI specific weights that shows the results of this analysis is contained in Figure 36. Note that the depicted dc RBI efficiency range is relatively narrow. Efficiencies higher than about 99.9% are not considered practical because the relay contact and semiconductor switch size will become unwieldy. It is not feasible to cut the RBI mass below a certain level because the relay contacts, semiconductor switch, and structural hardware simply will not be strong enough to withstand the stresses encountered while interrupting a fault current.

Redundancy Factor

$$DRBM=0.12*((EXP(0.0008/(1-DRBE)))/1.7)*\underline{(DRBAM/DRBRM)}*DRBP_0*(DRBP_0/DRBRM)^{-0.15}*(DRBV_0/200)^{0.13}$$

The mass of a dc RBI network will rise if a modular design approach is used to enhance reliability. The mass increase is estimated by the factor above. The "available modules" number is the actual number of modules present in the component; the "required modules" value is the actual number of modules required to provide the full output power level. If the reliability requirements of a system force a design to use 4/3 redundancy, each channel is designed to carry 33% of the power. Although 4 channels are available, only 3 channels are needed to supply full power. The mass of the fourth channel is the penalty paid to obtain the higher specified reliability.

Power Level Multiplier

$$DRBM=0.12*((EXP(0.0008/(1-DRBE)))/1.7)*(DRBAM/DRBRM)*\underline{DRBP_0}*(DRBP_0/DRBRM)^{-0.15}*(DRBV_0/200)^{0.13}$$

The equation can be used to calculate the mass or specific weight of the dc RBI. When the above multiplier is included, the value that results estimates the RBI mass. To obtain the specific weight of the RBI, remove this multiplier.

Figure 36

DC RBI SPWT vs Efficiency

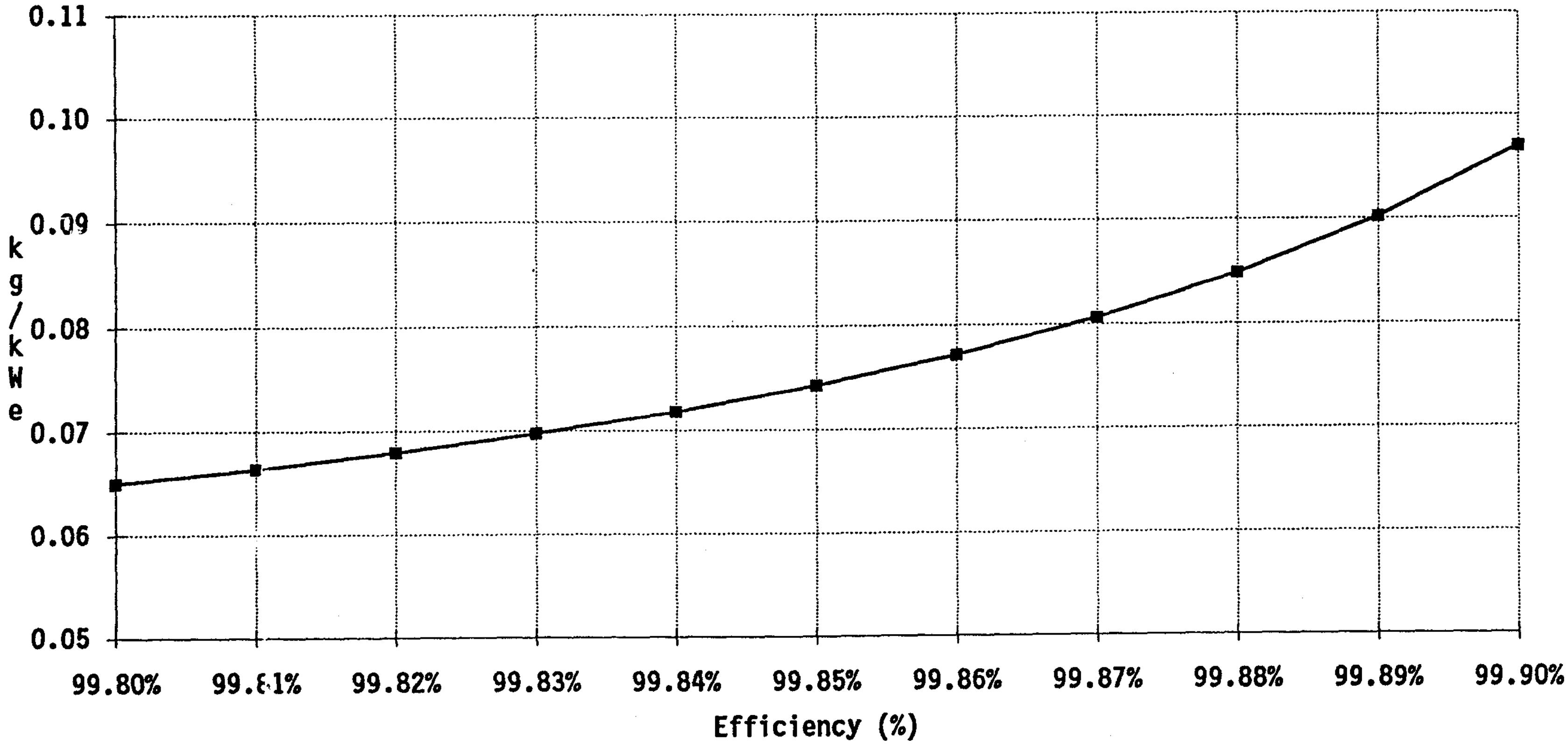

Power Level Factor

$$DRBM=0.12*((EXP(0.0008/(1-DRBE)))/1.7)*(DRBAM/DRBRM)*DRBP_0*\underline{(DRBP_0/DRBRM)^{-0.15}}*(DRBV_0/200)^{0.13}$$

The masses of the power conducting parts of the dc RBI, which are the relay contacts and the semiconductor switch, will increase nearly linearly with a rise in power. However, the mass of supporting hardware elements, such as driver modules, sensors, and control logic devices, grows at a slower rate. This results in some economies of scale as the dc RBI power level rises and causes its specific weight to decline. The change in the specific weight of a dc RBI as the power level rises is shown in Figure 37.

Voltage Level Factor

$$DRBM=0.12*((EXP(0.0008/(1-DRBE)))/1.7)*(DRBAM/DRBRM)*DRBP_0*(DRBP_0/DRBRM)^{-0.15}*\underline{(DRBV_0/200)^{0.13}}$$

As the voltage across a dc RBI increases, its mass was expected to rise at a slightly higher rate. This is because the elements in the RBI must be further isolated, more insulation is required, and the stresses are higher. The separation distance between the relay contacts in a dc RBI will need to increase as the voltage level rises to prevent vacuum breakdown and arcing. The mass of the semiconductor switch in parallel with the relay is also expected to rise. The semiconductor devices will need to be connected in series to handle higher voltages; however, series connected semiconductors do not inherently share voltages evenly. Additional hardware is needed to make them voltage share and protect them in case they do not. Finally, dc systems normally require capacitors to maintain voltage stability. Unfortunately, the capacitors will discharge into a fault and greatly increase the initial fault current. The RBI must be structurally strong enough to withstand the added stress of this discharge. Each of these factors increases the mass of the complete RBI. By referring to terrestrial RBI designs, an estimate of this mass increase was developed and it was utilized to generate the factor shown above. The results of this exercise are shown in Figure 38.

3.1.8 AC RBI Model

Ac RBIs are smart circuit protection switches that include current sensors. They are used to switch major ac power feeds and interrupt faults. They will be located in ac switchgear units. The equations developed to estimate ac RBI mass as it varies with power and voltage are discussed in this section. The equations provide rough mass estimates for component comparison purposes. For more accurate mass estimates specific component designs will need to be developed.

The ac RBI design will be similar in most respects to the dc RBI design. An ac RBI switchgear unit will also use a channelized approach because the card cage assembly that controls and monitors ac RBI operation can be shared between several RBIs. Two configurations are practical for an ac RBI channel, a hybrid arrangement consisting of a fast acting mechanical relay paralleled with a back-to-back pair of semiconductor switches, or just a back-to-back pair of semiconductor switches. A solitary mechanical relay is not fast enough to open during the zero current crossing; consequently, this configuration is not practical.

Figure 37

DC RBI SPWT vs Power Level

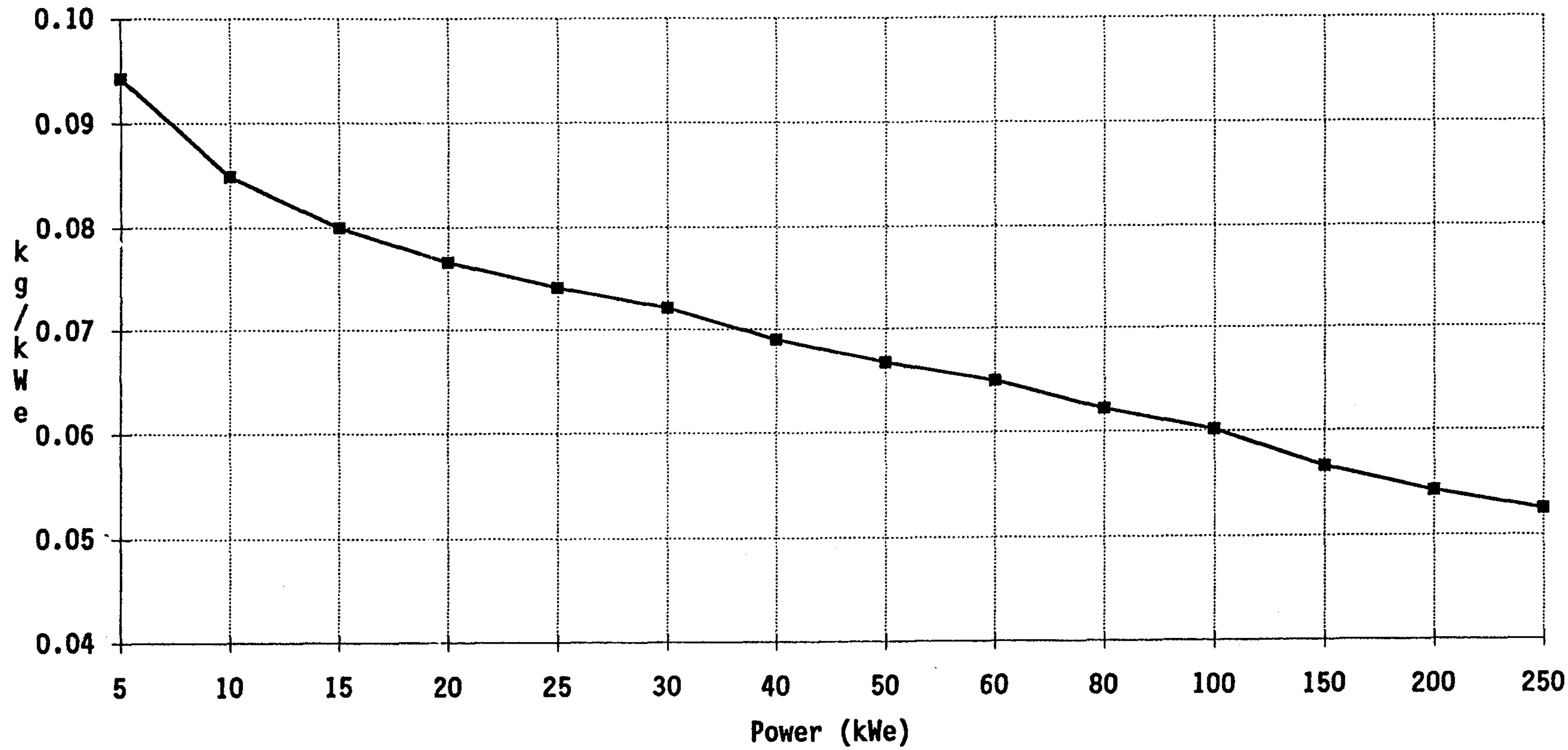

DRBIGRPH.XLS

9/16/91

Figure 38
DC RBI SPWT vs VOLTAGE

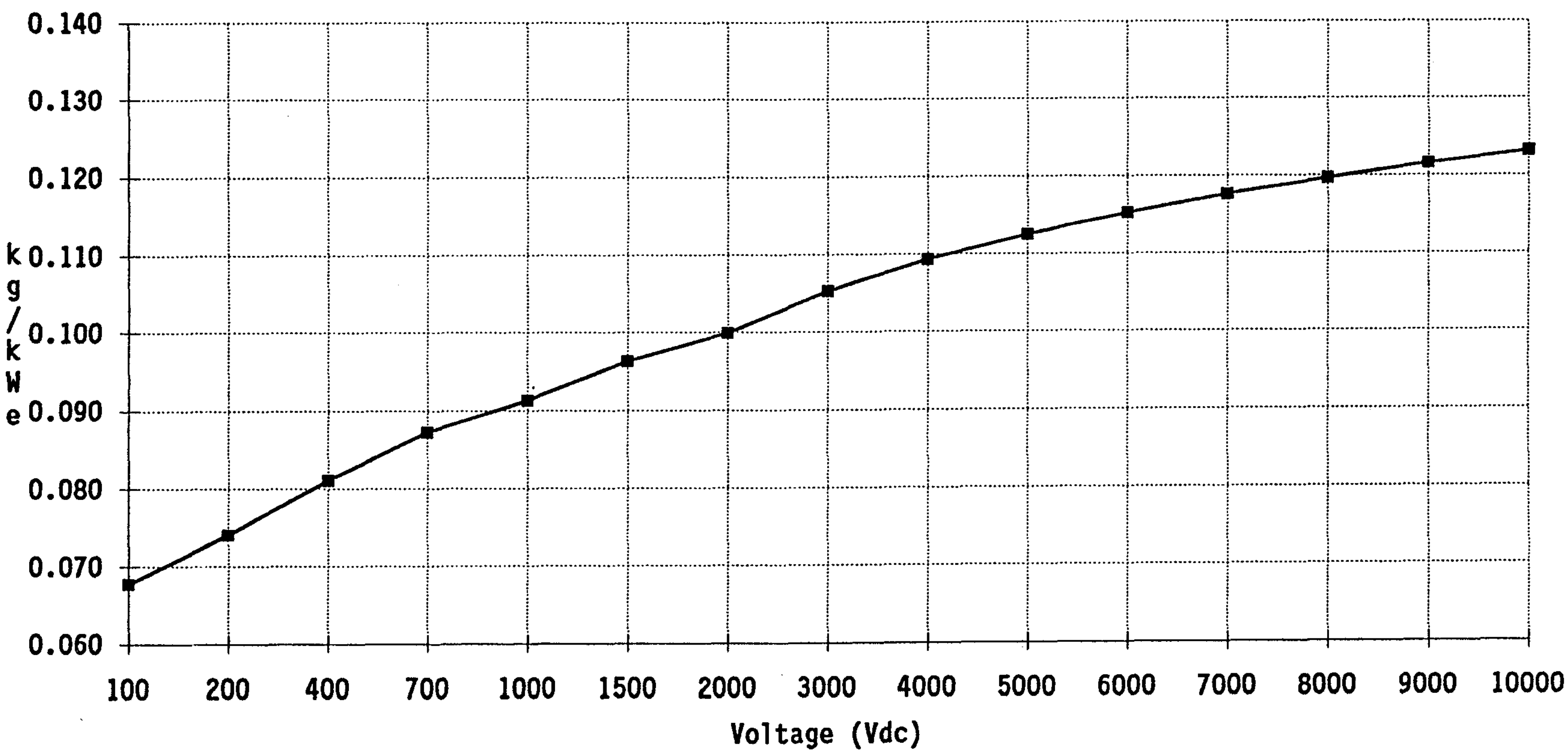

The hybrid arrangement is preferred because the relay and semiconductor switch can work together to improve the operating characteristics of the RBI switch. During normal power delivery periods, the relay carries the bulk of the current. The mechanical relay contacts greatly reduce conduction losses and allow high efficiency operation. The semiconductor switches are primarily required during opening and closing times. Only semiconductor switches can operate fast enough to close or open within the zero current crossing point limits. The semiconductor switches are closed immediately before relay closing to quell relay chatter transients, and opened after the relay to suppress opening transients. An RBI design using just semiconductor switches exhibits very good opening and closing characteristics; however, its conduction losses are much higher than a hybrid design with a relay. Consequently, the efficiency of this ac RBI design would be much poorer.

The ac RBI model described in this report is based on a hybrid switch configuration. This design was considered to provide the best combination of mass, efficiency, and switching characteristics. However, as the RBI voltage rises the RBI switch design will probably change from a relay in parallel with a single semiconductor to a vacuum switch in parallel with a number of series connected semiconductors. At the present time, the semiconductor devices in an ac RBI are typically SCRs. Future RBI designs may use MCTs. The mass breakdowns that were used as a basis for the development of an ac RBI mass estimation equation are in Appendix A on page A-8 and A-9. In a telephone conversation with Dave Fox of Westinghouse, he indicated that ac and dc RBIs rated to conduct the same amount of power would have similar masses (Ref. III-34). The data bus interface and control elements in the ac RBIs would probably be the same as those in the dc units. The relay in an ac RBI would be lighter because the existence of a zero current crossing point eases fault current interruption; however, the mass of the ac RBI must include the mass of a back-to-back pair of semiconductor switches and their drivers. Based on this discussion the masses of many of the elements in an ac RBI were obtained from the SSF dc RBI mass breakdown (Ref. III-6).

The ensuing paragraphs explain the development of single-phase and 3-phase ac RBI equations in detail. The equation formulation is explained via technical descriptions and graphs. The variables used in succeeding discussions are listed in Table 19.

Table 19
Ac RBI Model Variable Definitions

1ARB	Single-Phase ac RBI Mass
3ARB	Three-Phase ac RBI Mass
ARBE	Ac RBI Efficiency (99.85%)
ARBAM	Ac RBI Available Modules
ARBRM	Ac RBI Required Modules
$ARBP_o$	Ac RBI Power Output (kWe)
$ARBV_o$	Ac RBI Voltage Output (Vrms)

Mass Coefficient

$$1ARB=\underline{0.1}*((EXP(0.0008/(1-ARBE)))/1.7)*(ARBAM/ARBRM)*ARBP_0*(ARBP_0/ARBRM)^{-0.13}*(ARBV_0/200)^{0.05}$$

$$3ARB=\underline{0.135}*((EXP(0.0008/(1-ARBE)))/1.7)*(ARBAM/ARBRM)*ARBP_0*(ARBP_0/ARBRM)^{-0.15}*(ARBV_0/200)^{0.05}$$

The SSF dc RBI mass breakdowns were used as a starting point to generate mass breakdowns for ac RBIs. The resulting ac RBI mass breakdowns were then used to determine the mass coefficients underlined above. Many elements in dc and ac RBIs will be equivalent; therefore, the masses of these dc RBI elements were also used in the ac RBI case. The size of the relay in an ac RBI is smaller, but an ac RBI requires a back-to-back pair of semiconductor switches. The reduced relay mass and the mass of these semiconductor switches and their drivers was included in the ac RBI mass breakdowns. The ac RBI mass breakdown was completed by removing the snubber circuitry included in the SSF dc RBI design and incorporating the mass gains resulting from minor hardware advancements expected over the next ten years. The mass breakdowns generated for future ac RBIs are located in Appendix A on pages A-8 and A-9. The mass coefficients contained in the ac RBI mass equations were calculated to yield values consistent with these mass breakdowns.

The mass of the relay in a 3-phase ac RBI design was estimated to be about 50% heavier due to the need for two additional contact and semiconductor switch pairs. However, because the mass of the control logic and thermal management hardware is similar in both designs and the packaging weight difference becomes less as the RBI size grows, the relative difference in mass between the two designs also declines as the power level rises. The specific weights of single- and 3-phase ac RBI designs are compared in Figure 39.

Efficiency Factor

$$1ARB=0.1*\underline{((EXP(0.0008/(1-ARBE)))/1.7)}*(ARBAM/ARBRM)*ARBP_0*(ARBP_0/ARBRM)^{-0.13}*(ARBV_0/200)^{0.05}$$

$$3ARB=0.135*\underline{((EXP(0.0008/(1-ARBE)))/1.7)}*(ARBAM/ARBRM)*ARBP_0*(ARBP_0/ARBRM)^{-0.15}*(ARBV_0/200)^{0.05}.$$

The efficiency of an ac RBI was expected to be the same as a dc RBI; the reactive parasitics associated with ac operation were expected to be negligible. The efficiency of an ac RBI can be increased by enlarging the conduction area of the relay contacts and semiconductor switches to reduce their resistance. Doubling the mass of the relay contacts and semiconductor switches should cut conduction losses in half. The mass of the thermal management hardware should decline proportionally. Other RBI elements will change slightly to conform to the new relay, semiconductor, and thermal management hardware designs. Changes in RBI mass were estimated for efficiencies ranging from 99.8 to 99.9%. Efficiencies higher than 99.9% are not considered practical because the relay contact and semiconductor switch sizes would become unwieldy. Below an efficiency of 99.8% the structural integrity of the RBI, and the strength of its relay contacts and semiconductor switches would be suspect. The RBI mass breakdowns generated dur-

ACRBI1V3.XLC

Figure 39

AC RBI SPWT
1-PHASE VS 3-PHASE

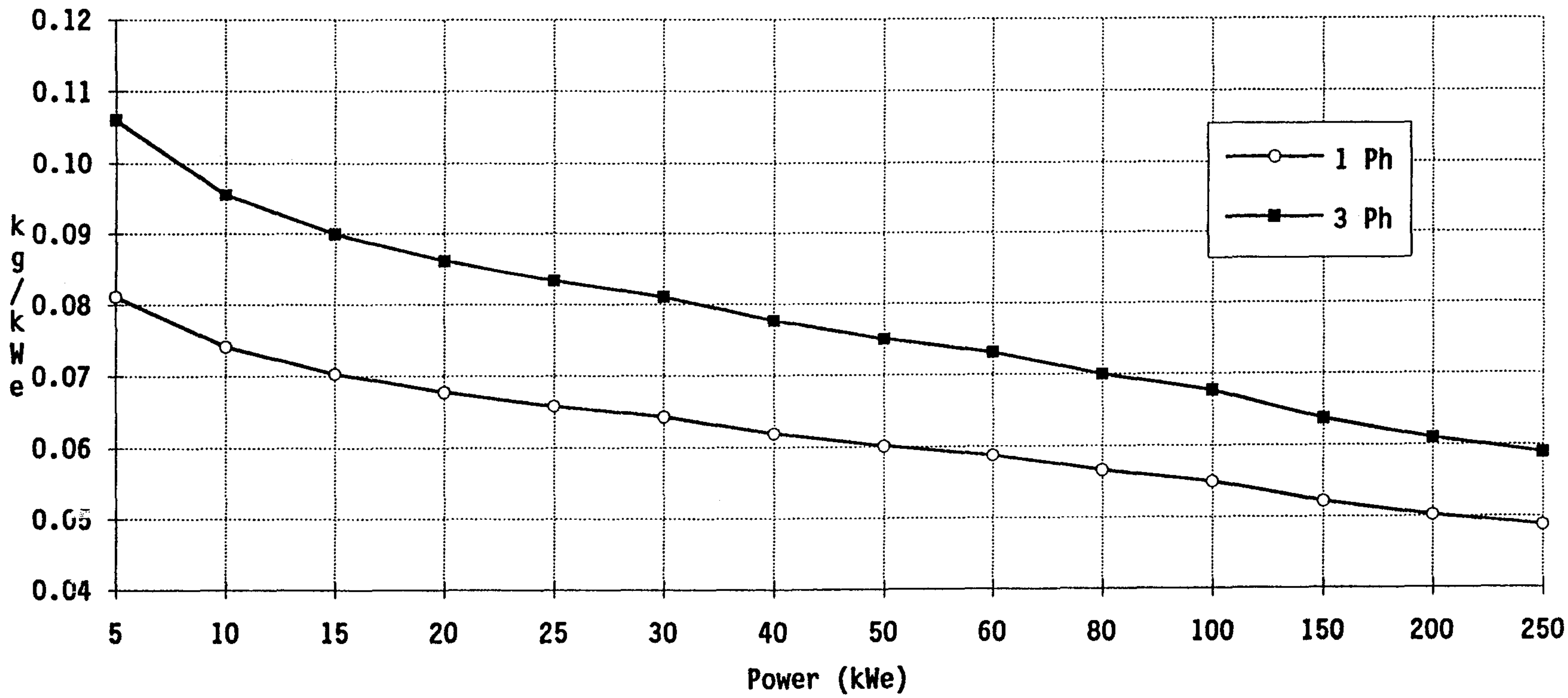

ARBIGRPH.XLS

9/16/91

ing this process were used to create the above efficiency factor. A graph of ac RBI specific weights as a function of efficiency is shown in Figure 40.

Redundancy Factor

$$1ARB=0.1*((EXP(0.0008/(1-ARBE)))/1.7)*\underline{(ARBAM/ARBRM)}*ARBP_O*(ARBP_O/ARBRM)^{-0.13}*(ARBV_O/200)^{0.05}$$

$$3ARB=0.135*((EXP(0.0008/(1-ARBE)))/1.7)*\underline{(ARBAM/ARBRM)}*ARBP_O*(ARBP_O/ARBRM)^{-0.15}*(ARBV_O/200)^{0.05}$$

If a modular design approach is used to enhance reliability, the total mass of the ac RBI units will rise. The above factor estimates this mass increase. The actual number of modules present in the system is defined by the "available modules" number; the number of modules required to deliver full power is specified by the "required modules" value. If a system is designed with 4/3 redundancy, each channel is capable of carrying 33% of the power. The fourth channel is not required to provide full power and its mass is the penalty paid to obtain a higher reliability.

Power Level Multiplier

$$1ARB=0.1*((EXP(0.0008/(1-ARBE)))/1.7)*(ARBAM/ARBRM)*\underline{ARBP_O}*(ARBP_O/ARBRM)^{-0.13}*(ARBV_O/200)^{0.05}$$

$$3ARB=0.135*((EXP(0.0008/(1-ARBE)))/1.7)*(ARBAM/ARBRM)*\underline{ARBP_O}*(ARBP_O/ARBRM)^{-0.15}*(ARBV_O/200)^{0.05}$$

The equations can be used to calculate the mass or specific weight of the ac RBI. When the above multiplier is included, the value that results estimates the RBI mass. To obtain the specific weight of the RBI, remove this multiplier.

Power Level Factor

$$1ARB=0.1*((EXP(0.0008/(1-ARBE)))/1.7)*(ARBAM/ARBRM)*ARBP_O*\underline{(ARBP_O/ARBRM)^{-0.13}}*(ARBV_O/200)^{0.05}$$

$$3ARB=0.135*((EXP(0.0008/(1-ARBE)))/1.7)*(ARBAM/ARBRM)*ARBP_O*\underline{(ARBP_O/ARBRM)^{-0.15}}*(ARBV_O/200)^{0.05}$$

The mass of the relay contacts and semiconductor switches will rise nearly linearly with an increase in power because they are the power conducting elements in the ac RBI. However, the mass of the drivers, sensors, and logic devices does not rise as fast. These trends result in some economies of scale as ac RBI power levels rise and they cause specific weights to decline. Because the mass of the ancillary hardware in a 3-phase ac RBI occupies a larger percentage of its total mass, the gains in specific weight that occur with power are greater in this RBI design than in the single-phase RBI design. This explains the difference between the single- and 3-phase power level multiplier exponents, -0.18 and -0.21. The difference in mass growth rates between single- and 3-phase ac RBIs can be seen

Figure 40

AC RBI SPWT vs EFFICIENCY

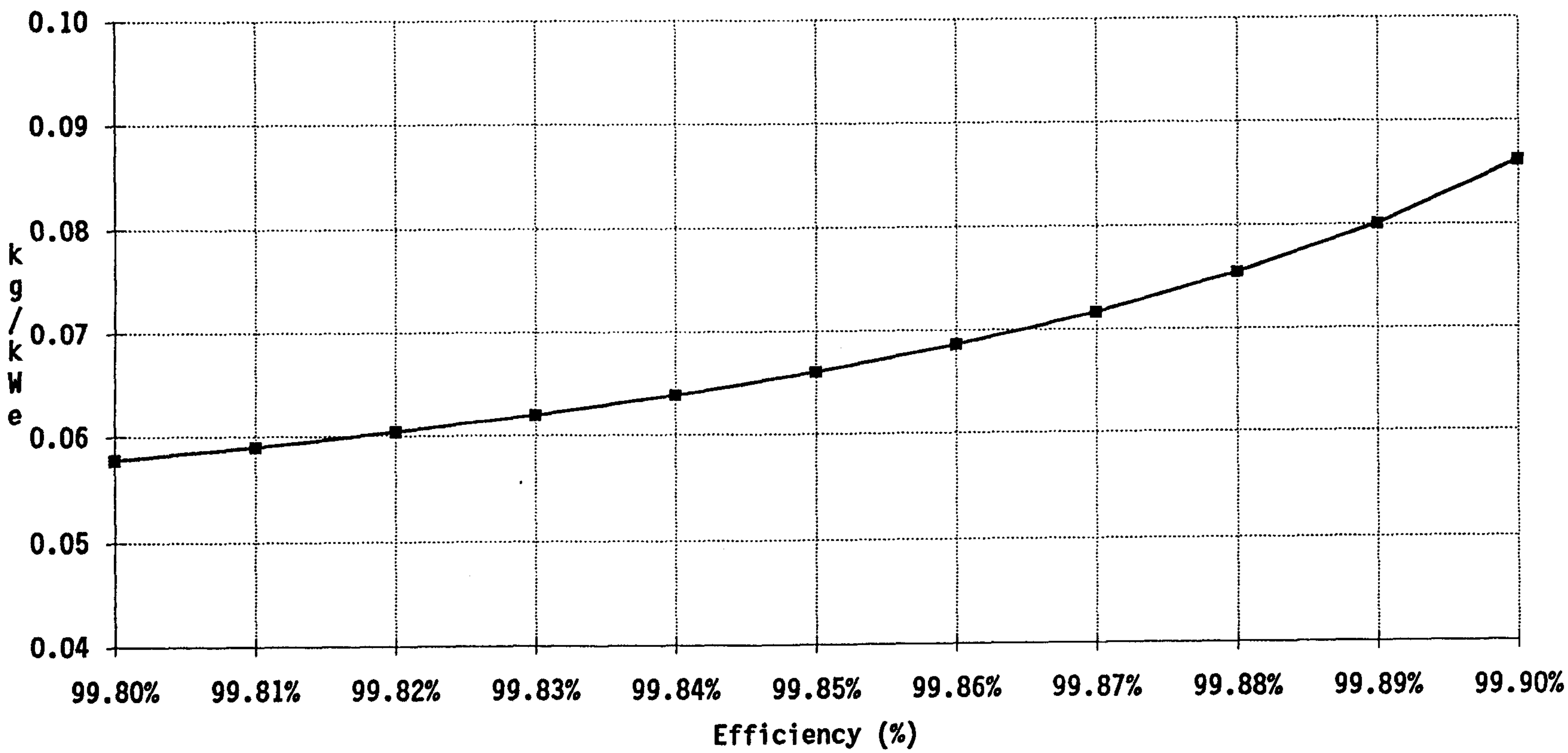

by referring back to Figure 39. An expanded view of only the single-phase ac RBI is shown in Figure 41.

Voltage Level Factor

$$1ARB=0.1*((EXP(0.0008/(1-ARBE)))/1.7)*(ARBAM/ARBRM)*ARBP_0*(ARBP_0/ARBRM)^{-0.13}*\underline{(ARBV_0/200)^{0.05}}$$

$$3ARB=0.135*((EXP(0.0008/(1-ARBE)))/1.7)*(ARBAM/ARBRM)*ARBP_0*(ARBP_0/ARBRM)^{-0.15}*\underline{(ARBV_0/200)^{0.05}}$$

A number of effects, some of them offsetting, occur as the voltage across an ac RBI increases. The internal RBI wiring and its devices will require more insulation to withstand the added voltage stresses. The relay contacts will need to be separated further to prevent vacuum breakdown. These effects tend to increase the RBI mass, especially the relay mass. However, assuming the RBI power level remains the same, the current conducted by the contacts will decline as the voltage rises. This reduces the mass of the relay contacts and the relay driver. Since the mechanical parts of the relay are heavier than insulation, the overall effect should be a slight reduction in relay mass as the ac RBI voltage increases. The mass of the semiconductor switches in parallel with the relay, however, is expected to rise as voltage increases. Semiconductor devices must be connected in series to switch higher voltages; however, series connected semiconductors will not naturally share voltages evenly. Additional hardware is needed to make them voltage share and protect them in case they do not. These factors increases the mass of the RBI. After weighing the increase in semiconductor mass against the reduction in relay mass, it appears the mass of a complete ac RBI will slowly rise as voltage levels rise. Figure 42 displays the results of this evaluation.

3.1.9 DC RPC Model

Dc remote power controllers (RPCs) are used to switch and monitor individual dc load circuits and provide circuit protection. These devices will be located in dc power distribution panels. This section explains the equation developed to estimate their masses as a function of power, efficiency, and voltage. This equation provides rough mass estimates for component comparison purposes. For more accurate mass estimates specific component designs must be developed.

The present dc RPC panel design uses a channelized approach similar to the dc RBI configuration since the card cage assembly that controls and monitors the operation of a dc RPC can be shared among several units. The current RPC channel employs a hybrid arrangement consisting of a mechanical relay paralleled with a semiconductor switch. A hybrid arrangement is appropriate because the relay and semiconductor switch can function together to yield a high efficiency switch that also exhibits good opening and closing characteristics. The dc RPC equation described in this section is based on this hybrid switch configuration. The attributes of a hybrid switch configuration and the reasons for selecting it over just a relay or only a semiconductor switch are explained in greater detail in the dc RBI section. Since a dc RPC is essentially a lower power dc RBI in many respects and most of their characteristics are similar, the paragraphs describing the RPC equation development and rationale will rely heavily on the previous dc RBI discussion. Explanations will be succinct to reduce the amount of repetition. If additional information is desired please refer back to the dc RBI discussion.

Figure 41
AC RBI SPWT vs POWER LEVEL

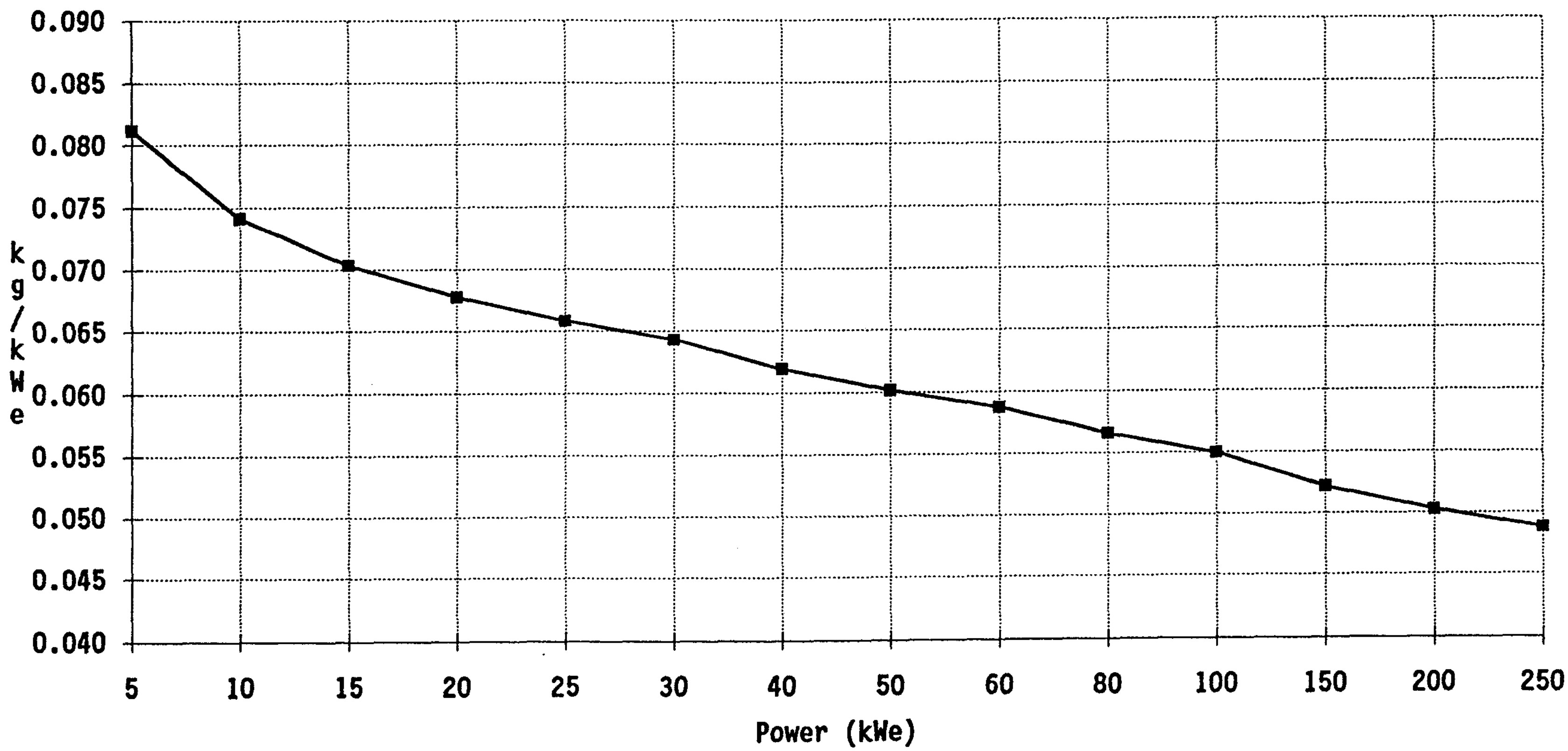

Figure 42

AC RBI SPWT vs VOLTAGE

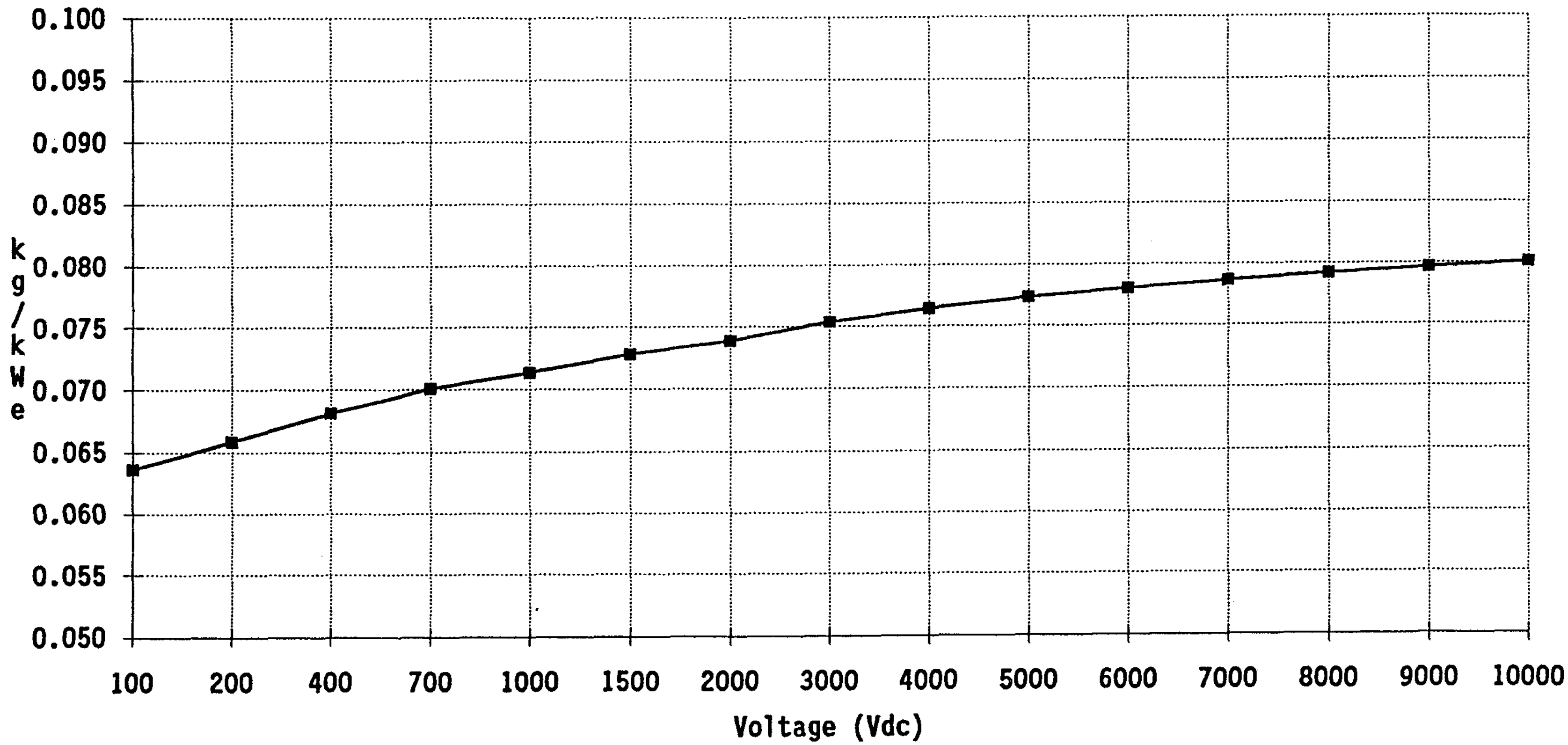

It was mentioned that the dc RBI and RPC configurations are similar; however, there are some differences that cause their specific weights to vary. The mass of the thermal management hardware occupies a larger percentage of the RPC mass. This is not because an RPC is less efficient, but because thermal management hardware does not scale linearly down to these smaller power levels. The mass of the housing and structure of an RPC also assumes a greater portion of the total mass for the same reason. The effect of these two items causes the specific weight of an RPC to be considerably higher than a RBI. Dc RPC mass breakdowns are contained in Appendix A on page A-10 and A-11. They were derived from SSF RPC mass breakdowns and were used as a basis for the subsequent equation development (Ref. III-6).

The dc RPC equation development is explained in the following paragraphs. Graphs are used in conjunction with technical descriptions to explain the equation rationale. Variables used in this discussion are shown in Table 20.

Table 20
Dc RPC Model Variable Definitions

DRPM	Dc RPC Mass
DRPE	Dc RPC Efficiency (99.85%)
DRPAM	Dc RPC Available Modules
DRPRM	Dc RPC Required Modules
$DRPP_o$	Dc RPC Power Output (kWe)
$DRPV_o$	Dc RPC Voltage Output (Vdc)

Mass Coefficient

$$DRPM=\underline{0.36}*((EXP(0.0003/(1-DRPE)))/1.22)*(DRPAM/DRPRM)*DRPP_o*(DRPP_o/DRPRM)^{-0.18}*(DRPV_o/120)^{0.04}$$

The dc RPC mass breakdowns located in Appendix A were derived from SSF dc RPC mass breakdowns. The SSF RPC mass breakdowns and those used for this equation development are based on a hybrid configuration consisting of a paralleled relay and semiconductor switch. Mass gains originating from technology improvements are incorporated into the breakdowns in Appendix A and they result in about a 15% reduction in total RPC mass. The above mass coefficient was calculated to yield values consistent with these mass breakdowns.

Efficiency Factor

$$DRPM=0.36*\underline{((EXP(0.0003/(1-DRPE)))/1.22)}*(DRPAM/DRPRM)*DRPP_o*(DRPP_o/DRPRM)^{-0.18}*(DRPV_o/120)^{0.04}$$

The above underlined factor estimates the change in specific weight occurring with a change in dc RPC efficiency. The efficiency of an RPC can be raised by enlarging the contact and semiconductor conduction area to reduce their resistance. The mass of the relay contacts and semiconductor switch will increase, but the thermal management hardware mass will decline. Other RPC elements must be reconfigured to conform to the new relay, semiconductor, and thermal management hardware designs. RPC mass estimates were generated for efficiencies ranging from 99.8 to 99.9% and they were used to generate the above efficiency factor. A graph of these RPC specific weights is shown in Figure 43.

Redundancy Factor

$$DRPM=0.36*((EXP(0.0003/(1-DRPE)))/1.22)*\underline{(DRPAM/DRPRM)}*DRPP_0*(DRPP_0/DRPRM)^{-0.18}*(DRPV_0/120)^{0.04}$$

The mass of a dc RPC network rises if a modular design approach is used to enhance reliability. The factor underlined above estimates this mass increase. The "available modules" number is the actual number of modules present in the component; the "required modules" value is the actual number of modules required to provide the full output power level. Assume the reliability requirements of a system drive a design to use 4/3 redundancy. Each channel will be designed to carry 33% of the power. 4 channels will be available, but only 3 are needed to supply full power. The mass of the fourth channel is the penalty paid to obtain the higher specified reliability.

Power Level Multiplier

$$DRPM=0.36*((EXP(0.0003/(1-DRPE)))/1.22)*(DRPAM/DRPRM)*\underline{DRPP_0}*(DRPP_0/DRPRM)^{-0.18}*(DRPV_0/120)^{0.04}$$

The equation can be used to calculate the mass or specific weight of the dc RPC. When the above multiplier is included, the value that results estimates the RPC mass. To obtain the specific weight of the RPC, remove this multiplier.

Power Level Factor

$$DRPM=0.36*((EXP(0.0003/(1-DRPE)))/1.22)*(DRPAM/DRPRM)*DRPP_0*\underline{(DRPP_0/DRPRM)^{-0.18}}*(DRPV_0/120)^{0.04}$$

The masses of the dc RPC relay contacts and the semiconductor switch, will increase proportionally with a rise in power. However, the masses of supporting hardware elements, such as driver modules, sensors, and control logic devices, will grow at a slower rate. This results in some economies of scale as the RPC power level rises and causes its specific weight to decline. The change in the specific weight of a dc RPC as the power level rises is shown in Figure 44.

Voltage Level Factor

$$DRPM=0.36*((EXP(0.0003/(1-DRPE)))/1.22)*(DRPAM/DRPRM)*DRPP_0*(DRPP_0/DRPRM)^{-0.18}*\underline{(DRPV_0/120)^{0.04}}$$

The mass of an RPC was expected to rise slowly as the voltage across it was increased. However, RPCs are located near the loads and experience voltages that are much lower than RBIs. Consequently, many effects identified with high volt-

Figure 43
DC RPC SPWT vs EFFICIENCY

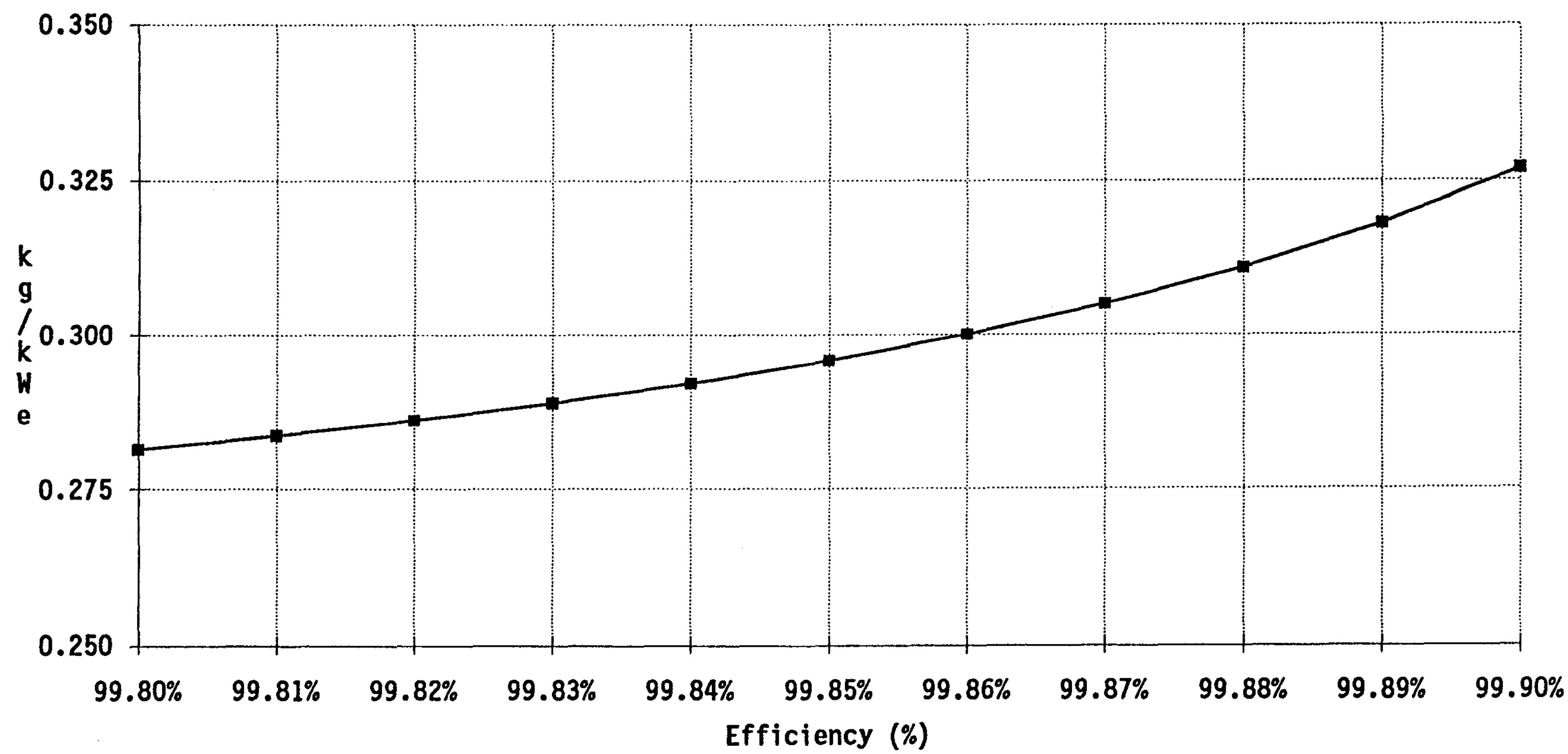

Figure 44

DC RPC SPWT vs Power Level

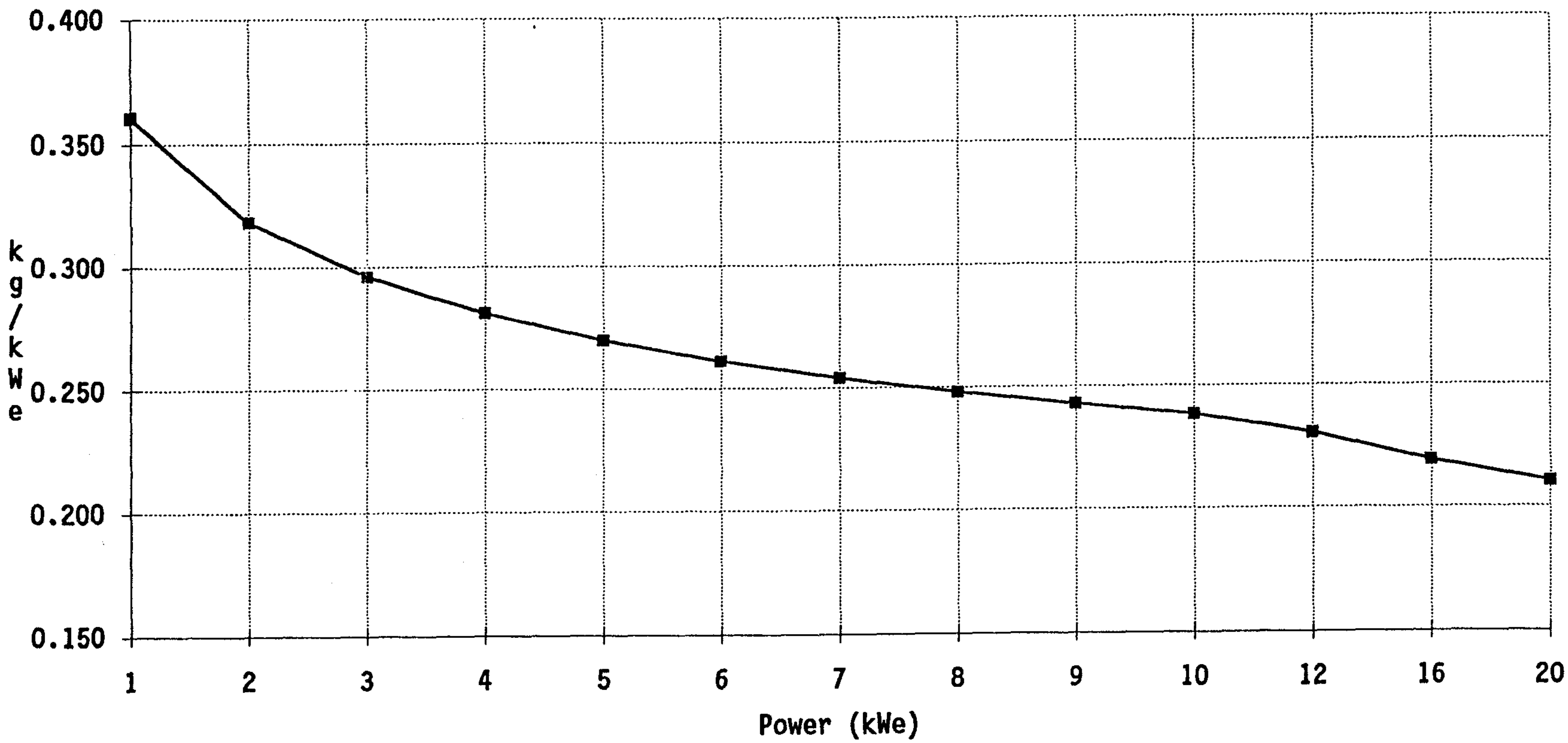

age operation, such as vacuum relay breakdown, presumably will not be a factor. RPC voltages also are not high enough to warrant connecting semiconductor switches in series. This means the problems associated with this form of operation will not occur and the mass of the semiconductor switches should not rise much with voltage. Finally, capacitors contained in dc systems are normally located in the dc switchgear units or near the power source. They will probably be separated from the RPCs by a considerable amount of cabling. This will greatly reduce the effects of capacitor discharge into a load fault and mitigate the stress imposed on the RPC. The main item that will increase the mass of the RPC is added insulation. This is needed to withstand higher voltages, but its effect on RPC mass should be minor. Figure 45 displays the results of this analysis.

3.1.10 AC RPC Model

Ac RPCs are used to switch and monitor individual ac load circuits and provide circuit protection. These devices will be located in ac power distribution panels. The following paragraphs explain the equations generated to estimate the masses of single- and 3-phase RPCs as a function of power, efficiency, and voltage. These equations are only capable of providing rough mass estimates for component comparison purposes. For more accurate mass estimates specific component designs will need to be developed.

The present ac RPC panel design uses a channelized approach like the ac RBI configuration. This allows the card cage assembly that controls and monitors ac RPC operation to be shared among several units. The current RPC channel employs a hybrid arrangement that consists of a fast acting mechanical relay in parallel with a back-to-back pair of semiconductor switches. This hybrid arrangement is preferred because it allows the relay and semiconductor switches to function together to yield a high efficiency switch with good opening and closing characteristics. The ac RPC equation described here is based on a hybrid switch configuration. The virtues of a hybrid switch configuration and the reasons for selecting it over a design utilizing only semiconductor switches were explained previously in the ac RBI section. Since an ac RPC is basically a low power ac RBI in many respects and most features are similar, the information presented in the ac RBI section will be relied on while describing the RPC equation development. The ac RPC discussion is shortened to reduce the amount of repetition. If additional information is desired please refer back to the ac RBI discussion.

The ac RPC and RBI configurations are similar; however, certain differences will cause their specific weights to differ considerably. The mass of the thermal management hardware, housing, and structure will assume a greater percentage of the RPC mass because it does not scale linearly down to the smaller RPC power levels. This results in the specific weight of an RPC being much higher than a RBI. In a telephone conversation with Dave Fox of Westinghouse, he indicated that comparably rated ac and dc RPCs should have similar masses (Ref. III-34). The data bus interface and control elements in the ac RPCs would probably be like those in the dc units. The relay in an ac RPC would be lighter because the zero current crossing point inherent in ac distribution eases fault current interruption; however, the mass of the ac RPC must include the mass of a back-to-back pair of semiconductor switches and their drivers. Based on this discussion the masses of many of the elements in an ac RPC were obtained from the SSF dc RPC mass breakdowns and they were utilized as a basis for the following equation development (Ref. III-6). The ac RPC mass breakdowns are located in Appendix A on page A-12 and A-13.

Figure 45

DC RPC SPWT vs VOLTAGE

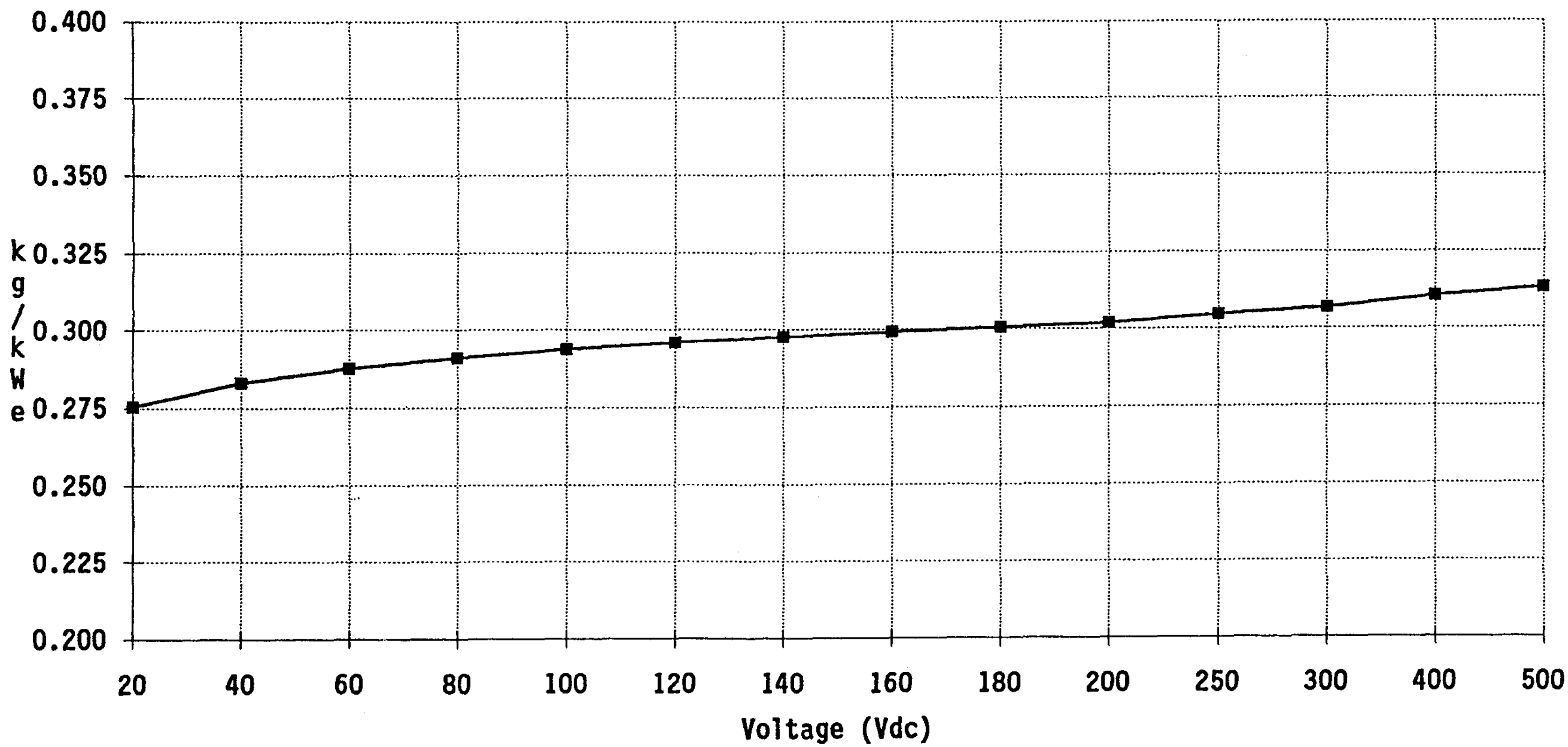

The ensuing paragraphs explain the formulation of single-phase and 3-phase ac RPC equations. Their development is explained by using technical descriptions and graphs. The variables used in these discussions are listed in Table 21.

Table 21
Ac RPC Model Variable Definitions

1ARP	Ac RPC Mass
3ARP	Ac RPC Mass
ARPE	Ac RPC Efficiency (99.85%)
ARPAM	Ac RPC Available Modules
ARPRM	Ac RPC Required Modules
$ARPP_o$	Ac RPC Power Output (kWe)
$ARPV_o$	Ac RPC Voltage Output (Vrms)

Mass Coefficient

$$1ARP=\underline{0.38}*((EXP(0.0003/(1-ARPE)))/1.22)*(ARPAM/ARPRM)*ARPP_o*(ARPP_o/ARPRM)^{-0.15}*(ARPV_o/120)^{0.01}$$

$$3ARP=\underline{0.5}*((EXP(0.0003/(1-ARPE)))/1.22)*(ARPAM/ARPRM)*ARPP_o*(ARPP_o/ARPRM)^{-0.2}*(ARPV_o/120)^{0.01}$$

The ac RPC mass breakdowns used the SSF dc RPC mass breakdowns as a starting point. Many items in dc and ac RPCs will be the same, so dc RPC component masses were also used for the ac RPC case. The relay in an ac RPC will be smaller, but an ac RPC contains a back-to-back pair of semiconductor switches. The mass differences resulting from these design differences were incorporated into the ac RPC mass breakdowns. To complete the ac RPC mass breakdowns, mass gains occurring as a result of minor hardware advancements were included. The above mass coefficients were then determined from these ac RPC mass breakdowns.

The mass of a 3-phase ac RPC will be higher than a single-phase RPC because the 3-phase design requires two additional relay contacts and two more back-to-back pairs of semiconductor switches. However, the control logic and thermal management hardware masses are similar in both designs and the packaging weight difference becomes less as the RPC size grows, so the relative difference in mass becomes less as the power level rises. Single- and 3-phase RPC specific weights are compared in Figure 46.

Efficiency Factor

$$1ARP=0.38*\underline{((EXP(0.0003/(1-ARPE)))/1.22)}*(ARPAM/ARPRM)*ARPP_o*(ARPP_o/ARPRM)^{-0.15}*(ARPV_o/120)^{0.01}$$

Figure 46

AC RPC SPWT
1-PHASE VS 3-PHASE

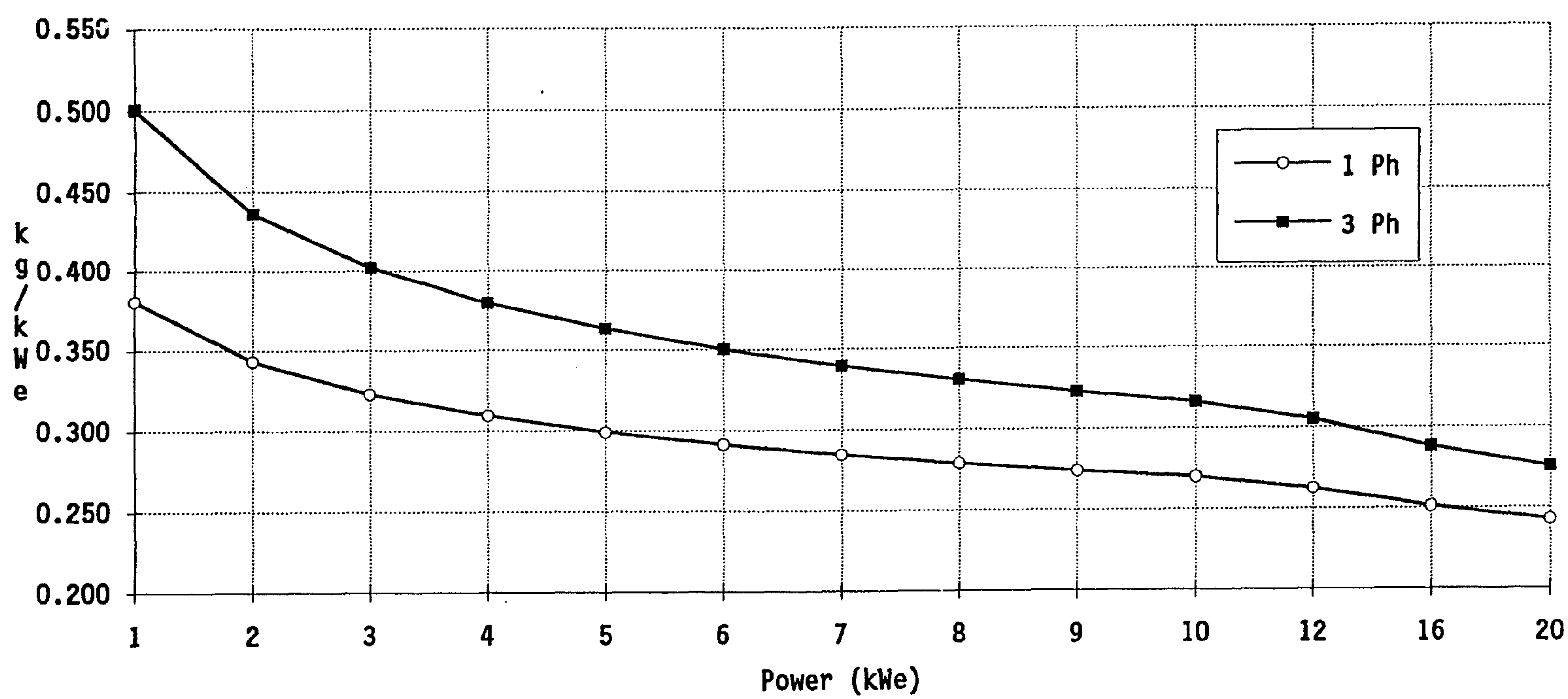

$$3ARP=0.5*\underline{((EXP(0.0003/(1-ARPE)))/1.22)}*(ARPAM/ARPRM)*ARPP_o*(ARPP_o/ARPRM)^{-0.2}*(ARPV_o/120)^{0.01}$$

The factor underlined above estimates the change in specific weight occurring with a change in ac RPC efficiency. The efficiency of an ac RPC was assumed to be the same as a dc RPC; the reactive parasitics associated with ac operation were expected to be negligible. The efficiency of an ac RPC can be increased by enlarging the conduction area of the relay contacts and semiconductor switches. This will reduce their resistance. The mass of the relay contacts and semiconductor switches will increase, but the thermal management hardware mass declines. Other RPC elements must be redesigned to conform to the new relay, semiconductor, and thermal management hardware configurations. RPC mass estimates were generated for efficiencies ranging from 99.8 to 99.9% and they were used to calculate this efficiency factor. A graph showing how RPC specific weights vary with power is shown in Figure 47.

Redundancy Factor

$$1ARP=0.38*((EXP(0.0003/(1-ARPE)))/1.22)*\underline{(ARPAM/ARPRM)}*ARPP_o*(ARPP_o/ARPRM)^{-0.15}*(ARPV_o/120)^{0.01}$$

$$3ARP=0.5*((EXP(0.0003/(1-ARPE)))/1.22)*\underline{(ARPAM/ARPRM)}*ARPP_o*(ARPP_o/ARPRM)^{-0.2}*(ARPV_o/120)^{0.01}$$

A modular design approach used to improve reliability will cause the total mass of an ac RPC assembly to rise. This mass increase is estimated by the above factor. The actual number of modules present in the assembly is specified by the "available modules" number; the number of modules required to deliver full power is defined by the "required modules" value. If a system is designed with 4/3 redundancy, each channel can carry up to 33% of the power. The fourth channel is included solely to improve reliability and its mass is the penalty paid to obtain the higher reliability.

Power Level Multiplier

$$1ARP=0.38*((EXP(0.0003/(1-ARPE)))/1.22)*(ARPAM/ARPRM)*\underline{ARPP_o}*(ARPP_o/ARPRM)^{-0.15}*(ARPV_o/120)^{0.01}$$

$$3ARP=0.5*((EXP(0.0003/(1-ARPE)))/1.22)*(ARPAM/ARPRM)*\underline{ARPP_o}*(ARPP_o/ARPRM)^{-0.2}*(ARPV_o/120)^{0.01}$$

The equations can be used to calculate the mass or specific weight of the ac RPC. When the above multiplier is included, the value that results estimates the RPC mass. To obtain the specific weight of the RPC, remove this multiplier.

Power Level Factor

$$1ARP=0.38*((EXP(0.0003/(1-ARPE)))/1.22)*(ARPAM/ARPRM)*ARPP_o*\underline{(ARPP_o/ARPRM)^{-0.15}}*(ARPV_o/120)^{0.01}$$

Figure 47
AC RPC SPWT vs EFFICIENCY

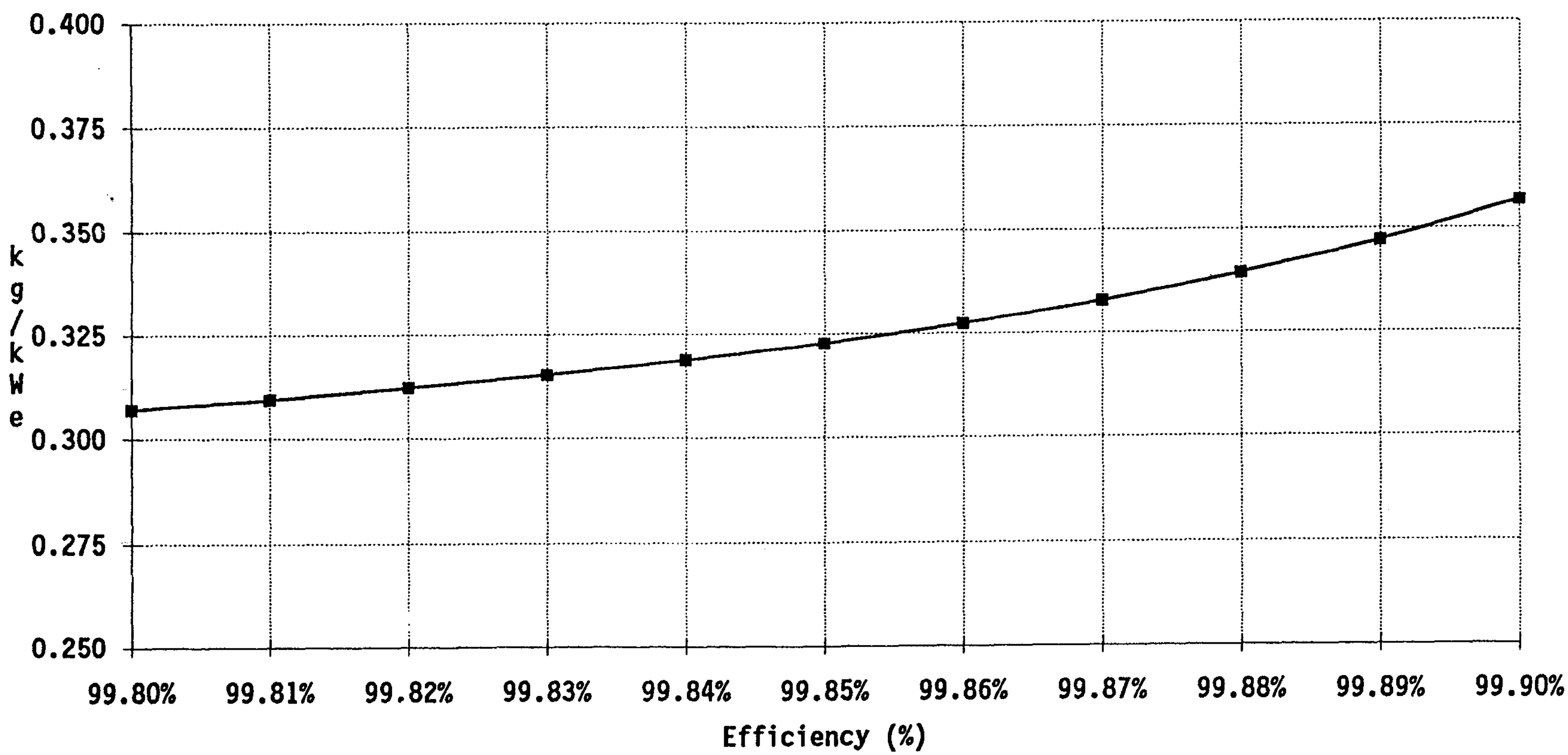

$$3ARP=0.5*((EXP(0.0003/(1-ARPE)))/1.22)*(ARPAM/ARPRM)*ARPP_0*\underline{(ARPP_0/ARPRM)^{-0.2}}*(ARPV_0/120)^{0.01}$$

The masses of the relay contacts and semiconductor switches in an ac RPC increase fairly linearly with a rise in power. However, the masses of supporting hardware elements, such as driver modules, sensors, and control logic devices, grow at a much slower rate. This results in some economies of scale as the RPC power level rises and causes its specific weight to decline. Because the mass of the ancillary hardware in a 3-phase ac RPC occupies a greater portion of its total mass, the reductions in specific weight that occur with power are greater in this RPC design than in the single-phase RPC design. This causes the difference in the single- and 3-phase power level multiplier exponents, -0.15 and -0.2. The difference in mass growth rates between single- and 3-phase ac RPCs can be seen by referring back to Figure 46. An expanded view of only the single-phase ac RPC is shown in Figure 48.

Voltage Level Factor

$$1ARP=0.38*((EXP(0.0003/(1-ARPE)))/1.22)*(ARPAM/ARPRM)*ARPP_0*(ARPP_0/ARPRM)^{-0.15}*\underline{(ARPV_0/120)^{0.01}}$$

$$3ARP=0.5*((EXP(0.0003/(1-ARPE)))/1.22)*(ARPAM/ARPRM)*ARPP_0*(ARPP_0/ARPRM)^{-0.2}*\underline{(ARPV_0/120)^{0.01}}$$

The ac RPCs will be located near the loads; consequently, the voltages they will experience will be lower than RBIs. This means that many effects associated with high voltage operation, such as vacuum relay breakdown, presumably will not occur. Some effects that will occur as the voltage across an RPC increases will also be offsetting. The RPC devices and internal wiring will require additional insulation to withstand the higher voltage stresses. While the RPC voltages are not high enough to warrant connecting the semiconductor switches in series, their masses will probably rise slowly to maintain comparable conducting properties at higher voltages. These factors will cause the mass of the RPC to rise. However, assuming the RPC power level remains constant, the current carried by the relay contacts will decline as the voltage rises. This will lower the mass of the relay contacts and relay driver. After considering the weight increases occurring from added insulation and semiconductor design changes against the reduction in relay mass, it appears the mass of a complete ac RPC will gradually rise as voltage levels rise. The results of this evaluation are displayed in Figure 49.

3.2 Power Conditioning Component Models

A complete power conditioning component model is created by linking individual stages and combining these with ancillary component hardware. The equations must undergo a few changes to integrate them into a component model. The power and voltage levels for each stage must be computed within their respective equations to obtain the most accurate mass estimates. These values are calculated by inserting the efficiencies of the subsequent stages and including the voltage coefficients associated with inversion and rectification. The equations that define the voltage relationships for single- and 3-phase rectification are shown below. These equations are simply reversed to obtain the corresponding relationships for inversion.

Figure 48

AC RPC SPWT vs Power Level

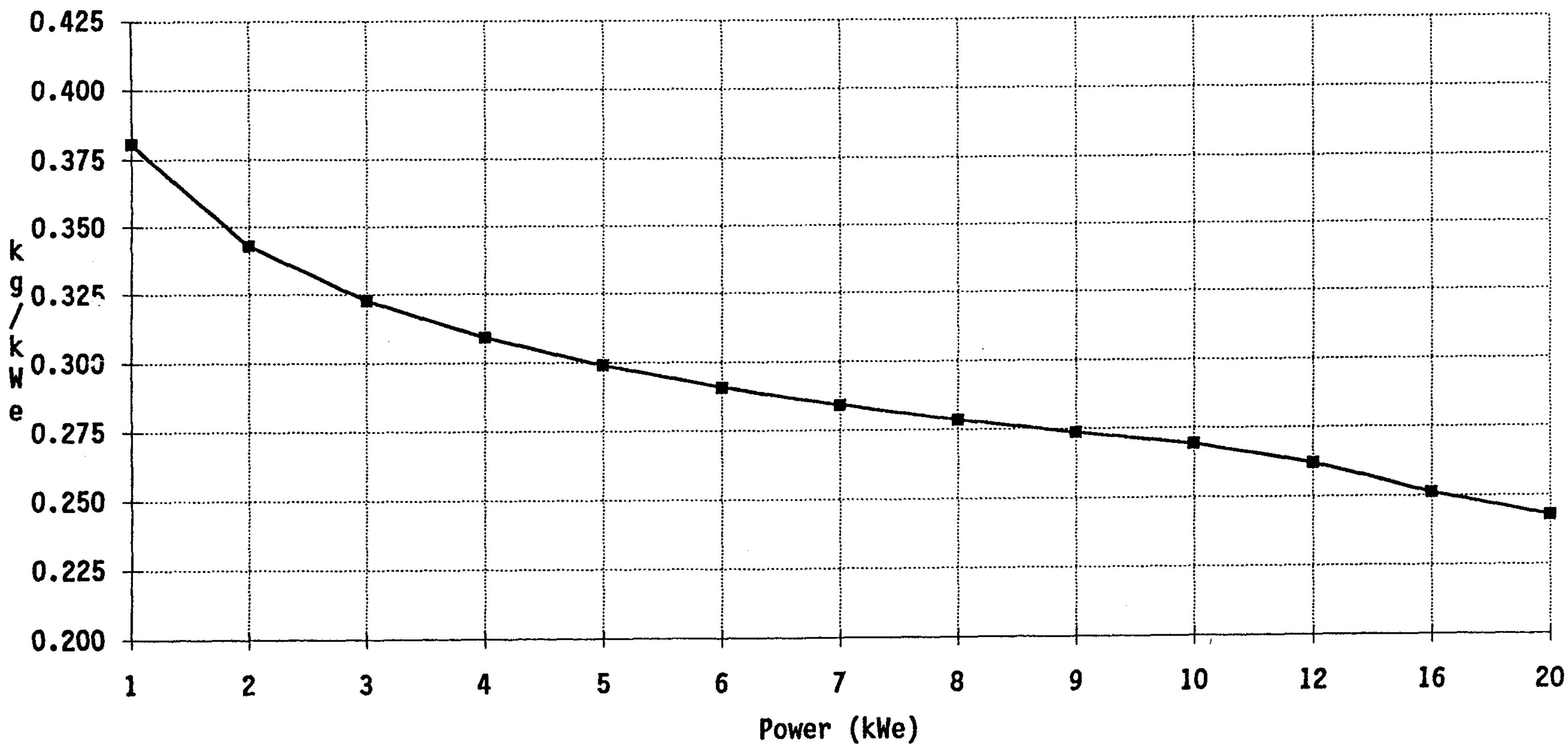

Figure 49

AC RPC SPWT vs VOLTAGE

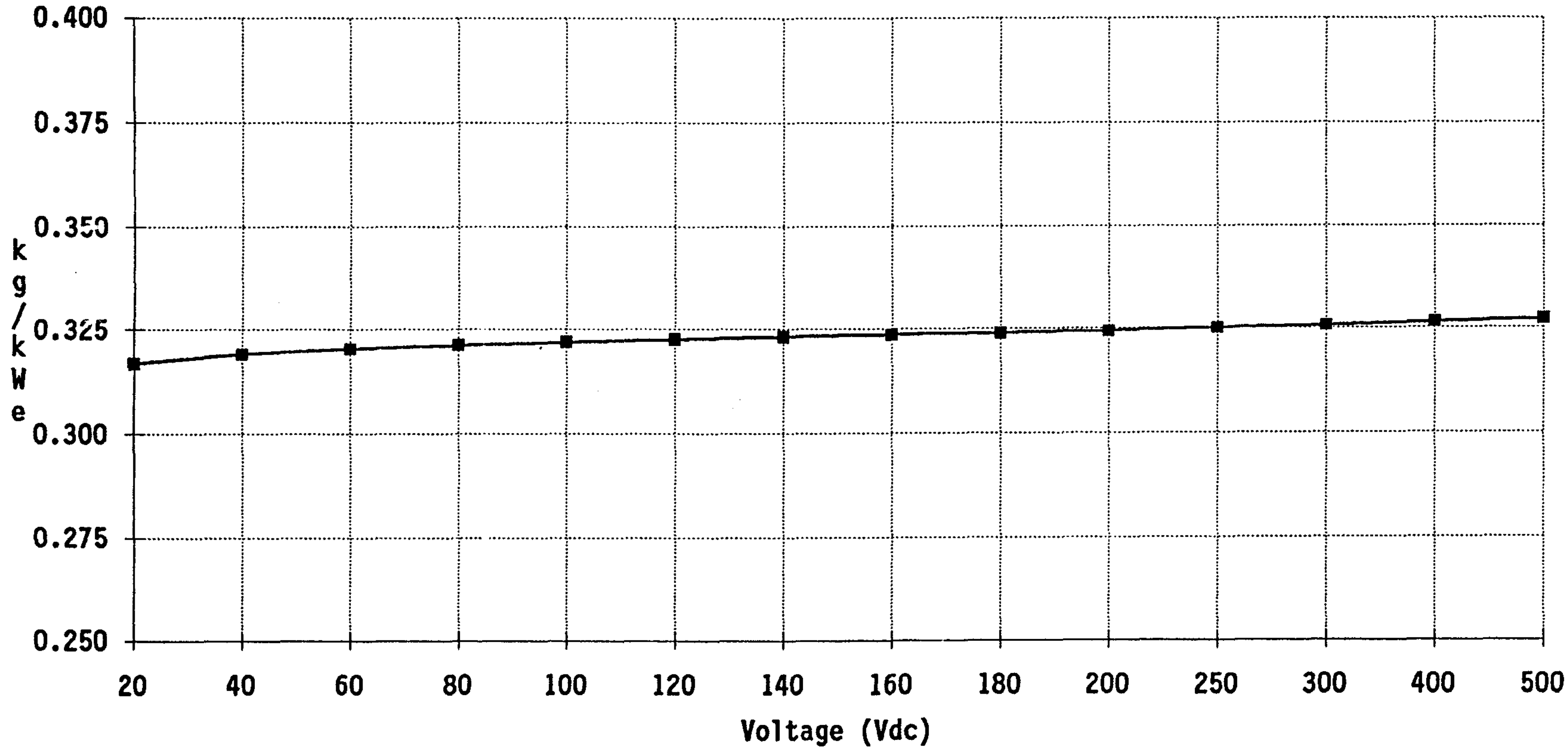

Single-Phase: Vdc=0.9*Vrms

3-Phase: Vdc=1.35*Vrms

where: Vdc = the output dc voltage from a rectifier or the input dc voltage to a chopper
Vrms = the line-to-line ac voltage from a chopper or the input line-to-line ac voltage fed to a rectifier

The subsequent component mass equations incorporate these voltage factors and the efficiencies of the interacting stages. Because the parasitic power demands of a component are supplied through the input filter, its mass equation also includes a value for this. The masses of the various stages and ancillary hardware are calculated for both single- and 3-phase designs. Based on the numerical input for the number of phases, "1" or "3", the appropriate values are selected.

3.2.1 DC/DC Converter Model

The dc/dc converter model incorporates equations for a chopper, inverter transformer, and rectifier stage. The model is completed with the addition of input and output dc filtering and ancillary hardware equations. Figure 50 shows a diagram of the dc/dc converter stages.

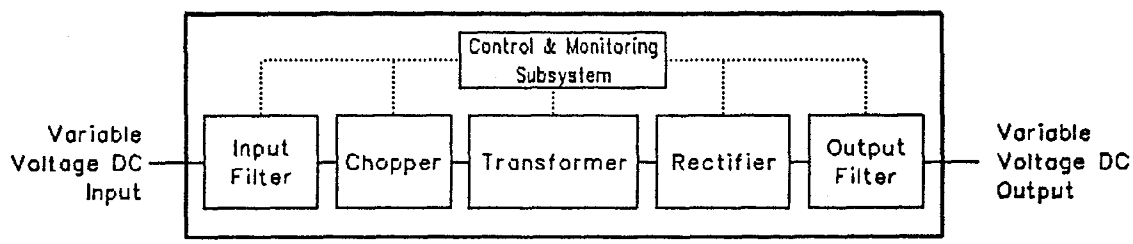

Figure 50 DC/DC Converter Diagram

Application Notes: Dc/dc converters are used to change the input dc voltage to a higher or lower value. They also provide isolation between the input and output to reduce transmitted interference. The dc/dc converter models can be used to estimate the masses of converters that directly follow a dc power source or those located near the load within a distribution network. In the two applications, the main difference is expected to be the filtering demands. The filter requirements will be determined by the particular applications; however, a ripple factor of 5% is suggested for converters that follow sources and feed industrial power devices such as heaters, and 1% is proposed for converters that distribute power to sensitive user loads.

The dc/dc converter models described in this report incorporate a resonant converter topology. A resonant converter exhibits low mass and high efficiency, and it is well suited for high frequency, space based applications. It also uses zero current switching, which reduces switching losses and switching induced EMI. These items improve chopper efficiency and cut the mass of the dc filter stages. There have been concerns raised about the technological maturity of the resonant converter. The resonant converter is a recent development and it does have a higher parts count and tend to be more complex. However, the models here are for components expected to available after the year 2000 and sufficient time should be available to fully resolve any resonant converter technology issues.

Spreadsheet Printout: Figure 51 is a printout of the dc/dc converter spreadsheet model. Subsequent sections explain the operation of this spreadsheet.

Model Input Parameter Ranges: The spreadsheet is designed to cover a specific range of input parameters. Using input parameters outside of these ranges could result in inaccurate mass estimates and it is not recommended. Table 22 lists appropriate input ranges and the values recommended to yield the best results. It also identifies the sources that should be consulted for certain items. It is considered to be the users responsibility to select nonconflicting input parameters that are suitable for the application and operating conditions.

Date: September 10, 1991					File Name: DCDCCONR.XLS		
					Originator: K. J. Metcalf		
		DC/DC Converter Design Model					
		(Resonant Chopper Type)					
		Input Parameters					
Output Power (kWe)		6.25		Inversion Frequency (kHz)			40
Input Voltage (Vdc)		140		Chopper Efficiency (%)			96.0%
Output Voltage (Vdc)		120		Transformer Efficiency (%)			99.0%
Number of Phases		1		Rectifier Efficiency (%)			98.5%
Ripple Factor (%)		1.0%		Filter Efficiency (%)			99.5%
Enclosure (FH or CP)		FH		Coldplate Temperature (C)			40
Available Modules		1		Coldplate-Rad. Temp. Delta (C)			16.7
Required Modules		1					
		Component Mass Characteristics					
Input Filter Mass (kg)	Chopper Mass (kg)	XFMR Mass (kg)	Rectifier Mass (kg)	Output Filter Mass (kg)	Cable & Conn. Mass (kg)	Cntrl & Mon. Mass (kg)	Enclosure Mass (kg)
0.84	2.52	1.72	0.69	1.03	2.82	3.39	9.38
Radiator Mass (kg)		Component Mass without Radiator (kg)	Component Specific Mass (kg/kW)		Total Mass with Radiator (kg)	Total Specific Mass (kg/kW)	
6.88		22.40	3.58		29.28	4.68	

Figure 51

Page 1

		Component Volume and Dimensions					
Single Module Parameters				Complete Assembly Parameters			
Volume (cu meters)		0.038		Volume (cu meters)		0.038	
Height (meters)		0.24		Height (meters)		0.24	
Width (meters)		0.37		Width (meters)		0.37	
Length (meters)		0.44		Length (meters)		0.44	
Radiator Area, Input Power, Parasitic Power, and Efficiencies							
Radiator Area (square meters)		Input Power Requirements (kWe)		Parasitic Power Demand (watts)	Eff. of Component Stages (%)	Total DC/DC Converter Eff. (%)	
1.65		6.81		66.78	92.7%	91.8%	

Figure 51

Page 2

Intermediate Calculation Values			
1 Ph Input Filter Mass (kg)	0.84	1 Phase Chopper Mass (kg)	2.52
3 Ph Input Filter Mass (kg)	0.28	3 Phase Chopper Mass (kg)	2.59
1 Phase XFMR Mass (kg)	1.72	1 Phase Rectifier Mass (kg)	0.69
3 Phase XFMR Mass (kg)	3.00	3 Phase Rectifier Mass (kg)	0.76
1 Ph Output Filter Mass (kg)	1.03	1 Phase Conductor Mass (kg)	2.82
3 Ph Output Filter Mass (kg)	0.35	3 Phase Conductor Mass (kg)	2.44
1 Phase Cntl & Mon Mass (kg)	3.39	1 Ph Cntl & Mon Power (watts)	66.78
3 Phase Cntl & Mon Mass (kg)	7.63	3 Ph Cntl & Mon Power (watts)	95.37
Single Module Finned HEX	9.38	Single Module Coldplate	6.67
Enclosure Mass (kg)		Enclosure Mass (kg)	
Total Assembly Finned HEX	9.38	Total Assembly Coldplate	6.67
Enclosure Mass (kg)		Enclosure Mass (kg)	

Figure 51

Page 3

Table 22
DC/DC Converter Model Input Parameter Ranges

DC/DC Converter Input Parameter	Recommended Input Range
Output Power Level	0.5 to 250 kWe
Input Voltage Level(1)	20 to 10,000 Vdc (Refer to Table 3 for voltages below 120 Vdc)
Output Voltage Level(1)	20 to 10,000 Vdc (Refer to Table 3 for voltages below 120 Vdc)
Number of Phases	1 or 3
Ripple Factor Percentage	0.5 to 8%
Enclosure Type (FH or CP)	Finned Heat Exchanger (FH) Coldplate (CP)
Available Modules	Equal to or Greater than Required Modules
Required Modules	No Limit
Inversion Frequency	10 to 60 kHz (Refer to Table 4)
Chopper Efficiency	Normal Range: 95 to 97% 96% is Recommended
Transformer Efficiency	Range: 97.5 to 99.5% 99% is Recommended
Rectifier Efficiency	Normal Range: 97.5 to 99.5% 98.5% is Recommended
DC Filter Efficiency	Range: 99.0 to 99.9% 99.5% is Recommended
Coldplate Temperature(2)	10 to 100° C 40° C Suggested for FH Enclosure 60° C Suggested for CP Enclosure
Coldplate to Radiator Temperature Delta	0 to 20° C 16.7° C is Recommended

1. The voltage step ratio should not exceed the limits defined in Table 6. To obtain the voltage step ratio, divide the higher, input or output voltage by the other, input or output voltage.

2. Because the Coldplate Enclosure has a lower thermal resistance than the Finned Heat Exchanger Enclosure, the coldplate temperature can be set 20° C higher when the Coldplate Enclosure is selected.

Model Equation Listing: Table 23 defines the variables utilized in the dc/dc converter model equations.

Table 23
DC/DC Converter Model Variable Definitions

P_O	Output Power Level (kWe)
P_I	Input Power Level (kWe)
V_I	Voltage Input (Vdc)
V_O	Voltage Output (Vdc)
AM	Available Modules
RM	Required Modules
IF	Inversion Frequency (kHz)
RF	Ripple Factor (%)
1IFM	Single-Phase Input Dc Filter Mass (kg)
3IFM	3-Phase Input Dc Filter Mass (kg)
1CM	Single-Phase Chopper Mass (kg)
3CM	3-Phase Chopper Mass (kg)
1TM	Single-Phase Transformer Mass (kg)
3TM	3-Phase Transformer Mass (kg)
1RM	Single-Phase Rectifier Mass (kg)
3RM	3-Phase Rectifier Mass (kg)
1OFM	Single-Phase Output Dc Filter Mass (kg)
3OFM	3-Phase Output Dc Filter Mass (kg)
FE	Dc Filter Efficiency (%)
CE	Chopper Efficiency (%)
TE	Transformer Efficiency (%)
RE	Rectifier Efficiency (%)
1CCM	Single-Phase Conductor and Connector Mass (kg)
3CCM	3-Phase Conductor and Connector Mass (kg)

1CMM	Single-Phase Control and Monitoring Mass (kg)
3CMM	3-Phase Control and Monitoring Mass (kg)
1CMP	Single-Phase Control and Monitoring Power (kg)
3CMP	3-Phase Control and Monitoring Power (kg)
DDCEM	DC/DC Converter Electronics Mass (kg)
DDCE	DC/DC Converter Efficiency (%)
DDCSE	DC/DC Converter Stage Efficiency (%)
CV	Component Volume (m^3)
CH	Component Height (m)
CW	Component Width (m)
CL	Component Length (m)
FHEM	Finned Heat Exchanger Enclosure Mass (kg)
CPEM	Coldplate Based Enclosure Mass (kg)
RA	Radiator Area (m^2)
RAM	Radiator Mass (kg)
TD	Coldplate to Radiator Temperature Delta (°C)
T	Coldplate Temperature (°C)

The EXCEL model "DCDCCONR.XLS" is for a resonant based dc/dc converter. The following equations are contained in this model.

DC/DC Converter Component Equations

$P_I=P_O/DDCE$

Single- and 3-Phase: DDCSE=FE*CE*TE*RE*FE

Single-Phase: DDCE=P_O/((P_O/FE/RE/TE/CE+1CMP/1000)/FE)

3-Phase: DDCE=P_O/((P_O/FE/RE/TE/CE+3CMP/1000)/FE)

Single-Phase: DDCEM=1IFM+1CM+1TM+1RM+1OFM+1CCM+1CMM

3-Phase: DDCEM=3IFM+3CM+3TM+3RM+3OFM+3CCM+3CMM

DC/DC Converter Input Dc Filter Equations

$$1IFM=4700*(1/(RF/0.01)^{0.5})*((1-0.995)/(1-FE))*(AM/RM)*(P_O/FE/RE/TE/CE+1CMP/1000)*((FE*V_I)^{-2}+0.000001)*(20/IF)$$

$$3IFM=4700*(1/(RF/0.01)^{0.5})*((1-0.995)/(1-FE))*(AM/RM)*(P_O/FE/RE/TE/CE+3CMP/1000)*((FE*V_I)^{-2}+0.000001)*(6.7/IF)$$

DC/DC Converter Chopper Equations

$$1CM=0.39*((EXP(0.025/(1-CE)))/1.86)*(AM/RM)*(P_O/FE/RE/TE)*((P_O/RM/FE/RE/TE)^{-0.05}*(V_I*FE/(V_I*FE-2))^{7}*EXP(V_I*FE/40000)*(20/IF)^{0.45}*EXP(P_O{}^{0.1}*IF/160))$$

$$3CM=0.4*((EXP(0.025/(1-CE)))/1.86)*(AM/RM)*(P_O/FE/RE/TE)*((P_O/RM/FE/RE/TE)^{-0.05}*(V_I*FE/(V_I*FE-2))^{7}*EXP(V_I*FE/40000)*(20/IF)^{0.45}*EXP(P_O{}^{0.1}*IF/160))$$

DC/DC Converter Transformer Equations

$$1TM=1.27*((EXP(0.003/(1-TE)))/1.35)*(AM/RM)*(P_O/FE/RE)*((P_O/RM/FE/RE)^{-0.08}*EXP(0.9*V_I*FE*CE/200000)*EXP(V_O/0.9/FE/RE/200000)*IF^{-0.47}+(IF/300)^{1.4})$$

$$3TM=2.75*((EXP(0.003/(1-TE)))/1.35)*(AM/RM)*(P_O/FE/RE)*((P_O/RM/FE/RE)^{-0.25}*EXP(1.35*V_I*FE*CE/200000)*EXP(V_O/1.35/FE/RE/200000)*IF^{-0.47}+(IF/300)^{1.4})$$

DC/DC Converter Rectifier Equations

$$1RM=0.1*((EXP(0.005/(1-RE)))/1.4)*(AM/RM)*(P_O/FE)*(V_O/FE/(V_O/FE-2))^{6}*EXP(V_O/FE/80000)$$

$$3RM=0.11*((EXP(0.005/(1-RE)))/1.4)*(AM/RM)*(P_O/FE)*(V_O/FE/(V_O/FE-2))^{6}*EXP(V_O/FE/80000)$$

DC/DC Converter Output Dc Filter Equations

$$1OFM=4700*(1/(RF/0.01)^{0.5})*((1-0.995)/(1-FE))*(AM/RM)*P_O*(V_O{}^{-2}+0.000001)*(20/IF)$$

$$3OFM=4700*(1/(RF/0.01)^{0.5})*((1-0.995)/(1-FE))*(AM/RM)*P_O*(V_O{}^{-2}+0.000001)*(6.7/IF)$$

DC/DC Converter Conductor and Connector Equations

$$1CCM=(AM/RM)*(0.028*((P_O*1000)/V_O)+0.028*(((P_O*1000)/DDCE)/V_I))$$

$$3CCM=(AM/RM)*((3^{0.5}/2)*0.028*((P_O*1000)/V_O)+(3^{0.5}/2)*0.028*(((P_O*1000)/DDCE)/V_I))$$

DC/DC Converter Control and Monitoring Equations

$$1CMM=AM*(1.4+0.9*(P_O/RM)^{0.3}+0.25*(P_O/RM)^{0.3})$$

$$3CMM=AM*(2+2.5*(P_O/RM)^{0.3}+0.75*(P_O/RM)^{0.3})$$

$$1CMP=AM*55.6*(P_o/RM)^{0.1}$$

$$3CMM=AM*79.4*(P_o/RM)^{0.1}$$

DC/DC Converter Volume and Dimension Equations

$$CV=DDCEM/(0.342*1000)$$

$$CH=0.7*CV^{0.3333}$$

$$CW=1.1*CV^{0.3333}$$

$$CL=1.3*CV^{0.3333}$$

DC/DC Converter Enclosure Equations

$$FHEM=44.26*CV^{0.6666}+27*(CL*CW)$$

$$CPEM=44.26*CV^{0.6666}+10.25*(CL*CW)$$

DC/DC Converter Radiator Equations

$$RA=(1.1212E+10*(P_o/DDCE-P_o)/((T+273-TD)^4-250^4)$$

$$RAM=4.159*RA$$

3.2.2 Inverter Model

The dc/ac inverter model integrates equations for a chopper and inverter transformer stage. An input dc filter, output ac filter, and ancillary hardware are added to obtain a complete inverter model. Figure 52 shows a diagram of the dc/ac inverter stages.

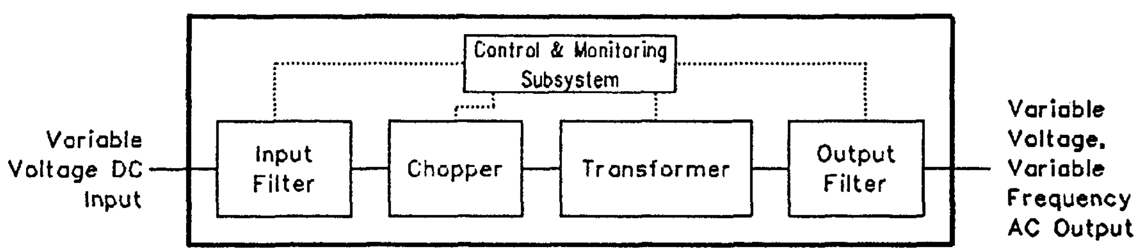

Figure 52 DC/AC Inverter Diagram

Application Notes: Dc/ac inverters are utilized to convert a dc input into an ac waveform. The transformer stage allows the generated ac voltage to be changed to a higher or lower value and also provides isolation between the input and output to reduce transmitted interference. These inverter models can be used to estimate the masses of inverters following a dc power source or those located near a load. Indications are the main difference in these two cases will be the filtering demands. Each application will have specific filtering requirements; however as a starting point, a ripple factor of 5% is suggested for inverters that follow sources and feed industrial power devices such as motors or heaters, and 1% is proposed for inverters supplying sensitive loads.

The dc/ac inverter models described in this section utilize a resonant converter topology. A resonant converter is lightweight and efficient, and well suited for high frequency, space based applications. This topology also employs zero current switching, which reduces switching losses and switching induced EMI. These items improve chopper efficiency and cut the mass of the input dc filter stage. There have been concerns raised about the technological maturity of the resonant converter. The resonant converter is a recent development and it does have a higher parts count and tend to be more complex. However, this model is for inverters deployed after the year 2000 and enough time should be available to fully resolve any resonant converter technology issues.

Spreadsheet Printout: A printout of the dc/ac inverter spreadsheet model is shown in Figure 53. The operation of this spreadsheet is explained in later sections.

Model Input Parameter Ranges: The spreadsheets are designed to cover a specific range of input parameters. Using input parameters outside of these ranges could result in inaccurate mass estimates and it is not recommended. Table 24 lists suitable input ranges and the values suggested for best results. It also identifies tables containing additional information. It is considered to be the users responsibility to select nonconflicting input parameters that are suitable for the application and operating conditions.

Date: September 10, 1991					File Name: DCACINVR.XLS		
					Originator: K. J. Metcalf		
		DC/AC Inverter Design Model					
		(Resonant Chopper Type)					
		Input Parameters					
Output Power (kWe)		25		Inversion Frequency (kHz)			20
Input Voltage (Vdc)		140		Filter Efficiency (%)			99.5%
Output Voltage (Vrms		440		Chopper Efficiency (%)			96.0%
Number of Phases		1		Transformer Efficiency (%)			99.0%
Ripple Factor (%)		1.0%		Coldplate Temperature (C)			40
Available Modules		1		Coldplate-Rad. Temp. Delta (C)			16.7
Required Modules		1		Enclosure (FH or CP)			FH
		Component Mass Characteristics					
Input Filter Mass (kg)	Chopper Mass (kg)	XFMR Mass (kg)	Output Filter Mass (kg)	Cable & Conn. Mass (kg)	Cntrl & Mon. Mass (kg)	Enclosure Mass (kg)	
6.55	11.16	6.77	2.27	6.92	4.42	19.18	
Radiator Mass (kg)		Component Mass without Radiator (kg)	Component Specific Mass (kg/kW)		Total Mass with Radiator (kg)	Total Specific Mass (kg/kW)	
20.20		57.27	2.29		77.47	3.10	

Figure 53

Page 1

DCACINVR.XLS

		Component Volume and Dimensions					
Single Module Parameters				Complete Assembly Parameters			
Volume (cu meters)		0.111		Volume (cu meters)		0.111	
Height (meters)		0.34		Height (meters)		0.34	
Width (meters)		0.53		Width (meters)		0.53	
Length (meters)		0.63		Length (meters)		0.63	
Radiator Area, Input Power, Parasitic Power, and Efficiencies							
Radiator Area (square meters)		Input Power Requirements (kWe)		Parasitic Power Demand (watts)	Eff. of Component Stages (%)	Total DC/AC Inverter Eff. (%)	
4.86		26.65		76.71	94.1%	93.8%	

Figure 53

Page 2

DCACINVR.XLS

Intermediate Calculation Values			
1 Ph Input Filter Mass (kg)	6.55	1 Phase Chopper Mass (kg)	11.16
3 Ph Input Filter Mass (kg)	2.19	3 Phase Chopper Mass (kg)	11.45
1 Phase XFMR Mass (kg)	6.77	1 Ph Output Filter Mass (kg)	2.27
3 Phase XFMR Mass (kg)	9.13	3 Ph Output Filter Mass (kg)	2.38
1 Phase Conductor Mass (kg)	6.92		
3 Phase Conductor Mass (kg)	5.99		
1 Phase Cntl & Mon Mass (kg)	4.42	1 Ph Cntl & Mon Power (watts)	76.71
3 Phase Cntl & Mon Mass (kg)	10.54	3 Ph Cntl & Mon Power (watts)	109.55
Single Module Finned HEX	19.18	Single Module Coldplate	13.64
Enclosure Mass (kg)		Enclosure Mass (kg)	
Total Assembly Finned HEX	19.18	Total Assembly Coldplate	13.64
Enclosure Mass (kg)		Enclosure Mass (kg)	

Figure 53

Page 3

Table 24
DC/AC Inverter Model Input Parameter Ranges

DC/AC Inverter Input Parameter	Recommended Input Range
Output Power Level	0.5 to 250 kWe
Input Voltage Level[1]	20 to 10,000 Vdc (Refer to Table 3 for voltages below 120 Vdc)
Output Voltage Level[1]	20 to 10,000 Vrms
Number of Phases	1 or 3
Ripple Factor Percentage	0.5 to 8%
Enclosure Type (FH or CP)	Finned Heat Exchanger (FH) Coldplate (CP)
Available Modules	Equal to or Greater than Required Modules
Required Modules	No Limit
Inversion Frequency	10 to 60 kHz (Refer to Table 4)
DC Filter Efficiency	Range: 99.0 to 99.9% 99.5% is Recommended
Chopper Efficiency	Normal Range: 95 to 97% 96% is Recommended
Transformer Efficiency	Range: 97.5 to 99.5% 99% is Recommended
AC Filter Efficiency	Range: 99.0 to 99.9% 99.5% is Recommended
Coldplate Temperature[2]	10 to 100° C 40° C Suggested for FH Enclosure 60° C Suggested for CP Enclosure
Coldplate to Radiator Temperature Delta	0 to 20° C 16.7° C is Recommended

1. The voltage step ratio should not exceed the limits defined in Table 6. To obtain the voltage step ratio, divide the higher, input or output voltage by the other, input or output voltage.

2. Because the Coldplate Enclosure has a lower thermal resistance than the Finned Heat Exchanger Enclosure, the coldplate temperature can be set 20° C higher when the Coldplate Enclosure is selected.

Model Equation Listing: Table 25 defines the variables utilized in the dc/ac inverter model equations.

Table 25
DC/AC Inverter Model Variable Definitions

P_O	Output Power Level (kWe)
P_I	Input Power Level (kWe)
V_I	Voltage Input (Vdc)
V_O	Voltage Output (Vdc)
AM	Available Modules
RM	Required Modules
IF	Inversion Frequency (kHz)
RF	Ripple Factor (%)
1IFM	Single-Phase Input Dc Filter Mass (kg)
3IFM	3-Phase Input Dc Filter Mass (kg)
1CM	Single-Phase Chopper Mass (kg)
3CM	3-Phase Chopper Mass (kg)
1TM	Single-Phase Transformer Mass (kg)
3TM	3-Phase Transformer Mass (kg)
1OFM	Single-Phase Output Ac Filter Mass (kg)
3OFM	3-Phase Output Ac Filter Mass (kg)
FE	Filter Efficiency (%)
CE	Chopper Efficiency (%)
TE	Transformer Efficiency (%)
1CCM	Single-Phase Conductor and Connector Mass (kg)
3CCM	3-Phase Conductor and Connector Mass (kg)
1CMM	Single-Phase Control and Monitoring Mass (kg)
3CMM	3-Phase Control and Monitoring Mass (kg)
1CMP	Single-Phase Control and Monitoring Power (kg)

3CMP 3-Phase Control and Monitoring Power (kg)

DAIEM DC/AC Inverter Electronics Mass (kg)

DAIE DC/AC Inverter Efficiency (%)

DAISE DC/AC Inverter Stage Efficiency (%)

CV Component Volume (m^3)

CH Component Height (m)

CW Component Width (m)

CL Component Length (m)

FHEM Finned Heat Exchanger Enclosure Mass (kg)

CPEM Coldplate Based Enclosure Mass (kg)

RA Radiator Area (m^2)

RAM Radiator Mass (kg)

TD Coldplate to Radiator Temperature Delta (°C)

T Coldplate Temperature (°C)

The EXCEL model "DCACCONR.XLS" is for a resonant based dc/ac inverter. The following equations are contained in this model.

DC/AC Inverter Component Equations

$$P_I=P_O/DAIE$$

Single- and 3-Phase: DAISE=FE*CE*TE*FE

Single-Phase: $DAIE=P_O/((P_O/FE/TE/CE+1CMP/1000)/FE)$

3-Phase: $DAIE=P_O/((P_O/FE/TE/CE+3CMP/1000)/FE)$

Single-Phase: DAIEM=1IFM+1CM+1TM+1OFM+1CCM+1CMM

3-Phase: DAIEM=3IFM+3CM+3TM+3OFM+3CCM+3CMM

DC/AC Inverter Input Dc Filter Equations

$$1IFM=4700*(1/(RF/0.01)^{0.5})*((1-0.995)/(1-FE))*(AM/RM)*(P_O/FE/TE/CE+1CMP/1000)*((FE*V_I)^{-2}+0.000001)*(20/IF)$$

$$3IFM=4700*(1/(RF/0.01)^{0.5})*((1-0.995)/(1-FE))*(AM/RM)*(P_O/FE/TE/CE+3CMP/1000)*((FE*V_I)^{-2}+0.000001)*(6.7/IF)$$

DC/AC Inverter Chopper Equations

$$1CM=0.39*((EXP(0.025/(1-CE)))/1.86)*(AM/RM)*(P_O/FE/TE)*((P_O/RM/FE/TE)^{-0.05} *(V_I*FE/(V_I*FE-2))^7*EXP(V_I*FE/40000)*(20/IF)^{0.45}*EXP(P_O^{0.1}*IF/160))$$

$$3CM=0.4*((EXP(0.025/(1-CE)))/1.86)*(AM/RM)*(P_O/FE/TE)*((P_O/RM/FE/TE)^{-0.05} *(V_I*FE/(V_I*FE-2))^7*EXP(V_I*FE/40000)*(20/IF)^{0.45}*EXP(P_O^{0.1}*IF/160))$$

DC/AC Inverter Transformer Equations

$$1TM=1.27*((EXP(0.003/(1-TE)))/1.35)*(AM/RM)*(P_O/FE)*((P_O/RM/FE)^{-0.08} *EXP(0.9*V_I*FE*CE/200000)*EXP(V_O/0.9/FE/200000)*IF^{-0.47}+(IF/300)^{1.4})$$

$$3TM=2.75*((EXP(0.003/(1-TE)))/1.35)*(AM/RM)*(P_O/FE)*((P_O/RM/FE)^{-0.25} *EXP(1.35*V_I*FE*CE/200000)*EXP(V_O/1.35/FE/200000)*IF^{-0.47}+(IF/300)^{1.4})$$

DC/AC Inverter Output Ac Filter Equations

$$1OFM=0.1*((1-0.995)/(1-FE))*(AM/RM)*P_O*(P_O/RM)^{-0.03}*(IF/20)^{-0.6}$$

$$3OFM=0.105*((1-0.995)/(1-FE))*(AM/RM)*P_O*(P_O/RM)^{-0.03}*(IF/20)^{-0.6}$$

DC/AC Inverter Conductor and Connector Equations

$$1CCM=(AM/RM)*(0.028*((P_O*1000)/V_O)+0.028*(((P_O*1000)/DAIE)/V_I))$$

$$3CCM=(AM/RM)*((3^{0.5}/2)*0.028*((P_O*1000)/V_O)+(3^{0.5}/2)*0.028*(((P_O*1000)/DAIE)/V_I))$$

DC/AC Inverter Control and Monitoring Equations

$$1CMM=AM*(1.4+0.9*(P_O/RM)^{0.3}+0.25*(P_O/RM)^{0.3})$$

$$3CMM=AM*(2+2.5*(P_O/RM)^{0.3}+0.75*(P_O/RM)^{0.3})$$

$$1CMP=AM*55.6*(P_O/RM)^{0.1}$$

$$3CMM=AM*79.4*(P_O/RM)^{0.1}$$

DC/AC Inverter Volume and Dimension Equations

$$CV=DAIEM/(0.342*1000)$$

$$CH=0.7*CV^{0.3333}$$

$$CW=1.1*CV^{0.3333}$$

$$CL=1.3*CV^{0.3333}$$

DC/AC Inverter Enclosure Equations

$$FHEM=44.26*CV^{0.6666}+27*(CL*CW)$$

$$CPEM=44.26*CV^{0.6666}+10.25*(CL*CW)$$

DC/AC Inverter Radiator Equations

$$RA=(1.1212E+10*(P_0/DAIE-P_0)/((T+273-TD)^4-250^4)$$

$$RAM=4.159*RA$$

3.2.3 AC/AC Frequency Converter Model

The ac/ac frequency converter model is based on a dc link frequency converter design. The ac input is rectified and lightly filtered to obtain dc, the dc is then fed to an inverter to obtain a new ac frequency output. The model contains the same stages as a dc/dc converter with the addition of an intermediate dc bus filter. The sequence of the stages is rearranged to obtain an alternate function. With the addition of input and output filtering and ancillary hardware, the model is completed. Figure 54 shows a diagram of the ac/ac frequency converter stages.

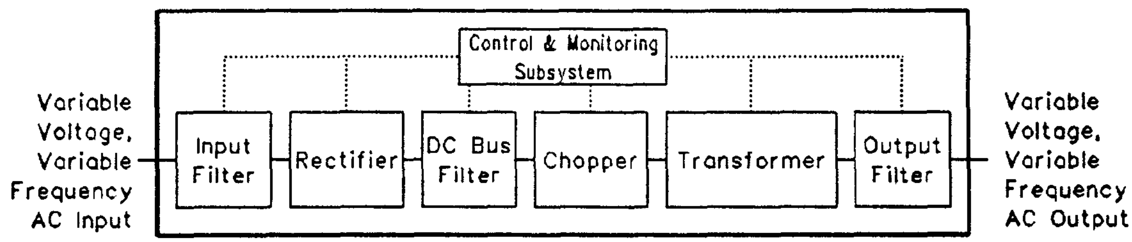

Figure 54 AC/AC Frequency Converter Diagram

Application Notes: Ac/ac frequency converters are used to change an incoming ac frequency to a higher or lower value. The internal transformer also isolates the input and output, thus reducing transmitted interference. The frequency converter model described here is best suited for estimating the masses of converters directly following an alternator power source. In this application, the alternator's low frequency output is typically stepped up to a higher frequency for transmission. The primary purpose of this frequency conversion is to reduce the mass of subsequent distribution transformers. This frequency converter model can also be used at the load end if the input frequency is relatively low, 2 kHz or less, and the waveform has a low harmonic content. These models are not suitable for high frequency inputs. Frequency converters designed to receive high frequency inputs are typically referred to as ac load receivers and they use a different topology.

The coefficients used in the input and dc bus filter equations were reduced to one-tenth of their previous values to yield lower, hopefully more realistic filter masses for this application. The ac filter design described in this report is actually a series harmonic trap. The primary purpose of a harmonic trap is to prevent a resonant circuit from amplifying external harmonics. The passive rectifier stage contained in the frequency converter is not capable of amplifying harmonics; and furthermore, the low harmonic content exhibited by an alternator would probably deter harmonic amplification anyway. Because alternators can tolerate reasonably high levels of harmonic distortion, it should also be relatively easy to suppress the harmonics reflected back to the alternator by the rectifier. The combined filtering of the input and intermediate dc bus filters should be adequate to prevent harmonic amplification in the subsequent resonant converter stage. A ripple factor of 5% for the intermediate dc bus filter is considered sufficient to prevent interference between the rectifier and resonant converter stages. It is necessary to define power quality requirements and generate low frequency filter designs consistent with this type of application to improve these filter mass estimates. Most of the dc and ac filter designs noted to date are oriented toward high frequency uses. However, low frequency filter designs will be required in these types of locations even if high frequency distribution is ultimately selected.

Spreadsheet Printout: Figure 55 is a printout of the ac/ac frequency converter spreadsheet model. Later sections describe this spreadsheet and its operation.

Model Input Parameter Ranges: The results generated by this spreadsheet are only valid for a certain range of input parameters. Inaccurate mass estimates may result if input parameters outside of the ranges defined in Table 26 are used and it is not recommended. Table 26 also identifies the values that should yield the best results, and lists sources that should be consulted in certain cases. The user is responsible for selecting input parameters that do not conflict and are reasonable for the application and operating conditions.

Date: September 10, 1991					File Name: ACACFREQ.XLS		
					Originator: K. J. Metcalf		

AC/AC Frequency Converter Design Model

(DC Link Resonant Chopper Type)

Input Parameters

Output Power (kWe)	25	Number of Input Phases	1
Input Voltage (Vrms)	500	Number of Output Phases	1
Output Voltage (Vrms	2000	DC Bus Ripple Factor (%)	5.0%
Input Freq. (kHz)	0.07	Filter Efficiency (%)	99.5%
Output Freq. (kHz)	20	Rectifier Efficiency (%)	98.5%
Enclosure (FH or CP)	FH	Chopper Efficiency (%)	96.0%
Available Modules	1	Transformer Efficiency (%)	99.0%
Required Modules	1	Coldplate Temperature (C)	40
		Coldplate-Rad. Temp. Delta (C)	16.7

Component Mass Characteristics

Input Filter Mass (kg)	Rectifier Mass (kg)	DC Bus Filter Mass (kg)	Chopper Mass (kg)	XFMR Mass (kg)	Output Filter Mass (kg)	Cable & Conn. Mass (kg)	Cntrl & Mon. Mass (kg)
7.29	2.74	9.83	10.47	6.82	2.27	2.46	4.42

Enclosure Mass (kg)	Radiator Mass (kg)		Component Mass without Radiator (kg)	Component Specific Mass (kg/kW)		Total Mass with Radiator (kg)	Total Specific Mass (kg/kW)
21.85	26.83		68.15	2.73		94.98	3.80

Figure 55

Page 1

		Component Volume and Dimensions					
Single Module Parameters				Complete Assembly Parameters			
Volume (cu meters)		0.135		Volume (cu meters)		0.135	
Height (meters)		0.36		Height (meters)		0.36	
Width (meters)		0.56		Width (meters)		0.56	
Length (meters)		0.67		Length (meters)		0.67	
Radiator Area, Input Power, Parasitic Power, and Efficiencies							
Radiator Area (square meters)		Input Power Requirements (kWe)		Parasitic Power Demand (watts)	Eff. of Component Stages (%)	Total Frequency Converter Eff. (%)	
6.45		27.19		76.71	92.2%	92.0%	

Figure 55

Page 2

Intermediate Calculation Values			
1 Ph Input Filter Mass (kg)	7.29	1 Phase Rectifier Mass (kg)	2.74
3 Ph Input Filter Mass (kg)	7.66	3 Phase Rectifier Mass (kg)	3.01
1 Ph DC Bus Filter Mass (kg)	9.83	1 Phase Chopper Mass (kg)	10.47
3 Ph DC Bus Filter Mass (kg)	3.29	3 Phase Chopper Mass (kg)	10.74
1 Phase XFMR Mass (kg)	6.82	1 Ph Output Filter Mass (kg)	2.27
3 Phase XFMR Mass (kg)	9.21	3 Ph Output Filter Mass (kg)	2.38
1 Phase Conductor Mass (kg)	2.46		
3 Phase Conductor Mass (kg)	2.13		
1 Phase Cntl & Mon Mass (kg)	4.42	1 Ph Cntl & Mon Power (watts)	76.71
3 Phase Cntl & Mon Mass (kg)	10.54	3 Ph Cntl & Mon Power (watts)	109.55
Single Module Finned HEX Enclosure Mass (kg)	21.85	Single Module Coldplate Enclosure Mass (kg)	15.54
Total Assembly Finned HEX Enclosure Mass (kg)	21.85	Total Assembly Coldplate Enclosure Mass (kg)	15.54

Figure 55

Page 3

Table 26
AC/AC Frequency Converter Model Input Parameter Ranges

AC/AC Frequency Converter Input Parameter	Recommended Input Range
Output Power Level	0.5 to 250 kWe
Input Voltage Level(1)	20 to 10,000 Vrms (Refer to Tables 3 and 10 for voltages below 120 Vrms)
Output Voltage Level(1)	20 to 10,000 Vrms
Input Frequency	60 Hz to 2 kHz
Output Frequency	10 to 60 kHz (Refer to Table 4)
Enclosure Type (FH or CP)	Finned Heat Exchanger (FH) Coldplate (CP)
Available Modules	Equal to or Greater than Required Modules
Required Modules	No Limit
Number of Input Phases	1 or 3
Number of Output Phases	1 or 3
DC Bus Ripple Factor Percentage	0.5 to 8%
AC and DC Filter Efficiencies	Range: 99.0 to 99.9% 99.5% is Recommended
Rectifier Efficiency	Normal Range: 97.5 to 99.5% 98.5% is Recommended
Chopper Efficiency	Normal Range: 95 to 97% 96% is Recommended
Transformer Efficiency	Range: 97.5 to 99.5% 99% is Recommended
Coldplate Temperature(2)	10 to 100° C 40° C Suggested for FH Enclosure 60° C Suggested for CP Enclosure
Coldplate to Radiator Temperature Delta	0 to 20° C 16.7° C is Recommended

1. The voltage step ratio should not exceed the limits defined in Table 6. To obtain the voltage step ratio, divide the higher, input or output voltage by the other, input or output voltage.

2. Because the Coldplate Enclosure has a lower thermal resistance than the Finned Heat Exchanger Enclosure, the coldplate temperature can be set 20° C higher when the Coldplate Enclosure is selected.

Model Equation Listing: Table 27 defines the variables utilized in the ac/ac frequency converter model equations.

Table 27
AC/AC Frequency Converter Model Variable Definitions

P_O	Output Power Level (kWe)
P_I	Input Power Level (kWe)
V_I	Voltage Input (Vdc)
V_O	Voltage Output (Vdc)
AM	Available Modules
RM	Required Modules
IF	Input Frequency (kHz)
OF	Output Frequency (kHz)
RF	Dc Bus Ripple Factor (%)
1IFM	Single-Phase Input Filter Mass (kg)
3IFM	3-Phase Input Filter Mass (kg)
1RM	Single-Phase Rectifier Mass (kg)
3RM	3-Phase Rectifier Mass (kg)
1DCFM	Single-Phase Dc Bus Filter Mass (kg)
3DCFM	3-Phase Dc Bus Filter Mass (kg)
1CM	Single-Phase Chopper Mass (kg)
3CM	3-Phase Chopper Mass (kg)
1TM	Single-Phase Transformer Mass (kg)
3TM	3-Phase Transformer Mass (kg)
1OFM	Single-Phase Output Dc Filter Mass (kg)
3OFM	3-Phase Output Dc Filter Mass (kg)
FE	Ac and Dc Filter Efficiencies (%)
RE	Rectifier Efficiency (%)
CE	Chopper Efficiency (%)

TE	Transformer Efficiency (%)
1CCM	Single-Phase Conductor and Connector Mass (kg)
3CCM	3-Phase Conductor and Connector Mass (kg)
1CMM	Single-Phase Control and Monitoring Mass (kg)
3CMM	3-Phase Control and Monitoring Mass (kg)
1CMP	Single-Phase Control and Monitoring Power (kg)
3CMP	3-Phase Control and Monitoring Power (kg)
AACEM	AC/AC Frequency Converter Electronics Mass (kg)
AACE	AC/AC Frequency Converter Efficiency (%)
AACSE	AC/AC Frequency Converter Stage Efficiency (%)
CV	Component Volume (m^3)
CH	Component Height (m)
CW	Component Width (m)
CL	Component Length (m)
FHEM	Finned Heat Exchanger Enclosure Mass (kg)
CPEM	Coldplate Based Enclosure Mass (kg)
RA	Radiator Area (m^2)
RAM	Radiator Mass (kg)
TD	Coldplate to Radiator Temperature Delta (°C)
T	Coldplate Temperature (°C)

The EXCEL model "ACACFREQ.XLS" is for a dc link resonant based ac/ac frequency converter. The following equations are contained in this model.

AC/AC Frequency Converter Component Equations

$$P_I=P_O/AACE$$

Single- and 3-Phase: AACSE=FE*RE*FE*CE*TE*FE

Single-Phase: $AACE=P_O/((P_O/FE/TE/CE/FE/RE+1CMP/1000)/FE)$

3-Phase: $AACE=P_O/((P_O/FE/TE/CE/FE/RE+3CMP/1000)/FE)$

Single-Phase: AACEM=1IFM+1RM+1DCFM+1CM+1TM+1OFM+1CCM+1CMM

3-Phase: AACEM=3IFM+3RM+3DCFM+3CM+3TM+3OFM+3CCM+3CMM

AC/AC Frequency Converter Input Ac Filter Equations

$1IFM=0.01*((1-0.995)/(1-FE))*(AM/RM)*(P_O/FE/TE/CE/FE/RE+1CMP/1000)*$
$(P_O/RM/FE/TE/CE/FE/RE+1CMP/RM/1000)^{-0.03}*(IF/20)^{-0.6}$

$3IFM=0.0105*((1-0.995)/(1-FE))*(AM/RM)*(P_O/FE/TE/CE/FE/RE+3CMP/1000)*$
$(P_O/RM/FE/TE/CE/FE/RE+3CMP/RM/1000)^{-0.03}*(IF/20)^{-0.6}$

AC/AC Frequency Converter Rectifier Equations

$1RM=0.1*((EXP(0.005/(1-RE)))/1.4)*(AM/RM)*(P_O/FE/TE/CE/FE)*$
$(V_O/FE/TE/CE/FE/(V_O/FE/TE/CE/FE-2))^6*EXP(V_O/FE/TE/CE/FE/80000)$

$3RM=0.11*((EXP(0.005/(1-RE)))/1.4)*(AM/RM)*(P_O/FE/TE/CE/FE)*$
$(V_O/FE/TE/CE/FE/(V_O/FE/TE/CE/FE-2))^6*EXP(V_O/FE/TE/CE/FE/80000)$

AC/AC Frequency Converter Dc Bus Filter Equations

$1DCFM=470*(1/(RF/0.01)^{0.5})*((1-0.995)/(1-FE))*(AM/RM)*(P_O/FE/TE/CE)*$
$((FE*0.9*RE*FE*V_I)^{-2}+0.000001)*(20/IF)$

$3DCFM=470*(1/(RF/0.01)^{0.5})*((1-0.995)/(1-FE))*(AM/RM)*(P_O/FE/TE/CE)*$
$((FE*0.9*RE*FE*V_I)^{-2}+0.000001)*(6.7/IF)$

AC/AC Frequency Converter Chopper Equations

$1CM=0.39*((EXP(0.025/(1-CE)))/1.86)*(AM/RM)*(P_O/FE/TE)*((P_O/RM/FE/TE)^{-0.05}*$
$(V_I*FE*RE*FE/(V_I*FE*RE*FE-2))^7*EXP(V_I*FE*RE*FE/40000)*$
$(20/OF)^{0.45}*EXP(P_O{}^{0.1}*OF/160))$

$3CM=0.4*((EXP(0.025/(1-CE)))/1.86)*(AM/RM)*(P_O/FE/TE)*((P_O/RM/FE/TE)^{-0.05}$
$*(V_I*FE*RE*FE/(V_I*FE*RE*FE-2))^7*EXP(V_I*FE*RE*FE/40000)*$
$(20/OF)^{0.45}*EXP(P_O{}^{0.1}*OF/160))$

AC/AC Frequency Converter Transformer Equations

$1TM=1.27*((EXP(0.003/(1-TE)))/1.35)*(AM/RM)*(P_O/FE)*((P_O/RM/FE)^{-0.08}$
$*EXP(0.9*V_I*FE*RE*FE*CE/200000)*EXP(V_O/FE/200000)*OF^{-0.47}+(OF/300)^{1.4})$

$3TM=2.75*((EXP(0.003/(1-TE)))/1.35)*(AM/RM)*(P_O/FE)*((P_O/RM/FE)^{-0.25}$
$*EXP(1.35*V_I*FE*RE*FE*CE/200000)*EXP(V_O/FE/200000)*OF^{-0.47}+(OF/300)^{1.4})$

AC/AC Frequency Converter Output Ac Filter Equations

$$1OFM=0.1*((1-0.995)/(1-FE))*(AM/RM)*P_O*(P_O/RM)^{-0.03}*(IF/20)^{-0.6}$$

$$3OFM=0.105*((1-0.995)/(1-FE))*(AM/RM)*P_O*(P_O/RM)^{-0.03}*(IF/20)^{-0.6}$$

AC/AC Frequency Converter Conductor and Connector Equations

$$1CCM=(AM/RM)*(0.014*((P_O*1000)/V_O)+0.042*(((P_O*1000)/AACE)/V_I))$$

$$3CCM=(AM/RM)*((3^{0.5}/2)*0.014*((P_O*1000)/V_O)+(3^{0.5}/2)*0.042*(((P_O*1000)/AACE)/V_I))$$

The coefficients "0.014" and "0.042" used in these equations differ from the coefficients "0.028" and "0.028" previously defined for components having two voltage levels. Since the input filter, rectifier, dc bus filter, chopper and transformer primary will be at the input voltage level and only the transformer secondary and output filter will be at the output voltage level, this adjustment was considered necessary to properly weight the conductor mass calculations.

AC/AC Frequency Converter Control and Monitoring Equations

$$1CMM=AM*(1.4+0.9*(P_O/RM)^{0.3}+0.25*(P_O/RM)^{0.3})$$

$$3CMM=AM*(2+2.5*(P_O/RM)^{0.3}+0.75*(P_O/RM)^{0.3})$$

$$1CMP=AM*55.6*(P_O/RM)^{0.1}$$

$$3CMM=AM*79.4*(P_O/RM)^{0.1}$$

AC/AC Frequency Converter Volume and Dimension Equations

$$CV=AACEM/(0.342*1000)$$

$$CH=0.7*CV^{0.3333}$$

$$CW=1.1*CV^{0.3333}$$

$$CL=1.3*CV^{0.3333}$$

AC/AC Frequency Converter Enclosure Equations

$$FHEM=44.26*CV^{0.6666}+27*(CL*CW)$$

$$CPEM=44.26*CV^{0.6666}+10.25*(CL*CW)$$

AC/AC Frequency Converter Radiator Equations

$$RA=(1.1212E+10*(P_O/AACE-P_O)/((T+273-TD)^4-250^4)$$

$$RAM=4.159*RA$$

3.2.4 Transformer/Rectifier Model

The transformer/rectifier model combines the standard transformer and rectifier stage models. Filtering and ancillary hardware are included to complete the package. A diagram of the transformer/rectifier model is shown in Figure 56.

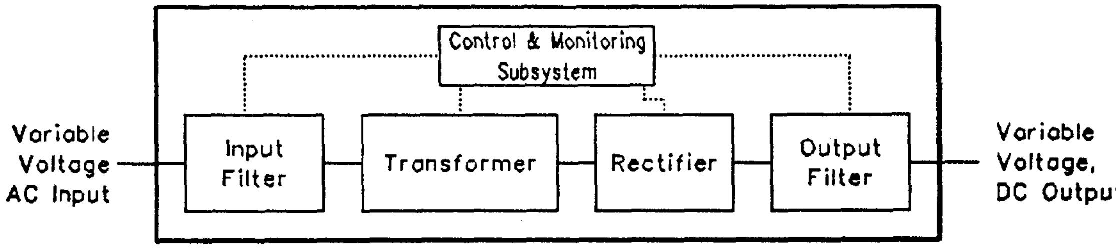

Figure 56 Transformer/Rectifier Diagram

<u>Application Notes:</u> Transformer/rectifiers are utilized to change an incoming ac voltage to an alternate value and provide a rectified dc output. The transformer stage also isolates the input and output, which reduces the level of transmitted interference. This transformer/rectifier model is intended primarily for applications near the load. Normally, these applications require a high voltage input to be stepped down and rectified for distribution. However, it can also estimate the mass of a transformer/rectifier unit that follows an alternator power source. The main difference in the two applications is typically the output dc filter design. The characteristics of a particular application will determine its filter requirements; however, a ripple factor of 1% is suggested for converters that provide power to sensitive user loads, and 5% is recommended for units that follow an alternator or feed industrial power devices such as heaters. This model is only designed to accept low frequency inputs, 2 kHz or less, with a low harmonic content. It is not designed to accept a high frequency input. Units configured to accept high frequency inputs are generally referred to as dc load receivers and they incorporate a resonant tank circuit.

The coefficient in the input filter equation was cut to one-tenth of the value specified in the ac filter equations listed in section 3.1.5. This will yield a filter mass that is more consistent with this application. The ac filter design described in section 3.1.5 is a series harmonic trap and its main purpose is to prevent the resonant circuit in the chopper from amplifying external harmonics. The rectifier stage in the transformer/rectifier unit does not contain a resonant circuit, so it is not capable of amplifying harmonics. The transformer also acts as a filter and it limits the noise reflected back to the input by the rectifier. Finally, alternators can tolerate fairly high levels of harmonic distortion so it is not necessary to completely suppress these harmonics anyway. To improve these filter mass estimates, system power quality requirements must be defined and low frequency filter designs suitable for this type of application must be generated. Most of the ac filter designs noted to date are intended for high frequency uses.

Spreadsheet Printout: A printout of the transformer/rectifier model is shown in Figure 57. It is described in later sections.

Model Input Parameter Ranges: The results generated by this spreadsheet are only valid for a certain range of input parameters. Inaccurate mass estimates may result if input parameters outside of the ranges defined in Table 28 are used and it is not recommended. Table 28 also identifies the values that should yield the best results, and lists sources that should be consulted for certain input parameters. The user is responsible for selecting input parameters that do not conflict and are reasonable for the application and operating conditions.

Date: September 10, 1991

File Name: XFMRRECT.XLS

Originator: K. J. Metcalf

Transformer/Rectifier Design Model

Input Parameters

Output Power (kWe)	25	Transformer Frequency (kHz)	1
Input Voltage (Vrms)	2000	Filter Efficiency (%)	99.5%
Output Voltage (Vdc)	200	Transformer Efficiency (%)	99.0%
Number of Phases	3	Rectifier Efficiency (%)	98.5%
Ripple Factor (%)	1.0%	Coldplate Temperature (C)	60
Available Modules	1	Coldplate-Rad. Temp. Delta (C)	16.7
Required Modules	1	Enclosure (FH or CP)	CP

Component Mass Characteristics

Input Filter Mass (kg)	XFMR Mass (kg)	Rectifier Mass (kg)	Output Filter Mass (kg)	Cable & Conn. Mass (kg)	Cntrl & Mon. Mass (kg)	Enclosure Mass (kg)
1.49	28.70	2.93	20.47	3.35	7.67	19.40

Radiator Mass (kg)		Component Mass without Radiator (kg)	Component Specific Mass (kg/kW)		Total Mass with Radiator (kg)	Total Specific Mass (kg/kW)
7.51		84.01	3.36		91.52	3.66

Figure 57

Page 1

XFMRRECT.XLS

		Component Volume and Dimensions					
Single Module Parameters				Complete Assembly Parameters			
Volume (cu meters)		0.189		Volume (cu meters)		0.189	
Height (meters)		0.40		Height (meters)		0.40	
Width (meters)		0.63		Width (meters)		0.63	
Length (meters)		0.75		Length (meters)		0.75	
Radiator Area, Input Power, Parasitic Power, and Efficiencies							
Radiator Area (square meters)		Input Power Requirements (kWe)		Parasitic Power Demand (watts)	Eff. of Component Stages (%)	Total XFMR Rectifier Eff. (%)	
1.81		25.98		87.61	96.5%	96.2%	

Figure 57

Page 2

Intermediate Calculation Values			
1 Ph Input Filter Mass (kg)	1.42	1 Phase XFMR Mass (kg)	22.90
3 Ph Input Filter Mass (kg)	1.49	3 Phase XFMR Mass (kg)	28.70
1 Phase Rectifier Mass (kg)	2.67	1 Ph Output Filter Mass (kg)	61.10
3 Phase Rectifier Mass (kg)	2.93	3 Ph Output Filter Mass (kg)	20.47
1 Phase Conductor Mass (kg)	3.86		
3 Phase Conductor Mass (kg)	3.35		
1 Phase Cntl & Mon Mass (kg)	3.41	1 Ph Cntl & Mon Power (watts)	61.40
3 Phase Cntl & Mon Mass (kg)	7.67	3 Ph Cntl & Mon Power (watts)	87.61
Single Module Finned HEX Enclosure Mass (kg)	27.29	Single Module Coldplate Enclosure Mass (kg)	19.40
Total Assembly Finned HEX Enclosure Mass (kg)	27.29	Total Assembly Coldplate Enclosure Mass (kg)	19.40

Figure 57

Page 3

Table 28
Transformer/Rectifier Unit Model Input Parameter Ranges

Transformer/Rectifier Unit Input Parameter	Recommended Input Range
Output Power Level	0.5 to 250 kWe
Input Voltage Level[1]	20 to 10,000 Vrms
Output Voltage Level[1]	20 to 10,000 Vdc (Refer to Table 3 for voltages below 120 Vdc)
Number of Phases	1 or 3
Ripple Factor Percentage	0.5 to 8%
Available Modules	Equal to or Greater than Required Modules
Required Modules	No Limit
Transformer Frequency	60 Hz to 2 kHz
AC and DC Filter Efficiencies	Range: 99.0 to 99.9% 99.5% is Recommended
Transformer Efficiency	Range: 97.5 to 99.5% 99% is Recommended
Rectifier Efficiency	Normal Range: 97.5 to 99.5% 98.5% is Recommended
Coldplate Temperature[2]	10 to 100° C 40° C Suggested for FH Enclosure 60° C Suggested for CP Enclosure
Coldplate to Radiator Temperature Delta	0 to 20° C 16.7° C is Recommended
Enclosure Type (FH or CP)	Finned Heat Exchanger (FH) Coldplate (CP)

1. The voltage step ratio should not exceed the limits defined in Table 6. To obtain the voltage step ratio, divide the higher, input or output voltage by the other, input or output voltage.

2. Because the Coldplate Enclosure has a lower thermal resistance than the Finned Heat Exchanger Enclosure, the coldplate temperature can be set 20° C higher when the Coldplate Enclosure is selected.

Model Equation Listing: Table 29 defines the variables utilized in the transformer/rectifier unit model equations.

Table 29
Transformer/Rectifier Unit Model Variable Definitions

P_O	Output Power Level (kWe)
P_I	Input Power Level (kWe)
V_I	Voltage Input (Vdc)
V_O	Voltage Output (Vdc)
AM	Available Modules
RM	Required Modules
TF	Transformer Frequency (kHz)
RF	Ripple Factor (%)
1IFM	Single-Phase Input Ac Filter Mass (kg)
3IFM	3-Phase Input Ac Filter Mass (kg)
1TM	Single-Phase Transformer Mass (kg)
3TM	3-Phase Transformer Mass (kg)
1RM	Single-Phase Rectifier Mass (kg)
3RM	3-Phase Rectifier Mass (kg)
1OFM	Single-Phase Output Dc Filter Mass (kg)
3OFM	3-Phase Output Dc Filter Mass (kg)
FE	Ac and Dc Filter Efficiencies (%)
TE	Transformer Efficiency (%)
RE	Rectifier Efficiency (%)
1CCM	Single-Phase Conductor and Connector Mass (kg)
3CCM	3-Phase Conductor and Connector Mass (kg)
1CMM	Single-Phase Control and Monitoring Mass (kg)
3CMM	3-Phase Control and Monitoring Mass (kg)
1CMP	Single-Phase Control and Monitoring Power (kg)

3CMP	3-Phase Control and Monitoring Power (kg)
TRUEM	Transformer/Rectifier Unit Electronics Mass (kg)
TRUE	Transformer/Rectifier Unit Efficiency (%)
TRUSE	Transformer/Rectifier Unit Stage Efficiency (%)
CV	Component Volume (m^3)
CH	Component Height (m)
CW	Component Width (m)
CL	Component Length (m)
FHEM	Finned Heat Exchanger Enclosure Mass (kg)
CPEM	Coldplate Based Enclosure Mass (kg)
RA	Radiator Area (m^2)
RAM	Radiator Mass (kg)
TD	Coldplate to Radiator Temperature Delta (°C)
T	Coldplate Temperature (°C)

The EXCEL model "XFMRRECT.XLS" is for a transformer/rectifier unit configured to accept frequency inputs from 60 Hz to 2 kHz. The following equations are contained in this model.

Transformer/Rectifier Unit Component Equations

$$P_I=P_O/TRUE$$

Single- and 3-Phase: TRUSE=FE*TE*RE*FE

Single-Phase: $TRUE=P_O/((P_O/FE/RE/TE+1CMP/1000)/FE)$

3-Phase: $TRUE=P_O/((P_O/FE/RE/TE+3CMP/1000)/FE)$

Single-Phase: TRUEM=1IFM+1TM+1RM+1OFM+1CCM+1CMM

3-Phase: TRUEM=3IFM+3TM+3RM+3OFM+3CCM+3CMM

Transformer/Rectifier Unit Input Ac Filter Equations

$$1IFM=0.01*((1-0.995)/(1-FE))*(AM/RM)*(P_O/FE/RE/TE+1CMP/1000)*(P_O/RM/FE/RE/TE+1CMP/RM/1000)^{-0.03}*(TF/20)^{-0.6}$$

$$3IFM=0.0105*((1-0.995)/(1-FE))*(AM/RM)*(P_O/FE/RE/TE+3CMP/1000)*(P_O/RM/FE/RE/TE+3CMP/RM/1000)^{-0.03}*(TF/20)^{-0.6}$$

Transformer/Rectifier Unit Transformer Equations

$$1TM=1.15*((EXP(0.003/(1-TE)))/1.35)*(AM/RM)*(P_O/FE/RE)*((P_O/RM/FE/RE)^{-0.08}*EXP(V_I*FE/200000)*EXP(V_O/0.9/FE/RE/200000)*OF^{-0.47}+(OF/300)^{1.4})$$

$$3TM=2.5*((EXP(0.003/(1-TE)))/1.35)*(AM/RM)*(P_O/FE/RE)*((P_O/RM/FE/RE)^{-0.25}*EXP(V_I*FE/200000)*EXP(V_O/1.35/FE/RE/200000)*OF^{-0.47}+(OF/300)^{1.4})$$

Transformer/Rectifier Unit Rectifier Equations

$$1RM=0.1*((EXP(0.005/(1-RE)))/1.4)*(AM/RM)*(P_O/FE)*(V_O/FE/(V_O/FE-2))^{6}*EXP(V_O/FE/80000)$$

$$3RM=0.11*((EXP(0.005/(1-RE)))/1.4)*(AM/RM)*(P_O/FE)*(V_O/FE/(V_O/FE-2))^{6}*EXP(V_O/FE/80000)$$

Transformer/Rectifier Unit Output Dc Filter Equations

$$1OFM=4700*(1/(RF/0.01)^{0.5})*((1-0.995)/(1-FE))*(AM/RM)*P_O*(V_O^{-2}+0.000001)*(20/TF)$$

$$3OFM=4700*(1/(RF/0.01)^{0.5})*((1-0.995)/(1-FE))*(AM/RM)*P_O*(V_O^{-2}+0.000001)*(6.7/TF)$$

Transformer/Rectifier Unit Conductor and Connector Equations

$$1CCM=(AM/RM)*(0.028*((P_O*1000)/V_O)+0.028*(((P_O*1000)/TRUE)/V_I))$$

$$3CCM=(AM/RM)*((3^{0.5}/2)*0.028*((P_O*1000)/V_O)+(3^{0.5}/2)*0.028*(((P_O*1000)/TRUE)/V_I))$$

Transformer/Rectifier Unit Control and Monitoring Equations

$$1CMM=AM*(1.4+0.6*(P_O/RM)^{0.3}+0.167*(P_O/RM)^{0.3})$$

$$3CMM=AM*(2+1.66*(P_O/RM)^{0.3}+0.5*(P_O/RM)^{0.3})$$

$$1CMP=AM*44.5*(P_O/RM)^{0.1}$$

$$3CMM=AM*63.5*(P_O/RM)^{0.1}$$

The normally used coefficients "0.9" and "0.25", and "2.5" and "0.75" in the control and monitoring mass equations were reduced to "0.6" and "0.167", and "1.66" and "0.5" respectively. This was done because a transformer/rectifier unit has fewer stages and is less complex than components such as a dc/dc converter or frequency converter; consequently, the number of sensors and their corresponding wiring was judged to be about two-thirds of the amounts in these components.

The normally used coefficients "55.6" and "79.4" in the control and monitoring power demand equations were reduced to "44.5" and "63.5" respectively. This was done because a transformer/rectifier unit has fewer sensors than components such as a dc/dc converter or frequency converter; consequently, the control and monitoring power demand was judged to be about 80% of the demand in these components.

Transformer/Rectifier Unit Volume and Dimension Equations

$$CV=TRUEM/(0.342*1000)$$

$$CH=0.7*CV^{0.3333}$$

$$CW=1.1*CV^{0.3333}$$

$$CL=1.3*CV^{0.3333}$$

Transformer/Rectifier Unit Enclosure Equations

$$FHEM=44.26*CV^{0.6666}+27*(CL*CW)$$

$$CPEM=44.26*CV^{0.6666}+10.25*(CL*CW)$$

Transformer/Rectifier Unit Radiator Equations

$$RA=(1.1212E+10*(P_0/TRUE-P_0)/((T+273-TD)^4-250^4)$$

$$RAM=4.159*RA$$

3.2.5 Rectifier Unit Model

The rectifier unit model is created by adding filtering after the rectifier stage and including ancillary hardware. A diagram of the rectifier unit model is shown in Figure 58.

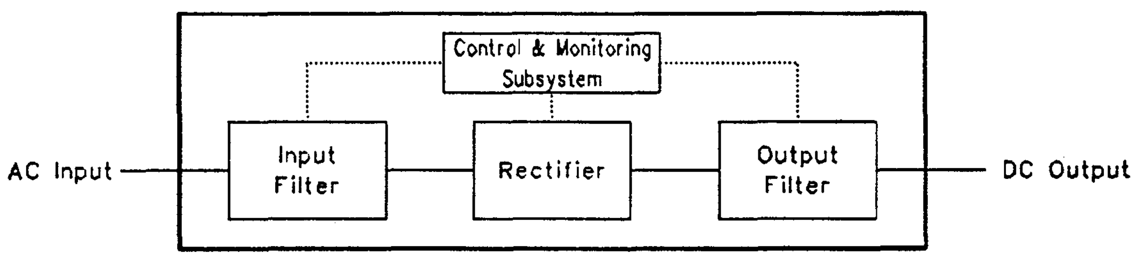

Figure 58 Rectifier Unit Diagram

<u>Application Notes:</u> Rectifier units are used to convert an incoming ac waveform to a dc output. This rectifier unit model is suitable for applications following an alternator or feeding a load or distribution network. The main difference in the two applications will probably be the output dc filter design. The characteristics of a particular application will determine its filter specifications; however, a ripple factor of 1% is suggested for rectifier units that supply power to sensitive user loads, and 5% is recommended for units that follow an alternator or feed industrial power devices such as heaters. This model is only suitable to accept low frequency inputs, 2 kHz or less, with a low harmonic content.

It is not designed to accept a high frequency input. A dc load receiver with a resonant tank circuit is normally preferred for high frequency inputs.

The input filter equation coefficient was reduced to a value that is one-tenth of the value contained in the ac filter equations listed in section 3.1.5. This will yield a filter mass that is more indicative of this application. The ac filter design described in section 3.1.5 is a series harmonic trap and its main purpose is to prevent the resonant circuit in the chopper from amplifying external harmonics. A rectifier does not contain a resonant circuit, so it is not capable of amplifying harmonics. Alternators can also tolerate fairly high levels of harmonic distortion so it is not necessary to completely suppress these harmonics anyway. To improve these filter mass estimates, system power quality requirements must be defined and low frequency filter designs suitable for this type of application must be generated. The majority of the ac filter designs noted to date are intended for high frequency uses.

Spreadsheet Printout: A printout of the rectifier unit model is shown in Figure 59. Subsequent sections describe its characteristics and operation.

Model Input Parameter Ranges: The results generated by this spreadsheet are only valid for a certain range of input parameters. Inaccurate mass estimates may result if input parameters outside of the ranges defined in Table 30 are used and it is not recommended. Table 30 also identifies the values that should yield the best results, and lists sources that should be consulted for certain input parameters. The user is responsible for selecting input parameters that do not conflict and are reasonable for the application and operating conditions.

Date: September 18, 1991					File Name:		ACDCRECT.XLS
					Originator:		K. J. Metcalf
		Rectifier Design Model					
		Input Parameters					
Output Power (kWe)		25		Transmission Frequency (kHz)			1
Output Voltage (Vdc)		500		Filter Efficiency (%)			99.5%
Number of Phases		3		Rectifier Efficiency (%)			98.5%
Ripple Factor (%)		5.0%		Coldplate Temperature (C)			60
Available Modules		1		Coldplate-Rad. Temp. Delta (C)			16.7
Required Modules		1		Enclosure (FH or CP)			CP
		Component Mass Characteristics					
Input Filter Mass (kg)	Rectifier Mass (kg)	Output Filter Mass (kg)	Cable & Conn. Mass (kg)	Cntrl & Mon. Mass (kg)	Enclosure Mass (kg)		
1.47	2.84	1.76	2.42	4.84	6.78		
Radiator Mass (kg)		Component Mass without Radiator (kg)	Component Specific Mass (kg/kW)		Total Mass with Radiator (kg)	Total Specific Mass (kg/kW)	
5.37		20.11	0.80		25.47	1.02	

Figure 59

Page 1

		Component Volume and Dimensions					
Single Module Parameters				Complete Assembly Parameters			
Volume (cu meters)		0.039		Volume (cu meters)		0.039	
Height (meters)		0.24		Height (meters)		0.24	
Width (meters)		0.37		Width (meters)		0.37	
Length (meters)		0.44		Length (meters)		0.44	
Radiator Area, Input Power, Parasitic Power, and Efficiencies							
Radiator Area (square meters)		Input Power Demand (kWe)	Input Voltage Level (Vrms)		Parasitic Power Demand (watts)	Eff. of Component Stages (%)	Total Rectifier Eff. (%)
1.29		25.70	379.80		65.68	97.5%	97.3%

Figure 59

Page 2

Intermediate Calculation Values			
1 Ph Input Filter Mass (kg)	1.40	1 Phase Rectifier Mass (kg)	2.58
3 Ph Input Filter Mass (kg)	1.47	3 Phase Rectifier Mass (kg)	2.84
1 Ph Output Filter Mass (kg)	5.25	1 Phase Conductor Mass (kg)	2.80
3 Ph Output Filter Mass (kg)	1.76	3 Phase Conductor Mass (kg)	2.42
1 Phase Cntl & Mon Mass (kg)	2.41	1 Ph Cntl & Mon Power (watts)	46.08
3 Phase Cntl & Mon Mass (kg)	4.84	3 Ph Cntl & Mon Power (watts)	65.68
Single Module Finned HEX Enclosure Mass (kg)	9.53	Single Module Coldplate Enclosure Mass (kg)	6.78
Total Assembly Finned HEX Enclosure Mass (kg)	9.53	Total Assembly Coldplate Enclosure Mass (kg)	6.78

Figure 59

Page 3

Table 30
Rectifier Unit Model Input Parameter Ranges

Rectifier Unit Input Parameter	Recommended Input Range
Output Power Level	0.5 to 250 kWe
Output Voltage Level	20 to 10,000 Vdc (Refer to Table 3 for voltages below 120 Vdc)
Number of Phases	1 or 3
Ripple Factor Percentage	0.5 to 8%
Available Modules	Equal to or Greater than Required Modules
Required Modules	No Limit
Transmission Frequency	60 Hz to 2 kHz
AC and DC Filter Efficiencies	Range: 99.0 to 99.9% 99.5% is Recommended
Rectifier Efficiency	Normal Range: 97.5 to 99.5% 98.5% is Recommended
Coldplate Temperature(1)	10 to 100° C 40° C Suggested for FH Enclosure 60° C Suggested for CP Enclosure
Coldplate to Radiator Temperature Delta	0 to 20° C 16.7° C is Recommended
Enclosure Type (FH or CP)	Finned Heat Exchanger (FH) Coldplate (CP)

1. Because the Coldplate Enclosure has a lower thermal resistance than the Finned Heat Exchanger Enclosure, the coldplate temperature can be set 20° C higher when the Coldplate Enclosure is selected.

Model Equation Listing: Table 31 defines the variables used in the rectifier unit model equations.

Table 31
Rectifier Unit Model Variable Definitions

P_O	Output Power Level (kWe)
P_I	Input Power Level (kWe)
V_O	Voltage Output (Vdc)
AM	Available Modules
RM	Required Modules
TF	Transmission Frequency (kHz)
RF	Ripple Factor (%)
1IFM	Single-Phase Input Ac Filter Mass (kg)
3IFM	3-Phase Input Ac Filter Mass (kg)
1RM	Single-Phase Rectifier Mass (kg)
3RM	3-Phase Rectifier Mass (kg)
1OFM	Single-Phase Output Dc Filter Mass (kg)
3OFM	3-Phase Output Dc Filter Mass (kg)
FE	Ac and Dc Filter Efficiencies (%)
RE	Rectifier Efficiency (%)
1CCM	Single-Phase Conductor and Connector Mass (kg)
3CCM	3-Phase Conductor and Connector Mass (kg)
1CMM	Single-Phase Control and Monitoring Mass (kg)
3CMM	3-Phase Control and Monitoring Mass (kg)
1CMP	Single-Phase Control and Monitoring Power (kg)
3CMP	3-Phase Control and Monitoring Power (kg)
RUEM	Rectifier Unit Electronics Mass (kg)
RUE	Rectifier Unit Efficiency (%)
RUSE	Rectifier Unit Stage Efficiency (%)

CV Component Volume (m^3)

CH Component Height (m)

CW Component Width (m)

CL Component Length (m)

FHEM Finned Heat Exchanger Enclosure Mass (kg)

CPEM Coldplate Based Enclosure Mass (kg)

RA Radiator Area (m^2)

RAM Radiator Mass (kg)

TD Coldplate to Radiator Temperature Delta (°C)

T Coldplate Temperature (°C)

The EXCEL model "ACDCRECT.XLS" is for a rectifier unit capable of accepting frequency inputs ranging from 60 Hz to 2 kHz. The model utilizes the following equations.

Rectifier Unit Component Equations

$$P_I=P_O/RUE$$

Single- and 3-Phase: RUSE=FE*TE*RE*FE

Single-Phase: $RUE=P_O/((P_O/FE/RE/TE+1CMP/1000)/FE)$

3-Phase: $RUE=P_O/((P_O/FE/RE/TE+3CMP/1000)/FE)$

Single-Phase: RUEM=1IFM+1TM+1RM+1OFM+1CCM+1CMM

3-Phase: RUEM=3IFM+3TM+3RM+3OFM+3CCM+3CMM

Rectifier Unit Input Ac Filter Equations

$$1IFM=0.01*((1-0.995)/(1-FE))*(AM/RM)*(P_O/FE/RE+1CMP/1000)*(P_O/RM/FE/RE+1CMP/RM/1000)^{-0.03}*(TF/20)^{-0.6}$$

$$3IFM=0.0105*((1-0.995)/(1-FE))*(AM/RM)*(P_O/FE/RE+3CMP/1000)*(P_O/RM/FE/RE+3CMP/RM/1000)^{-0.03}*(TF/20)^{-0.6}$$

Rectifier Unit Rectifier Equations

$$1RM=0.1*((EXP(0.005/(1-RE)))/1.4)*(AM/RM)*(P_O/FE)*(V_O/FE/(V_O/FE-2))^{6}*EXP(V_O/FE/80000)$$

$$3RM=0.11*((EXP(0.005/(1-RE)))/1.4)*(AM/RM)*(P_o/FE)*(V_o/FE/(V_o/FE-2))^6 *EXP(V_o/FE/80000)$$

Rectifier Unit Output Dc Filter Equations

$$1OFM=4700*(1/(RF/0.01)^{0.5})*((1-0.995)/(1-FE))*(AM/RM)*P_o*(V_o^{-2}+0.000001)*(20/TF)$$

$$3OFM=4700*(1/(RF/0.01)^{0.5})*((1-0.995)/(1-FE))*(AM/RM)*P_o*(V_o^{-2}+0.000001)*(6.7/TF)$$

Rectifier Unit Conductor and Connector Equations

$$1CCM=0.056*(AM/RM)*((P_o*1000)/V_o)$$

$$3CCM=0.056*(AM/RM)*(3^{0.5}/2)*((P_o*1000)/V_o)$$

Rectifier Unit Control and Monitoring Equations

$$1CMM=AM*(1.4+0.3*(P_o/RM)^{0.3}+0.083*(P_o/RM)^{0.3})$$

$$3CMM=AM*(2+0.83*(P_o/RM)^{0.3}+0.25*(P_o/RM)^{0.3})$$

$$1CMP=AM*33.4*(P_o/RM)^{0.1}$$

$$3CMM=AM*47.6*(P_o/RM)^{0.1}$$

The normally used coefficients "0.9" and "0.25", and "2.5" and "0.75" in the control and monitoring mass equations were reduced to "0.3" and "0.083", and "0.83" and "0.25" respectively. This was done because a rectifier unit has fewer stages and is less complex than components such as a dc/dc converter or frequency converter; consequently, the number of sensors and their corresponding wiring was judged to be about one-third of the amounts in these components.

The normally used coefficients "55.6" and "79.4" in the control and monitoring power demand equations were reduced to "33.4" and "47.6" respectively. This was done because a rectifier unit has fewer sensors than components such as a dc/dc converter or frequency converter; consequently, the control and monitoring power demand was judged to be about 60% of the demand in these components.

Rectifier Unit Volume and Dimension Equations

$$CV=RUEM/(0.342*1000)$$

$$CH=0.7*CV^{0.3333}$$

$$CW=1.1*CV^{0.3333}$$

$$CL=1.3*CV^{0.3333}$$

Rectifier Unit Enclosure Equations

$$FHEM=14.26*CV^{0.6666}+27*(CL*CW)$$

$$CPEM=44.26*CV^{0.6666}+10.25*(CL*CW)$$

Rectifier Unit Radiator Equations

$$RA=(1.1212E+10*(P_0/RUE-P_0)/((T+273-TD)^4-250^4)$$

$$RAM=4.159*RA$$

3.2.6 Transformer Unit Model

The transformer unit model is the easiest to create. It simply incorporates the standard transformer stage with its associated ancillary hardware. A diagram of the transformer unit model is shown in Figure 60.

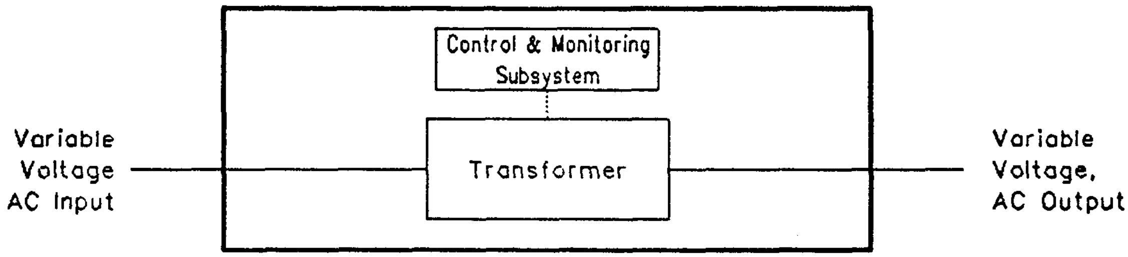

Figure 60 Transformer Unit Diagram

Application Notes: The transformer unit is used to change the input ac voltage to an different level. The transformer stage also isolates the input and output, which reduces the level of transmitted interference. The transformer unit can be used anywhere in the power system where a change in voltage is required. In applications near a load the high transmission voltage is normally stepped down to the level desired by the load or selected for distribution. It can also be used after an alternator power source, but normally an alternator is capable of providing the desired voltage directly. Since the transformer unit does not use filtering, there are no filter considerations. This model is designed to accept any frequency input from 60 Hz to 60 kHz, but the waveform should exhibit a fairly low harmonic content consistent with external sinusoidal power transmission.

Spreadsheet Printout: A printout of the transformer unit model is shown in Figure 61. Its format and operation is described in later sections.

Model Input Parameter Ranges: The results generated by this spreadsheet are only valid for a certain range of input parameters. Inaccurate mass estimates may result if input parameters outside of the ranges defined in Table 32 are used and it is not recommended. Table 32 also identifies the values that should yield the best results, and lists sources that should be consulted for certain input parameters. The user is responsible for selecting input parameters that do not conflict and are reasonable for the application and operating conditions.

Date: September 10, 1991						File Name: ACACXFMR.XLS	
						Originator: K. J. Metcalf	
		Transformer Design Model					
		Input Parameters					
Output Power (kWe)		100		Transformer Frequency (kHz)			1
Input Voltage (Vrms)		500		Transformer Efficiency (%)			99.0%
Output Voltage (Vdc)		5000		Coldplate Temperature (C)			60
Number of Phases		3		Coldplate-Rad. Temp. Delta (C)			16.7
Available Modules		1		Enclosure (FH or CP)			CP
Required Modules		1					
		Component Mass Characteristics					
XFMR Mass (kg)	Cable & Conn. Mass (kg)	Cntrl & Mon. Mass (kg)	Enclosure Mass (kg)				
81.34	5.39	6.30	24.74				
Radiator Mass (kg)		Component Mass without Radiator (kg)	Component Specific Mass (kg/kW)		Total Mass with Radiator (kg)	Total Specific Mass (kg/kW)	
8.29		117.76	1.18		126.06	1.26	

Figure 61

Page 1

ACACXFMR.XLS

		Component Volume and Dimensions					
Single Module Parameters				Complete Assembly Parameters			
Volume (cu meters)		0.272		Volume (cu meters)		0.272	
Height (meters)		0.45		Height (meters)		0.45	
Width (meters)		0.71		Width (meters)		0.71	
Length (meters)		0.84		Length (meters)		0.84	
Radiator Area, Input Power, Parasitic Power, and Efficiencies							
Radiator Area (square meters)		Input Power Requirements (kWe)		Parasitic Power Demand (watts)	Eff. of Component Stages (%)	Total XFMR Rectifier Eff. (%)	
1.99		101.09		75.44	99.0%	98.9%	

Figure 61

Page 2

Intermediate Calculation Values

1 Phase XFMR Mass (kg)	81.81	1 Phase Conductor Mass (kg)	6.22
3 Phase XFMR Mass (kg)	81.34	3 Phase Conductor Mass (kg)	5.39
1 Phase Cntl & Mon Mass (kg)	2.92	1 Ph Cntl & Mon Power (watts)	52.94
3 Phase Cntl & Mon Mass (kg)	6.30	3 Ph Cntl & Mon Power (watts)	75.44
Single Module Finned HEX Enclosure Mass (kg)	34.79	Single Module Coldplate Enclosure Mass (kg)	24.74
Total Assembly Finned HEX Enclosure Mass (kg)	34.79	Total Assembly Coldplate Enclosure Mass (kg)	24.74

Figure 61

Page 3

Table 32
Transformer Unit Model Input Parameter Ranges

Transformer Unit Input Parameter	Recommended Input Range
Output Power Level	0.5 to 250 kWe
Input Voltage Level(1)	20 to 10,000 Vrms
Output Voltage Level(1)	20 to 10,000 Vrms
Number of Phases	1 or 3
Available Modules	Equal to or Greater than Required Modules
Required Modules	No Limit
Transformer Frequency	60 Hz to 60 kHz
Transformer Efficiency	Range: 97.5 to 99.5% 99% is Recommended
Coldplate Temperature(2)	10 to 100° C 40° C Suggested for FH Enclosure 60° C Suggested for CP Enclosure
Coldplate to Radiator Temperature Delta	0 to 20° C 16.7° C is Recommended
Enclosure Type (FH or CP)	Finned Heat Exchanger (FH) Coldplate (CP)

1. The voltage step ratio should not exceed the limits defined in Table 6. To obtain the voltage step ratio, divide the higher, input or output voltage by the other, input or output voltage.

2. Because the Coldplate Enclosure has a lower thermal resistance than the Finned Heat Exchanger Enclosure, the coldplate temperature can be set 20° C higher when the Coldplate Enclosure is selected.

Model Equation Listing: Table 33 defines the variables utilized in the transformer unit model equations.

Table 33
Transformer Unit Model Variable Definitions

P_O	Output Power Level (kWe)
P_I	Input Power Level (kWe)
V_I	Voltage Input (Vdc)
V_O	Voltage Output (Vdc)
AM	Available Modules
RM	Required Modules
TF	Transformer Frequency (kHz)
1TM	Single-Phase Transformer Mass (kg)
3TM	3-Phase Transformer Mass (kg)
TE	Transformer Efficiency (%)
1CCM	Single-Phase Conductor and Connector Mass (kg)
3CCM	3-Phase Conductor and Connector Mass (kg)
1CMM	Single-Phase Control and Monitoring Mass (kg)
3CMM	3-Phase Control and Monitoring Mass (kg)
1CMP	Single-Phase Control and Monitoring Power (kg)
3CMP	3-Phase Control and Monitoring Power (kg)
TUEM	Transformer Unit Electronics Mass (kg)
TUE	Transformer Unit Efficiency (%)
TUSE	Transformer Unit Stage Efficiency (%)
CV	Component Volume (m^3)
CH	Component Height (m)
CW	Component Width (m)
CL	Component Length (m)
FHEM	Finned Heat Exchanger Enclosure Mass (kg)

CPEM Coldplate Based Enclosure Mass (kg)

RA Radiator Area (m^2)

RAM Radiator Mass (kg)

TD Coldplate to Radiator Temperature Delta (°C)

T Coldplate Temperature (°C)

The EXCEL model "ACACXFMR.XLS" is for a transformer unit and the following equations are contained in this model.

Transformer Unit Component Equations

$$P_I=P_O/TUE$$

Single- and 3-Phase: TUSE=TE

Single-Phase: $TUE=P_O/(P_O/TE+1CMP/1000)$

3-Phase: $TUE=P_O/(P_O/TE+3CMP/1000)$

Single-Phase: TUEM=1TM+1CCM+1CMM

3-Phase: TUEM=3TM+3CCM+3CMM

Transformer Unit Transformer Equations

$$1TM=1.15*((EXP(0.003/(1-TE)))/1.35)*(AM/RM)*P_O*((P_O/RM)^{-0.08} *EXP(V_I/200000)*EXP(V_O/200000)*TF^{-0.47}+(TF/300)^{1.4})$$

$$3TM=2.5*((EXP(0.003/(1-TE)))/1.35)*(AM/RM)*P_O*((P_O/RM)^{-0.25} *EXP(V_I/200000)*EXP(V_O/200000)*TF^{-0.47}+(TF/300)^{1.4})$$

Transformer Unit Conductor and Connector Equations

$$1CCM=(AM/RM)*(0.028*((P_O*1000)/V_O)+0.028*(((P_O*1000)/TUE)/V_I))$$

$$3CCM=(AM/RM)*((3^{0.5}/2)*0.028*((P_O*1000)/V_O)+(3^{0.5}/2)*0.028*(((P_O*1000)/TUE)/V_I))$$

Transformer Unit Control and Monitoring Equations

$$1CMM=AM*(1.4+0.3*(P_O/RM)^{0.3}+0.083*(P_O/RM)^{0.3})$$

$$3CMM=AM*(2+0.83*(P_O/RM)^{0.3}+0.25*(P_O/RM)^{0.3})$$

$$1CMP=AM*33.4*(P_O/RM)^{0.1}$$

$$3CMM=AM*47.6*(P_O/RM)^{0.1}$$

The normally used coefficients "0.9" and "0.25", and "2.5" and "0.75" in the control and monitoring mass equations were reduced to "0.3" and "0.083", and "0.83" and "0.25" respectively. This was done because a transformer unit has fewer stages and is less complex than components such as a dc/dc converter or frequency converter; consequently, the number of sensors and their corresponding wiring was judged to be about one-third of the amounts in these components.

The normally used coefficients "55.6" and "79.4" in the control and monitoring power demand equations were reduced to "33.4" and "47.6" respectively. This was done because a transformer unit has fewer sensors than components such as a dc/dc converter or frequency converter; consequently, the control and monitoring power demand was judged to be about 60% of the demand in these components.

Transformer Unit Volume and Dimension Equations

$$CV=TUEM/(0.342*1000)$$

$$CH=0.7*CV^{0.3333}$$

$$CW=1.1*CV^{0.3333}$$

$$CL=1.3*CV^{0.3333}$$

Transformer Unit Enclosure Equations

$$FHEM=44.26*CV^{0.6666}+27*(CL*CW)$$

$$CPEM=44.26*CV^{0.6666}+10.25*(CL*CW)$$

Transformer Unit Radiator Equations

$$RA=(1.1212E+10*(P_o/TUE-P_o)/((T+273-TD)^4-250^4)$$

$$RAM=4.159*RA$$

3.2.7 DC RBI Switchgear Model

The dc RBI switchgear model integrates several dc RBIs into a single unit. The RBIs are interconnected by a main bus. A bus capacitor is included to stabilize the output power during a switching operation. The model is completed with the addition of control and monitoring, an enclosure, and a radiator.

Application Notes: The dc switchgear unit interconnects the system power sources and load distribution networks. The RBIs contained in the switchgear unit allow the sources and load distribution networks to be disconnected from the power system during maintenance periods, and provide fault protection for these components when they are operating. In a large power system, one dc switchgear unit is typically located near the power sources, while another unit is situated by the load distribution networks. The unit close to the power sources makes it possible to bring individual sources on line separately, and remove a source from the system if it is malfunctioning or requires maintenance. Switchgear units located near the loads typically feed local power distribution networks. The dc RBI switchgear model is intended to very flexible. The designer is able to specify one to eight input RBIs, and one to eight RBI power feeds.

Spreadsheet Printout: A printout of the dc RBI Switchgear model is shown in Figure 62. Its format and operation are explained in the following sections.

Model Input Parameter Ranges: The results generated by this spreadsheet are only valid for a certain range of input parameters. Inaccurate mass estimates may result if input parameters outside of the ranges defined in Table 34 are used and it is not recommended. Table 34 also identifies the values that should yield the best results, and lists sources that should be consulted for some input parameters. The user is responsible for selecting input parameters that do not conflict and are reasonable for the application and operating conditions.

Table 34
DC RBI Switchgear Unit Model Input Parameter Ranges

DC RBI Switchgear Unit Input Parameter	**Recommended Input Range**
Number of Input RBI Units	1 to 8
Number of Output RBI Units	1 to 8
RBI Unit Output Power Level	5 to 250 kWe
RBI Unit Output Voltage Level	100 to 10,000 Vdc
RBI Efficiency	Range: 99.8 to 99.9% 99.85% is Recommended
Capacitor Energy Storage Factor	Range: 1 to 2 Joules/kWe 1.8 Joules/kWe is Recommended
Enclosure Type (FH or CP)	Finned Heat Exchanger (FH) Coldplate (CP)
Coldplate Temperature(1)	10 to 100° C 40° C Suggested for FH Enclosure 60° C Suggested for CP Enclosure
Coldplate to Radiator Temperature Delta	0 to 20° C 16.7° C is Recommended
Available Switchgear Modules	Equal to or Greater than Required Modules
Required Switchgear Modules	No Limit

1. Because the Coldplate Enclosure has a lower thermal resistance than the Finned Heat Exchanger Enclosure, the coldplate temperature can be set 20° C higher when the Coldplate Enclosure is selected.

Model Equation Listing: Table 35 defines the variables utilized in the dc RBI switchgear unit model equations.

Date: September 17, 1991		File Name: DCRBI.XLS	
		Originator: K. J. Metcalf	
DC RBI Switchgear Design Model			
Switchgear Input Parameters			
Number of Input RBI Units	1	Switchgear Enclosure (FH or CP)	FH
Number of Output RBI Units	5	Coldplate Temperature (C)	40
RBI Output Voltage (Vdc)	200	Coldplate-Rad. Temp. Delta (C)	16.7
RBI Efficiency (%)	99.85%	Available Switchgear Modules	1
Capacitor Storage (Joules/kWe)	1.8	Required Switchgear Modules	1
RBI Unit Input Parameters			
Input RBI #1 Output Power (kWe)	45	Output RBI #1 Output Power (kWe	25
		Output RBI #2 Output Power (kWe	25
		Output RBI #3 Output Power (kWe	25
		Output RBI #4 Output Power (kWe	25
		Output RBI #5 Output Power (kWe	45

Figure 62

Page 1

		Component Mass Characteristics					
Input RBI Mass (kg)	Output RBI Mass (kg)	Cable & Conn. Mass (kg)	Capacitor Bank Mass (kg)	Cntrl & Mon. Mass (kg)	Enclosure Mass (kg)		
3.06	10.48	12.55	22.28	5.00	24.02		
Radiator Mass (kg)		Component Mass without Radiator (kg)	Component Specific Mass (kg/kW)		Total Mass with Radiator (kg)	Total Specific Mass (kg/kW)	
3.20		77.39	1.73		80.59	1.80	
		Component Volume and Dimensions					
Single Module Parameters				Complete Assembly Parameters			
Volume (cu meters)		0.156		Volume (cu meters)		0.156	
Height (meters)		0.38		Height (meters)		0.38	
Width (meters)		0.59		Width (meters)		0.59	
Length (meters)		0.70		Length (meters)		0.70	
Radiator Area, Input Power, Parasitic Power, and Efficiencies							
Radiator Area (square meters)		Input Power Requirements (kWe)		Parasitic Power Demand (watts)	Eff. of Bus & RBI Sections (%)	Total SWGR Eff. (%)	
0.77		45.07		81.36	99.6%	99.4%	

Figure 62

Page 2

Intermediate Calculation Values			
Input RBI #1 Mass (kg)	3.06	Output RBI #1 Mass (kg)	1.86
		Output RBI #2 Mass (kg)	1.86
		Output RBI #3 Mass (kg)	1.86
		Output RBI #4 Mass (kg)	1.86
		Output RBI #5 Mass (kg)	3.06
Connector and Bus Mass (kg)	12.55		
Capacitor Size (microfarads)	4050	Capacitor Mass (kg)	22
Control & Monitor Mass (kg)	5.00	Cntrl & Mntr Power (watts)	81.36
Single Module Finned HEX Enclosure Mass (kg)	24.02	Single Module Coldplate Enclosure Mass (kg)	17.08
Total Assembly Finned HEX Enclosure Mass (kg)	24.02	Total Assembly Coldplate Enclosure Mass (kg)	17.08

Figure 62

Page 3

Table 35
DC RBI Switchgear Model Variable Definitions

RBP_O	RBI Output Power Level (kWe) The variable RBP_O will be prefaced with the letter I or O and a number to identify a specific RBI Unit. For example $I2RBP_O$ is input RBI unit #2.
$SWRP_I$	Switchgear Input Power Level (kWe)
$SWRP_B$	Switchgear Bus Power Level (kWe)
RBV_O	RBI Voltage Output (Vdc)
AM	Available Modules
RM	Required Modules
RBUM	RBI Unit Mass (kg)
IRBM	Input RBI Mass (kg) The variable RBM will be prefaced with the letter I or O and a number to identify a specific RBI Unit. For example I2RBM is input RBI unit #2.
ORBM	Output RBI Mass (kg) The variable RBM will be prefaced with the letter I or O and a number to identify a specific RBI Unit. For example O4RBM is output RBI unit #4.
RBE	RBI Efficiency (%)
CESF	Capacitor Energy Storage Factor (Joules/kWe)
CBS	Capacitor Bank Size (microfarads)
CBM	Capacitor Bank Mass (kg)
CCM	Conductor and Connector Mass (kg)
CMM	Control and Monitoring Mass (kg)
CMP	Control and Monitoring Power (kg)
SWREM	Switchgear Electronics Mass (kg)
SWRE	Switchgear Efficiency (%)
RBSE	Combined RBI and Bus Section Efficiency (%)
CV	Component Volume (m^3)
CH	Component Height (m)

CW Component Width (m)

CL Component Length (m)

FHEM Finned Heat Exchanger Enclosure Mass (kg)

CPEM Coldplate Based Enclosure Mass (kg)

RA Radiator Area (m^2)

RAM Radiator Mass (kg)

TD Coldplate to Radiator Temperature Delta (°C)

T Coldplate Temperature (°C)

The EXCEL model "DCRBI.XLS" estimates the mass of a dc RBI switchgear unit. The following equations are contained in this model.

Dc RBI Switchgear Unit Component Equations

$$SWRP_B=I1RBP_O+I2RBP_O+I3RBP_O+I4RBP_O+I5RBP_O+I6RBP_O+I7RBP_O+I8RBP_O$$

$$SWRP_I=(I1RBP_O+I2RBP_O)/RBE$$

$$RBSE=RBE*0.999*RBE$$

The efficiency of the switchgear bus was assumed to be 99.9%.

$$SWRE=((SWRP_I*RBE-CMP/1000)*0.999*RBE)/SWRP_I$$

$$SWREM=IRBM+ORBM+CBM+CCM+CMM$$

Dc RBI Switchgear Unit RBI Equations

$$RBUM=0.12*((EXP(0.0008/(1-RBE)))/1.7)*(AM/RM)*RBP_O*(RBP_O/RM)^{-0.15}*(RBV_O/200)^{0.13}$$

This equation is repeated for each of the RBI units at its output power level.

$$IRBM=I1RBM+I2RBM+I3RBM+I4RBM+I5RBM+I6RBM+I7RBM+I8RBM$$

$$ORBM=O1RBM+O2RBM+O3RBM+O4RBM+O5RBM+O6RBM+O7RBM+O8RBM$$

Dc RBI Switchgear Unit Capacitor Equations

$$CBS=(AM/RM)*(2*1000000*((SWRP_B*CESF)/RBV_O^2))$$

To calculate an appropriate size for the capacitor bank that stabilizes the dc switchgear bus, an energy storage value based on the switchgear bus's power level was derived from the present SSF dc switching unit (DCSU). A figure of "1.8" yields a capacitor bank size of 4050 µF for a 45 kWe switchgear bus power level. This is roughly equivalent to the capacitor bank size in the present SSF DCSU.

Utilizing the relationship:

$$E=1/2*C*V^2$$

where: E is the energy stored in the capacitor expressed in joules,
C is the capacitor value in farads, and
V is the voltage across the capacitor in volts;

the capacitor size can be calculated from the switchgear bus power level and a user defined capacitor energy storage factor. Note that an increase in the switchgear bus voltage will exponentially reduce the capacitor size, since its stored energy is proportional to the voltage squared.

$$CBM=0.0055*CBS$$

Dc RBI Switchgear Unit Conductor and Connector Equation

$$CCM=(AM/RM)*(0.056*(SWRP_I*1000)*SWRE/RBV_O)$$

Dc RBI Switchgear Unit Control and Monitoring Equations

$$CMM=AM*(1.4+0.9*(SWRP_B/RM)^{0.3}+0.25*(SWRP_B/RM)^{0.3})$$

$$CMP=AM*55.6*(P_O/RM)^{0.1}$$

Dc RBI Switchgear Unit Volume and Dimension Equations

$$CV=SWREM/(0.342*1000)$$

$$CH=0.7*CV^{0.3333}$$

$$CW=1.1*CV^{0.3333}$$

$$CL=1.3*CV^{0.3333}$$

Dc RBI Switchgear Unit Enclosure Equations

$$FHEM=44.26*CV^{0.6666}+27*(CL*CW)$$

$$CPEM=44.26*CV^{0.6666}+10.25*(CL*CW)$$

Dc RBI Switchgear Unit Radiator Equations

$$RA=(1.1212E+10*(SWRP_I-SWRE*SWRP_I)/((T+273-TD)^4-250^4)$$

$$RAM=4.159*RA$$

3.2.8 AC RBI Switchgear Model

The ac RBI switchgear model integrates several ac RBIs into a single unit by interconnecting them with a main bus. The model is completed by adding control and monitoring, an enclosure, and a radiator.

Application Notes: The ac switchgear unit interconnects the system power sources and load distribution networks. The RBIs contained in the switchgear unit allow the sources and load distribution networks to be disconnected from the power system during maintenance periods, and provide fault protection for these components during operation. In a large power system, one ac switchgear unit will probably be close to the power sources, while another unit is situated near the load distribution networks. The unit near the power sources makes it possible to bring individual sources on line separately, and remove a source from the system if it is malfunctioning or requires maintenance. Switchgear units located close to the loads typically feed local power distribution networks. The ac RBI switchgear model is designed to be quite flexible and it allows the designer to specify one to eight input RBIs, and one to eight RBI power feeds.

Spreadsheet Printout: A printout of the ac RBI Switchgear model is shown in Figure 63. Its format and operation are explained in the following sections.

Model Input Parameter Ranges: The results generated by this spreadsheet are only valid for a certain range of input parameters. Inaccurate mass estimates may result if input parameters outside of the ranges defined in Table 36 are used and it is not recommended. Table 36 also identifies the values that should yield the best results, and lists sources that should be consulted for some input parameters. The user is responsible for selecting input parameters that do not conflict and are reasonable for the application and operating conditions.

Date: September 17, 1991			File Name: ACRBI.XLS
			Originator: K. J. Metcalf
AC RBI Switchgear Design Model			
Switchgear Input Parameters			
Number of Input RBI Units	1	Switchgear Enclosure (FH or CP)	FH
Number of Output RBI Units	5	Coldplate Temperature (C)	40
Number of Phases	1	Coldplate-Rad. Temp. Delta (C)	16.7
RBI Output Voltage (Vrms)	200	Available Switchgear Modules	1
RBI Efficiency (%)	99.85%	Required Switchgear Modules	1
RBI Unit Input Parameters			
Input RBI #1 Output Power (kWe)	45	Output RBI #1 Output Power (kWe	25
		Output RBI #2 Output Power (kWe	25
		Output RBI #3 Output Power (kWe	25
		Output RBI #4 Output Power (kWe	25
		Output RBI #5 Output Power (kWe	45

Figure 63

Page 1

ACRBI.XLS

Component Mass Characteristics

Input RBI Mass (kg)	Output RBI Mass (kg)	Cable & Conn. Mass (kg)	Cntrl & Mon. Mass (kg)	Enclosure Mass (kg)
2.75	9.35	12.55	5.00	16.24

Radiator Mass (kg)		Component Mass without Radiator (kg)	Component Specific Mass (kg/kW)		Total Mass with Radiator (kg)	Total Specific Mass (kg/kW)
3.20		45.88	1.02		49.09	1.10

Component Volume and Dimensions

Single Module Parameters		Complete Assembly Parameters	
Volume (cu meters)	0.087	Volume (cu meters)	0.087
Height (meters)	0.31	Height (meters)	0.31
Width (meters)	0.49	Width (meters)	0.49
Length (meters)	0.58	Length (meters)	0.58

Radiator Area, Input Power, Parasitic Power, and Efficiencies

Radiator Area (square meters)	Input Power Requirements (kWe)	Parasitic Power Demand (watts)	Eff. of Bus & RBI Sections (%)	Total SWGR Eff. (%)
0.77	45.07	81.36	99.6%	99.4%

Figure 63
Page 2

Intermediate Calculation Values			
1 Ph Input RBI #1 Mass (kg)	2.75	1 Ph Output RBI #1 Mass (kg)	1.65
3 Ph Input RBI #1 Mass (kg)	3.44	3 Ph Output RBI #1 Mass (kg)	2.09
		1 Ph Output RBI #2 Mass (kg)	1.65
		3 Ph Output RBI #2 Mass (kg)	2.09
		1 Ph Output RBI #3 Mass (kg)	1.65
		3 Ph Output RBI #3 Mass (kg)	2.09
		1 Ph Output RBI #4 Mass (kg)	1.65
		3 Ph Output RBI #4 Mass (kg)	2.09
		1 Ph Output RBI #5 Mass (kg)	2.75
		3 Ph Output RBI #5 Mass (kg)	3.44
1 Ph Conn and Bus Mass (kg)	12.55		
3 Ph Conn and Bus Mass (kg)	10.86		
1 Ph Cntl & Mon Mass (kg)	5.00	1 Ph Cntl & Mon Power (watts)	81.36
3 Ph Cntl & Mon Mass (kg)	12.18	3 Ph Cntl & Mon Power (watts)	116.18
Single Module Finned HEX Enclosure Mass (kg)	16.24	Single Module Coldplate Enclosure Mass (kg)	11.54
Total Assembly Finned HEX Enclosure Mass (kg)	16.24	Total Assembly Coldplate Enclosure Mass (kg)	11.54

Figure 63

Page 3

Table 36
AC RBI Switchgear Unit Model Input Parameter Ranges

AC RBI Switchgear Unit Input Parameter	Recommended Input Range
Number of Input RBI Units	1 to 8
Number of Output RBI Units	1 to 8
RBI Unit Output Power Level	5 to 250 kWe
RBI Unit Output Voltage Level	100 to 10,000 Vrms
RBI Efficiency	Range: 99.8 to 99.9% 99.85% is Recommended
Number of Phases	1 or 3
Enclosure Type (FH or CP)	Finned Heat Exchanger (FH) Coldplate (CP)
Coldplate Temperature[1]	10 to 100° C 40° C Suggested for FH Enclosure 60° C Suggested for CP Enclosure
Coldplate to Radiator Temperature Delta	0 to 20° C 16.7° C is Recommended
Available Switchgear Modules	Equal to or Greater than Required Modules
Required Switchgear Modules	No Limit

1. Because the Coldplate Enclosure has a lower thermal resistance than the Finned Heat Exchanger Enclosure, the coldplate temperature can be set 20° C higher when the Coldplate Enclosure is selected.

Model Equation Listing: Table 37 defines the variables utilized in the ac RBI switchgear unit model equations.

Table 37
AC RBI Switchgear Model Variable Definitions

RBP_O RBI Output Power Level (kWe)
The variable RBP_O will be prefaced with the letter I or O and a number to identify a specific RBI Unit. For example $I2RBP_O$ is input RBI unit #2.

$SWRP_I$ Switchgear Input Power Level (kWe)

$SWRP_B$ Switchgear Bus Power Level (kWe)

RBV_O RBI Voltage Output (Vdc)

AM Available Modules

RM Required Modules

1RBUM Single-Phase RBI Unit Mass (kg)

3RBUM 3-Phase RBI Unit Mass (kg)

1IRBM Single-Phase Input RBI Mass (kg)
The variable RBM will be prefaced with the letter I or O and a number to identify a specific RBI Unit. For example 1I2RBM is single-phase input RBI #2. This is also done with the 3-Phase input RBIs, and the single- and 3-phase output RBIs.

3IRBM 3-Phase Input RBI Mass (kg)

1ORBM Single-Phase Output RBI Mass (kg)

3ORBM 3-Phase Output RBI Mass (kg)

RBE RBI Efficiency (%)

1CCM Single-Phase Conductor and Connector Mass (kg)

3CCM 3-Phase Conductor and Connector Mass (kg)

1CMM Single-Phase Control and Monitoring Mass (kg)

3CMM 3-Phase Control and Monitoring Mass (kg)

1CMP Single-Phase Control and Monitoring Power (kg)

3CMP 3-Phase Control and Monitoring Power (kg)

SWREM Switchgear Electronics Mass (kg)

SWRE Switchgear Efficiency (%)

RBSE Combined RBI and Bus Section Efficiency (%)

CV Component Volume (m^3)

CH Component Height (m)

CW Component Width (m)

CL Component Length (m)

FHEM Finned Heat Exchanger Enclosure Mass (kg)

CPEM Coldplate Based Enclosure Mass (kg)

RA Radiator Area (m^2)

RAM Radiator Mass (kg)

TD Coldplate to Radiator Temperature Delta (°C)

T Coldplate Temperature (°C)

The EXCEL model "ACRBI.XLS" estimates the mass of an ac RBI switchgear unit. The following equations are contained in this model.

Ac RBI Switchgear Unit Component Equations

$$SWRP_B = I1RBP_O + I2RBP_O + I3RBP_O + I4RBP_O + I5RBP_O + I6RBP_O + I7RBP_O + I8RBP_O$$

The number of input RBI power feeds is defined by the user. One to eight input RBI units can be selected.

$$SWRP_I = (I1RBP_O + I2RBP_O)/RBE$$

$$RBSE = RBE*0.999*RBE$$

The efficiency of the switchgear bus was assumed to be 99.9%.

Single-Phase: $SWRE = ((SWRP_I*RBE-1CMP/1000)*0.999*RBE)/SWRP_I$

3-Phase: $SWRE = ((SWRP_I*RBE-3CMP/1000)*0.999*RBE)/SWRP_I$

Single-Phase: $SWREM = 1IRBM+1ORBM+1CBM+1CCM+1CMM$

3-Phase: $SWREM = 3IRBM+3ORBM+3CBM+3CCM+3CMM$

Ac RBI Switchgear Unit RBI Equations

$$1RBUM = 0.1*((EXP(0.0008/(1-RBE)))/1.7)*(AM/RM)*RBP_O*(RBP_O/RM)^{-0.13}*(RBV_O/200)^{0.05}$$

$$3RBUM = 0.135*((EXP(0.0008/(1-RBE)))/1.7)*(AM/RM)*RBP_O*(RBP_O/RM)^{-0.15}*(RBV_O/200)^{0.05}$$

The proper equation, either single-phase or 3-phase, is automatically selected by the model based on the number of phases input by the user. The individual RBI mass is then calculated for each of the RBI units at its output power level.

Single-Phase: $1IRBM = 1I1RBM+1I2RBM+1I3RBM+1I4RBM+1I5RBM+1I6RBM+1I7RBM+1I8RBM$

3-Phase: $3IRBM = 3I1RBM+3I2RBM+3I3RBM+3I4RBM+3I5RBM+3I6RBM+3I7RBM+3I8RBM$

Single-Phase: $1ORBM = 1O1RBM+1O2RBM+1O3RBM+1O4RBM+1O5RBM+1O6RBM+1O7RBM+1O8RBM$

3-Phase: $3ORBM = 3O1RBM+3O2RBM+3O3RBM+3O4RBM+3O5RBM+3O6RBM+3O7RBM+3O8RBM$

The number of individual RBI unit masses is determined by the user. One to eight input and output RBI units can be defined.

Ac RBI Switchgear Unit Capacitor Equation

An equation was not included in the ac switchgear unit model to calculate a mass for a capacitor bank because capacitive storage is not necessary to provide bus stability. However, later design developments may indicate a capacitor bank is required for power factor correction, especially if the transmission lines are highly inductive. If switchgear capacitors are incorporated into future designs, the model can be revised.

Ac RBI Switchgear Unit Conductor and Connector Equations

$$1CCM=(AM/RM)*(0.056*(SWRP_I*1000)*SWRE/RBV_O)$$

$$3CCM=(AM/RM)*((3^{0.5}/2)*0.056*(SWRP_I*1000)*SWRE/RBV_O)$$

Ac RBI Switchgear Unit Control and Monitoring Equations

$$1CMM=AM*(1.4+0.9*(SWRP_B/RM)^{0.3}+0.25*(SWRP_B/RM)^{0.3})$$

$$3CMM=AM*(2+2.5*(SWRP_B/RM)^{0.3}+0.75*(SWRP_B/RM)^{0.3})$$

$$1CMP=AM*55.6*(P_O/RM)^{0.1}$$

$$3CMP=AM*79.4*(P_O/RM)^{0.1}$$

Ac RBI Switchgear Unit Volume and Dimension Equations

$$CV=SWREM/(0.342*1000)$$

$$CH=0.7*CV^{0.3333}$$

$$CW=1.1*CV^{0.3333}$$

$$CL=1.3*CV^{0.3333}$$

Ac RBI Switchgear Unit Enclosure Equations

$$FHEM=44.26*CV^{0.6666}+27*(CL*CW)$$

$$CPEM=44.26*CV^{0.6666}+10.25*(CL*CW)$$

Ac RBI Switchgear Unit Radiator Equations

$$RA=(1.1212E+10*(SWRP_I-SWRE*SWRP_I)/((T+273-TD)^4-250^4)$$

$$RAM=4.159*RA$$

3.2.9 DC RPC Distribution Panel Model

The dc RPC distribution panel model integrates several dc RPC modules into a single unit. The RPC modules themselves consist of individual RPC units; each RPC unit is a separate power feed. The RPC modules are connected to a main bus. The RPC panel model is completed with the addition of control and monitoring, an enclosure, and a radiator.

Application Notes: Dc RPC distribution panels are normally located in the secondary distribution network. The RPC units contained in these panels provide power to individual loads. The design of an RPC allows its power feed to be turned on and off frequently. In this regard RPCs differ from RBIs. RBIs only interrupt power delivery during off-normal times, such as a failure or maintenance. When the RPC is supplying power, it is capable of monitoring load power demand and providing fault protection. It is assumed the RPCs in future panels will be programmable so that the current interrupt value can be changed to correspond to different load requirements.

The dc RPC distribution panel model design is intended to be very flexible. The designer is able to specify from one to four RPC modules, and within a module up to twenty RPC units. Because it was necessary to evenly allocate the mass of the RPC module packaging and housing between individual RPC units, it is recommended that the user define RPC unit configurations that will generate RPC module power levels between 10 and 20 kWe. For example, ten 1 kWe RPCs results in 10 kWe, four 3 kWe RPCs delivers 12 kWe, and one 16 kWe RPC provides 16 kWe.

This dc RPC distribution panel model is intended for external environments. For applications in a habitat module, it is suggested that the coldplate enclosure option be selected, and the user utilize the component mass figure that does not include the mass of the radiator. It is assumed that a common radiator will be available for the habitat. Naturally, the power losses occurring in the various distribution panels must be factored into the habitat thermal management system calculations.

Spreadsheet Printout: A printout of the dc RPC distribution panel model is shown in Figure 64. This figure illustrates the capability of the model to provide a mass estimate for four different RPC module configurations. Model format and operation are explained in greater detail in the following sections.

Model Input Parameter Ranges: The results generated by this spreadsheet are only valid for a certain range of input parameters. Inaccurate mass estimates may result if input parameters outside of the ranges defined in Table 38 are used and it is not recommended. Table 38 also identifies the values that should yield the best results, and lists sources that should be consulted for some input parameters. The user is responsible for selecting input parameters that do not conflict and are reasonable for the application and operating conditions.

Date: September 17, 1991		File Name: DCRPC.XLS	
		Originator: K. J. Metcalf	
DC RPC Distribution Panel Design Model			
Distribution Panel Input Parameters		**RPC Module Input Parameters**	
Number of RPC Modules	4	RPC Unit #1 Output Power (kWe)	1
		No. of RPC Units in Module #1	10
Distribution Panel Input Power	25		
RPC Output Voltage (Vdc)	120	RPC Unit #2 Output Power (kWe)	3
RPC Efficiency (%)	99.85%	No. of RPC Units in Module #2	4
Dist Panel Enclosure (FH or CP)	FH		
Coldplate Temperature (C)	40	RPC Unit #3 Output Power (kWe)	6
Coldplate-Rad. Temp. Delta (C)	16.7	No. of RPC Units in Module #3	2
Available Distribution Panels	1		
Required Distribution Panels	1	RPC Unit #4 Output Power (kWe)	16
		No. of RPC Units in Module #4	1

Component Mass Characteristics

RPC Mass (kg)	Cable & Conn. Mass (kg)	Cntrl & Mon. Mass (kg)	Enclosure Mass (kg)
13.79	11.60	4.42	16.29

Radiator Mass (kg)	Component Mass without Radiator (kg)	Component Specific Mass (kg/kW)	Total Mass with Radiator (kg)	Total Specific Mass (kg/kW)
1.70	46.10	1.85	47.81	1.92

Figure 64

Page 1

		Component Volume and Dimensions					
Single Module Parameters				Complete Assembly Parameters			
Volume (cu meters)		0.087		Volume (cu meters)		0.087	
Height (meters)		0.31		Height (meters)		0.31	
Width (meters)		0.49		Width (meters)		0.49	
Length (meters)		0.58		Length (meters)		0.58	
Radiator Area, Input Power, Parasitic Power, and Efficiencies							
Radiator Area (square meters)				Parasitic Power Demand (watts)	Eff. of Bus & RPC Sections (%)	Total Dist. Panel Eff. (%)	
0.41				76.71	99.8%	99.4%	

Figure 64

Page 2

Intermediate Calculation Values			
RPC Unit #1 Mass (kg)	0.36	**RPC Module #1 Mass (kg)**	3.60
RPC Unit #2 Mass (kg)	0.89	**RPC Module #2 Mass (kg)**	3.55
RPC Unit #3 Mass (kg)	1.57	**RPC Module #3 Mass (kg)**	3.13
RPC Unit #4 Mass (kg)	3.50	**RPC Module #4 Mass (kg)**	3.50
Connector and Bus Mass (kg)	11.60		
Control & Monitor Mass (kg)	4.42	**Cntrl & Mntr Power (watts)**	76.71
Single Module Finned HEX Enclosure Mass (kg)	16.29	**Single Module Coldplate Enclosure Mass (kg)**	11.58
Total Assembly Finned HEX Enclosure Mass (kg)	16.29	**Total Assembly Coldplate Enclosure Mass (kg)**	11.58

Figure 64

Page 3

Table 38
DC RPC Distribution Panel Model Input Parameter Ranges

DC RPC Distribution Panel Input Parameter	Recommended Input Range
Number of RPC Modules	1 to 4
Distribution Panel Input Power Level[1]	10 to 100 kWe
RPC Unit Output Power Level	1 to 20 kWe
RPC Unit Output Voltage Level	20 to 500 Vdc
Number of RPC Units in RPC Module[2]	1 to 20
RPC Efficiency	Range: 99.8 to 99.9% 99.85% is Recommended
Enclosure Type (FH or CP)	Finned Heat Exchanger (FH) Coldplate (CP)
Coldplate Temperature[3]	10 to 100° C 40° C Suggested for FH Enclosure 60° C Suggested for CP Enclosure
Coldplate to Radiator Temperature Delta	0 to 20° C 16.7° C is Recommended
Available Distribution Panels	Equal to or Greater than Required Panels
Required Distribution Panels	No Limit

1. The distribution panel input power level must be defined by the user. The input power to a distribution panel is often less than the connected output power load. The user may also specify an input power level larger than the connected load to allow for future growth.
2. The number of units depends on the power level of the individual RPC units. The defined RPC Module power level should be between 10 and 20 kWe. Refer to Application Notes for more information.
3. Because the Coldplate Enclosure has a lower thermal resistance than the Finned Heat Exchanger Enclosure, the coldplate temperature can be set 20° C higher when the Coldplate Enclosure is selected.

Model Equation Listing: Table 39 defines the variables utilized in the dc RPC distribution panel model equations.

Table 39
DC RPC Distribution Panel Model Variable Definitions

RPP_o RPC Unit Output Power Level (kWe)

DPP_I Distribution Panel Input Power Level (kWe)

RPV_O RPC Unit Voltage Output (Vdc)

ADP Available Distribution Panels

RDP Required Distribution Panels

RPUM RPC Unit Mass (kg)
The variable RPUM will be suffixed with a number to identify an RPC Unit located in a specific module. For example RPUM2 is an RPC Unit located in RPC module #2. This nomenclature is also used for the variables NRPU and RPMM.

NRPU Number of RPC Units in a Module

RPMM RPC Module Mass (kg)

RPE RPC Efficiency (%)

CCM Conductor and Connector Mass (kg)

CMM Control and Monitoring Mass (kg)

CMP Control and Monitoring Power (kg)

DPEM Distribution Panel Electronics Mass (kg)

DPE Distribution Panel Efficiency (%)

RBSE Combined RPC and Bus Section Efficiency (%)

CV Component Volume (m^3)

CH Component Height (m)

CW Component Width (m)

CL Component Length (m)

FHEM Finned Heat Exchanger Enclosure Mass (kg)

CPEM Coldplate Based Enclosure Mass (kg)

RA Radiator Area (m^2)

RAM Radiator Mass (kg)

TD Coldplate to Radiator Temperature Delta (°C)

T Coldplate Temperature (°C)

The EXCEL model "DCRPC.XLS" estimates the mass of a dc RPC distribution panel. The following equations are contained in this model.

DC RPC Distribution Panel Component Equations

$$RBSE=0.999*RPE$$

The efficiency of the distribution panel bus was assumed to be 99.9%.

$$DPE=((DPP_I-CMP/1000)*0.999*RPE)/DPP_I$$

$$DPEM=RPMM+CCM+CMM$$

DC RPC Distribution Panel RPC Equations

$$RPUM=0.36*((EXP(0.0003/(1-RPE)))/1.22)*(ADP/RDP)*RPP_O*(RPP_O/RDP)^{-0.18}*(RPV_O/120)^{0.04}$$

$$RPMM1=NRPU1*RPUM1$$

The RPC module mass is also calculated for RPC modules #2, #3, and #4 depending on the number of user defined modules. The mass of an RPC module is calculated from the user defined RPC unit power level and the number of RPC units specified in the module.

$$RPMM=RPMM1+RPMM2+RPMM3+RPMM4$$

DC RPC Distribution Panel Conductor and Connector Equation

$$CCM=(ADP/RDP)*(0.056*(DPP_I*1000)*DPE/RPV_O)$$

DC RPC Distribution Panel Control and Monitoring Equations

$$CMM=ADP*(1.4+0.9*(DPP_I/RDP)^{0.3}+0.25*(DPP_I/RDP)^{0.3})$$

$$CMP=ADP*55.6*(P_O/RDP)^{0.1}$$

DC RPC Distribution Panel Volume and Dimension Equations

$$CV=DPEM/(0.342*1000)$$

$$CH=0.7*CV^{0.3333}$$

$$CW=1.1*CV^{0.3333}$$

$$CL=1.3*CV^{0.3333}$$

DC RPC Distribution Panel Enclosure Equations

$$FHEM=44.26*CV^{0.6666}+27*(CL*CW)$$

$$CPEM=44.26*CV^{0.6666}+10.25*(CL*CW)$$

DC RPC Distribution Panel Radiator Equations

$$RA=(1.1212E+10*(DPP_1-DPE*DPP_1)/((T+273-TD)^4-250^4)$$

$$RAM=4.159*RA$$

3.2.10 AC RPC Distribution Panel Model

The ac RPC distribution panel model integrates several ac RPC modules into a single unit. The RPC modules themselves consist of individual RPC units; each RPC unit is a separate power feed. The RPC modules are connected to a main bus. The RPC panel model is completed with the addition of control and monitoring, an enclosure, and a radiator.

Application Notes: Ac RPC distribution panels are normally located in the secondary distribution network. The RPC units contained in these panels provide power to individual loads. The design of an RPC allows its power feed to be turned on and off frequently. In this regard RPCs differ from RBIs. RBIs only interrupt power delivery during off-normal times, such as a failure or maintenance. When the RPC is supplying power, it is capable of monitoring load power demand and providing fault protection. It is assumed the RPCs in future panels will be programmable so that the current interrupt value can be changed to correspond to different load requirements.

The ac RPC distribution panel model design is intended to be very flexible. The designer is able to specify from one to four RPC modules, and within a module up to twenty RPC units. The designer can also specify the number of phases that are incorporated into an RPC module. If all the RPC modules are single-phase, a single-phase, two-wire bus is automatically selected; if only 3-phase RPCs are specified, a 3-phase, 3-wire bus is selected by the model; if the panel contains a mixture of single- and 3-phase RPCs, the model selects a 3-phase, 4-wire bus. Because it was necessary to allocate the RPC module packaging and housing mass evenly between individual RPC units, it is recommended that the user define RPC unit configurations that will generate RPC module power levels between 10 and 20 kWe. For example, ten 1 kWe RPCs results in 10 kWe, four 3 kWe RPCs delivers 12 kWe, and one 16 kWe RPC provides 16 kWe.

This ac RPC distribution panel model is intended for external environments. For applications in a habitat module, it is suggested that the coldplate enclosure option be selected, and the user utilize the component mass figure that does not include the mass of the radiator. It is assumed that a common radiator will be available for the habitat. Naturally, the power losses occurring in the various distribution panels must be factored into the habitat thermal management system calculations.

Spreadsheet Printout: A printout of the ac RPC distribution panel model is shown in Figure 65. This figure illustrates the capability of the model to provide a mass estimate for four different RPC module configurations. Model format and operation are explained in greater detail in the following sections.

Date: September 18, 1991					File Name: ACRPC.XLS		
					Originator: K. J. Metcalf		
AC RPC Distribution Panel Design Model							
Distribution Panel Input Parameters				**RPC Module Input Parameters**			
Number of RPC Modules			4	RPC Unit #1 Output Power (kWe)			1
				No. of RPC Units in Module #1			10
Distribution Panel Input Power			25	No. of Phases in RPC Module #1			1
RPC Output Voltage (Vrms)			120	RPC Unit #2 Output Power (kWe)			3
RPC Efficiency (%)			99.85%	No. of RPC Units in Module #2			4
Dist Panel Enclosure (FH or CP)			FH	No. of Phases in RPC Module #2			1
Coldplate Temperature (C)			40	RPC Unit #3 Output Power (kWe)			6
Coldplate-Rad. Temp. Delta (C)			16.7	No. of RPC Units in Module #3			2
Available Distribution Panels			1	No. of Phases in RPC Module #3			1
Required Distribution Panels			1	RPC Unit #4 Output Power (kWe)			16
				No. of RPC Units in Module #4			1
				No. of Phases in RPC Module #4			1
		Component Mass Characteristics					
RPC Mass (kg)	**Cable & Conn. Mass (kg)**	**Cntrl & Mon. Mass (kg)**	**Enclosure Mass (kg)**				
15.18	11.60	4.42	16.80				
Radiator Mass (kg)		**Component Mass without Radiator (kg)**	**Component Specific Mass (kg/kW)**		**Total Mass with Radiator (kg)**	**Total Specific Mass (kg/kW)**	
1.70		48.00	1.93		49.71	2.00	

Figure 65

Page 1

		Component Volume and Dimensions					
Single Module Parameters				Complete Assembly Parameters			
Volume (cu meters)		0.091		Volume (cu meters)		0.091	
Height (meters)		0.32		Height (meters)		0.32	
Width (meters)		0.50		Width (meters)		0.50	
Length (meters)		0.59		Length (meters)		0.59	
Radiator Area, Input Power, Parasitic Power, and Efficiencies							
Radiator Area (square meters)				Parasitic Power Demand (watts)	Eff. of Bus & RPC Sections (%)	Total Dist. Panel Eff. (%)	
0.41				76.71	99.8%	99.4%	

Figure 65

Page 2

Intermediate Calculation Values

1 Ph RPC Unit #1 Mass (kg)	0.38	1 Ph RPC Module #1 Mass (kg)	3.80
3 Ph RPC Unit #1 Mass (kg)	0.50	3 Ph RPC Module #1 Mass (kg)	5.01
1 Ph RPC Unit #2 Mass (kg)	0.97	1 Ph RPC Module #2 Mass (kg)	3.87
3 Ph RPC Unit #2 Mass (kg)	1.21	3 Ph RPC Module #2 Mass (kg)	4.82
1 Ph RPC Unit #3 Mass (kg)	1.74	1 Ph RPC Module #3 Mass (kg)	3.49
3 Ph RPC Unit #3 Mass (kg)	2.10	3 Ph RPC Module #3 Mass (kg)	4.20
1 Ph RPC Unit #4 Mass (kg)	4.02	1 Ph RPC Module #4 Mass (kg)	4.02
3 Ph RPC Unit #4 Mass (kg)	4.60	3 Ph RPC Module #4 Mass (kg)	4.60
1 Ph Conn and Bus Mass (kg)	11.60	3 Ph, 4 W Conn and Bus Mass (kg	13.40
3 Ph, 3W Conn and Bus Mass (kg)	10.05		
1 Ph Cntl & Mon Mass (kg)	4.42	1 Ph Cntl & Mon Power (watts)	76.71
3 Ph Cntl & Mon Mass (kg)	10.54	3 Ph Cntl & Mon Power (watts)	109.55
Single Module Finned HEX Enclosure Mass (kg)	16.80	Single Module Coldplate Enclosure Mass (kg)	11.94
Total Assembly Finned HEX Enclosure Mass (kg)	16.80	Total Assembly Coldplate Enclosure Mass (kg)	11.94

Figure 65

Page 3

Model Input Parameter Ranges: The results generated by this spreadsheet are only valid for a certain range of input parameters. Inaccurate mass estimates may result if input parameters outside of the ranges defined in Table 40 are used and it is not recommended. Table 40 also identifies the values that should yield the best results, and lists sources that should be consulted for some input parameters. The user is responsible for selecting input parameters that do not conflict and are reasonable for the application and operating conditions.

Table 40
AC RPC Distribution Panel Model Input Parameter Ranges

AC RPC Distribution Panel Input Parameter	Recommended Input Range
Number of RPC Modules	1 to 4
Distribution Panel Input Power Level(1)	10 to 100 kWe
RPC Unit Output Power Level	1 to 20 kWe
RPC Unit Output Voltage Level	20 to 500 Vdc
Number of RPC Units in RPC Module(2)	1 to 20
RPC Efficiency	Range: 99.8 to 99.9% 99.85% is Recommended
Number of Phases	1 or 3
Enclosure Type (FH or CP)	Finned Heat Exchanger (FH) Coldplate (CP)
Coldplate Temperature(3)	10 to 100° C 40° C Suggested for FH Enclosure 60° C Suggested for CP Enclosure
Coldplate to Radiator Temperature Delta	0 to 20° C 16.7° C is Recommended
Available Distribution Panels	Equal to or Greater than Required Panels
Required Distribution Panels	No Limit

1. The distribution panel input power level must be defined by the user. The input power to a distribution panel is often less than the connected output power load. The user may also specify an input power level larger than the connected load to allow for future growth.

2. The number of units depends on the power level of the individual RPC units. The defined RPC Module power level should be between 10 and 20 kWe. Refer to Application Notes for more information.

3. Because the Coldplate Enclosure has a lower thermal resistance than the Finned Heat Exchanger Enclosure, the coldplate temperature can be set 20° C higher when the Coldplate Enclosure is selected.

Model Equation Listing: Table 41 defines the variables utilized in the dc RPC distribution panel model equations.

Table 41
AC RPC Distribution Panel Model Variable Definitions

RPP_O	RPC Unit Output Power Level (kWe)
DPP_I	Distribution Panel Input Power Level (kWe)
RPV_O	RPC Unit Voltage Output (Vrms)
ADP	Available Distibution Panels
RDP	Required Distribution Panels
1RPUM	Single-Phase RPC Unit Mass (kg) The variable RPUM will be suffixed with a number to identify an RPC Unit located in a specific module. For example 1RPUM2 is a single-phase RPC Unit located in RPC module #2. This nomenclature is also used for 3-phase RPCs and for the variables NRPU and RPMM.
3RPUM	3-Phase RPC Unit Mass (kg)
NRPU	Number of RPC Units in a Module
RPMM	RPC Module Mass (kg)
RPE	RPC Efficiency (%)
1CCM	Single-Phase Conductor and Connector Mass (kg)
3CCM	3-Phase Conductor and Connector Mass (kg)
1CMM	Single-Phase Control and Monitoring Mass (kg)
3CMM	3-Phase Control and Monitoring Mass (kg) .
1CMP	Single-Phase Control and Monitoring Power (kg)
3CMP	3-Phase Control and Monitoring Power (kg)
DPEM	Distribution Panel Electronics Mass (kg)
DPE	Distribution Panel Efficiency (%)
RBSE	Combined RPC and Bus Section Efficiency (%)
CV	Component Volume (m^3)
CH	Component Height (m)

CW Component Width (m)

CL Component Length (m)

FHEM Finned Heat Exchanger Enclosure Mass (kg)

CPEM Coldplate Based Enclosure Mass (kg)

RA Radiator Area (m^2)

RAM Radiator Mass (kg)

TD Coldplate to Radiator Temperature Delta (°C)

T Coldplate Temperature (°C)

The EXCEL model "ACRPC.XLS" estimates the mass of a ac RPC distribution panel. The following equations are contained in this model.

AC RPC Distribution Panel Component Equations

RBSE=0.999*RPE

The efficiency of the distribution panel bus was assumed to be 99.9%.

Single-Phase: $DPE=((DPP_I-1CMP/1000)*0.999*RPE)/DPP_I$

3-Phase: $DPE=((DPP_I-3CMP/1000)*0.999*RPE)/DPP_I$

Single-Phase: DPEM=1RPMM+1CCM+1CMM

3-Phase: DPEM=3RPMM+3CCM+3CMM or DPEM=3RPMM+4CCM+3CMM

AC RPC Distribution Panel RPC Equations

$$1RPUM=0.38*((EXP(0.0003/(1-RPE)))/1.22)*(ADP/RDP)*RPP_O*(RPP_O/RDP)^{-0.15}*(RPV_O/120)^{0.01}$$

$$3RPUM=0.5*((EXP(0.0003/(1-RPE)))/1.22)*(ADP/RDP)*RPP_O*(RPP_O/RDP)^{-0.2}*(RPV_O/120)^{0.01}$$

The number of phases is defined for each active RPC module by the user. The RPC unit mass equation that is selected, single- or 3-phase, is determined by the number of phases input by the user for the module that it resides in.

1RPMM1=1NRPU1*1RPUM1

3RPMM1=3NRPU1*3RPUM1

The RPC module mass is also calculated for RPC modules #2, #3, and #4 depending on the number of user defined modules. The mass of an RPC module is calculated from the user defined RPC unit power level and the number of RPC units specified in the module.

$$\text{Single-Phase: } RPMM=1RPMM1+1RPMM2+1RPMM3+1RPMM4$$

$$\text{3-Phase: } RPMM=3RPMM1+3RPMM2+3RPMM3+3RPMM4$$

The RPC Module Mass (RPMM) can also be calculated for a mixture of single- and 3-phase RPC modules.

AC RPC Distribution Panel Conductor and Connector Equation

$$1CCM=(ADP/RDP)*(0.056*(DPP_I*1000)*DPE/RPV_O)$$

$$3CCM=(ADP/RDP)*((3^{0.5}/2)*0.056*(DPP_I*1000)*DPE/RPV_O)$$

$$4CCM=(ADP/RDP)*((2/3^{0.5})*0.056*(DPP_I*1000)*DPE/RPV_O)$$

The 3-phase, 4-wire conductor and connector mass (4CCM) is automatically selected by the model if a mixture of single- and 3-phase RPC modules is specified by the user. This combination would require a 4-wire bus.

AC RPC Distribution Panel Control and Monitoring Equations

$$1CMM=ADP*(1.4+0.9*(DPP_I/RDP)^{0.3}+0.25*(DPP_I/RDP)^{0.3})$$

$$3CMM=ADP*(2+2.5*(DPP_I/RDP)^{0.3}+0.75*(DPP_I/RDP)^{0.3})$$

$$1CMP=ADP*55.6*(P_O/RDP)^{0.1}$$

$$3CMP=ADP*79.4*(P_O/RDP)^{0.1}$$

AC RPC Distribution Panel Volume and Dimension Equations

$$CV=DPEM/(0.342*1000)$$

$$CH=0.7*CV^{0.3333}$$

$$CW=1.1*CV^{0.3333}$$

$$CL=1.3*CV^{0.3333}$$

AC RPC Distribution Panel Enclosure Equations

$$FHEM=44.26*CV^{0.6666}+27*(CL*CW)$$

$$CPEM=44.26*CV^{0.6666}+10.25*(CL*CW)$$

AC RPC Distribution Panel Radiator Equations

$$RA=(1.1212E+10*(DPP_I-DPE*DPP_I)/((T+273-TD)^4-250^4)$$

$$RAM=4.159*RA$$

4.0 CREATING PMAD SYSTEM MODELS

A complete PMAD system model is created by defining the power system architecture, selecting components consistent with this architecture, and then linking the input and output parameters of all the components with their interconnecting transmission lines. By creating a complete PMAD system model, the impact of changes in power, voltage, frequency, etc. can be seen on the total power system mass. To create a system model, individual component models must be connected to show the flow of power through the system and the voltage reductions that occur because of component losses. To assist the user in interconnecting models, the locations of the input and output power and voltage levels are mentioned. If these parameters are not specifically identified in the model, techniques for calculating them are discussed.

The input power provided to a component is equal to the output power of the transmission line that feeds it. This component's input voltage is also equivalent to the output voltage of the line supplying it. In the model input section, the output power level of a component is normally defined by the user. The input power level is typically provided as an output to facilitate interconnecting the models; however, if it is not available, it can be calculated by using the total component efficiency. In the RBI switchgear unit models, the output power rating of each RBI is specified by the user. The total output power can be determined by summing these individual values; the input power is provided as a model output. In the RPC distribution panel models, the power output for each of the RPCs and the power supplied to the panel are defined by the user because the panel power feed can differ considerably from the connected load. In models that contain a transformer stage, the user must define both the input and output voltage levels since they determine the transformer step ratio. The input voltage level for the rectifier model is provided, because it will be different depending on whether a single- or 3-phase rectifier is selected. In the RBI and RPC models, the input voltage level can be calculated by dividing the output voltage by the "Efficiency of the Bus and RBI (RPC) Section" value provided by the model.

Since a complete PMAD system model consists of several power conditioning and transmission line models that are linked together to display the total impact of different power, voltage, and frequency levels; it is probably best to define a parameter that is common throughout the system, such as the transmission frequency, in a systems input section. It may also be convenient to locate many of the component input parameters in this same systems input section. Key systems output parameters can be obtained by combining the values obtained from individual component models. For example, total system mass is determined by summing the masses of the individual components and lines; the efficiency of the power system is calculated by multiplying the efficiencies of the series connected elements together. Locating these power system parameters in a system output section that is close to the system input section will allow a person to immediately see the impact of changing an input parameter without having to go to another location on the spreadsheet or individually assessing the effect on each component.

5.0 CONCLUSIONS AND RECOMMENDATIONS

The purpose of this task was to create the first set of power conditioning models that will eventually be part of a library of PMAD component models. After this library has been completed, it will allow PMAD system designers to evaluate different power distribution approaches in a timely manner. The first steps in this process are developing a modeling approach that is acceptable to NASA LeRC, and refining these models to ensure that they generate results that are both useful and accurate. It is important to realize that these models are just a beginning and that the best way to improve them is to continue to compare the output obtained from them with the information acquired from ongoing component designs. The present power conditioning component data base is relatively small and confined to lower power and voltage levels. Because of this shortage, it was necessary extrapolate a considerable distance to generate component models that will be consistent with future power and voltage levels. To acquire the information used to create these models, many different sources were consulted; however, the final models were generated by one person and consequently they must be reviewed carefully to ensure this information was understood and properly applied.

To create these power conditioning models, it was necessary to generate equations for each of the stages and elements in a component. This process was particularly difficult in the case of the component filter stages. In many power system designs, the power quality and filtering requirements appear to be one of the last areas defined in detail, possibly because it also seems to be one of the most hotly debated areas. Consequently, the filter designs in many preliminary component assessments are rather immature. In addition, filter designs suitable for space applications also tend to be for high frequency applications. Up until this point in time, it has not been necessary to address in detail low frequency filter designs and requirements. However, in the future many high power systems will use alternators for power conversion. So regardless of the power distribution form ultimately selected, the filtering requirements for components immediately following the alternator output must be addressed. The component models in this report reflect the lack of information present in the filtering area, and consequently the equations pertaining to the filter stages are probably the least accurate and require the most work.

The models included in this report are primarily oriented toward lunar surface applications; however, they are considered to be flexible enough to permit them to be used in a wide variety of applications. To properly define the model inputs and interconnect them to form a system, the user must be familiar with the characteristics of an application, and formulate a rough design. The power system architecture should be defined, and issues such as component maintainability and system filtering should be considered. To illustrate the use of these models in an alternate application, the characteristics of a nuclear electric propulsion (NEP) power system will be considered. An NEP system will probably employ a modular architecture to enhance reliability; therefore, the model option that allows a person to define the number of required and available modules should be used. An NEP system will probably use coldplates for cooling and mount many components on them. Components probably will not be replaced if they fail since this vehicle transports people and hardware far from earth orbit. These last two features favor the use of the model coldplate option. A coldplate enclosure is also much lighter than a finned heat exchanger enclosure. The last issue is are the power, voltage, and frequency characteristics incorporated into the models adequate for this application. The model capabilities defined in Table 42 indicate a system

Table 42
Power Conditioning Model
Input Parameter Options and Ranges

Component Model	Output Power Range	Input Voltage Range	Output Voltage Range	Input Power Capability	Output Power Capability
Transformer	500 W to 1 MWe	20 to 10,000 Vrms	20 to 10,000 Vrms	1 or 3 Phase ac 60 Hz to 60 kHz	1 or 3 Phase ac 60 Hz to 60 kHz
Inverter	500 W to 250 kWe	20 to 10,000 Vdc	20 to 10,000 Vrms	dc	1 or 3 Phase ac 1 to 60 kHz
Rectifier	500 W to 250 kWe	20 to 10,000 Vrms	20 to 10,000 Vdc	1 or 3 Phase ac 60 Hz to 60 kHz	dc
Transformer/Rectifier	500 W to 250 kWe	20 to 10,000 Vrms	20 to 10,000 Vdc	1 or 3 Phase ac 60 Hz to 60 kHz	dc
DC/DC Converter	500 W to 250 kWe	20 to 10,000 Vdc	20 to 10,000 Vdc	dc	dc
DC Link Frequency Converter	500 W to 250 kWe	20 to 10,000 Vrms	20 to 10,000 Vrms	1 or 3 Phase ac 60 Hz to 60 kHz	1 or 3 Phase ac 60 Hz to 60 kHz
DC Switchgear (DC RBIs)	5 to 250 kWe	100 to 10,000 Vdc	100 to 10,000 Vdc	dc	dc
AC Switchgear (AC RBIs)	5 to 250 kWe	100 to 10,000 Vrms	100 to 10,000 Vrms	1 or 3 Phase ac 60 Hz to 50 kHz	1 or 3 Phase ac 60 Hz to 50 kHz
DC Power Distribution Panel (DC RPCs)	10 to 100 kWe	20 to 500 Vdc	20 to 500 Vdc	dc	dc
AC Power Distribution Panel (AC RPCs)	10 to 100 kWe	20 to 500 Vrms	20 to 500 Vrms	1 or 3 Phase ac 60 Hz to 50 kHz	1 or 3 Phase ac 60 Hz to 50 kHz

Note 1: The inversion frequency of the intermediate transformer stage in the dc/dc converter can be varied from 10 to 60 kHz.

model with components rated up to 250 kWe can be created. An NEP power system will probably require some power conditioning components that are rated for over 1 MWe. While the power levels listed in Table 42 seem to indicate these models are not suitable for an NEP application, this probably is not the case. These models were primarily intended for a lunar application that did not appear to require component power levels in excess of 250 kWe. Although these component models must be evaluated at power levels around 1 MWe, it is expected they will prove to yield meaningful results. The voltage capabilities already incorporated into the models, up to 10,000 volts, seem to be adequate for an NEP applications. It is felt that enough component models were created during this task to evaluate dc and lower frequency ac PMAD systems; however, ac and dc load receiver models must be created to evaluate a high frequency system. Finally, the filter stages incorporated into the models may not even be needed in an NEP application because an electric propulsion system is already extremely noisy. It does not appear to be necessary to provide a filtered output to these devices. Based on this evaluation, the current models can be reconfigured and used for NEP power system analyses. This assignment is highly recommended for a future task order study.

Although several power conditioning component models were created and documented during this task order, it has already been mentioned that other models are required to allow a thorough evaluation of lunar base PMAD alternatives and to perform PMAD system studies for other applications. Ac and dc load receiver models are required to evaluate high frequency power distribution systems. Load receivers are used to convert the high frequency input into a form suitable for the loads. At the power source end, dc shunt regulator and ac speed regulator models are required. These components shunt excess power to a parasitic load. A parasitic load radiator model is also necessary. Linear alternators will generally require a capacitor bank for power factor correction; a model to estimate the mass of this hardware would be beneficial. Finally, the power sources may need a battery for backup power and to start the alternators. A model of a battery charge/discharge unit is required to fully estimate the mass of this energy storage system. It is suggested that models be created for these power conditioning components during a follow up task order.

In addition to the power conditioning components, a PMAD system includes transmission lines. Auburn University addressed dc transmission line models in their report: "Electrical Transmission on the Lunar Surface - Part I DC Transmission". Under a separate contract, it is understood that they documented a detailed study on ac transmission lines. During Task Order No. 8, it was discovered that the equations contained in Auburn's dc transmission line report could be used to create comprehensive dc transmission line models. It is assumed that the equations in their ac transmission line report could also be used to create high fidelity ac transmission line models. These two items are recommended for future task orders. However, the ac transmission model development should only be undertaken if Auburn's report on ac transmission lines is available. Otherwise, it would be necessary to basically repeat this study to generate ac transmission line models.

References

II-1 Metcalf, Kenneth; Harty, Richard; and James Robin. "Issues Concerning Centralized vs. Decentralized Power Deployment." Rockwell International, Rocketdyne Division. NASA Contractor Report CR-187121, March 1991.

II-2 Gilmour, A. "High Power Study - Power Conditioning." Department of Electrical Engineering, State University of New York at Buffalo. Technical Report AFAPL-TR-76-101, January 1976.

II-3 Moriarty, J. "Power Conditioning Subsystem Design." Raytheon Company, Missile Systems Division, Bedford Laboratories. Technical Report AFWAL-TR-82-2108, November 1982.

II-4 Gerry, Edward, and Wally Shaefer. "Advanced Weapons Concept Evaluation Study", Appendix J. Technical Report AFSTC-TR-84-03, April 1985.

III-1 Harris Semiconductor. "Power MOSFETs", A data book on power MOSFETs prepared by Harris Semiconductor, 1989.

III-2 Kozik, Robert. "High Power MOSFETs for Multi-Megawatt Inverters", In-house Rocketdyne Survey, IL No. 119-88-RK-087, September 1988. (Copies can be provided on request).

III-3 Yates, Warren. "MOSFET Availability and Performance Continues on the Upswing." Electronic Products, Vol. 33, No. 6, (November 1990), pp. 67-69.

III-4 Anderson, Paul, and Rene Thibodeaux. " Power Distribution Study for 10-100 kW Baseload Space Power Systems." IECEC '90, August 1990, Vol. I, pp. 428-433.

III-5 Boylestad, Robert, and Louis Nashelsky. Electronic Devices and Circuit Theory. Englewood Cliffs, New Jersey: Prentice-Hall, 1978.

III-6 Hui, Shimooi. "Space Station WP-04 Mass Properties", An internal Rocketdyne report generated by the Space Station Freedom mass properties group.

III-7 TRW. "Bidirectional Power Driver/Receiver", Final technical review report prepared under contract NAS3-24653. Engineering and Test Division, TRW Space & Technology Group, 1988.

III-8 Ford Aerospace & Communications Corporation. "Space Station Electric Power System Phase C/D Option I", Volume I - Technical, June 1987.

III-9 Levy, Stephen, John Carter, and John Creedon. "Comparison of Solid State with Gaseous Switches for Space Based Megawatt Inverter Applications." IECEC '87, August 1987, Vol. IV, pp. 2034-2039.

III-10 Borger, William, and Lowell Massie. "Space System Requirements and Issues: The Next Decade." IECEC '90, August 1990, Vol. I, pp. 1-5.

III-11 Informal Meeting Record. "Power Conditioning Component Mass and Efficiency Modeling", Attendees: Irv Hansen, John Biess, Ron Cull, Ken Metcalf. June 4, 1991.

III-12 Hansen, Irving, and Gale Sundberg. "Space Station 20-kHz Power Management and Distribution System." 1986 Power Electronics Specialists Conference.

III-13 Mullet, Charles. "Designing Multi-Output Power Converters", Course notes for a tutorial seminar presented during The Power Electronics Conference/88 West, 1988.

III-14 Conversation with Jim Mildice of General Dynamics. "Mass and Volume Estimates for 70 kWe Motor Driver". June 5, 1991.

III-15 Mildice, J. W. "Performance of Resonant Power Processors in Direct Load PMAD Systems", High Frequency Power Distribution and Control Technology Conference, June 1991.

III-16 Koerner, G., and E. Siddiqui. Permanent Magnet Variable Speed Constant Frequency Power Generation System. General Electric Company, Binghamton, New York. Technical Report AFWAL-TR-85-2112, November 1984.

III-17 Kraus, Robert, Ira Meyers, and Eric Baumann. "Light Weight, High Power, High Voltage DC/DC Converter Technologies." IECEC '90, August 1990, Vol. I, pp. 380-385.

III-18 Hall, James. "Notes on Telecon with Ira Myer NASA LeRC", Documented telecon between Ira Myer of NASA LeRC and Jim Hall of Rocketdyne on the status of the NASA 1 MWe power inverter program. (Copies can be provided on request).

III-19 Magnetics. "Power Transformer and Inductor Design", Design notes and procedures prepared by the Magnetics Division of Spang and Company.

III-20 Ferroxcube. "Linear Ferrite Magnetic Design Manual", Design notes and procedures prepared by the Ferroxcube Division of Amperex Electronic Corporation.

III-21 McLyman, Colonel Willian T. "Transformer and Inductor Design Handbook". New York, N.Y.: Marcel Dekker, 1978.

III-22 Fink, Donald and H. Wayne Beaty. "Standard Handbook for Electrical Engineers", Eleventh Edition. New York, N.Y.: McGraw-Hill Book Company, 1978.

III-23 Westinghouse Electric Corporation. "Westinghouse Quick Selector", Catalog 25-000, 1988.

III-24 Kuhlmann, John H. "Design of Electrical Apparatus". New York, N.Y.: John Wiley & Sons, 1957.

III-25 Ferroxcube. "Linear Ferrite Materials and Components", A characterization of Ferrite materials prepared by the Ferroxcube Division of Amperex Electronic Corporation.

III-26 Unitrode Corporation. "Unitrode Applications Handbook", Application Note U-108, "Schottky Rectifiers for Low-Voltage Outputs", pp 290-297, 1988.

III-27 Hearst Business Communications, Inc. "Electronic Engineers Master Catalog", Product Section 4800, "High Voltage Diodes". p A-2159, 1991.

III-28 Yu, Yuan, Max Bachmann, and Fred Lee. "Formulation of a Methodology for Power Circuit Design Optimization." 1976 Power Electronics Specialists Conference Record, pp. 35-44.

III-29 Rockwell International, Rocketdyne Division. "SP-100 Reactor-Stirling Power System GES Baseline System Definition and Characterization Study", JPL Contract No. 956935, 1985.

III-30 Biess, John J. "Power Management and Distribution (PMAD) Technology Overview", High Frequency Power Distribution and Control Technology Conference, June 1991.

III-31 Ford Aerospace & Communications Corporation. "PWR Splinter Meeting Power Electronics." A tabulated mass and power loss breakdown for the sequential shunt unit (SSU), battery charge/discharge unit (BCDU), and direct current switching unit (DCSU). November, 1989.

III-32 Metcalf, Kenneth. "EPS Voltage and Power Supply", Rockwell International, Rocketdyne Division, EID-00355. December, 1989.

III-33 Dupass, W. "Parasitics - Based on the Standard ORU DC Architecture", Rockwell International, Rocketdyne Division, EID-00344. November, 1989.

III-34 Telephone conversation with Dave Fox of Westinghouse. "Design Details and Mass Estimates for AC RBIs and RPCs". September 9, 1991.

Appendix A

Mass Breakdowns of Component Stages and Elements

Chopper Mass Breakdown Tables

Single Phase Mass Breakdowns by Power Level
(Resonant Toplogy, 20 kHz Resonant Frequency)

		Notes 1 and 2					Note 3									
Power Level (kWe)	0.5	1	5	10	15	20	25	30	40	50	60	80	100	150	200	250
Active Switch Eleme	3	5	25	50	75	100	125	150	200	250	300	400	500	750	1000	1250
Snubber Circuitry	8	15	75	150	225	300	375	450	600	750	900	1200	1500	2250	3000	3750
Heat Sink, Thermal	18	35	175	350	525	700	875	1050	1400	1750	2100	2800	3500	5250	7000	8750
Gate Drive	12	15	24	30	34	37	39	42	45	49	51	56	60	67	74	79
Switch Control Logi	5	5	6	6	7	7	7	7	7	7	8	8	8	8	8	9
Packaging	15	25	101	193	286	377	469	561	743	926	1108	1473	1837	2747	3657	4566
Ancilliary Hardware	155	300	1452	2865	4263	5651	7032	8408	11147	13871	16585	21986	27360	40709	53967	67159
Total Mass (grams)	273	500	2264	4424	6565	8693	10813	12927	17138	21335	25519	33859	42170	62855	83445	103966

Note 1: Values derived from mass breakdown of 6.25 kWe SSF DDCU. Converter uses Current Fed Push-Pull Topology and operates at 40 kHz (Ref. III-6).
Note 2: Values derived from mass breakdown of 5 kWe DC-Inductor Resonant Driver developed by TRW (Ref. III-7).
Note 3: 20 kHz SSF PMAD development work indicated an optimized 25 kVA, 20 kHz Resonant Converter would weigh about 20 lbs or 9 kg (Ref. III-11).

Three Phase Mass Breakdowns by Power Level
(Resonant Toplogy, 20 kHz Resonant Frequency)

											Notes 4 and 5					
Power Level (kWe)	0.5	1	5	10	15	20	25	30	40	50	60	80	100	150	200	250
Active Switch Eleme	1	2	10	20	30	40	50	60	80	100	120	160	200	300	400	500
Snubber Circuitry	3	5	25	50	75	100	125	150	200	250	300	400	500	750	1000	1250
Heat Sink, Thermal	6	12	60	120	180	240	300	360	480	600	720	960	1200	1800	2400	3000
Gate Drive	9	11	18	22	25	27	29	31	33	36	38	41	44	49	54	58
Switch Control Logi	4	4	5	5	5	5	6	6	6	6	6	6	6	7	7	7
Packaging	7	11	39	72	104	136	168	200	264	327	391	517	644	959	1274	1589
Ancilliary Hardware	164	317	1485	2929	4357	5777	7189	8595	11394	14179	16953	22475	27968	41613	55166	68651
Total Mass (grams)	341	588	2423	4660	6871	9068	11254	13432	17771	22091	26398	34980	43530	64804	85975	107071

Note 4: Flight packaged 70 kVA DC Link Resonant Driver being developed for ALS by General Dynamics estimated to weigh 60 lbs, 27 kg (Ref. III-14).
Note 5: Air cooled aircraft 60 kVA cycloinverter that accepts 1350 to 2500 Hz and supplies a constant 400 Hz weighs about 56 lbs, 25 kg (Ref. III-16).

Single-Phase Mass Breakdowns by Efficiency
(Resonant Topology, 1 kWe Power Level, 20 kHz Resonant Frequency)

			Note 6						
Efficiency (%)	95.00%	95.25%	95.50%	95.75%	96.00%	96.25%	96.50%	96.75%	97.00%
Active Switch Eleme	4	4	4	5	5	5	6	6	7
Snubber Circuitry	12	13	13	14	15	16	17	18	20
Heat Sink, Thermal	39	38	37	36	35	34	33	32	30
Gate Drive	15	15	15	15	15	15	15	15	15
Switch Control Logi	5	5	5	5	5	5	5	5	5
Packaging	25	25	25	25	25	25	25	25	25
Ancilliary Hardware	243	255	268	283	300	320	342	368	398
Total Mass (grams)	443	454	467	482	500	520	543	570	602

Note 6: A Resonant Converter design exhibiting an efficiency of 95.5% and THD of 5% has been developed by General Dynamics (Ref. III-15).

Single Phase Mass Breakdowns by Frequency
(Resonant Topology, 1 kWe Power Level)

					Note 7				Note 8		
Frequency (kHz)	1	5	10	15	20	25	30	35	40	45	50
Active Switch Eleme	5.0	5.0	5.0	5.0	5.0	5.0	5.0	5.0	5.0	5.0	5.0
Snubber Circuitry	15	15	15	15	15	15	15	15	15	15	15
Heat Sink, Thermal	35	35	35	35	35	35	35	35	35	35	35
Gate Drive	15	15	15	15	15	15	15	15	15	15	15
Switch Control Logi	5	5	5	5	5	5	5	5	5	5	5
Packaging	25	25	25	25	25	25	25	25	25	25	25
Ancilliary Hardware	1342	600	424	346	300	274	255	240	227	217	208
Total Mass (grams)	1541	800	624	546	500	474	455	439	427	416	407

Note 7: Values based on 5 kWe, 20 kHz DC-Inductor Resonant Driver developed by TRW (Note 2 and Ref. III-7).
Note 8: Values based on 6.25 kWe, 40 kHz Current Fed Push-Pull SSF DDCU developed by Rocketdyne (Note 1 and Ref. III-6).

Three Phase Mass Breakdowns by Frequency
(Resonant Topology, 10 kWe Power Level)

Frequency (kHz)	1	5	10	15	20	25	30	35	40	45	50
Active Switch Eleme	20	20	20	20	20	20	20	20	20	20	20
Snubber Circuitry	50	50	50	50	50	50	50	50	50	50	50
Heat Sink, Thermal	120	120	120	120	120	120	120	120	120	120	120
Gate Drive	22	22	22	22	22	22	22	22	22	22	22
Switch Control Logi	8	8	8	8	8	8	8	8	8	8	8
Packaging	72	72	72	72	72	72	72	72	72	72	72
Ancilliary Hardware	13099	5858	4001	3334	2929	2679	2490	2408	2379	2353	2329
Total Mass (grams)	14851	7610	5753	5086	4681	4431	4243	4160	4131	4105	4081

Rectifier Mass Breakdown Tables

Single-Phase Mass Breakdowns by Power Level

			Note 1													
Power Level (kWe)	0.5	1	5	10	15	20	25	30	40	50	60	80	100	150	200	250
Active Switch Elemen	3	5	25	50	75	100	125	150	200	250	300	400	500	750	1000	1250
Heat Sink, Thermal	18	35	175	350	525	700	875	1050	1400	1750	2100	2800	3500	5250	7000	8750
Packaging	7	15	74	148	222	296	370	444	592	740	888	1184	1480	2220	2960	3700
Total Mass (grams)	55	110	548	1096	1644	2192	2740	3288	4384	5480	6576	8768	10960	16440	21920	27400

Note 1: Values derived from mass breakdown of 6.25 kWe SSF DDCU. Rectifier follows Current Fed Push-Pull Topology Converter (Ref. III-6).

3-Phase Mass Breakdowns by Power Level

Power Level (kWe)	0.5	1	5	10	15	20	25	30	40	50	60	80	100	150	200	250
Active Switch Elemen	1	2	10	20	30	40	50	60	80	100	120	160	200	300	400	500
Heat Sink, Thermal	6	12	60	120	180	240	300	360	480	600	720	960	1200	1800	2400	3000
Packaging	3	5	26	52	78	104	130	155	207	259	311	414	518	777	1036	1295
Total Mass (grams)	58	115	575	1151	1726	2302	2877	3452	4603	5754	6905	9206	11508	17262	23016	28770

Single-Phase Mass Breakdowns by Efficiency

Efficiency (%)	97.50%	97.75%	98.00%	98.25%	98.50%	98.75%	99.00%	99.25%	99.50%
Active Switch Elemen	2	2	3	4	5	7	11	20	45
Heat Sink, Thermal	36	36	36	35	35	35	34	34	33
Packaging	14	14	14	14	15	15	17	20	29
Total Mass (grams)	103	104	105	107	110	115	125	147	214

DC Filter Mass Breakdown Tables

Single-Phase Mass Breakdowns by Power Level
40 kHz Ripple Frequency)
(1% Ripple Factor)

Power Level (kWe)	0.5	1	5	10	15	20	25	30	40	50	60	80	100	150	200	250
Inductor Mass (kg)	1	3	7	12	16	20	23	26	32	38	43	53	62	83	102	120
Capacitor Mass (kg)	162	324	1620	3240	4860	6480	8100	9720	12960	16200	19440	25920	32400	48600	64800	81000
Filter Mass (kg)	163	327	1627	3252	4876	6500	8123	9746	12992	16238	19483	25973	32462	48683	64902	81120

3-Phase Mass Breakdowns by Power Level
(120 kHz Ripple Frequency)
(1% Ripple Factor)

Power Level (kWe)	0.5	1	5	10	15	20	25	30	40	50	60	80	100	150	200	250
Inductor Mass (kg)	1	1	3	5	6	7	8	9	11	12	14	16	19	24	28	32
Capacitor Mass (kg)	54	108	549	1079	1618	2157	2696	3236	4314	5393	6471	8628	10785	16178	21571	26963
Filter Mass (kg)	55	109	552	1083	1624	2164	2704	3245	4325	5405	6485	8645	10804	16202	21599	26996

Single-Phase Mass Breakdowns by Efficiency
40 kHz Ripple Frequency)
(1% Ripple Factor)

Efficiency (%)	99.30%	99.35%	99.40%	99.45%	99.50%	99.55%	99.60%	99.65%	99.70%
Inductor Mass (kg)	5	5	5	5	4	4	4	4	3
Capacitor Mass (kg)	231	249	269	294	324	360	405	463	540
Filter Mass (kg)	236	254	274	299	328	364	409	467	544

Single-Phase Mass Breakdowns by Frequency
(1% Ripple Factor)
(99.5% Efficiency)

Frequency (kHz)	0.07	0.1	0.2	0.3	0.4	0.5	0.6	0.7	0.8	0.9	1	1.1	1.2	1.3	1.4	1.5
Inductor Mass (kg)	5928	3864	1682	1034	732	560	450	374	319	277	243	218	196	178	163	150
Capacitor Mass (kg)	239	167	84	56	42	33	28	24	21	19	17	15	14	13	12	11
Filter Mass (kg)	6166	4031	1765	1090	774	594	478	398	340	295	260	233	210	191	175	161

AC Filter Mass Breakdown Tables

Single-Phase Mass Breakdowns by Power Level
(20 kHz Resonant Frequency)

Power Level (kWe)	0.5	1	5	10	15	20	25	30	40	50	60	80	100	150	200	250
Transformer Mass	26	50	220	416	604	787	966	1143	1489	1828	2162	2817	3459	5023	6545	8037
Inductor Mass	13	25	125	250	375	500	625	750	1000	1250	1500	2000	2500	3750	5000	6250
Capacitor Mass	8	15	75	150	225	300	375	450	600	750	900	1200	1500	2250	3000	3750
Resistor Mass	5	10	50	100	150	200	250	300	400	500	600	800	1000	1500	2000	2500
Filter Mass (grams)	51	100	470	916	1354	1787	2216	2643	3489	4328	5162	6817	8459	12523	16545	20537

3-Phase Mass Breakdowns by Power Level
(20 kHz Resonant Frequency)

Power Level (kWe)	0.5	1	5	10	15	20	25	30	40	50	60	80	100	150	200	250
Transformer Mass	29	55	240	454	659	859	1055	1248	1626	1996	2361	3076	3777	5485	7146	8775
Inductor Mass	13	25	125	250	375	500	625	750	1000	1250	1500	2000	2500	3750	5000	6250
Capacitor Mass	8	15	75	150	225	300	375	450	600	750	900	1200	1500	2250	3000	3750
Resistor Mass	5	10	50	100	150	200	250	300	400	500	600	800	1000	1500	2000	2500
Filter Mass (grams)	54	105	490	954	1409	1859	2305	2748	3626	4496	5361	7076	8777	12985	17146	21275

Single-Phase Mass Breakdowns by Efficiency
(20 kHz Resonant Frequency)

Efficiency (%)	99.30%	99.35%	99.40%	99.45%	99.50%	99.55%	99.60%	99.65%	99.70%
Transformer Mass	36	38	42	45	50	56	63	71	83
Inductor Mass	18	19	21	23	25	28	31	36	42
Capacitor Mass	11	12	13	14	15	17	19	21	25
Resistor Mass	7	8	8	9	10	11	13	14	17
Filter Mass (grams)	71	77	83	91	100	111	125	143	167

Single-Phase Mass Breakdowns by Frequency
(99.5% Efficiency)

Frequency (kHz)	10	15	20	25	30	35	40	45	50	55	60
Transformer Mass	69	57	50	45	41	38	36	34	33	31	30
Inductor Mass	50	33	25	20	17	14	13	11	10	9	8
Capacitor Mass	30	20	15	12	10	9	8	7	6	5	5
Resistor Mass	10	10	10	10	10	10	10	10	10	10	10
Filter Mass (grams)	159	121	100	87	78	71	66	62	59	56	53

DC RBI Mass Breakdown Tables

Mass Breakdowns by Power Level
(200 Vdc Voltage Level, 99.85% Efficiency)

					Note 1		Note 2							
Power Level (kWe)	5	10	15	20	25	30	40	50	60	80	100	150	200	250
Relay Element	179	312	432	544	650	752	947	1132	1309	1648	1970	2725	3431	4101
Semiconductor Element	12	24	36	48	60	72	96	120	144	192	240	360	480	600
Relay Driver	19	32	42	51	60	68	83	97	111	135	158	210	257	301
Semiconductor Driver	12	15	17	19	20	21	23	25	26	28	30	34	37	40
Sensors	19	23	26	28	30	32	35	37	39	43	45	51	56	60
Control Logic	4	5	5	5	5	5	5	5	5	6	6	6	6	6
Heat Sink Thermal	70	140	210	280	350	420	560	700	840	1120	1400	2100	2800	3500
Packaging	158	275	384	487	588	685	874	1058	1237	1586	1925	2744	3534	4304
Total Mass (grams)	474	826	1151	1462	1763	2055	2623	3174	3712	4758	5775	8231	10601	12912

Note 1: Values developed from 130 Amp SSF RBI mass. The RBI was changed to a hybrid design with a relay and semiconductor switch in parallel (Ref. III-6).

Note 2: Values developed from 225 Amp SSF RBI mass. The RBI was changed to a hybrid design with a relay and semiconductor switch in parallel (Ref. III-6).

Mass Breakdowns by Efficiency
(25 kWe Power Level, 200 Vdc Voltage Level)

						Note 3					
Efficiency (%)	99.80%	99.81%	99.82%	99.83%	99.84%	99.85%	99.86%	99.87%	99.88%	99.89%	99.90%
Relay Element	487	513	542	574	609	650	696	750	812	886	975
Semiconductor Element	45	47	50	53	56	60	64	69	75	82	90
Relay Driver	45	47	50	53	56	60	64	69	75	82	90
Semiconductor Driver	15	16	17	18	19	20	21	23	25	27	30
Sensors	30	30	30	30	30	30	30	30	30	30	30
Control Logic	5	5	5	5	5	5	5	5	5	5	5
Heat Sink, Thermal	467	443	420	397	373	350	327	303	280	257	233
Packaging	547	551	557	564	574	588	604	625	651	684	727
Total Mass (grams)	1641	1653	1670	1693	1723	1763	1812	1875	1954	2053	2180

Note 3: Based on the contact resistance of the present 130 Amp and 225 Amp dc RBI designs, the efficiency of these units will be 99.85% (Ref. III-33).

Mass Breakdowns by Voltage Level
(25 kWe Power Level, 99.85% Efficiency)

		Note 4													
Voltage Level (Vdc)	100	200	400	700	1000	1500	2000	3000	4000	5000	6000	7000	8000	9000	10000
Relay Element	606	650	697	737	764	795	818	852	877	897	913	928	940	951	961
Semiconductor Element	56	60	64	68	70	73	76	79	81	83	84	86	87	88	89
Relay Driver	58	60	62	64	65	66	67	69	70	70	71	72	72	73	73
Semiconductor Driver	19	20	21	21	22	22	22	23	23	23	24	24	24	24	24
Sensors	24	30	37	44	49	55	60	68	74	79	83	87	91	94	97
Control Logic	5	5	5	5	5	5	5	5	5	5	5	5	5	5	5
Heat Sink, Thermal	350	350	350	350	350	350	350	350	350	350	350	350	350	350	350
Packaging	504	588	686	778	843	925	988	1085	1160	1221	1275	1322	1364	1402	1438
Total Mass (grams)	1623	1763	1921	2066	2167	2291	2386	2530	2639	2729	2805	2873	2933	2987	3037

Note 4: The present 130 Amp and 225 Amp dc RBI designs are capable of 200 Vdc operation.

AC RBI Mass Breakdown Tables

Single-Phase Mass Breakdowns by Power Level
(200 Vrms Voltage Level, 99.85% Efficiency)

					Note 1		Note 2							
Power Level (kWe)	5	10	15	20	25	30	40	50	60	80	100	150	200	250
Relay Element	110	192	266	335	400	463	583	696	806	1014	1213	1677	2111	2524
Semiconductor Element	24	48	72	96	120	144	192	240	288	384	480	720	960	1200
Relay Driver	13	21	28	34	40	45	56	65	74	90	106	140	171	200
Semiconductor Driver	20	24	27	30	32	34	37	39	42	45	49	55	60	64
Sensors	15	19	21	23	25	26	29	31	33	35	38	43	47	50
Control Logic	4	5	5	5	5	5	5	5	5	6	6	6	6	6
Heat Sink, Thermal	70	140	210	280	350	420	560	700	840	1120	1400	2100	2800	3500
Packaging	154	269	378	482	583	683	877	1066	1252	1617	1974	2845	3693	4527
Total Mass (grams)	411	719	1007	1285	1555	1820	2338	2843	3340	4312	5264	7586	9848	12071

Note 1: Values derived from 130 Amp SSF dc RBI mass. The RBI was changed to a hybrid design with a relay and semiconductor switch in parallel (Ref. III-6).
Note 2: Values derived from 225 Amp SSF dc RBI mass. The RBI was changed to a hybrid design with a relay and semiconductor switch in parallel (Ref. III-6).

Three-Phase Mass Breakdowns by Power Level
(200 Vrms Voltage Level, 99.85% Efficiency)

Power Level (kWe)	5	10	15	20	25	30	40	50	60	80	100	150	200	250
Relay Element	155	269	372	468	560	648	816	975	1128	1420	1698	2348	2956	3533
Semiconductor Element	30	60	90	120	150	180	240	300	360	480	600	900	1200	1500
Relay Driver	18	30	40	49	57	65	79	93	105	129	150	200	244	286
Semiconductor Driver	22	27	31	34	36	38	41	44	47	51	55	62	67	72
Sensors	46	57	64	70	75	79	86	92	98	106	114	128	140	150
Control Logic	5	5	6	6	6	6	6	6	7	7	7	7	7	8
Heat Sink, Thermal	70	140	210	280	350	420	560	700	840	1120	1400	2100	2800	3500
Packaging	208	353	488	616	740	862	1097	1326	1551	1988	2414	3447	4449	5429
Total Mass (grams)	555	942	1301	1643	1974	2298	2926	3537	4135	5301	6437	9192	11863	14477

Single-Phase Mass Breakdowns by Efficiency
(25 kWe Power Level, 200 Vrms Voltage Level)

						Note 3					
Efficiency (%)	99.80%	99.81%	99.82%	99.83%	99.84%	99.85%	99.86%	99.87%	99.88%	99.89%	99.90%
Relay Element	300	316	333	353	375	400	429	462	500	545	600
Semiconductor Element	90	95	100	106	112	120	129	138	150	164	180
Relay Driver	30	32	33	35	37	40	43	46	50	55	60
Semiconductor Driver	24	25	27	28	30	32	34	37	40	44	48
Sensors	25	25	25	25	25	25	25	25	25	25	25
Control Logic	5	5	5	5	5	5	5	5	5	5	5
Heat Sink, Thermal	467	443	420	397	373	350	327	303	280	257	233
Packaging	564	564	566	569	575	583	595	610	630	656	691
Total Mass (grams)	1505	1505	1509	1518	1533	1555	1586	1626	1680	1750	1842

Note 3: Based on the contact resistance of the present 130 Amp and 225 Amp dc RBI designs, the efficiency of these units will be 99.85% (Ref. III-33).

Single-Phase Mass Breakdowns by Voltage Level
(25 kWe Power Level, 99.85% Efficiency)

Voltage Level (Vrms)	100	200	400	700	1000	1500	2000	3000	4000	5000	6000	7000	8000	9000	10000
Relay Element	411	400	389	380	375	369	365	359	355	352	349	347	345	344	342
Semiconductor Element	112	120	129	136	141	147	151	157	162	166	169	171	174	176	177
Relay Driver	41	40	39	39	39	38	38	38	38	38	37	37	37	37	37
Semiconductor Driver	31	32	33	34	35	35	36	37	37	38	38	38	38	39	39
Sensors	20	25	31	36	41	46	50	56	61	66	69	73	76	78	81
Control Logic	5	5	5	5	5	5	5	5	5	5	5	5	5	5	5
Heat Sink, Thermal	350	350	350	350	350	350	350	350	350	350	350	350	350	350	350
Packaging	543	583	628	667	694	727	751	788	816	839	858	874	889	903	915
Total Mass (grams)	1513	1555	1604	1648	1679	1717	1746	1790	1824	1852	1875	1896	1914	1931	1946

DC RPC Mass Breakdown Tables

Mass Breakdowns by Power Level
(120 Vdc Voltage Level, 99.85% Efficiency)

	Note 1		Note 2			Note 3						Note 4	
Power Level (kWe)	1	2	3	4	5	6	7	8	9	10	12	16	20
Relay Element	19	33	46	58	69	80	90	100	110	120	139	175	209
Semiconductor Element	2	5	7	10	12	14	17	19	22	24	29	38	48
Relay Driver	6	10	14	17	19	22	25	27	29	32	36	44	51
Semiconductor Driver	4	5	5	6	6	7	7	7	7	8	8	9	9
Sensors	8	9	11	12	12	13	14	14	15	15	16	17	19
Control Logic	14	16	16	17	17	17	18	18	18	18	19	19	20
Heat Sink, Thermal	40	80	120	160	200	240	280	320	360	400	480	640	800
Packaging & Housing	281	473	656	834	1008	1180	1349	1518	1684	1850	2179	2828	3468
Total Mass (grams)	375	631	875	1112	1344	1573	1799	2023	2246	2467	2905	3770	4624

Note 1: The masses of the dc RPC elements were derived from the 10 Amp SSF dc RPC mass breakdown (Ref. III-6).
Note 2: The masses of the dc RPC elements were derived from the 25 Amp SSF dc RPC mass breakdown (Ref. III-6).
Note 3: The masses of the dc RPC elements were derived from the 50 Amp SSF dc RPC mass breakdown (Ref. III-6).
Note 4: The masses of the dc RPC elements were derived from the 130 Amp SSF dc RPC mass breakdown (Ref. III-6).

Mass Breakdowns by Efficiency
(3 kWe Power Level, 120 Vdc Voltage Level)

						Note 5					
Efficiency (%)	99.80%	99.81%	99.82%	99.83%	99.84%	99.85%	99.86%	99.87%	99.88%	99.89%	99.90%
Relay Element	34	36	38	40	43	46	49	53	57	62	69
Semiconductor Element	5	6	6	6	7	7	8	8	9	10	11
Relay Driver	10	11	11	12	13	14	15	16	17	19	20
Semiconductor Driver	4	4	4	5	5	5	6	6	7	7	8
Sensors	11	11	11	11	11	11	11	11	11	11	11
Control Logic	16	16	16	16	16	16	16	16	16	16	16
Heat Sink, Thermal	135	132	129	126	123	120	117	113	110	106	102
Packaging & Housing	646	646	647	649	652	656	662	669	679	693	710
Total Mass (grams)	861	862	863	866	869	875	882	892	906	923	947

Note 5: Based on efficiency estimates for the 10 Amp, 25 Amp, 50 Amp, and 130 Amp SSF dc RPCs, the efficiency of these units will be 99.85% (Ref. III-33).

Mass Breakdowns by Voltage Level
(3 kWe Power Level, 99.85% Efficiency)

						Note 6								
Voltage Level (Vdc)	20	40	60	80	100	120	140	160	180	200	250	300	400	500
Relay Element	38	41	43	44	45	46	47	47	48	48	49	50	52	53
Semiconductor Element	6	6	7	7	7	7	7	7	7	8	8	8	8	8
Relay Driver	12	13	13	13	13	14	14	14	14	14	14	14	14	15
Semiconductor Driver	5	5	5	5	5	5	5	5	5	5	5	6	6	6
Sensors	6	8	9	9	10	11	11	12	12	12	13	14	15	16
Control Logic	16	16	16	16	16	16	16	16	16	16	16	16	16	16
Heat Sink, Thermal	120	120	120	120	120	120	120	120	120	120	120	120	120	120
Packaging & Housing	612	628	638	645	651	656	661	664	668	671	678	684	694	702
Total Mass (grams)	816	837	850	860	868	875	881	886	891	895	904	912	925	936

Note 6: The present 10 Amp, 25 Amp, 50 Amp, and 130 Amp dc RPC designs are rated for 120 Vdc operation.

AC RPC Mass Breakdown Tables

Single-Phase Mass Breakdowns by Power Level
(120 Vrms Voltage Level, 99.85% Efficiency)

	Note 1		Note 2			Note 3						Note 4	
Power Level (kWe)	1	2	3	4	5	6	7	8	9	10	12	16	20
Relay Element	11	20	28	35	41	48	54	60	66	72	83	105	125
Semiconductor Element	5	10	14	19	24	29	34	38	43	48	58	77	96
Relay Driver	4	7	9	11	13	15	16	18	20	21	24	29	34
Semiconductor Driver	8	9	11	12	12	13	14	14	15	15	16	17	19
Sensors	6	7	8	9	9	10	10	11	11	11	12	13	14
Control Logic	14	16	16	17	17	17	18	18	18	18	19	19	20
Heat Sink, Thermal	40	80	120	160	200	240	280	320	360	400	480	640	800
Packaging	318	534	740	942	1141	1338	1532	1726	1918	2109	2490	3243	3989
Total Mass (grams)	406	682	946	1204	1458	1709	1958	2205	2451	2695	3181	4144	5097

Note 1: The masses of the 10 Amp ac RPC elements were derived from the 10 Amp SSF dc RPC mass breakdown (Ref. III-6).
Note 2: The masses of the 25 Amp ac RPC elements were derived from the 25 Amp SSF dc RPC mass breakdown (Ref. III-6).
Note 3: The masses of the 50 Amp ac RPC elements were derived from the 50 Amp SSF dc RPC mass breakdown (Ref. III-6).
Note 4: The masses of the 130 Amp ac RPC elements were derived from the 130 Amp SSF dc RPC mass breakdown (Ref. III-6).

Three-Phase Mass Breakdowns by Power Level
(120 Vrms Voltage Level, 99.85% Efficiency)

Power Level (kWe)	1	2	3	4	5	6	7	8	9	10	12	16	20
Relay Element	16	28	39	48	58	67	76	84	93	101	117	147	176
Semiconductor Element	6	12	18	24	30	36	42	48	54	60	72	96	120
Relay Driver	6	10	13	16	18	21	23	26	28	30	34	42	49
Semiconductor Driver	14	17	19	21	22	23	25	26	26	27	29	31	34
Sensors	13	16	19	20	22	23	24	25	26	27	28	31	33
Control Logic	17	19	19	20	20	21	21	21	22	22	22	23	23
Heat Sink, Thermal	40	80	120	160	200	240	280	320	360	400	480	640	800
Packaging	405	653	887	1113	1334	1552	1767	1980	2191	2400	2816	3635	4443
Total Mass (grams)	517	835	1134	1422	1705	1983	2258	2530	2799	3067	3598	4645	5678

REPORT DOCUMENTATION PAGE

Form Approved
OMB No. 0704-0188

1. AGENCY USE ONLY (*Leave blank*)

2. REPORT DATE
February 1992

3. REPORT TYPE AND DATES COVERED
Final Contractor Report

4. TITLE AND SUBTITLE
Lunar PMAD Technology Assessment

5. FUNDING NUMBERS
WU–953–20–0D–00
NAS3–25808

6. AUTHOR(S)
Kenneth J. Metcalf

7. PERFORMING ORGANIZATION NAME(S) AND ADDRESS(ES)
Rockwell International
Rocketdyne Division
Canoga Park, California

8. PERFORMING ORGANIZATION REPORT NUMBER
E–12691

9. SPONSORING/MONITORING AGENCY NAME(S) AND ADDRESS(ES)
National Aeronautics and Space Administration
Washington, DC 20546–0001

10. SPONSORING/MONITORING AGENCY REPORT NUMBER
NASA CR–189225

11. SUPPLEMENTARY NOTES
Project Manager, Robert Cataldo, Power and Propulsion Office, NASA Glenn Research Center, organization code 6920, 216–977–7082.

12a. DISTRIBUTION/AVAILABILITY STATEMENT
Unclassified - Unlimited
Subject Category: 20
Available electronically at http://gltrs.grc.nasa.gov/GLTRS
This publication is available from the NASA Center for AeroSpace Information, 301–621–0390.

12b. DISTRIBUTION CODE

13. ABSTRACT ***(Maximum 200 words)***

The purpose of this report is to document the initial set of power conditioning models created to estimate power management and distribution (PMAD) component masses and sizes. This first set contains converter, rectifier, inverter, transformer, remote bus isolator (RBI), and remote power controller (RPC) models. The objective is to form a library of PMAD models that will allow system designers to assess various power system architectures and distribution techniques quickly and consistently. It is recommended that the models developed during this study only be used for conceptual design studies which require “ballpark” PMAD mass estimates. To determine specific PMAO design choices such as component topologies, and transmission and distribution voltages and frequencies requires specific power system requirements and more detailed analyses. These models are designed primarily for space exploration initiative (SKI) missions that require continuous power and support manned operations. The model development is based on the fact that power conditioning components have common stages and that their interconnection and control determines the function and operation of the component. The stages contained in a component are defined, their masses calculated, and the control and monitoring, enclosure, and thermal management masses are added to determine the mass of the complete component. The models are based on components that use passive or active thermal management and they estimate component heat sink, coldplate, and radiator masses (the masses of pumps, plumbing, etc. are not included). The model documentation explains the component equations, including their constants and exponents; identifies model limitations; specifies valid input ranges; and discusses methods for applying the component models. A separate section explains how to link individual models to form a complete power transmission and distribution system model. Before creating the power conditioning models, a power element technology assessment was conducted to gauge the amount of advancement one could reasonably expect by the year 2000.

14. SUBJECT TERMS
Power conditioning; Power converters

15. NUMBER OF PAGES
221

16. PRICE CODE
A10

17. SECURITY CLASSIFICATION OF REPORT	18. SECURITY CLASSIFICATION OF THIS PAGE	19. SECURITY CLASSIFICATION OF ABSTRACT	20. LIMITATION OF ABSTRACT
Unclassified	Unclassified	Unclassified	